Malformations of Cortical Development
- Clinical and genetic characterization -

Renske Oegema

Cover design and layout: Optima Grafische Communicatie, Rotterdam, the Netherlands
Cover image: Tom de Vries-Lentsch

ISBN/EAN 9789070116705

Part of the research presented in this thesis was supported by an Erasmus MC grant, an EMBO short term fellowship and the NVHG Simonsfonds.
Printing of this thesis was supported by the Erasmus Universiteit, Klinische Genetica Erasmus MC, and ChipSoft B.V.

Malformations of Cortical Development
- Clinical and genetic characterization -

Aanlegstoornissen van de hersenschors
- Een klinische en genetische studie -

Proefschrift

ter verkrijging van de graad van doctor aan de
Erasmus Universiteit Rotterdam
op gezag de
rector magnificus
prof.dr. H.A.P. Pols
en volgens besluit van het College voor Promoties.

De openbare verdediging zal plaatsvinden op
dinsdag 10 mei om 13.30 uur

door

Renske Oegema
geboren te Zaanstad

Erasmus University Rotterdam

Promotiecommissie

Promotor	Prof.dr. R.M.W. Hofstra
Overige leden	Prof.dr. V.V.A. Knoers Prof.dr. A.C. Jansen Dr. J.E.M.M. de Klein
Copromotor	Dr. G.M.S. Mancini

CONTENTS

Chapter 1

General introduction

GENERAL INTRODUCTION

The folded surface of the human brain, the brain cortex, has intrigued scientists for centuries. It was recently discovered that the mathematical formula predicting the degree of folding of a paper ball can also be applied to predicting the degree of folding of the brain cortex, and that its pattern depends on the cortical thickness and total surface area.[1]
As this thesis will show, finding an explanation for abnormal development of the cortex has been less straightforward, although our knowledge regarding its mechanisms is rapidly expanding.
The human brain is roughly built up of two main structures, the cortex which is the outer layer (the grey matter) and the inner white matter. The cortex contains the cell bodies of the neurons, and the white matter contains the axons connecting neurons from the same or from different brain regions to each other. All congenital abnormalities related to the development of the brain cortex are collectively called malformations of cortical development (MCD). The majority of MCD are either forms of microcephaly, megalencephaly, lissencephaly, heterotopia or polymicrogyria.[2] This thesis focuses on heterotopia and microcephaly. Before describing the details of these malformations, I will briefly summarize the normal development of the brain cortex.

DEVELOPMENT OF THE BRAIN CORTEX

The adult male brain contains around 86 billion neurons and 85 billion non-neuronal cells. [3] It is thought that the majority of these neurons are already present in the newborn brain.

Early development

After formation of the neural tube around the fourth week, the cranial region develops into three, and later five structures: the rhombencephalon, from which the myelencephalon and metencephalon are formed, the mesencephalon, and the prosencephalon, which later forms the diencephalon and telencephalon (cerebrum). The ventricles are formed from the hollow cavity of the neural tube.
Intriguingly, neurons are born within deep brain structures and then migrate outwards to form the cortex. Therefore, the formation of the cortex can roughly be divided into three main stages; neurogenesis, neuronal migration and cortical organization.

Neurogenesis

Neurogenesis starts from the pool of neuroepithelial cells (NECs) lining the surface of the ventricles (Fig. 1). During cell cycle, the nucleus moves from the basal side during S phase towards the apical (ventricular) side during M phase and then back to the basal side. This is a critical process and disturbance will lead to cell cycle exit and /or

apoptosis and thus to depletion of the progenitor pool. The NECs give rise to apical radial glial cells (RGCs). Both NECs and RGCs are polarized and connected through adherens junctions. The RGCs undergo both symmetric and asymmetric cell divisions, in turn expanding the cell pool by giving rise to RGCs, neurons (direct neurogenesis), and intermediary progenitor cells (IPCs), which in turn will also give rise to neurons (indirect neurogenesis).[4]

Neuronal migration – radial

Newborn neurons migrate toward the cortical plate on the outer surface to eventually form a six-layered folded cortex (Fig. 1). The RGCs form long processes extending

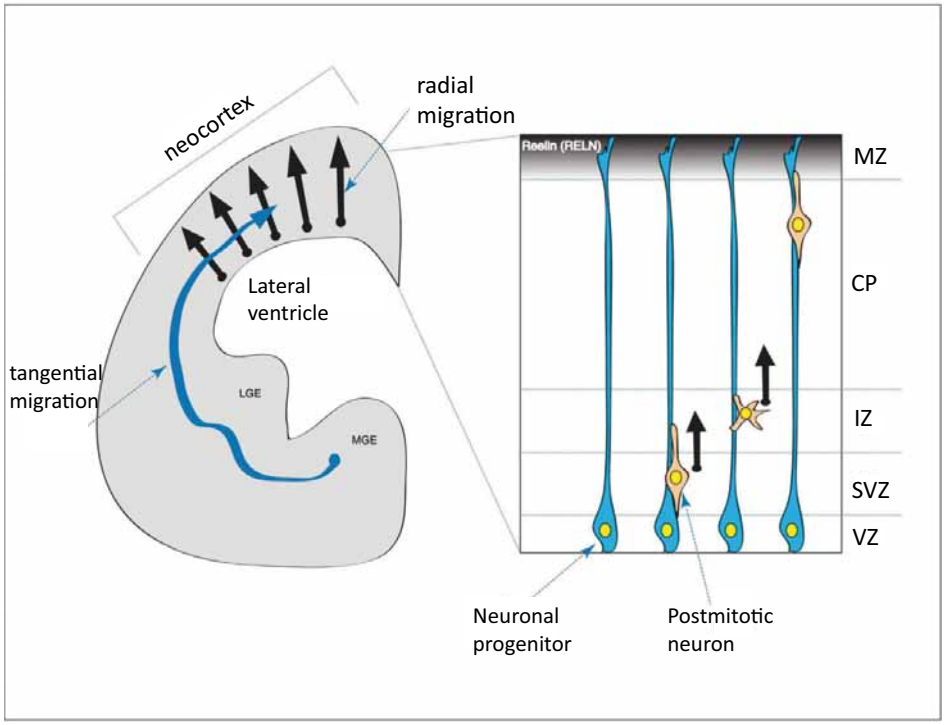

Figure 1. Schematic representation of the developing mammalian brain.
(A) Coronal section of one half of the mammalian developing forebrain. There are two main migratory streams of post-mitotic neurons: the radial migration of excitatory cortical pyramidal neurons from the ventricular zone (VZ) to the cortical plate (CP) (black arrow) and the tangential migration of inhibitory GABAergic interneurons from lateral- and medial- ganglionic eminences (LGE/MGE) into the neocortex (blue arrow). (B) The developing cerebral cortex in mammals is multi-layered with different neuronal cell populations. Near the lateral ventricle surface, neural progenitors (NPs) reside in the ventricular zone (VZ). This progenitor zone is extended to subventricular and intermediate zones (SVZ and IZ, respectively). Newly born neurons from the division of NPs undergo extensive radial neuronal migration to enter the cortical plate (CP). The marginal zone (MZ) is the most superficial layer (66). [reused with permission from John Wiley and Sons]

through the cortical plate and connecting to the pial lamina, hereby forming a scaffold for the migration of newborn neurons to the cortical plate. These neurons migrate radially along the RGC extensions and are also guided by extracellular cues. The migrating neuron first extends its leading process, and then the centrosome moves into the leading process followed by the nucleus. The cytoskeleton (actin filaments and microtubules) and its associated proteins are crucial components of these processes.[4] Neurons that migrated radially to the cortex will become glutamatergic excitatory pyramidal neurons.

Neuronal migration - tangential

In contrast to the pyramidal neurons, the inhibitory GABAergic interneurons migrate tangentially and originate in the ganglionic eminences (Fig. 1). The ganglionic eminences (GE) form transiently during brain development and provide a source of neurons destined for the cortex and for the basal ganglia. The GE disappear around one year of age.[5] The caudal GE is the major source of cortical interneurons, but the medial and lateral GE also contribute.[6] The GABAergic neurons travel tangentially from the GEs through the subventricular zone or through the marginal zone, and, in contrast to the glutamatergic neurons, without a radial glia scaffold.[6] As a consequence, interneurons seem to end up randomly dispersed throughout the mammalian cortex.[7,8]

Cortical organization

The normal human cortex is built up of six distinct cellular layers. Its size is unique to humans and other primates, and this is achieved by expansion of neuronal progenitors and folding (gyrification) of the cortical plate. When the neurons have reached their final destination in the cortex, their axons and dendrites mature, they commence synaptogenesis and assemble into microcircuits.[9]

Malformations of cortical development

Malformations of cortical development (MCD) comprise a large and heterogeneous group of malformations resulting from defects in the process of cortical formation, from ventricular and subventricular zone neurogenesis to neuronal migration to post-migrational development.[2] This term is preferred to "cortical malformations" to include gray matter heterotopia which are located beneath the cortex but also result from defective corticogenesis.

Prevalence and impact

The prevalence of MCD in the general population is unknown. In the 2012 MCD classification [2], 200 MCD subtypes are recognized, each subtype being very rare. Taken together, however, they form a substantial burden on health care and society, account-

ing for 3% of intellectual disability, 25% of pediatric partial seizures, 5-15% of adult epilepsy, and 20-40% of therapy-resistant epilepsy. [10-14]
Symptoms can present at all ages; from pregnancy into late adulthood.[15-17] In the majority of individuals, the brain abnormalities are discovered on brain imaging (MRI= magnetic resonance imaging) during childhood, initiated by the presence of developmental delay and/or seizures. As for the majority of patients, only symptomatic therapy and no curative therapy is available, MCD have a lifelong impact on the health and wellbeing of the affected patients and their families.

Classification

Classically, MCD are grouped into the presumed stage of defective development;

I) proliferation or apoptosis disorders (primary microcephaly, megalencephaly),
II) migration disorders (heterotopia, lissencephaly, cobblestone malformation),
III) organization disorders (polymicrogyria, schizencephaly, focal cortical dysplasia, postmigrational microcephaly).[2]

It was anticipated that mutations in genes unique to each disorder and developmental stage would be identified. Data from imaging and genetic studies and subsequent functional and animal studies have greatly advanced our understanding of MCD pathophysiology. It has however also led to the recognition that the current classification is not comprehensive, as malformations from more than one group can occur in a single patient. The discovery of mutations in for example *WDR62* and *TUBA1A* has further strengthened the concept that mutations in a single gene can lead to multiple malformations originating in different stages of brain development.[18-20]
The range of malformations associated with *WDR62* mutations is broad and includes primary microcephaly, lissencephaly, and polymicrogyria. [19,21] WDR62 localizes to the centrosome and to the nucleus and in mouse embryonic brain it is expressed in both the ventricular zone and the cortical plate.[22,23] It has been proposed that the *WDR62*-related malformations result from the combined effects on nucleokinesis, centrosome assembly and movement in both progenitors and differentiating post-mitotic neurons, leading to a diminished progenitor pool, altered migration and disturbed cortical organization.[4,22] Ultimately, a new classification based on integrated clinical, imaging, genetic and biological pathway data will be established.[16]

Imaging

MCD were first described by neuropathologists. In the early seventies, respectively early eighties, the compute tomography (CT) scans and magnetic resonance imaging (MRI) scans became clinically available. It has taken several more years however before these were implemented into routine clinical practice. The use of CT scans for diagnosing patients with severe MCD during their lifetime emerged in the eighties.[24]

MRI, a powerful tool for recognizing MCD allowing a more detailed description of morphology and localization than CT, emerged in clinical practice only from the late eighties.[25] During the nineties, more and more MCD subtypes were described and in 1996, the first MCD classification was published.[26] Comparing the first classification (1996) with the most recent (2012) emphasizes the explosively increased recognition of these disorders over less than two decades:
Group I: in 1996 16, in 2012 65 subtypes;
Group II: in 1996 40, in 2012 65 subtypes;
Group III: in 1996 8, in 2012 70 subtypes. [2,26]
This growing complexity is due in part to increased use of high resolution brain imaging, and in part to the discovery of dozens of genes involved in MCD, much more than was first anticipated.
When diagnosing MCD on brain imaging, it is extremely important to systematically review all brain structures in order 1) to make accurate prognostic predictions 2), to not overlook subtle abnormalities and 3) to enable a precise diagnosis. In MCD, extra-cortical abnormalities can be a clue to the underlying diagnosis, for example basal ganglia abnormalities in the tubulinopathies.[18] A useful approach would be to systematically review at least these structures in the following sequence: date of review, age of MRI, head contour/skull; extra-axial spaces, cerebral hemispheres, gyral pattern, hippocampus, basal ganglia and thalami, white matter, lateral ventricles, third ventricle, corpus callosum, brain stem, cerebellum and cerebellar vermis, posterior fossa (adapted from W.B. Dobyns, personal communication).

The majority of individuals described in this thesis have heterotopia and/or microcephaly, and in the next section, these disorders are described in more detail.

HETEROTOPIA

Neuronal heterotopia are macroscopic clusters of misplaced neurons, most often situated along the ventricular walls or within the subcortical white matter. The cortex itself can be normal or abnormal. Naming in literature has been inconsistent and has included grey matter heterotopia, subependymal heterotopia, white matter heterotopias, and neuronal heterotopia. According to the Barkovich classification the following terms are to be used for the different subtypes: subcortical band heterotopia, periventricular nodular heterotopia, periventricular linear heterotopia, columnar heterotopia and large subcortical heterotopia.[2] When situated above the cortex (e.g. overmigration of neurons) they form a distinct entity named leptomeningeal glioneuronal heterotopia. The different subtypes can be distinguished on MRI (Fig. 2). Both periventricular nodular heterotopia and subcortical heterotopia are the subject of this thesis.

Periventricular nodular heterotopia

Although its true prevalence is unknown, in multiple cohort studies periventricular nodular heterotopia (PNH) were one of the most frequently occurring MCD.[27-29] Patients most commonly present with seizures, which will develop in 80-90% of individuals.[16] However the severity and the age of presentation depends largely on the underlying etiology and associated malformations, rendering it very important to establish a specific and whenever possible, an etiological diagnosis.

Imaging

PNH are clusters (nodules) of mislocalized neurons and glial cells along the walls of the lateral ventricles.[30] They are recognized on brain imaging as an irregular or bumpy surface lining of the ventricular walls. The nodules display the same signal intensity as the cortex, and are more easily recognized in the mature (myelinated) brain. Their localization can be anywhere along the ventricular wall, bilateral or unilateral, continuous or scattered. The differential diagnosis includes subcortical heterotopia, white matter abnormalities, and tubers associated with tuberous sclerosis complex, although these can be very well differentiated by careful MRI review. Single or scattered PNH are sometimes overlooked, especially on low-resolution imaging and/or in young children in whom myelination is still ongoing. PNH can be an isolated finding on brain imaging, or occur in combination with a wide range of other brain malformations. X-linked PNH caused by *FLNA* mutations is commonly associated with posterior fossa abnormalities, mainly mega cisterna magna.[31] Patients with *ARFGEF2*- associated PNH have microcephaly and hyperintensities of the basal ganglia on T2-weighted and FLAIR images (Fig. 2).[32,33] In a large retrospective study of 200 patients with PNH, additional MCD were found in 33%, subcortical heterotopia, polymicrogyria, and microcephaly being most common.[8] Polymicrogyria is commonly observed in combination with PNH, with polymicrogyria most commonly found in the perisylvian areas or more posterior in the occipital-parietal-temporal cortex.[5,34] The latter pattern has been associated with the 6q terminal deletion syndrome [35] and was found in a female with large chromosome Xq21 deletion (G.M.S. Mancini, personal communication). We and others have observed PNH in patients with neural tube defects.[36] Sometimes a thin curvilinear gray-matter band can be seen within the white matter.[37]

Etiology

The number of genes associated with PNH is still small, but several chromosomal imbalances and monogenetic syndromes have been reported to include PNH as a main or minor feature (Table 1). The Baraitser-Winter Neurogenetics database [v.1.0.32 London Medical Databases] lists 39 syndromes with PNH. Non-genetic causes are not

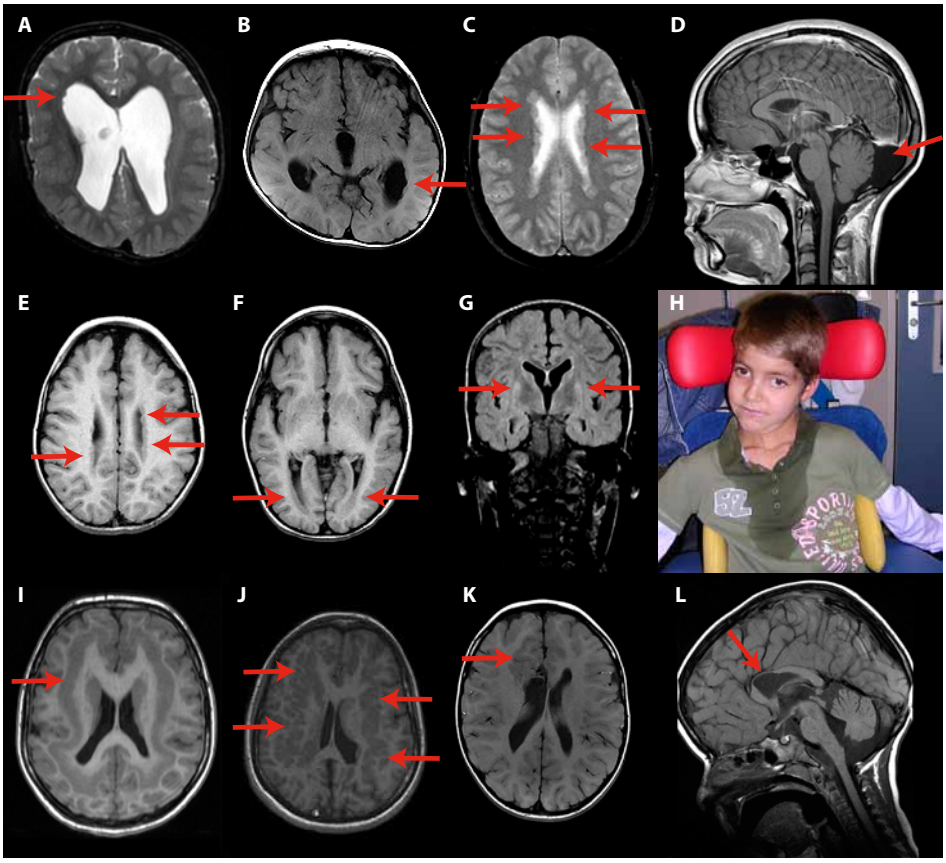

Figure 2. Magnetic resonance imaging of heterotopia patients.
(A) scattered PNH, bilateral perisylvian polymicrogyria and enlarged lateral ventricles. (B) PNH in patient with Smith-Magenis syndrome caused by a 17p11.2 deletion. (C) extensive bilateral PNH in a female patient with a *FLNA* mutation. (D) mega cisterna magna in the same *FLNA* patient. (E-H) patient with biallelic *ARFGEF2* mutations showing bilateral PNH (E) extending to the occipital horns (F) and hyperintensity of the putamen on FLAIR imaging. (H) she had dystonic posturing and excessive drooling. (I) subcortical band heterotopia in male patient with a mosaic *DCX* mutation. (J) extensive bilateral curvilinear subcortical heterotopia. (K) curvilinear subcortical heterotopia limited to the frontal lobes. (L) same patient as in (K) showing partial agenesis of the corpus callosum.

very well studied. There has been one report on the association with prenatal alcohol exposure.[38]

The most studied form is that of X-linked dominant periventricular heterotopia caused by mutations in the *FLNA* gene. In around half of bilateral PNH cases *FLNA* mutations can be identified, and this number rises to 83-100% in familial cases.[39,40] Females can be asymptomatic or present with mildly disturbed cognitive functioning, seizures, connective tissue abnormalities, lung disease, and cardiovascular malformations.[41-43] Mutations in males usually result in embryonic lethality, however the few surviving

males present with a plethora of congenital abnormalities affecting the CNS, cardiovascular, pulmonary, gastro-intestinal, and genito-urinary systems.[40,44] The intra- and interfamilial variability is great, and outcome largely depends on the associated abnormalities.

A clinically distinct disorder is caused by autosomal recessive mutations in *ARFGEF2*.[32] Since its discovery in 2004 only 6 families, with 13 affected patients, have been described.[32,33,45-47] Patients suffer from severe neurological disease with seizures, spastic quadriplegia, profound ID, progressive microcephaly, and movement disorder. Recently obstructive cardiomyopathy has been recognized as an additional feature.[46,47] MRI shows progressive generalized cerebral atrophy, bilateral PNH, which can be continuous or scattered, abnormal intensity of the putamen, hippocampal atrophy, thin corpus callosum, and relatively preserved brainstem and cerebellum.[32,33,45-47]

Several studies have reported deletions of chromosome band 6q27 in patients with variable combinations of the following structural brain malformations: PNH predominantly situated in the temporal horns, polymicrogyria, agenesis or hypoplasia of the corpus callosum, colpocephaly, under-rotated hypoplastic hippocampi, and cerebellar hypoplasia.[35,48,49] In a patient who had PNH, developmental delay, and seizures a heterozygous missense mutation in the *ERMARD* gene (located on 6q27, previously named *C6orf70*) was identified.[35] Additional studies are warranted to clarify the role of *ERMARD* mutations in PNH.

Subcortical band heterotopia

Subcortical band heterotopia (SBH) is considered the mild end of the lissencephaly spectrum. In contrast to lissencephaly, where the cortex is thickened and has diminished number of gyri (agyria or pachygyria), in SBH the cortex is normally organized into six layers, although the sulci can be shallow.[16] A normal white matter layer is present right beneath the cortex, followed by a layer of varying depth consisting of misplaced neurons. On brain MRI, this appears as a smooth band of similar signal intensity to the cortex.[16] Patients can have seizures and mild to moderate intellectual disability, or be entirely asymptomatic.[50]

SBH is caused by mutations in genes also causing lissencephaly, most commonly *DCX* (Table 2), but the migration defect is less severe due to X-linked dominant inheritance (*DCX* mutations causing lissencephaly in males and SBH in females), milder (missense) mutations (*LIS1*), or mosaicism (*LIS1, DCX*).[51,52] Together *DCX* and *LIS1* constitute about 80% of mutations causing SBH.[50]

Other subcortical heterotopia

All other heterotopia located between the cortex and lateral ventricles have collectively been referred to as subcortical heterotopia. The few available reports of subcorti-

cal heterotopia show remarkable heterogeneity in location, size and pattern.[15,53-56] Its cause is largely unknown, but for a few, mostly rare, subtypes a possibly or likely genetic etiology has been implied (Table 3). Exogenic causes have also been suggested due to the occurrence of subcortical heterotopia in patients with a prenatal history of twinning, near miscarriage or trauma.[54,57]

Rare other heterotopia

Other types of heterotopia exist, but reports are rare. Bilateral undulating ribbon-like heterotopia have been reported in two adults with epilepsy and normal intelligence, but was also observed in a girl with severe developmental delay, seizures, and cataracts.[39,58] Van Maldergem syndrome is a disorder characterized by intellectual disability, craniofacial, auditory, renal, skeletal and limb malformations.[59] Affected individuals variably have periventricular heterotopia ranging from nodular to confluent "laminar" heterotopia, and occasionally extending into the white matter. [59,60]

MICROCEPHALY

Microcephaly is defined by a head circumference equal to or less than 2 – 3 standard deviations below the mean for age.[61] Post-migrational microcephaly is characterized by a severe postnatal slowing in brain growth.[2] When present at birth is it referred to as congenital microcephaly. Congenital microcephaly is due to either reduced proliferation or accelerated apoptosis.[2] Primary microcephaly is traditionally defined as a congenital microcephaly, <-3SD at birth, with a non-progressive mental retardation and, apart from a simplified gyral pattern, with normal brain architecture.[62]

Imaging

Brain imaging is not obligatory, but should be carefully considered in any child with microcephaly, especially when neurological deficits or seizures are present. In children with severe microcephaly (<-3 SD), imaging abnormalities are found in 80%.[63] This is in contrast to children with milder microcephaly (between -2 and -3 SD) in whom abnormalities are found in 40%.[63] Most frequently MCD or abnormalities of the corpus callosum are identified. Congenital microcephaly is often associated with a simplified gyral pattern, resulting in fewer gyri and sulci, especially of the frontal lobes. Although usually considered a separate entity in combination with microcephaly, it has become evident that this is the direct result of the diminished brain volume, and therefore not a separate malformation.[1,64]

Etiology

Dozens of genes have already been associated with microcephaly, and the majority encode proteins involved in the cell cycle and DNA repair mechanisms. [61] This is especially true for the genes associated with primary microcephaly, of which already 16 have been identified (OMIM MCPH1-16). It is thought that mutations in these genes lead to cell cycle arrest or cell death and ultimately a diminished neuroprogenitor pool. Genes associated with micrcocephaly in combination with MCD are listed in Table 4. Many syndromes and chromosomal aberrations also have microcephaly as a key feature, as well as prenatal teratogen exposures. This heterogeneity complicates the diagnostic trajectory of the microcephaly patient, and any additional features which might point to the diagnosis should be actively sought for. A practical for the diagnostic approach was proposed by Woods and Parker.[65]

BACKGROUND OF THE THESIS

In the Erasmus MC-Sophia, multidisciplinary expertise on MCD has been built by dedicated professionals from the departments of Clinical Genetics, Radiology and Pediatric Neurology starting in the late nineties. This has resulted in the joint neurogenetics clinic, now embedded within the " national expertise center for central nervous system malformations"(registered by the Dept. of Health in 2015); and a laboratory offering state-of-the-art molecular diagnostics, first targeted Sanger sequencing, FISH or MLPA of individual genes, and currently SNP arrays, a next-generation sequencing panel with 103 genes and whole-exome sequencing.

The main purpose of this study was to enhance our knowledge on MCD and to disseminate our findings to the clinical and the scientific community. Therefore we aimed to improve the existing classification, to identify genetic causes of MCD and to describe in great detail imaging manifestations and associated symptoms and malformations. In particular I have focused on two common types of MCD: heterotopia, one of the poorly explained types of MCD, and microcephaly, which is etiological very heterogeneous and is frequently associated with structural MCD.

SCOPE OF THE THESIS

In **Chapter 1**, a general introduction to the presentation and etiology of MCD is given. In the Erasmus MC-Sophia we identified several patients with rare, unpublished forms of subcortical heterotopia. For the research described in **Chapter 2**, I visited the Center for Integrative Brain Research, Seattle Children's / University of Washington (U.S.A.) to search the world's largest database of MCD patients (>7,500) collected by professor W. B. Dobyns, for additional patients. This, in combination with searches of three other large databases of MCD patients collected by professor A.J. Barkovich, professor R. Guerrini, and dr. G.M.S. Mancini, has resulted in a classification for subcortical malformations, with data of >100 patients (**Chapter 2.1**). In the next chapter, patients from the Seattle database of dr. D. Doherty are described who presented with a distinct cerebellar dysplasia. We identified mutations in multiple tubulin genes and named the mild cortical abnormalities associated with tubulinopathies *dysgyria* (**Chapter 2.2**).

In **Chapter 3**, Expanding phenotypes, we diagnosed MCD in patients with known syndromes and/or gene mutations: PNH in KBG syndrome (**Chapter 3.1**); microcephaly, PNH and cortical dysplasia associated with chromosome 21q22 deletions (**Chapter 3.2**); polymicrogyria and PNH in a boy with an *ARX* mutation (**Chapter 3.3**); multi-organ involvement and PNH in a *FLNA* pedigree with three affected males (**Chapter 3.4**); and progressive neurodegeneration with microcephaly and ataxia associated with *PNKP* mutations (**Chapters 3.5 and 3.6**).

In **Chapter 4**, New gene and mechanism, we describe the discovery of a novel gene for profound intellectual disability, microcephaly and PNH, *INTS8* (**Chapter 4.1**).
Finally, in **Chapter 5**, our findings and future studies are discussed.

REFERENCES

1. Mota B, Herculano-Houzel S. BRAIN STRUCTURE. Cortical folding scales universally with surface area and thickness, not number of neurons. Science. 2015 Jul 3;349(6243):74-7.
2. Barkovich AJ, Guerrini R, Kuzniecky RI, Jackson GD, Dobyns WB. A developmental and genetic classification for malformations of cortical development: update 2012. Brain. 2012 May;135(Pt 5):1348-69.
3. Azevedo FA, Carvalho LR, Grinberg LT, Farfel JM, Ferretti RE, Leite RE, et al. Equal numbers of neuronal and nonneuronal cells make the human brain an isometrically scaled-up primate brain. J Comp Neurol. 2009 Apr 10;513(5):532-41.
4. Jiang X, Nardelli J. Cellular and molecular introduction to brain development. Neurobiol Dis. 2015 Jul 13.
5. Wieck G, Leventer RJ, Squier WM, Jansen A, Andermann E, Dubeau F, et al. Periventricular nodular heterotopia with overlying polymicrogyria. Brain. 2005 Dec;128(Pt 12):2811-21.
6. Hansen DV, Lui JH, Flandin P, Yoshikawa K, Rubenstein JL, Alvarez-Buylla A, et al. Non-epithelial stem cells and cortical interneuron production in the human ganglionic eminences. Nat Neurosci. 2013 Nov;16(11):1576-87.
7. Barkovich AJ, Kjos BO. Schizencephaly: correlation of clinical findings with MR characteristics. AJNR Am J Neuroradiol. 1992 Jan-Feb;13(1):85-94.
8. Gonzalez G, Vedolin L, Barry B, Poduri A, Walsh C, Barkovich AJ. Location of periventricular nodular heterotopia is related to the malformation phenotype on MRI. AJNR Am J Neuroradiol. 2013 Apr;34(4):877-83.
9. Hippenmeyer S. Chapter 1: Molecular pathways controllling the sequential steps of cortical projection neuron migration. In: Nguyen LP, Hippenmeyer S, editors. Cellular and molecular control of neuronal migration. Dordrecht: Springer; 2014.
10. Hunter A. Brain. In: Stevenson RE, Hall JG, Goodman R, editors. Human malformations and related anomalies: Oxford University Press; 1993. p. 1-52.
11. Jacobs MP, Fischbach GD, Davis MR, Dichter MA, Dingledine R, Lowenstein DH, et al. Future directions for epilepsy research. Neurology. 2001 Nov 13;57(9):1536-42.
12. Kuzniecky R, Murro A, King D, Morawetz R, Smith J, Powers R, et al. Magnetic resonance imaging in childhood intractable partial epilepsies: pathologic correlations. Neurology. 1993 Apr;43(4):681-7.
13. Mischel PS, Nguyen LP, Vinters HV. Cerebral cortical dysplasia associated with pediatric epilepsy. Review of neuropathologic features and proposal for a grading system. J Neuropathol Exp Neurol. 1995 Mar;54(2):137-53.
14. Papayannis CE, Consalvo D, Kauffman MA, Seifer G, Oddo S, D'Alessio L, et al. Malformations of cortical development and epilepsy in adult patients. Seizure. 2012 Jun;21(5):377-84.
15. Dubeau F, Tampieri D, Lee N, Andermann E, Carpenter S, Leblanc R, et al. Periventricular and subcortical nodular heterotopia. A study of 33 patients. Brain. 1995 Oct;118 (Pt 5):1273-87.
16. Guerrini R, Dobyns WB. Malformations of cortical development: clinical features and genetic causes. Lancet Neurol. 2014 Jul;13(7):710-26.
17. Stutterd CA, Leventer RJ. Polymicrogyria: a common and heterogeneous malformation of cortical development. Am J Med Genet C Semin Med Genet. 2014 Jun;166C(2):227-39.
18. Bahi-Buisson N, Poirier K, Fourniol F, Saillour Y, Valence S, Lebrun N, et al. The wide spectrum of tubulinopathies: what are the key features for the diagnosis? Brain. 2014 Jun;137(Pt 6):1676-700.

19. Bilguvar K, Ozturk AK, Louvi A, Kwan KY, Choi M, Tatli B, et al. Whole-exome sequencing identifies recessive WDR62 mutations in severe brain malformations. Nature. 2010 Sep 9;467(7312):207-10.
20. Poulton CJ, Schot R, Seufert K, Lequin MH, Accogli A, Annunzio GD, et al. Severe presentation of WDR62 mutation: is there a role for modifying genetic factors? Am J Med Genet A. 2014 Sep;164A(9):2161-71.
21. Yu TW, Mochida GH, Tischfield DJ, Sgaier SK, Flores-Sarnat L, Sergi CM, et al. Mutations in WDR62, encoding a centrosome-associated protein, cause microcephaly with simplified gyri and abnormal cortical architecture. Nat Genet. 2010 Nov;42(11):1015-20.
22. Bhat V, Girimaji SC, Mohan G, Arvinda HR, Singhmar P, Duvvari MR, et al. Mutations in WDR62, encoding a centrosomal and nuclear protein, in Indian primary microcephaly families with cortical malformations. Clin Genet. 2011 Dec;80(6):532-40.
23. Nicholas AK, Khurshid M, Desir J, Carvalho OP, Cox JJ, Thornton G, et al. WDR62 is associated with the spindle pole and is mutated in human microcephaly. Nat Genet. 2010 Nov;42(11):1010-4.
24. Dobyns WB, McCluggage CW. Computed tomographic appearance of lissencephaly syndromes. AJNR Am J Neuroradiol. 1985 Jul-Aug;6(4):545-50.
25. Barkovich AJ, Chuang SH, Norman D. MR of neuronal migration anomalies. AJR Am J Roentgenol. 1988 Jan;150(1):179-87.
26. Barkovich AJ, Kuzniecky RI, Dobyns WB, Jackson GD, Becker LE, Evrard P. A classification scheme for malformations of cortical development. Neuropediatrics. [Review]. 1996 Apr;27(2):59-63.
27. Barkovich AJ, Kjos BO. Gray matter heterotopias: MR characteristics and correlation with developmental and neurologic manifestations. Radiology. 1992 Feb;182(2):493-9.
28. Raymond AA, Fish DR, Sisodiya SM, Alsanjari N, Stevens JM, Shorvon SD. Abnormalities of gyration, heterotopias, tuberous sclerosis, focal cortical dysplasia, microdysgenesis, dysembryoplastic neuroepithelial tumour and dysgenesis of the archicortex in epilepsy. Clinical, EEG and neuroimaging features in 100 adult patients. Brain. 1995 Jun;118 (Pt 3):629-60.
29. Tinuper P, D'Orsi G, Bisulli F, Zaniboni A, Piraccini A, Bernardi B, et al. Malformation of cortical development in adult patients. Epileptic Disord. 2003 Sep;5 Suppl 2:S85-90.
30. Tassi L, Colombo N, Cossu M, Mai R, Francione S, Lo Russo G, et al. Electroclinical, MRI and neuropathological study of 10 patients with nodular heterotopia, with surgical outcomes. Brain. 2005 Feb;128(Pt 2):321-37.
31. Fox JW, Lamperti ED, Eksioglu YZ, Hong SE, Feng Y, Graham DA, et al. Mutations in filamin 1 prevent migration of cerebral cortical neurons in human periventricular heterotopia. Neuron. 1998 Dec;21(6):1315-25.
32. Sheen VL, Ganesh VS, Topcu M, Sebire G, Bodell A, Hill RS, et al. Mutations in ARFGEF2 implicate vesicle trafficking in neural progenitor proliferation and migration in the human cerebral cortex. Nat Genet. 2004 Jan;36(1):69-76.
33. de Wit MC, de Coo IF, Halley DJ, Lequin MH, Mancini GM. Movement disorder and neuronal migration disorder due to ARFGEF2 mutation. Neurogenetics. 2009 Oct;10(4):333-6.
34. Leventer RJ, Jansen A, Pilz DT, Stoodley N, Marini C, Dubeau F, et al. Clinical and imaging heterogeneity of polymicrogyria: a study of 328 patients. Brain. 2010 May;133(Pt 5):1415-27.
35. Conti V, Carabalona A, Pallesi-Pocachard E, Parrini E, Leventer RJ, Buhler E, et al. Periventricular heterotopia in 6q terminal deletion syndrome: role of the C6orf70 gene. Brain. 2013 Nov;136(Pt 11):3378-94.

36. Lotfi M, Iranpour P, As'adi K. Cervical meningocele associated with subependymal nodular heterotopia. Clin Imaging. 2011 May-Jun;35(3):214-6.
37. Battaglia G, Chiapparini L, Franceschetti S, Freri E, Tassi L, Bassanini S, et al. Periventricular nodular heterotopia: classification, epileptic history, and genesis of epileptic discharges. Epilepsia. 2006 Jan;47(1):86-97.
38. Nicita F, Verrotti A, Pruna D, Striano P, Capovilla G, Savasta S, et al. Seizures in fetal alcohol spectrum disorders: evaluation of clinical, electroencephalographic, and neuroradiologic features in a pediatric case series. Epilepsia. 2014 Jun;55(6):e60-6.
39. Parrini E, Ramazzotti A, Dobyns WB, Mei D, Moro F, Veggiotti P, et al. Periventricular heterotopia: phenotypic heterogeneity and correlation with Filamin A mutations. Brain. 2006 Jul;129(Pt 7):1892-906.
40. Sheen VL, Dixon PH, Fox JW, Hong SE, Kinton L, Sisodiya SM, et al. Mutations in the X-linked filamin 1 gene cause periventricular nodular heterotopia in males as well as in females. Hum Mol Genet. 2001 Aug 15;10(17):1775-83.
41. Clapham KR, Yu TW, Ganesh VS, Barry B, Chan Y, Mei D, et al. FLNA genomic rearrangements cause periventricular nodular heterotopia. Neurology. 2012 Jan 24;78(4):269-78.
42. de Wit MC, de Coo IF, Lequin MH, Halley DJ, Roos-Hesselink JW, Mancini GM. Combined cardiological and neurological abnormalities due to filamin A gene mutation. Clin Res Cardiol. 2011 Jan;100(1):45-50.
43. Reinstein E, Frentz S, Morgan T, Garcia-Minaur S, Leventer RJ, McGillivray G, et al. Vascular and connective tissue anomalies associated with X-linked periventricular heterotopia due to mutations in Filamin A. Eur J Hum Genet. 2012 Oct 3.
44. Guerrini R, Mei D, Sisodiya S, Sicca F, Harding B, Takahashi Y, et al. Germline and mosaic mutations of FLN1 in men with periventricular heterotopia. Neurology. 2004 Jul 13;63(1):51-6.
45. Banne E, Atawneh O, Henneke M, Brockmann K, Gartner J, Elpeleg O, et al. West syndrome, microcephaly, grey matter heterotopia and hypoplasia of corpus callosum due to a novel ARFGEF2 mutation. J Med Genet. 2013 Nov;50(11):772-5.
46. Tanyalcin I, Verhelst H, Halley DJ, Vanderhasselt T, Villard L, Goizet C, et al. Elaborating the phenotypic spectrum associated with mutations in ARFGEF2: case study and literature review. Eur J Paediatr Neurol. 2013 Nov;17(6):666-70.
47. Yilmaz S, Gokben S, Serdaroglu G, Eraslan C, Mancini GM, Tekin H, et al. The expanding phenotypic spectrum of ARFGEF2 gene mutation: Cardiomyopathy and movement disorder. Brain Dev. 2015 Jun 27.
48. Dobyns WB, Mirzaa G, Christian SL, Petras K, Roseberry J, Clark GD, et al. Consistent chromosome abnormalities identify novel polymicrogyria loci in 1p36.3, 2p16.1-p23.1, 4q21.21-q22.1, 6q26-q27, and 21q2. Am J Med Genet A. 2008 Jul 1;146A(13):1637-54.
49. Peddibhotla S, Nagamani SC, Erez A, Hunter JV, Holder JL, Jr., Carlin ME, et al. Delineation of candidate genes responsible for structural brain abnormalities in patients with terminal deletions of chromosome 6q27. Eur J Hum Genet. 2015 Jan;23(1):54-60.
50. Bahi-Buisson N, Souville I, Fourniol FJ, Toussaint A, Moores CA, Houdusse A, et al. New insights into genotype-phenotype correlations for the doublecortin-related lissencephaly spectrum. Brain. 2013 Jan;136(Pt 1):223-44.
51. Pilz DT, Kuc J, Matsumoto N, Bodurtha J, Bernadi B, Tassinari CA, et al. Subcortical band heterotopia in rare affected males can be caused by missense mutations in DCX (XLIS) or LIS1. Hum Mol Genet. 1999 Sep;8(9):1757-60.

52. Sicca F, Kelemen A, Genton P, Das S, Mei D, Moro F, et al. Mosaic mutations of the LIS1 gene cause subcortical band heterotopia. Neurology. 2003 Oct 28;61(8):1042-6.
53. Barkovich AJ. Morphologic characteristics of subcortical heterotopia: MR imaging study. AJNR Am J Neuroradiol. 2000 Feb;21(2):290-5.
54. Novegno F, Battaglia D, Chieffo D, Frassanito P, Leoni C, Tamburrini G, et al. Giant subcortical heterotopia involving the temporo-parieto-occipital region: a challenging cause of drug-resistant epilepsy. Epilepsy Res. [Case Reports]. 2009 Nov;87(1):88-94.
55. Poduri A, Golja A, Riviello JJ, Jr., Bourgeois BF, Duffy FH, Takeoka M. A distinct asymmetrical pattern of cortical malformation: large unilateral malformation of cortical development with contralateral periventricular nodular heterotopia in three pediatric cases. Epilepsia. [Case Reports Research Support, Non-U.S. Gov't]. 2005 Aug;46(8):1317-21.
56. Barkovich AJ. Malformations of cortical development. In: Kuzniecky RI, G.D. J, editors. Magnetic Resonance of Epilepsy. Burlington: Elsevier; 2005. p. 221-48.
57. Preul MC, Leblanc R, Cendes F, Dubeau F, Reutens D, Spreafico R, et al. Function and organization in dysgenic cortex. Case report. J Neurosurg. [Case ReportsResearch Support, Non-U.S. Gov't]. 1997 Jul;87(1):113-21.
58. Tsuburaya R, Uematsu M, Kikuchi A, Hino-Fukuyo N, Kunishima S, Kato M, et al. Unusual ribbon-like periventricular heterotopia with congenital cataracts in a Japanese girl. Am J Med Genet A. [Case Reports]. 2012 Mar;158A(3):674-7.
59. Cappello S, Gray MJ, Badouel C, Lange S, Einsiedler M, Srour M, et al. Mutations in genes encoding the cadherin receptor-ligand pair DCHS1 and FAT4 disrupt cerebral cortical development. Nat Genet. 2013 Nov;45(11):1300-8.
60. Mansour S, Swinkels M, Terhal PA, Wilson LC, Rich P, Van Maldergem L, et al. Van Maldergem syndrome: further characterisation and evidence for neuronal migration abnormalities and autosomal recessive inheritance. Eur J Hum Genet. 2012 Oct;20(10):1024-31.
61. Alcantara D, O'Driscoll M. Congenital microcephaly. Am J Med Genet C Semin Med Genet. 2014 Jun;166C(2):124-39.
62. Woods CG, Bond J, Enard W. Autosomal recessive primary microcephaly (MCPH): a review of clinical, molecular, and evolutionary findings. Am J Hum Genet. 2005 May;76(5):717-28.
63. Ashwal S, Michelson D, Plawner L, Dobyns WB, Quality Standards Subcommittee of the American Academy of N, the Practice Committee of the Child Neurology S. Practice parameter: Evaluation of the child with microcephaly (an evidence-based review): report of the Quality Standards Subcommittee of the American Academy of Neurology and the Practice Committee of the Child Neurology Society. Neurology. 2009 Sep 15;73(11):887-97.
64. Germanaud D, Lefevre J, Fischer C, Bintner M, Curie A, des Portes V, et al. Simplified gyral pattern in severe developmental microcephalies? New insights from allometric modeling for spatial and spectral analysis of gyrification. Neuroimage. 2014 Nov 15;102 Pt 2:317-31.
65. Woods CG, Parker A. Investigating microcephaly. Arch Dis Child. 2013 Sep;98(9):707-13.

Table 1. Genetic etiology associated with periventricular heterotopia

disorder	OMIM	locus/ gene	inheritance	PNH	imaging features	additional features	references
X-linked dominant periventricular heterotopia	#300049	FLNA	XLD	common	confluent or scattered PNH, mega cisterna magna, rarely CTXD	seizures, LD, cardiovascular anomalies, GI abnormalities, facial dysmorphism, severe/lethal phenotype in males	(31, 39)
Periventricular nodular heterotopia (PVNH6)	#615544	del 6q27/ ERMARD (1 case)	AD	common	PNH predominant in temporal horns, corpus callosum abnormalities, colpocephaly, polymicrogyria, under-rotated or hypoplastic hippocampi, cerebellar/vermis hypoplasia, mega cisterna magna, hydrocephalus	seizures, DD, ataxic or clumsy gait, joint laxity, facial dysmorphism	(35, 49)
Autosomal recessive periventricular heterotopia with microcephaly	#608097	ARFGEF2	AR	common	PNH, thin corpus callosum, cerebral atrophy, T2 image hyperintensity of putamen	seizures, spastic quadriplegia, severe ID, progressive microcephaly, movement disorder, obstructive cardiomyopathy	(32, 33, 46)
Pettigrew syndrome	#304340	AP1S2	XLR	rare	scattered PNH in frontal horns and mid-body, vermis hypoplasia, enlarged posterior fossa, DWM, hydrocephalus, iron and calcium depositions in basal ganglia	iron depositions in basal ganglia, ID, athetoid movements, facial dysmorphism, self-abusive behavior	(67)
Donnai-Barrow syndrome	#222448	LRP2	AR	UK	PNH, partially empty sella turcica, hypoplastic or absent corpus callosum, abnormally placed central sulcus, small pons, small optic nerves and chiasm, ocular colobomas	congenital diaphragmatic hernia, proteinuria, omphalocele, sensorineural deafness, myopia, skeletal abnormalities, DD, facial dysmorphism	(68)
Van Maldergem syndrome	#601390	DCHS1, FAT4	AR	common	laminar PH posterior predominant, overlying simplified cortical gyri	ID, craniofacial, auditory, renal, skeletal and limb malformations	(59)
KBG syndrome	#148050	del 16q24.3 (incl ANKRD11)	CHR/ AD	sporadic	PNH, corpus callosum abnormalities, posterior fossa cyst	mild ID, facial dysmorphism, macrodontia, short stature.	(69, 70), this thesis

Table 1. Genetic etiology associated with periventricular heterotopia (continued)

disorder	OMIM	locus/ gene	inheritance	PNH	imaging features	additional features	references
Pyruvate dehydrogenase E1-alpha deficiency	#312170	PDHA1	XLD	UK	PNH, agenesis corpus callosum, cerebral atrophy, enlarged ventricles	seizures, movement disorder, DD, facial dysmorphism, lactic acidosis	(71)
Jacobsen syndrome	#147791	del 11q24		rare	PNH, cortical dysplasia, white matter abnormalities, cerebellar hypoplasia, agenesis corpus callosum	variable ID, microcephaly, facial dysmorphism, growth retardation, thrombocytopenia, cardiac defects, limb reduction (rare)	(72), personal observation
Chromosome 1p36 deletion syndrome	#607872	del 1p36	CHR	sporadic	PNH, enlarged ventricles, cerebral atrophy, polymicrogyria, pachygyria, white matter abnormalities, corpus callosum abnormalities	ID, variable congenital abnormalities, facial dysmorphism, seizures, cardiomyopathy, hearing loss	(73, 74)
Smith-Magenis syndrome	#182290	del 17p11.2	CHR	4 cases	PNH, enlarged ventricles, vermis hypoplasia, mega cisterna magna	ID, behavorial problems, facial dysmorphism, congenital abnormalities	(75, 76), personal observation
Williams-Beuren syndrome	#194050	del 7q11.23	CHR	rare	PNH, Chiari I malformations	ID, facial dysmorphism, variable congenital abnormalities	(77, 78)
22q11 deletion syndrome	#611867	del 22q11	CHR	rare	PNH, polymicrogyria	variable ID, congenital abnormalities, facial dysmorphism	(78, 79)
AR ID with microcephaly and PNH	NA	INTS8	AR	common	PNH, microcephaly, cerebellar hypoplasia	severe ID, spasticity, cortical blindness	this thesis
West syndrome with ACC, PNH, and PMG	*300382	ARX	XLR	rare	PNH, agenesis corpus callosum, polymicrogyria	ID, seizures, cleft lip/palate	(80), this thesis
Autosomal dominant mental retardation-7	#614104	del 21q22.1–q22.2	CHR	rare	single PNH, mild cortical dysplasia, microcephaly	ID, no speech, behavorial problems, facial dysmorphism, epilepsy	(81), this thesis

Table 1. Genetic etiology associated with periventricular heterotopia (continued)

disorder	OMIM	locus/ gene	inheritance	PNH	imaging features	additional features	references
Malonyl-CoA decarboxylase deficiency	#248360	MLYCD	AR	rare	PNH, pachygyria, cerebral atropy, white matter abnormalities	DD, seizures, hypotonia, diarrhea, vomiting, metabolic acidosis, hypoglycemia, ketosis, abnormal urinary compounds, lactic acidemia, hypertrophic cardiomyopathy	(82)
Periventricular heterotopia associated with 5p anomalies	%608098	5p	CHR	UK	periventricular and subcortical nodular heterotopia, hippocampal sclerosis	DD, seizures, club feet, congenital heart defects	(83-85)
Ventriculomegaly with cystic kidney disease	#219730	CRB2	AR	UK	PNH, hydrocephalus	nephrotic syndrome, cystic kidney disease (prenatal onset), increased alpha-fetoprotein in amniotic fluid	(86), personal observation
Miller-Dieker syndrome with PNH	NA	t(12;17) (q24.31;p13.3)	CHR	1 case	PNH, lissencephaly, Hypoplasia of corpus callosum, altered white matter myelination	facial dysmorphisms consistent with Miller–Dieker syndrome, passed away 22m.	(87)
Renpenning syndrome	#309500	PQBP1	XLR	1 case	PNH	dysmorphism, ID, hearing loss	(88)
Noonan-like syndrome with loose anagen hair	#607721	SHOC2	AD	1 case	PNH, thick corpus callosum, small posterior fossa	Noonan syndrome	(89)
Mismatch repair cancer syndrome	#276300	PMS2	AR	1 case	PNH, ACC, IHEM	B-cell NHL, carcinoma of the parotis	(90)
Xp22.3 contiguous gene deletion syndrome	NA	del Xp22.3	CHR	1 case	PNH, DWM	ID, ichthyosis	(91)
Generalized epilepsy with febrile seizures plus, type 2	#604403	SCN1A	AD	2 cases	PNH, FCD type IIA, cerebellar atrophy	seizures, ID	(92)

Table 1. Genetic etiology associated with periventricular heterotopia (continued)

disorder	OMIM	locus/ gene	inheritance	PNH	imaging features	additional features	references
PNH with overlying PMG	NA	Xq26.1-26.2	CHR	1 case	PNH, PMG, microcephaly	mild ID, distinctive facial features, short stature, cardiac disorder	(93)
Distal chromosome 5q14.3 deletion syndrome	#612881	del 5q14.3-q15	CHR	3 cases	PNH, polymicrogyria	epilepsy, mental retardation	(94)
Fragile X syndrome	#300624	FMR1	XLR	2 cases	PNH, underrotated hippocampi	ID, ADD, macroorchidism, dysmorphism, cleft lip in 1.	(95)
Rett syndrome, congenital variant	#613454	dup 14q12 (incl FOXG1)	CHR	1 case	1 PNH	ID, epilepsy	(96)
Koolen- De Vries syndrome	#610443	del 17q21.31 (incl. KANSL1)	CHR	3 cases	PNH	ID, dysmorphism	(97, 98)
Baraitser-Winter cerebrofrontofacial syndrome	#243310	ACTB/ ACTG1	AD	rare	PNH, subcortical band heterotopia, pachygyria	ID, facial dysmorphism, ptosis, contractures, eye coloboma, hearing loss	(99, 100)
TARP syndrome		RBM10	XLR	UK	PNH, hypoplastic CC dysplastic caudate + hippocampi, cavum septum et vergae, megacisterna magna	Multiple congenital anomalies, childhood demise, facial dysmorphism	(101, 102)

Abbreviations: AD= autosomal dominant, AR= autosomal recessive, CC= corpus callosum CHR= chromosomal, CTXD= cortical dysplasia, DD= developmental delay, DWM= Dandy-Walker malformation, ID= intellectual disability, LD= learning difficulties, PH= periventricular heterotopia, PNH= periventricular nodular heterotopia, UK= unknown, XLR= X-linked recessive

Table 2. Genetic etiology associated with subcortical band heterotopia (SBH)

disorder	OMIM	locus/ gene	inheritance	PNH	imaging features	additional features	references
X-linked lissencephaly 1	#300067	DCX	XLD	common	SBH in females, lissencephaly in males	ID, seizures	(103, 104)
Lissencephaly 1	#607432	LIS1	AD	sporadic	lissencephaly, SBH with milder/mosaic mutations	ID, seizures	(51)
Lissencephaly 3	#611603	TUBA1A	AD	AD	SBH, agyria, pachygyria, polymicrogyria, simplified gyral pattern, corpus callosum abnormalities, brainstem and cerebellum abnormalities, abnormal basal ganglia	ID, seizures	(18, 105)
Lissencephaly 5	#615191	LAMB1	AR	UK	SBH, cobblestone lissencephaly P>A, white matter abnormalities, brainstem and cerebellum hypoplasia, posterior encephalocele	severe DD, seizures	(106)
Complex cortical dysplasia with other brain malformations 3	#615411	KIF2A	AD	UK	SBH, agyria, pachygyria, thin corpus callosum, dysmorphic basal ganglia, microcephaly	severe DD, seizures,	(107)
Complex cortical dysplasia with other brain malformations 4	#615412	TUBG1	AD	UK	posterior SBH, posterior pachygyria, corpus callosum abnormalities	ID, seizures, cataract, spastic tetraplegia	(107)
Primary microcephaly 2, autosomal recessive, with or without cortical malformations	#604317	WDR62	AR	rare	SBH, pachygyria, polymicrogyria, microcephaly, corpus callosum abnormalities	ID, seizures	(21)
Baraitser-Winter cerebrofrontofacial syndrome	#243310	ACTB, ACTG1	AD	rare	pachygyria, PNH, SBH	ID, facial dysmorphism, ptosis, contractures, hearing loss	(99)
STX7- subcortical band heterotopia	NA	STX7	AD	1 family	SBH		(108)
Familial focal epilepsy with variable foci	#604364	DEPDC5	AD	1 case	focal SBH	seizures	(109)

Abbreviations: AD= autosomal dominant, AR= autosomal recessive, ID= intellectual disability, DD= developmental delay, P>A = posterior predominant, PNH= periventricular nodular heterotopia, SBH= subcortical band heterotopia, UK= unknown, XLD= X-linked dominant

Table 3. Genetic etiology associated with other subcortical heterotopia (SH)

disorder	OMIM	locus/ gene	inheritance	PNH	imaging features	additional features	references
Deletion 15q11	NA	del 15q11	CHR	1 case	bilateral subcortical perisylvian nodules, abnormal claustrum, polymicrogyria	arthrogryposis, intestinal atresia, ASD, PDA, dysmorphism	(110)
Mismatch repair cancer syndrome	#276300	MLH1	AR	1 case	unilateral SH, ACC, IHEM and intracerebral cysts	glioblastoma, T-cell lymphoma	(90)
BRCA1- neuronal migration defect	NA	BRCA1	AD?	2 cases	curvilinear SH	epilepsy	(111, 112)
Cortical dysplasia, complex, with other brain malformations 6	#615771	TUBB	AD?	2 cases	solid SH in optic radiation tract, abnormal corpus callosum, cortical dysplasia, cerebellar dysplasia, microcephaly	ID, motor delay	(113), this thesis
Lissencephaly-6 with microcephaly	#616212	KATNB1	AR	2 cases	solid SH in optic radiation tract, microcephaly	ID, seizures	(114)
Chudley-McCullough syndrome	#604213	GPSM2	AR	common	ribbon-like subcortical gray matter heterotopia along the cingulate gyri and in temporal lobes, cysts, dypslastic cerebellum, agenesis corpus callosum	mild ID, seizures, hearing loss	(115, 116)
Ribbon-like subcortical heterotopia	NA	EML1	AR	common	ribbon-like with SH, hydrocephalus, megalencephaly, agenesis corpus callosum	ID, seizures, short stature	(117), this thesis

Abbreviations: ACC= agenesis corpus callosum, AD= autosomal dominant, AR= autosomal recessive, ASD= atrial septal defect, CHR= chromosomal, ID= intellectual disability, IHEM= interhemispheric cysts, NA= not applicable, PDA= patent ductus arteriosus, SH= subcortical heterotopia.

Table 4. Genes associated with microcephaly and MCD

disorder	OMIM	locus/ gene	inheritance	MIC	imaging features	additional features
X-linked lissencephaly with ambiguous genitalia	#300215	ARX	XLR	common	"thin" lissencephaly, agenesis of the corpus callosum	intractable epilepsy, poor temperature regulation, chronic diarrhea, underdeveloped genitalia
Lissencephaly 1	#607432	LIS1	AD	postnatally in 40%	lissencephaly, SBH with milder/mosaic mutations	ID, refractory seizures, spasticity, early demise
Lissencephaly 3	#611603	TUBA1A	AD	common	SBH, agyria, pachygyria, polymicrogyria, simplified gyral pattern, corpus callosum abnormalities, brainstem and cerebellum abnormalities, abnormal basal ganglia	ID, seizures, spasticity
Lissencephaly 4	#614019	NDE1	AR	common	microlissencephaly	profound ID
Lissencephaly 6 with microcephaly	#616212	KATNB1	AR	2 cases	solid SH in optic radiation tract, microcephaly	ID, seizures
Lissencephaly 7 with cerebellar hypoplasia	#616342	CDK5	AR	1 family	extreme lissencephaly with complete agyria, cerebellar hypoplasia, and agenesis of the corpus callosum	lethal, contractures, intractable seizures, absent reflexes
Cortical dysplasia, complex, with other brain malformations 1	#614039	TUBB3	AD	in some	polymicrogyria, gyral disorganization, fusion of the basal ganglia, thin corpus callosum, hypoplastic brainstem, and dysplastic cerebellar vermis	mild to severe ID, spasticity, seizures
Cortical dysplasia, complex, with other brain malformations 2	#615282	KIF5C	AD	2 families	polymicrogyria, thin corpus callosum	severe ID, seizures, arthrogryposis, automutilation
Complex cortical dysplasia with other brain malformations 3	#615411	KIF2A	AD	2/2 cases	SBH, agyria, pachygyria, thin corpus callosum, dysmorphic basal ganglia	severe DD, seizures
Complex cortical dysplasia with other brain malformations 4	#615412	TUBG1	AD	2/3 cases	posterior SBH, posterior pachygyria, corpus callosum abnormalities	ID, seizures, cataract, spastic tetraplegia

Table 4. Genes associated with microcephaly and MCD (continued)

disorder	OMIM	locus/ gene	inheritance	MIC	imaging features	additional features
Cortical dysplasia, complex, with other brain malformations 6	#615771	TUBB	AD	common	solid SH in optic radiation tract, abnormal corpus callosum, cortical dysplasia, cerebellar dysplasia	ID, motor delay
Polymicrogyria, symmetric or asymmetric	#610031	TUBB2B	AD	common	polymicrogyria, microlissencephaly, corpus callosum abnormalities, brainstem and cerebellum abnormalities, abnormal basal ganglia	ID, seizures
Primary microcephaly 2, autosomal recessive, with or without cortical malformations	#604317	WDR62	AR	common	SBH, pachygyria, polymicrogyria, microcephaly, corpus callosum abnormalities	ID, seizures
Baraitser-Winter cerebrofrontofacial syndrome	#243310	ACTB, ACTG1	AD	in ~ 50%, postnatal	pachygyria, PNH, SBH	ID, facial dysmorphism, ptosis, contractures, hearing loss
STX7- subcortical band heterotopia	NA	STX7	AD	1 case	SBH	unknown
Autosomal recessive periventricular heterotopia with microcephaly	#608097	ARFGEF2	AR	common	PNH, thin corpus callosum, cerebral atrophy, T2 image hyperintensity of putamen	seizures, spastic quadriplegia, severe ID, movement disorder, cardiomyopathy
Warburg Micro syndrome 1	#600118	RAB3GAP1	AR	common	polymicrogyria	ocular and neurodevelopmental defects and hypothalamic hypogenitalism
Warburg Micro syndrome 2	614225	RAB3GAP2	AR	common	polymicrogyria	ID, cataracts, hypogonadism, and short stature

Table 4. Genes associated with microcephaly and MCD (continued)

disorder	OMIM	locus/ gene	inheritance	MIC	imaging features	additional features
Warburg Micro syndrome 3	#614222	RAB18	AR	common	polymicrogyria, atrophy, delayed myelinization, hypoplasia of the cerebellar vermis and corpus callosum, mild ventriculomegaly	microphthalmia, microcornea, spastic quadriplegia
Warburg Micro syndrome 4	#615663	TBC1D20	AR	common, postnatal	polymicrogyria, corpus callosum hypogenesis, widened lateral ventricles, and megacisterna magna due to cerebellar vermis hypoplasia	profound ID, spasticity, congenital cataracts, microphthalmia, microcornea, micropenis, cryptorchidism
Primary microcephaly 5	#608716	APSM	AR	common	simplified gyral pattern, enlarged ventricles, partial agenesis of the corpus callosum, rarely focal cortical dysplasia or polymicrogyria	ID, short stature, mild seizures
Primary microcephaly 6	#608393	CENPJ	AR	unknown	simplified gyral pattern, solid SUBH in the peritrigonal optic pathway	ID, short stature
AR ID with microcephaly and PNH	NA	INTS8	AR	common	PNH, microcephaly, cerebellar hypoplasia	severe ID, spasticity, cortical blindness
Immunodeficiency 26	#615966	PRKDC	AR	1 case	simplified gyral pattern, mild frontal pachygyria, small hippocampi, hypomyelinated white matter, thin corpus callosum, cerebellar vermis hypoplasia	Immunodeficiency, DD, hearing loss, visual impairment
Band-like calcification with simplified gyration and polymicrogyria	#251290	OCLN	AR	common	polymicrogyria, calcifications	seizures, ID
Polymicrogyria with seizures	#614833	RTTN	AR	common	polymicrogyria, pachygyria	ID, seizures, spasticity, microcephalic primordial dwarfism
Goldberg-Shprintzen syndrome	#609460	KIAA1279	AR	common	polymicrogyria, partial agenesis of the corpus callosum	ID, M. Hirschsprung, dysmorphism

Table 4. Genes associated with microcephaly and MCD (continued)

disorder	OMIM	locus/ gene	inheritance	MIC	imaging features	additional features
Muscular dystrophy-dystroglycanopathy with brain and eye anomalies (type A)/ Walker Warburg syndrome/ muscle-eye-brain disease	#236670	POMT1 and 13 other genes		micro- or macrocephaly	cobblestone (type II) lissencephaly, cerebellar malformations, hydrocephalus, encephalocele	profound ID, retinal abnormalities, muscular dystrophy, cleft lip/palate, congenital contractures, microphthalmia
Autosomal recessive cutis laxa type IIA	#219200	ATP6V0A2	AR	in ~ 50%	cobblestone-like malformation predominantly in the posterior frontal, perisylvian, and parietal regions, Dandy-Walker malformation	cutis laxa, abnormal growth, developmental delay, skeletal abnormalities

Abbreviations: DD= developmental delay, ID= intellectual disability, PNH= periventricular nodular heterotopia, SBH= subcortical band heterotopia, SH= subcortical heterotopia

Chapter 2

Defining imaging characteristics

Chapter 2.1

Subcortical heterotopia: clinical and imaging findings of 107 patients and a new classification

Renske Oegema, Grazia M.S. Mancini, A. James Barkovich, Renzo Guerrini, William B. Dobyns

Manuscript in preparation

ABSTRACT

Subcortical heterotopia (SUBH) represent a rare and heterogeneous brain malformation classified as a malformation of cortical development. From four large databases, we collected imaging and clinical data of 107 patients with subcortical heterotopia. This extensive survey led to the first comprehensive classification of these distinctive malformations. Curvilinear SUBH formed the largest group (n=66), followed by deeply infolded SUBH (n=19). We also describe several rare forms including solid SUBH in the peritrigonal optic pathway (n=5), brain-in-brain malformation (N=5), and ribbon-like SUBH (n=2). The large majority (84%) was scanned during childhood, and more than half (59%) before age 4 years. Although most patients had early developmental delay, learning difficulties, intellectual disability and/or spasticity, 19% had normal motor and cognitive development. Epilepsy occurred in 69%, the age of the onset ranging from the newborn period up to 25 years of age. For the majority, the etiology is unknown but its sporadic occurrence and often asymmetric appearance of the curvilinear SUBH suggests *de novo* germline or somatic mutations, or a prenatal disruptive event. Indeed several patients had a history of twinning. Several of the rare, bilateral forms are associated with mutations in microtubule- and centrosome-associated genes (*EML1*, *TUBB*, *KATNB1, CENPJ*, *GPSM2*), revealing a possible overlapping pathomechanism to primary microcephaly and other MCD. In conclusion, this study provides novel insights into the broad clinical and imaging spectrum of this malformation.

INTRODUCTION

Malformations of cortical development (MCD) comprise a large and heterogeneous group of brain malformations that result from defects in the formation of the human cortex. This process includes neurogenesis, neuronal migration, and post-migrational development.[1] While their prevalence is unknown, they account for 3% of intellectual disability, 25% of pediatric focal epilepsy, 5-15% of adult epilepsy, 20-40% of therapy-resistant epilepsy, and 42% of children undergoing epilepsy surgery.[2-6] Therefore, MCD collectively place a substantial burden on health care and society.

The increasing availability and resolution of magnetic resonance imaging (MRI) technology over the past 30 years has led to an immense change in our appreciation of MCD from fewer than 10 to currently more than 200 different types.[1,7-9] Several of these are classified as gray matter heterotopia, which represent clusters of neurons derived from neurogenesis in the ventricular or subventricular zone that failed to locate to their normal position in the cortex. The most commonly encountered heterotopia are those found as nodules along the walls of the lateral ventricles (periventricular nodular heterotopia). In contrast, the more rarely identified subcortical heterotopia (SUBH) are located between the cortex and lateral ventricles. Although, according to previous reports, SUBH are heterogeneous regarding nomenclature and imaging patterns, they frequently show extensive and asymmetric involvement of the cerebral hemispheres.[10-19] A distinct group is formed by the subcortical band heterotopia, which are classified within the lissencephaly spectrum.[1]

While analyzing brains scans from individuals with MCD, we recognized several novel SUBH with predominant subcortical localization, suggesting far more diversity of SUBH than had been previously recognized. This led us to systematically search our four large MCD databases containing records on more than 10,000 subjects (based in Chicago/Seattle, Rotterdam, Florence, and San Francisco) for subjects with SUBH. We selected 107 subjects with MCD and a prominent subcortical component, grouped them based on shared imaging characteristics, and analyzed the neuroimaging and clinical features for each subtype.

From this extensive survey, we reconceive subcortical heterotopia as a diverse class of MCD, and present the first comprehensive classification of these distinctive malformations. We hypothesize that SUBH result not only from defects in neuronal migration as previously proposed [1], but also from defects arising in the outer subventricular zone of the developing brain, the site of origin of a majority of neurons in the human brain.[20,21]

METHODS

Subjects

We identified subjects with SUBH by first searching our large Chicago/Seattle database of patients with developmental brain disorders (Lisdb, N>8000 subjects) using search terms for known SUBH as well as for potentially overlapping malformations including cortical dysplasia not otherwise specified, cortical infolding, schizencephaly especially rare familial forms, and transmantle malformations. After defining many different patterns of SUBH, we searched the other three MCD databases (Rotterdam, Florence, San Francisco) for patients with similar malformations. All patients were examined by, or referred for MRI review to one of the senior authors. Institutional review boards (IRBs) of Seattle Children's Hospital, The University of Chicago, University of Minnesota, Erasmus University Medical Center, University of Florence, and University of California – San Francisco approved our inclusion of these patients in research studies.
We selected for review all subjects with any SUBH, defined as grey matter visible in at least one region at a level where only white matter would normally be expected, for whom sufficient imaging was available to perform a detailed review (e.g. subjects were excluded when only a few images or only computed tomography scans were available). We excluded subjects who had PNH with no subcortical component or only a few small immediately adjacent subcortical heterotopia, and those with subcortical band heterotopia.

Clinical data

We searched available clinical notes and referral information and, whenever possible, re-contacted their referring physicians and parents or guardians. We sought a minimum data set comprising age at first MRI (as a surrogate for age at presentation); neurological outcome especially development and cognitive functioning; behavioral abnormalities such as autism; presence and age of onset of seizures; and head circumference (OFC). Data regarding pregnancy, other congenital anomalies, developmental milestones, type of seizures, relevant family history, and genetic testing were noted when available in our records.

Definitions

We use the terms subcortical malformation or subcortical heterotopia to include any MCD in which the most prominent and usually largest component is grey matter between the cortex and the lateral ventricles. In this context, this implies clusters of neurons located in an abnormal position within the subcortical white matter. Many SUBH contain cerebrospinal fluid (CSF) within a sulcus or cleft that clearly communicates with extra-axial CSF. Others contain short, discontinuous and often curvilinear spaces with the same signal intensity as CSF. When the connection to extra-axial or

intraventricular CSF is absent or not easily identified, we will describe these as "CSF-like" spaces. Several other descriptive terms are defined in Box 1.

Brain imaging

All patients selected for review underwent at least one T1-weighted or volumetric sequence and one T2-weighted sequence, and all underwent imaging in at least two planes. All available images were reviewed using a standardized approach by WBD and RO, with representative examples reviewed by all authors. We systematically assessed the location (bilateral symmetric or asymmetric, unilateral right or left; anterior-, central- or posterior-predominant, or diffuse; lobes affected), size including presence of mass effect on surrounding structures, morphology and general orientation (see Box 1), connection to the cortex and ventricular wall, and relationship to CSF spaces. Next, the imaging was scored for the presence and distribution of cortical malformations *per se*, PNH (only scored if clearly separated from SUBH), and any non-cortical brain malformations especially complete (ACC) and partial (pACC) agenesis of the corpus callosum; diffuse (CBLH) or vermis-predominant (CBVH) cerebellar hypoplasia, and Dandy Walker malformation (DWM).

Box 1. Definitions of descriptive terms used for brain imaging

Columnar	Vertical, narrow and generally cylindrical heterotopia that are usually transmantle
Curvilinear	Thick convoluted and generally longitudinal heterotopia with CSF-like spaces and blood vessels coursing within the gray matter mass
Fan-like	Generally radial heterotopia that appear narrow at or near the ventricular surface then fan out to become much wider at or near the cortex
Infolded	Inward folding of an area of cerebral cortex containing gyri and sulci thereby forming a longitudinal space connected to the extra-axial space and situated within the solid cerebral tissue
Laminar	Thin horizontal heterotopia, most of which are found in the deep white matter
Lobular	Continuous masses of gray matter with small round projections on the periphery of the main tissue mass
Longitudinal	Oriented from anterior to posterior, parallel to ventricular wall and cortex; also horizontal
Nodular	Solid and often round masses of gray matter without adjacent CSF-like spaces; may be single or multiple and if multiple, separate or contiguous
Radial	Oriented from ventricular wall outward to cortex, perpendicular to both; also vertical
Ribbon-like	Thin longitudinal heterotopia that undulate in and out along their course
Transmantle	Any subcortical malformation that extends from the ventricular wall to the cortex

Approach to classification

Our prior review of SUBH separated them into nodular (solid masses without CSF-like signal found in deep white matter), curvilinear (convoluted masses often containing CSF-like spaces and blood vessels within the central or peripheral white matter), and mixed heterotopia.[16] We have now added many additional patterns of subcortical-

predominant MCD, including several types with areas of infolded cortex that include linear sulci with direct and obvious communication with the extra-axial space. We therefore chose to continue using the pattern of CSF-containing spaces as our first criterion for separating SUBH into those with (1) abnormally deep infolded sulci enclosing linear CSF-containing spaces that have direct and obvious communication with the extra-axial space, (2) short often curvilinear areas with CSF-like signal and little or less obvious communication with the extra-axial space, and (3) no CSF signal at all (solid SUBH). We also considered using location, orientation (longitudinal or radial) and shape (Box 1), contiguity with the cortex, and associated CNS malformations, but these proved to be highly variable and indeterminate in many subjects. We used a combination of these features as secondary criteria.

In order to establish a comprehensive classification, we searched for publications of SUBH subtypes in PubMed. We limited our search to the English language literature, with publication dates between January 1985 and December 2015, and used key words including "subcortical heterotopia", "heterotopia AND brain", "brain-in-brain", and "aventriculy". We also searched our own libraries and references of relevant publications for additional papers.

Statistical analysis

Analysis was performed using IBM SPSS Statistics software v21. Frequencies and percentages were calculated to compare groups. To test for Normal distribution, the Shapiro-Wilk test was used. To compare characteristics between groups, the Chi square test and Fisher's exact test were used. The Kruskal–Wallis rank-sum was used to compare the age at presentation and age at seizure onset among groups. The non-parametric Mann-Whitney U test was used to compare seizure onset with the bilateral presence of the SUBH. When information on a given feature was not available, the patient was excluded for analysis of that feature.

RESULTS

From 188 patients identified by database searches, we identified 107 individuals with subcortical malformations and sufficient imaging available for classification, including 65 from Chicago/Seattle, 18 from Florence, 10 from Rotterdam, and 14 from San Francisco. Among 95 individuals with sex recorded (54 males, 41 females), a mild skewing of the sex ratio was observed: 57% to 43% (Table 1).

Table 1. Clinical characteristics of the 107 patients with subcortical heterotopia.

		All	Deeply infolded	Curvilinear	Solid	Bilateral complex
		n=107	n=19	n=66	n=8	n=14
Gender – male		54/95 (57%)	7/18 (39%)	34/57 (60%)	2/8 (25%)	11/12 (92%)
Age at first MRI	Child<1y	25/83 (30%)	4/17 (23%)	15/51 (29%)	0/5 (0%)	6/10 (60%)
	1y-4y	24/83 (29%)	8/17 (47%)	12/51 (24%)	2/5 (40%)	2/10 (20%)
	4y-18y	21/83 (25%)	3/17 (18%)	15/51 (29%)	1/5 (20%)	1/10 (10%)
	Adult	13/83 (16%)	2/17 (12%)	9/51 (18%)	2/5 (40%)	1/10 (10%)
Epilepsy		50/72 (69%)	9/15 (60%)	31/42 (74%)	3/6 (50%)	7/9 (78%)
Delayed development/ ID		55/68 (81%)	13/14 (93%)	28/38 (74%)	3/5 (60%)	10/10 (100%)
Abnormal behavior		17/44 (39%)	2/9 (22%)	10/28 (36%)	2/2 (100%)	3/5 (60%)
Head circumference	<p5	18/45 (40%)	5/10 (50%)	5/21 (24%)	4/6 (67%)	4/8 (50%)
	>p95	4/45 (9%)	0/10 (0%)	3/21 (14%)	0/6 (0%)	1/8 (13%)
Extra-CNS malformation		32/69 (46%)	7/12 (58%)	14/41 (34%)	3/5 (60%)	8/11 (72%)
Imaging	Bilateral SUBH	67/107 (63%)	17/19 (90%)	34/65 (52%)	4/8 (50%)	12/14 (86%)
	PNH	53/98 (54%)	6/16 (38%)	42/61 (69%)	2/8 (25%)	3/14 (21%)
Abnormalities of	Corpus callosum	65/102 (64%)	12/19 (63%)	40/65 (62%)	3/8 (36%)	10/12 (83%)
	Basal ganglia & thalami	42/104 (40%)	0/19 (0%)	29/64 (45%)	2/8 (25%)	11/12 (92%)
	Cerebellum/ posterior fossa	47/106 (44%)	5/19 (26%)	26/65 (40%)	4/8 (50%)	12/14 (86%)

Clinical features

Clinical records were available for most subjects. The data are summarized in Table 1, with complete data listed in Supplementary Table 1. Selected individual clinical summaries from each group are included in the Supplementary Clinical Reports section. For 83 individuals, age at first MRI was recorded and ranged from 2 days to 32 years. Unsurprisingly, age was significantly skewed towards infancy and early childhood (mean 6.4 years, median 2.0 years, $p= 1.5x10^{-10}$). A large majority of subjects were scanned during childhood (70/83, 84%), and more than half before age 4 years (49/83, 59%). Data regarding development were available for 68 individuals and almost one-fifth (13/68, 19%) had normal development. The remainder had developmental and neurologic dysfunction consisting of early developmental delay, intellectual disability, learning difficulties, and spasticity. The severity varied from isolated motor or language delay to profound global intellectual disability with no major developmental milestones reached. Behavioral abnormalities were noted for 17 of 44 (39%) subjects with data available. Most patients had epilepsy (50/72; 69%) with the age of first seizure ranging from the neonatal period to 25 years but significantly skewed towards towards infancy and early childhood (mean 7.3 years, median 4.5 years, $p<0.001$). We were able to document epilepsy surgery in only one patient. Almost half (32/69; 48%) had a major extra-CNS malformation. The range of malformations was wide, and the eyes, limbs and genitourinary system were most commonly affected.

Imaging patterns

Brain imaging studies on all 107 patients were reviewed and classified based first on the presence and type of CSF spaces, and secondarily on other features, including morphology, location and the presence of other brain malformations. We defined four major groups of heterotopia and 14 subgroups (Table 2), which are further described below. The most common pattern by far was curvilinear SUBH (66/107; 62%).
For only a few patients, we did not have sufficient imaging to assess all brain structures (Supplementary Table 1). We found that in addition to SUBH, most patients had non-cortical brain malformations that included abnormalities of the corpus callosum (65/102, 64%), basal ganglia, thalami or both (44/104, 40%), and cerebellum, posterior fossa or both (47/106, 44%). The prevalence of basal ganglia/thalami abnormalities, cerebellar/posterior fossa abnormalities, and PNH differed significantly among groups ($p= 2.591x10^{-7}$; $p= 0.004$; $p=0.004$, respectively). The group of all subjects with bilateral SUBH was significantly enriched for the presence of extra-CNS malformations ($p=0.01$), and also enriched, although non-significantly, for abnormal development ($p= 0.09$). Whether the SUBH were unilateral or bilateral did not influence the presence or age of onset of seizures.

Table 2. Proposed classification of subcortical heterotopia

1.	Deeply infolded subcortical heterotopia with longitudinal CSF spaces	
	a.	Deeply infolded SUBH – parieto-occipital subtype
	b.	Deeply infolded SUBH – parasagittal subtype
	c.	Deeply infolded SUBH – other subtypes
2.	Curvilinear SUBH with CSF-like spaces	
	a.	Curvilinear SUBH
	b.	Diffuse curvilinear SUBH with interhemispheric cysts and agenesis of the corpus callosum
3.	Solid subcortical heterotopia - no CSF-like signal	
	a.	Transmantle columnar SUBH
	b.	Nodular SUBH in region of peritrigonal optic pathway
	c.	Multinodular small SUBH, often anterior of frontal horns
4.	Subcortical heterotopia with bilateral complex patterns	
	a.	Aventriculy with SUBH
	b.	Brain-in-brain malformation
	c.	Transmantle columnar and fan-like SUBH with clefts
	d.	Ribbon-like SUBH (*EML1)*
	e.	Mesial parasagittal SUBH (Chudley-McCullough syndrome)
	f.	Complex chaotic SUBH

Groups

We observed no significant differences between groups regarding age at first MRI, age of seizure onset, development, behavioral abnormalities, presence of seizures, microcephaly or macrocephaly. Remarkably, all but one individual with normal development (13/14) had curvilinear SUBH (group 2a). Also, all subjects in group 4 with bilateral complex SUBH had developmental delay and ID and this group had the highest percentage of extra-CNS malformations (72%).

1. Deeply infolded subcortical heterotopia with longitudinal CSF spaces

This group is characterized by (1) extension of two opposing cortices separated by CSF into the deep white matter well beyond the usual cortical-white matter boundary but in clear continuity with the overlying cortex, (2) mild thickening (5-10 mm) and irregularity of all or most of the infolded cortex consistent with polymicrogyria, (3) and clear connection of CSF spaces with overlying sulci and extra-axial space. While the CSF spaces lined by dysplastic cortex resemble the clefts observed in schizencephaly [22], they have a branching pattern typical of sulci and do not communicate with the lateral ventricles. When the deeply infolded SUBH extend all the way down to the ependymal surface, the SUBH can be seen bulging into the ventricle, as opposed to closed-lip schizencephaly – where a dimple is seen at the ventricular surface.[23]

We observed **deeply infolded SUBH – parieto-occipital subtype** in 10 individuals with infolding patterns of similar morphology and variable, posterior predominant,

localization. The parietal and/or occipital regions were predominately affected, but the frontal and temporal lobe were sometimes involved as well (Fig. 1 LP97-007, LR12-324).

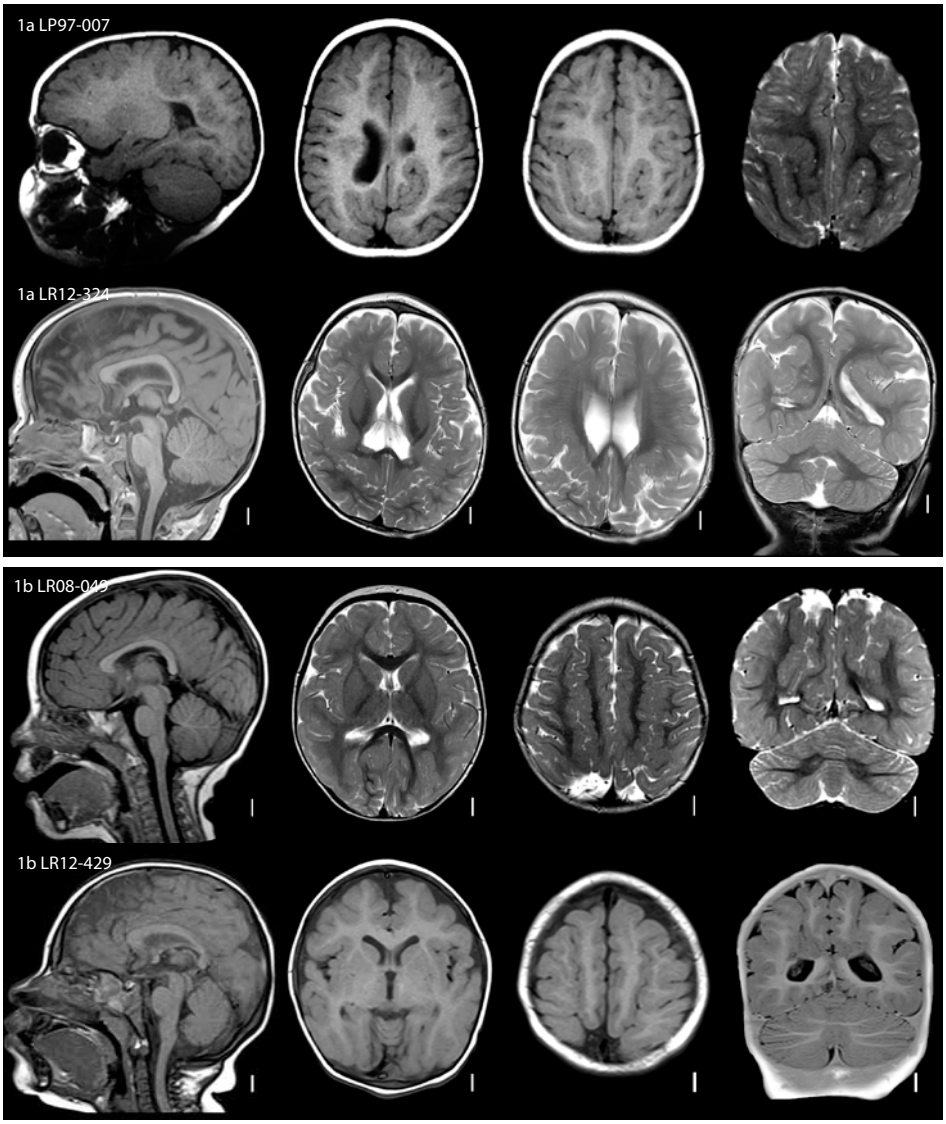

Figure 1. Representative MRI images from individuals from group 1; deeply infolded SUBH.
Each row depicts images from the same patient. First column: midline sagittal, second column: axial at the level of the basal ganglia (except LP97-007; axial), third column: axial, fourth column: coronal images (except LP97-007; axial). Deeply infolded SUBH was identified in LP97-007 and LR12-324 (parieto-occipital subtype), originating posteriorly in the perisylvian areas with an oblique orientation relative to the sagittal plane. Images from LR08-049 and LR12-429 (parasagittal subtype) show a highly similar pattern of bilateral parasagittal deep infolded SUBH touching the ependyma. Both individuals are microcephalic (OFC -3 SD and -5 SD, respectively). Other brain structures are relatively preserved.

The infolding always involves the mesial parietal and occipital cortex, and in several subjects a strictly mesial connection was observed. In its most complete form, the SUBH extends from the mesial parietal and occipital region behind the splenium of the corpus callosum, around the occipital horn and trigone of the lateral ventricles, and to the posterior perisylvian region. Other brain structures were preserved or only mildly affected in most patients. Thinning or partial agenesis of the corpus callosum occurred, but none had complete agenesis; all had normal deep grey nuclei except one patient with globular-shaped thalami; and five had mild cerebellar abnormalities. This was previously classified as unilateral or bilateral parasagittal parieto-occipital PMG [24], and was identified in 11/328 individuals with polymicrogyria.[25]

In **the parasagittal subtype**, a continuous band of deeply infolded SUBH that resembles polymicrogyric cortex is seen. It is located parallel to the mid-sagittal plane, extending from anterior-lateral to posterior medial and deeply into the white matter touching the ventricular walls (Fig. 1 LR08-049, LR12-429). The SUBH is bilateral and highly symmetric in appearance and is best recognized in axial and coronal planes. Although abnormalities of the corpus callosum were observed, none of the six patients had complete agenesis of the corpus callosum. Of note, all patients had normal deep grey nuclei and a normal cerebellum. We were able to identify only one previous mention of this subtype: a single image from one of our patients (LR01-283) was presented as bilateral superior parasaggittal PMG, and defined as unilateral or bilateral 'bands' of polymicrogyria lining abnormal lateral parasagittal sulci.[25] We collected clinical data on all six patients with this subtype. They all presented with early motor delay; four developed spasticity, and one had a normal neurological exam at 10 years. Three had intellectual disability, and two were cognitively normal. Seizures that began during puberty were seen in three patients. The other three, without seizures, had not yet reached puberty. For three individuals, OFC data were available and all had microcephaly ranging from -3 SD to -5 SD. Interestingly, four out of six had a feature (twinning or jejunal atresia) which has been previously associated with schizencephaly, suggesting the possibility of a similar pathogenesis.[26]

In the remaining three patients with deep infolding (**deeply infolded SUBH – other subtypes**), SUBH occurred in a different location, but all involved the frontal lobes.

2. Curvilinear SUBH were present in 61 patients, forming the largest group in our cohort. These malformations are usually large, occupying one or more lobes, and the CSF-like spaces may be prominent or subtle (Fig. 2). The overlying cortex is abnormally thin with shallow sulci and the SUBH always connects to the overlying cortex in at least one, but usually in multiple, locations. Sulci extending abnormally deep into the white matter are sometimes seen, although extensive cortical malformations are uncommon. They may resemble some deeply infolded SUBH, but curvilinear SUBH have a more

complex morphology making it difficult to define continuity of the CSF-like spaces with extra-axial spaces. The name curvilinear subcortical heterotopia was previously proposed by one of the authors [16] and we consider this the best descriptive term to describe this group. The morphology is variable – often even within the same individual – and besides the curvilinear spaces can contain areas with nodular, laminar and/or lobular appearance. Any lobe can be affected either unilaterally or bilaterally. We found an equal distribution of unilateral and bilateral examples (31 vs. 30), but even with bilateral curvilinear SUBH the brain appears asymmetrically affected. Evidence of pressure on surrounding structures is often apparent (e.g. compression of the adjacent lateral ventricle or contralateral hemisphere). The affected hemisphere is usually smaller than the unaffected one. Also, either or both hemispheres may cross the midline. Ipsilateral and/or contralateral PNH are seen in more than two-thirds (70%) of patients. Abnormal configuration or even partial obliteration of the ipsilateral ventricle and basal ganglia and abnormalities of the corpus callosum were also frequently observed (40% and 62%). We identified abnormalities of the cerebellum and/or posterior fossa in 36% of patients.

We identified five patients with a distinct subtype of **diffuse curvilinear SUBH combined with multiple interhemispheric cysts and agenesis of the corpus callosum** (Fig. 2, LR03-395). This pattern was reported in three individuals from a series of patients with callosal agenesis, and was designated as "callosal agenesis with cyst type 2c".[27] Another patient was reported to have mismatch-repair deficiency due to a biallelic *MLH1* mutation.[28] This suggests that this subtype represents a specific, recurrent pattern.

3. Solid subcortical heterotopia

Solid SUBH contain no CSF-like spaces. We reserve the term **transmantle columnar SUBH** for a small distinct band or wedge of gray matter perpendicular to the cortex that extends from the ependyma to the cortex (Fig. 3 LR08-415). These may be difficult to distinguish from closed lip schizencephaly, the primary distinction being the absence of a pia-ependymal cleft and dimple at the ventricular wall.[23] Also, transmantle columnar SUBH should not be confused with transmantle dysplasia (bottom-of-the-sulcus dysplasia) or sign associated with focal cortical dysplasia (FCD type IIb), which is a streak of abnormal signal intensity within the white matter.[23]

In five patients including two sisters, we encountered **solid nodular SUBH situated in the region of the peritrigonal optic pathway** posterior to the deep grey nuclei (bilateral in 4 of the 5) (Fig. 3 LR07-197, GM-R06). All had borderline to profound (-11 SD) microcephaly. We found previous mention of three microcephalic patients with similar SUBH, two of whom were sibling.[29,30]

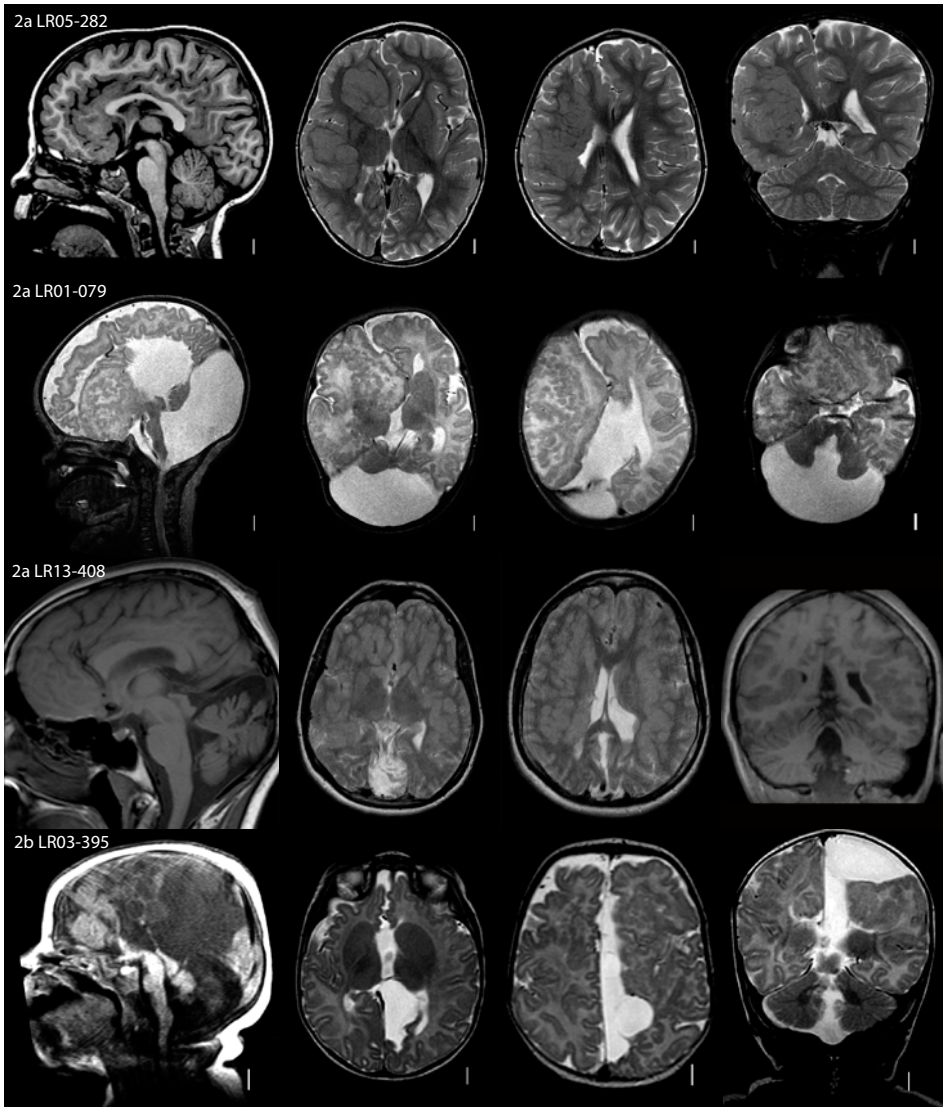

Figure 2. Representative MRI images from group 2; curvilinear SUBH.
Each row depicts images from the same patient. First column: midline sagittal, second column: axial at the level of the basal ganglia, third column: axial, fourth column: upper three coronal, lower two axial. Images from individual LR05-282 show extensive giant SUBH with curvilinear CSF-like spaces in the right hemisphere. The SUBH touches both the overlying cortex and the ependymal in several occasions. The left hemisphere crosses the midline. The right frontal horn and right caudate nucleus cannot be identified, instead a large heterotopic mass is seen. LR01-079: Curvilenar with subtle CSF-like spaces in the right hemisphere. The affected hemisphere is notably smaller, although there is a local mass effect, also the lateral ventricle and basal ganglia are not identified. Note ACC, brainstem hypoplasia and severe CBLH. LR13-408: extensive involvement of both hemispheres with both curvilinear SUBH connecting to the cortex and multiple nodular SUBH. LR03-395: bilateral asymmetric SUBH with IHEM. Note also ACC and hypoplastic pons and cerebellar vermis. CSF-like spaces are clearly identifiable in the third column.

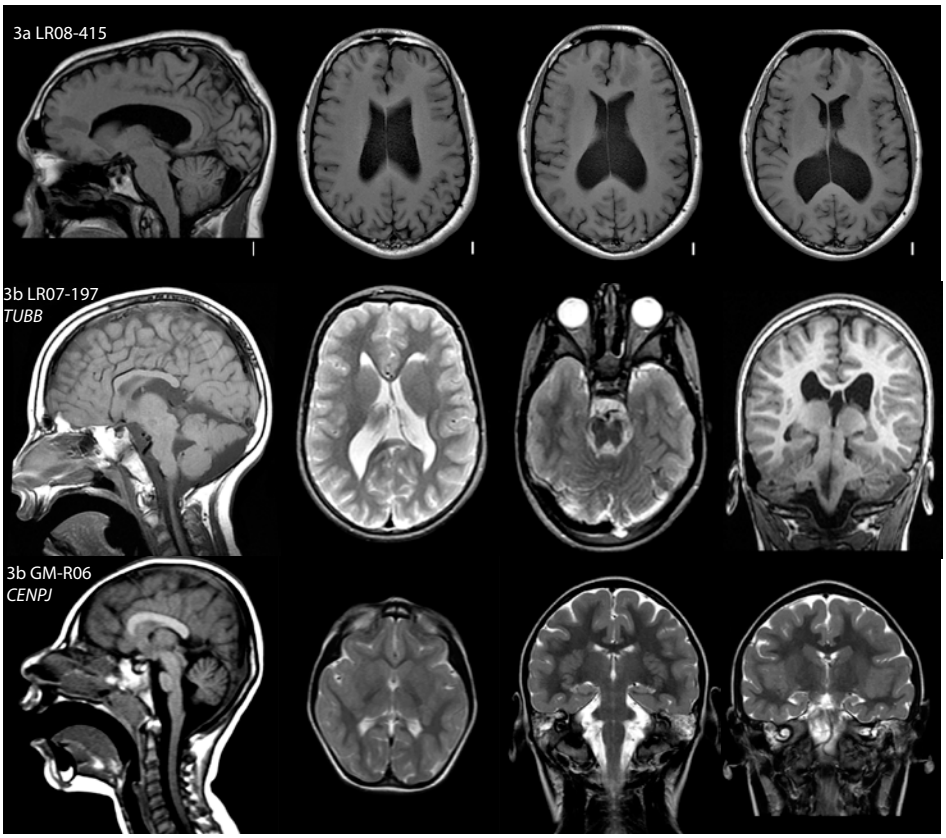

Figure 3. Representative MRI images from individuals from group 3; Solid SUBH.
Each row depicts images from the same patient. First column: midline sagittal, second column: axial at the level of the basal ganglia, third column: axial and coronal (GM-R06), fourth row: axial (LR08-415) and coronal images. LR08-415: Transmantle columnar SUBH in the left frontal lobe. The overlying cortex is dysplastic, the lateral ventricles are mildly enlarged. LR07-197 has bilateral, left larger than right, peritrigonal optic pathway SUBH (2nd and 4th column). The genu of the corpus callosum and brainstem are hypoplastic (1st column), the cerebellum is dysplastic (3rd column). This individual was found to have a de novo *TUBB* mutation c.860C>G (p.Pro287Arg). GM-R06 has bilateral peritrigonal optic pathway SUBH (2nd-4th column). She also has profound microcephaly (-11 SD). She is compound heterozygous for *CENPJ* mutations c.1805_1808del (p.Glu602fs) and c.289dupA (p.Thr97fs).

Figure 4 (opposite page). Representative MRI images from individuals from group 4; microventriculy with SUBH and brain-in-brain malformation.
Each row depicts images from the same patient. First column: midline sagittal, second column: axial at the level of the basal ganglia, third column: axial and coronal, fourth column: axial images of cerebellum (except LR00-237: coronal). All had absent or barely identifiable lateral ventricles (LV). The SUBH resemble disorganized sulci deeply infiltrating the white matter. LR00-237, LR05-320, and LR13-329 have high occipital encephalocele, LR05-320 and LR13-202 have turricephaly with high parietal interhemispheric cyst (1st column). Non-separated thalami are suspected in all and in addition, alobar holoprosencephaly in LR00-237 and middle interhemispheric fusion in LR99-240 (3rd column). The cerebellum is hypoplastic in all, and severe dysplastic in all but LR13-329 (4th column for all, except LR00-237, 2nd column).

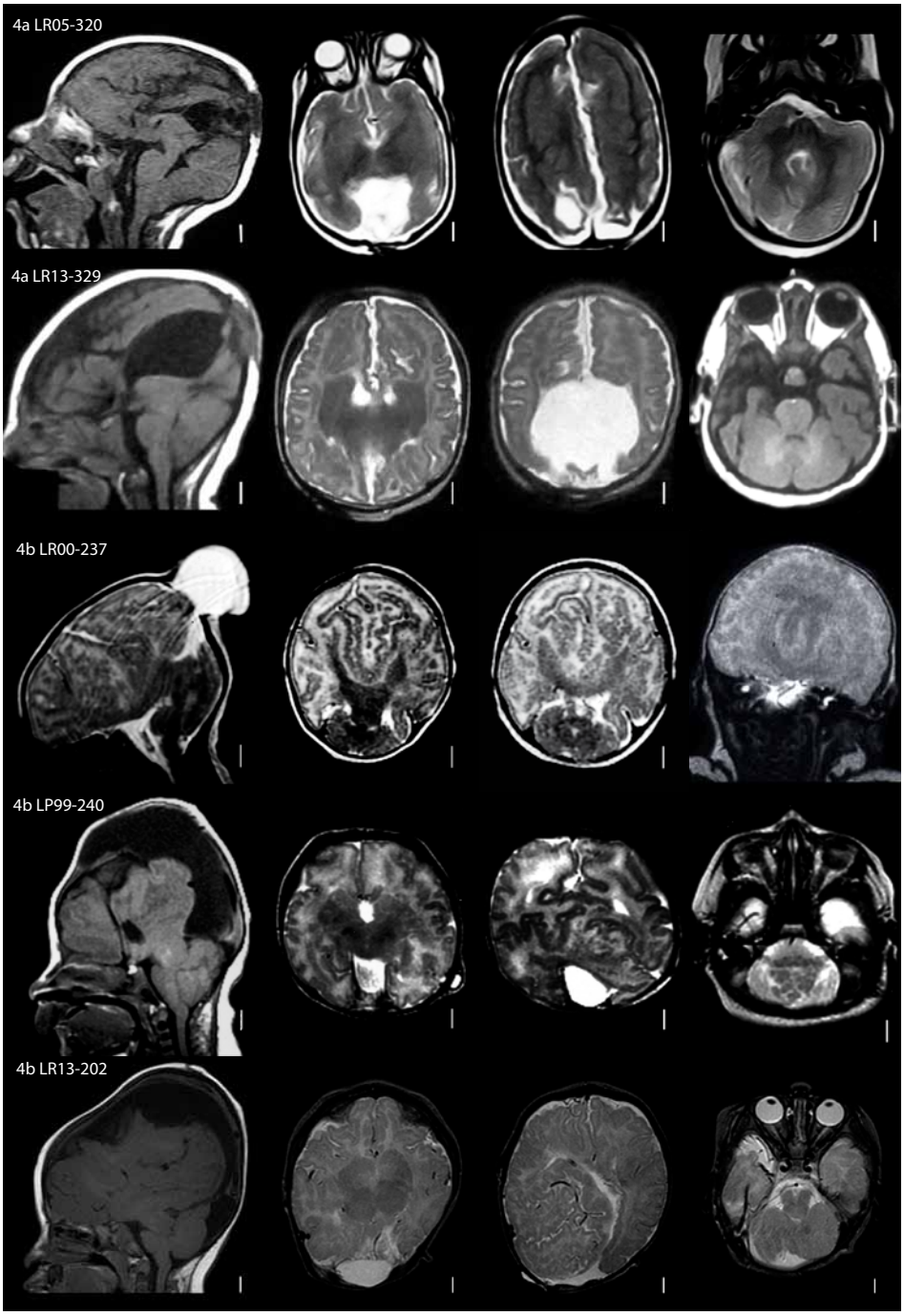

Figure 4. Representative MRI images from individuals from group 4; microventriculy with SUBH and brain-in-brain malformation.

Multinodular small SUBH anterior to the frontal horns can sometimes be identified in young babies, from birth until 2 months postnatally. These may represent residual neurons from the germinal zones, and are most likely a normal variant.

4. Subcortical heterotopia with bilateral complex patterns

The group **microventriculy with SUBH** is based on two patients with a distinctive complex brain malformation consisting of SUBH, absent or very small lateral ventricles, unseparated thalami, and encephalocele (Fig. 4 LR05-320, LR13-329). The SUBH consists of seemingly disorganized deeply infolded fissures lined with dysplastic cortex, combined with vessels, white matter, and CSF. Both patients also had cerebellar dysplasia. Absence of the ventricles (aventriculy) in combination with absent separation of midline structures was first described by Garfinkle in 1996.[31] Since then, only four additional patients have been reported.[32-35] SUBH were present in at least three of these patients.

The above group shows considerable overlap with the **brain-in-brain malformation**, originally defined as a midline mass of dysplastic cortex with holoprosencephalic features.[36] We classified four patients with a midline mass of grey and white matter signal intensity as brain-in-brain malformation. Two of these patients also had microventriculy and three had continuity of cerebral structures across the midline (the middle interhemispheric fusion subtype of holoprosencephaly, unseparated thalami and/or mesencephalosynapsis) (Fig. 4 LR00-237, LP99-240, LR13-202, LR15-229). Another key feature was an encephalocele or turricephaly with high parietal interhemispheric cysts. Also, CSF-like spaces and blood vessels may be present. We identified one patient who had SUBH and a midline mass with signal intensities suggesting a

Figure 5 (opposite page). Representative MRI images from individuals from group 4; Transmantle columnar and fan-like SUBH with clefts, ribbon-like SUBH, Chudley-McCullough syndrome and complex chaotic SUBH.

Each row depicts images from the same patient. First column: midline sagittal, second column: axial, third column: axial (except LR01-016a2, coronal), fourth column: axial images of cerebellum (LR03-112 and LR03-246), axial image T1-weighted (vs. T2-weighted in 3rd column, LP98-117), coronal images (LR01-016a2, LR13-260, LR11-273, LR11-450). LR01-016a2 has transmantle columnar and fan-like SUBH (right hemisphere) and bilateral clefts. LP98-117 and LR13-260 both show a bilateral single undulating ribbon-like SUBH throughout the white matter. The cortex is polymicrogyria-like. Both individuals are megalencephalic. The lateral ventricles are enlarged in LP98-117, LR13-260 received a VP-drain shortly after birth for treatment of hydrocephalus. A homozygous *EML1* mutation was identified in LR13-260. LR03-112 and LR03-246 have longitudinal SUBH in the parasagittal plane, on more upwards cuts the SUBH connects to the highly dysplastic mesial cortex (not shown). The cerebellum is dysplastic (4th column). Note also enlarged lateral ventricles and midline cyst in LR03-246 (2nd column). This pattern is associated with Chudley-McCullough syndrome. LR11-273 and LR11-450 show complex chaotic SUBH. Both show a mixed morphology of longitudinal undulating SUBH (especially in LR11-273) and smaller, more nodular shaped SUBH. Multiple CSF-like spaces can be identified. In LR11-450, lower cuts showed absence of SUBH (shown in 2nd column). The cortex is highly dysplastic in LR11-450, but relatively preserved in LR11-450.

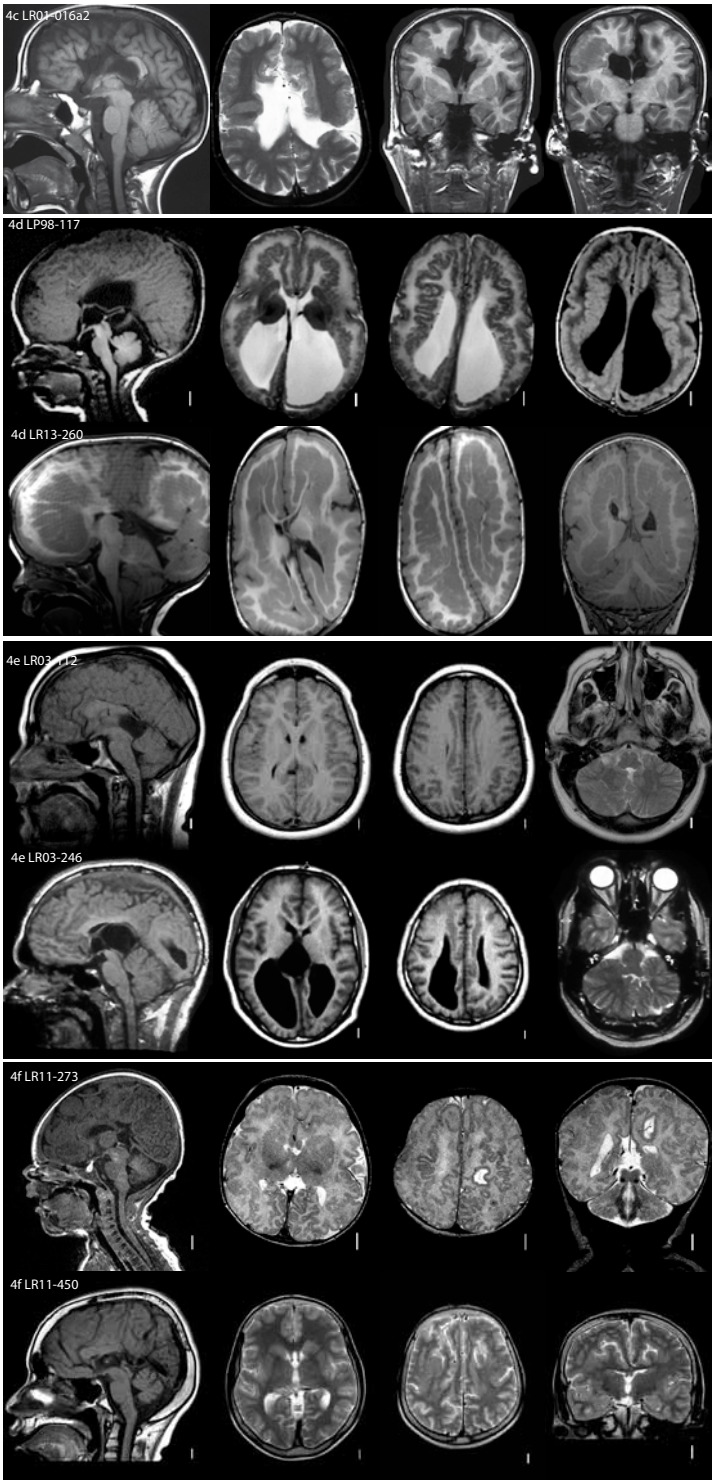
4c LR01-016a2
4d LP98-117
4d LR13-260
4e LR03-112
4e LR03-246
4f LR11-273
4f LR11-450

mix of grey and white matter, but with normal midline structures. This patient may possibly reflect the milder end of the spectrum. In hindsight, the patient described by Garfinkle also shows a midline mass and could possibly be classified as brain-in-brain malformation.[31] Shaw & Alvord published pathology studies of three patients with "global cerebral dysplasia" which in hindsight could also be classified as brain-in-brain malformations.[35] These patients had a large central mass without distinguishable deep grey nuclei. The ventricular system of a fetal case was filled with disorganized germinal cells that the authors presumed to be dislocated from the subependymal matrix.[35] The cause of these rare and complex malformations remains to be determined.

We observed two patients with solid **transmantle columnar and fan-like SUBH in addition to clefts typical of schizencephaly** (Fig. 5 LR01-016a2) In both, two or more distinct transmantle SUBH or clefts were seen in each hemisphere. One child had a sibling with bilateral severe open-lip schizencephaly and was previously published as a rare form of familial schizencephaly.[37] **Ribbon-like SUBH (*EML1*).** Two patients had recognizable SUBH with a ribbon-like appearance that consists of a bilateral and symmetric single continuous, undulating ribbon-like layer of gray matter located in the frontal, parietal and occipital lobes (Fig. 5 LP98-117, LR13-260). High-resolution imaging revealed a continuous thick undulating layer of gray matter with no or little connection to the overlying cortex. The absence of veins or CSF-like spaces distinguishes these malformations from those in Groups 1 and 2. The cortex appears diffusely thin and dysplastic with shallow sulci. Other features include prenatal-onset ventriculomegaly or hydrocephalus, megalencephaly, and agenesis of the corpus callosum. This is a rare malformation and only two families have been previously published, including a patient from this study, LR13-260.[38] In both families *EML1* mutations following an autosomal recessive inheritance pattern were identified. [38]

Mesial parasagittal SUBH (Chudley-McCullough). Two patients were found to have a distinct pattern of SUBH extending along the mesial side of the lateral ventricles, with direct connection to mesial PMG-like cortex at the anterior and posterior limits of the heterotopia (Fig. 5 LR03-112, LR03-246). A separate SUBH of similar morphology was present in the temporal lobes. Both also had dysmorphic cerebellar folia and arachnoid cysts. This same pattern has been reported in multiple patients with Chudley-McCullough syndrome associated with mutations of the *GPSM2* gene.[39,40]

Complex chaotic SUBH. This group includes two patients with a complex subcortical malformation with diffuse and bilateral involvement. The key features consist of both gyriform and nodular SUBH along with areas of CSF "inclusions" lined by grey matter (Fig. 5 LR11-273, LR11-450). Multiple SUBH connect to the cortex. These two patients may either represent distinct entities, or represent more extensive forms of the curvilinear SUBH.

Etiology

According to the available medical records, the etiology was unknown in the majority of patients. No pathogenic chromosomal aberrations were noted, although it is unknown in how many patients karyotyping or chromosome microarray was performed. In a few patients, single gene mutations were reported. In one patient with nodular SUBH in the region of the peritrigonal optic pathway (3b) a *de novo TUBB* mutation was identified, and in another patient compound heterozygous mutations in *CENPJ*. One patient with ribbon-like SUBH (4c) had a homozygous *EML1* mutation.[38] No DNA was available to test the second patient in this subgroup. An *OFD1* mutation was found in a patient with diffuse SUBH with interhemispheric cysts and agenesis of the corpus callosum (2b).[41] A summary of genes associated with SUBH in this and in previous studies is shown in Table 3.

Table 3. Genes associated with subcortical heterotopia

Gene Protein function	Inheritance	SUBH subtype, other imaging features	Reference
TUBB microtubule component	de novo dominant	In optic radiation tract, primary microcephaly	Breuss et al. 2012, this study
CENPJ regulation of microtubule assembly and nucleation	autosomal recessive	In optic radiation tract, primary microcephaly	This study
KATNB1 microtubule disassembly at centrosomes	autosomal recessive	In optic radiation tract, primary microcephaly	Mishra-Gorur et al. 2014
GPSM2 activation of G proteins, spindle pole orientation	autosomal recessive	mesial longitudinal in Chudley-McCullough syndrome, fronto-mesial PMG, partial ACC, ventriculomegaly, cerebellar dysplasia, arachnoid cysts	Doherty et al. 2012
EML1 microtubule-binding protein	autosomal recessive	ribbon-like with HYD, MEG, and ACC	Kielar et al. 2014, this study
BRCA1 DNA damage response, centrosome/ mitotic function	?type 2 mosaicism	Giant SUBH	Eccles et al. 2003 & 2005
MLH1 DNA mismatch repair	?autosomal recessive	Giant SUBH, ACC, and interhemispheric cysts	Baas et al. 2013
OFD1 regulation of centriole length, ciliogenesis	X-linked dominant	Giant SUBH, PMG, ACC, intracerebral cysts, cerebellar and brainstem abnormalities, porencephaly	Bisschoff et al. 2013; Del Giudice et al. 2014

DISCUSSION

We have described the imaging patterns and, when available, the associated clinical features of 107 patients with SUBH. We classified these patients into 14 distinct MCD

groups that predominately involve the subcortical regions, among which we define several new and rarely described subtypes. From prior experience, we had expected to find mostly localized focal-segmental SUBH, but also found numerous bilateral and diffuse forms.

As few pathological descriptions have appeared and for only few subtypes the underlying causes have been identified, this classification system is necessarily imaging-based. In our prior comprehensive MCD classification, MCD were classified in a framework of three main groups of malformations, namely those due (I) to abnormal neuronal proliferation, (II) to abnormal neuronal migration, or (III) to abnormal postmigrational development.[1] SUBH were classified in group II. It is arguable that other mechanisms play a role in its etiology, e.g. proliferation in abnormal locations, which has been suggested as a cause of the ribbon-like SUBH [38], or abnormal organization of the cortex, as several SUBH resemble abnormally deep infolded cortex. Therefore, for the SUBH, we chose not to use this framework but instead defined the group of SUBH by its anatomical location only. We have included genetic data when available, but so far this applies only to a few very rare subtypes of SUBH.

Previous studies focused mainly on neurological symptoms associated with the SUBH. As expected, abnormal cognitive and/or motor development and epilepsy were present in the majority of patients. We also observed a high frequency of extra-CNS malformations (46%), with eyes, limbs and genitourinary tract being most frequently affected. We therefore recommend, in addition to a careful neurological exam, a full physical examination focusing on congenital anomalies, an ophthalmological exam and renal ultrasound in all patients with SUBH.

Curvilinear SUBH

By far the largest group in our cohort consisted of curvilinear SUBH with CSF-like spaces (62%). In previous reports, several different terms have been used for this group including giant subcortical nodular heterotopia [10], focal subcortical heterotopia [23,42], massive heterotopia [11], subcortical nodular heterotopia [43], and curvilinear transmantle heterotopia [1]. We discourage the use of any secondary descriptive terms for the group as a whole - such as giant, large, focal, etc. – as the size and location vary considerably among patients with otherwise similar morphology. When assessed on a single plane, curvilinear heterotopia may have a multinodular appearance. However, high-resolution images in multiple planes show the curvilinear morphology. A few additional nodules may be seen surrounding the main body of the curvilinear SUBH, but these should be distinguished from the isolated solid nodules placed in group 3.

The clinical spectrum regarding development was very broad. Thirteen individuals within this group had normal cognitive and motor development, which seems remarkable judging from the size and extent of the malformation. Reports on this

malformation mostly involved single patient reports or small series.[10,12,13,15,17,43] The largest reported series described imaging and clinical features of 24 patients; all had seizures and almost all had pyramidal signs, mostly contralateral to the brain lesion.[16] No correlation between clinical outcome and radiological features was found in this published study. Another report compared nine patients with PNH only to nine other patients with both PNH and unilateral SUBH.[43] The latter group had lower average IQ scores and higher incidence of developmental delay and neurological signs compared to the PNH only group. In contrast to previous reports, we did not find an excess of subjects with unilateral curvilinear SUBH.[16,17,43] We cannot explain this difference, other than that the curvilinear SUBH usually affects the brain asymmetrically and subtle involvement of the contralateral hemisphere could be overlooked.

Etiology

It is striking that no syndrome or etiological diagnosis was noted for any patient with curvilinear SUBH, and we did not encounter any sibling recurrences. Based on incomplete data, two mechanisms have limited support. The first is a genetic etiology, most likely a postzygotic or mosaic mutation. The asymmetric and unilateral forms meet criteria for mosaicism [44], a mechanism already demonstrated for several other cortical malformations.[45-47] Two unrelated patients have been reported with germline *BRCA1* mutations and SUBH, leading the authors to propose a postzygotic, somatic mutation on the second allele as a cause for the brain malformation.[42,48] An exogenic cause, e.g. vascular disruptive or infectious, remains another possibility. In our cohort, one individual had an absent right internal carotid artery. In addition, 2 of 61 patients had a history of twinning, and another had absence of an arm. A vascular disruptive cause has also been suggested in other reports based on prenatal history of twinning, near miscarriage or trauma in patients with curvilinear SUBH. Further, both of the *BRCA1* patients with SUBH were one of twins.[11,12,14,42,48] However, from these small numbers of patients, no definitive conclusions may be drawn regarding a vascular disruptive cause. We identified a subgroup of curvilinear SUBH with interhemispheric cysts and corpus callosum agenesis. One patient in this subgroup was diagnosed with oro-facial-digital syndrome type 1 (OFD1, OMIM #311300). In OFD1 patients, brain malformations are frequent, including complex MCD with striking infolding, SUBH and PNH and abnormalities of the corpus callosum, interhemispheric cysts, ventriculomegaly, and cerebellar vermis abnormalities.[41,49] OFD1 can be diagnosed on the basis of recognizable clinical features, especially oral findings (bifid tongue, tongue hamartomas, teeth abnormalities, oral frenulae, (pseudo)cleft of the upper lip) and is caused by mutations in the X-linked *OFD1* gene. A syndrome to consider in females with SUBH and infantile spasms is Aicardi syndrome. In addition, patients have chorioretinal lacunae and

complex brain malformations with deficiency of the falx cerebri, subependymal heterotopia and polymicrogyria.[27,50] The etiology of Aicardi syndrome is unknown. We found strong evidence for a disruptive pathogenesis in the group of deeply infolded SUBH. Four of six patients from the parasagittal subtype had a feature (twinning or jejunal atresia) which has been previously associated with schizencephaly, suggesting a similar pathogenesis.[26] We had less prenatal data on the larger parieto-occipital subgroup, but the records of one patient noted a fetus papyraceus and in another heavy maternal vaginal bleeding either just before or early in the pregnancy.

Microtubule defects in rare bilateral forms

Several genes have been associated with rare forms of bilateral SUBH (table 3). Due to the high recurrence risk in autosomal recessive disorders, recognizing these groups is of high importance. All of these SUBH are bilateral and solid, and either microcephaly or megalencephaly are frequently observed in these patients. Interestingly, several of these genes can be associated to the mitotic spindle and microtubules. This is not surprising because both primary microcephalies as well as multiple MCD with complex brain malformations have been linked to similar mechanisms.[51,52] The *CENPJ* gene encodes a centrosomal protein with tubulin-dimer binding activity.[53] KATNB1 forms with KATNA1 the microtubule-severing protein katanin which localizes to the centrosomes.[30] *TUBB* encodes a beta-tubulin, and beta-tubulins together with alpha-tubulins form the core of the microtubules.[29] These findings suggest that defects in microtubule formation underlie solid SUBH in the peritrigonal optic pathway. Mutations in another microtubule-associated gene, *EML1,* cause an extensive ribbon-like SUBH, combined with agenesis of the corpus callosum, dysplastic cortex (PMG-like), hydrocephalus and megalencephaly.[38] The Eml1-deficient mouse (HeCo mouse) develops similar brain abnormalities and at the microscopic level shows ectopic neuronal progenitors and oblique mitotic spindle orientation.[38] Patients with Chudley-McCollough syndrome have a distinct bilateral form of SUBH. This syndrome is caused by mutations in *GPSM2*, a gene which is associated with cell polarity and mitotic spindle orientation. [39,54]

CONCLUSIONS

This study represents an attempt to increase awareness of the frequency and complexity of the heterogeneous group of malformations known as subcortical heterotopia (SUBH). Increased awareness of the imaging patterns of SUBH and its subtypes will lead to better recognition of the patients and stimulate scientific research regarding the causes, manifestations, and eventually therapies for this complex malformation. Although this study has contributed substantial knowledge to the field, it is striking that the causative mechanism is unknown for the great majority of the patients.

We have shown that the etiology is heterogeneous with both genetic and possibly prenatal disruptive factors.
Elucidating the pathomechanisms underlying SUBH should be the next crucial step in the understanding of these disorders and will enable the development of targeted therapies. As this classification is based on imaging appearance, it will probably need revision as underlying genes and pathways are discovered. However, this classification will not just be useful to the clinician, but also to the genetic researcher, as correct phenotyping is crucial when interpreting genetic variants.

Supplementary Table 1 is available online at http://cluster15.erasmusmc.nl/oegema. Username oegema, password renske.

ACKNOWLEDGEMENTS

The authors would like to thank all the patients and their families, and the referring physicians for their contributions to this study. For this study RO was supported by an EMBO short-term fellowship and a Simonsfonds grant from the Dutch society of Human Genetics.

SUPPLEMENTARY CLINICAL REPORTS

Deeply infolded SUBH

LP97-007 presented with developmental delay and right hemiparesis around 6 months of age. She was born after an uncomplicated pregnancy at 42 GW. Birth weight was 3485 grams, Apgar scores were unremarkable and OFC "normal". She spoke her first words at 9 months. She was able to crawl at 13 months and stand alone at 18 months. She has adequate social skills and speech development and has not had seizures up to 22 months. Height and weight are normal. She had mild to moderate spasticity of the right limbs. Family history was negative for brain malformations and brain MRI in the mother was normal.

LR01-283a1 & a2. These identical twin girls were born prematurely (35-36 GW) after an uneventful pregnancy. For LR01-283a2 neonatal asphyxia was reported in her medical records, without further detail. Motor milestones were delayed, she walked unassisted at age three and had mild mental delay. She spoke first words at age 3. On examination she had mild spastic paraparesis (more severe on the left), motor clumsiness in fine motor skills, and a bilateral deficit of stereognosis. Wechsler intelligene scale (age 33) showed IQ of 68. At age 11 years, she had a first seizure, focal somatosensitive involving the left hand. Since the age of 17 she suffers from two types of seizures 1) impaired awareness with forced grasping of objects, and 2) hypertonic extension of the left leg causing falling to the ground. The seizures occur in clusters, usually during menstruations, and are drug-resistant. EEG showed bilateral discharges.
Her sister, LR01-283a1, also showed early developmental delay. She walked independently at 4 years of age and spoke her first word at 3. She has short stature, scoliosis, lumbar hyperlordosis, an asymmetric spastic paraparesis (more severe on the right side), and bilateral deficit of stereognosis. Wechsler intelligence scale (33 years) showed IQ of 59 (VIQ 58 and PIQ 67). Her first seizure occurred at age 17 years. The seizures are manifested with a feeling of unfamiliarity, loss of contact, eye and head rotation towards the right, oral and hand automatisms. Occasionally a seizure is followed by slow falling to the ground. She has many seizures per day, intercalated with seizure-free intervals of a few days. EEG showed bilateral temporal foci. Lumbar spine X-ray showed the presence of 4 lumbar vertebral bodies, and schisis of the posterior laminae of S1.

LR09-150 was born at 40 GW, birth weight 3827 grams, length 53.3 inch. She experienced complex partial seizures at 2 months, rapidly evolving to infantile spasms. At 19 months she continues to have spasms and tonic seizures every couple of days despite AED. She has developmental delay, starting rolling at 16 months, and is not sitting

or standing at 19 months. At 6 months, her height is at p25, and weight >p95. On examination she has mild hypotonia, plagiocephaly, and mild facial dysmorphism with synophrys, short palpebral fissures, hypertelorism and poorly formed philtrum. She has a right optic nerve coloboma.

Curvilinear SUBH

LR02-038. She has bilateral iris coloboma, right chorioretinal coloboma, mild dysmorphic features (small chin, upturned nose with hypoplastic alae nasi, asymmetric narrow palpebral fissures, prominent ears), and right-sided subtle thumb hypoplasia. Echocardiogram at 2 months showed partial anomalous pulmonary venous return and patent foramen ovale. Torticollis at 4 months prompted MRI studies. She showed a mild motor delay (rolling at 6 moths, sitting supported at 7 months) but there were no cognitive concerns at 13 months. At 6.5 years, she is in general good health, has fluent speech, and uses miralax for constipation. She has not had seizures, she has occupational, speech and physical therapy. On neurological examination she had symmetric tendon reflexes with Babinski sign on the left, some difficulty with toe walking and intact coordination. Height, weight and FC fall within normal limits. No hearing loss, normal skeletal survey and abdominal ultrasound. She has normal female karyotype and normal FISH 22q11 results.

LR01-079. An intracranial cyst was noted on prenatal ultrasounds and confirmed after birth. 2 VP-drains were placed, one in posterior fossa cyst and one in a 3rd ventricle cyst. He had transient hypothyroidism. He has developmental delay, and at 2 years, he can arm craw but not sit up. He speaks several words and some two-word sentences. His failure to thrive with both weight and height <p3, improved on a high-caloric diet. He started walking with support at 3 years (at 4 years still using a walker) and speaks short sentences at this age. Facial features include a frontal upsweep, prominent forehead, hypertelorism, low nasal bridge, mild epicanthal folds, downturned corners of the mouth. He is normocephalic (p50). He has strabismus and myopia. He underwent surgery for hip dislocation at 3.5 years. His seizures started before 2 years and are well controlled with lamictal. Karyotyping and FISH 17p studies showed normal results.

LR11-239 was born to a healthy, 21-year old woman at 36 GW after a spontaneous, uncomplicated delivery. A 19 GW ultrasound was normal. The mother was diagnosed with hypertension at 31 GW. His BW was 7 pounds, 1 ounce. He received 3 days of phototherapy due to neonatal jaundice. He was admitted for GI reflux and hypertension at 5 weeks, and bilateral kidney cysts were noted on ultrasound. At age 2, he has global developmental delay, slight hypotonia and non-dysmorphic facies. He walked independently at 2.5 years. At 3 years, he is a clumsy walker, has no pencil grip, wears

insoles for his inward posture of the feet and has a significant language delay. He had brisk reflexes and mild hypotonia. Karyotype, microarray and extensive metabolic investigations were normal.

LR06-375. Prenatal ultrasound at 32 GW showed ventriculomegaly, subsequent MRI showed ACC, decreased WM and an arachnoid cyst. After birth, brain imaging showed several midline cysts and at surgery for fenestration at least five major and several smaller cysts were identified. Due to growth of several cysts at 5 months he underwent again craniotomy and fenestration. At 13 months he is crawling, pulling himself up, take assisted steps, has pincer grasp, can drink from a straw and is babbling and saying mama. He has had a single episode of stiffening and unresponsiveness. He showed left hand preference but used both hands. His weight was at p50-p75, height p10-p25 and OFC p25. Neurological exam was grossly normal.

LR04-376. Prenatal ultrasound at 25 GW showed enlarged ventricles and an irregular fetal heart rate. He was delivered at 41 GW by cesarean section due to large head size. BW was 4876 grams, length 56 cm. An occipital encephalocele was noted, two VP-shunts were placed after birth one in the posterior fossa cyst and in the enlarged ventricles. He was intubated neonatally due to recurrent apnea with oxygen need. Feeding difficulties necessitated tube feeding. Seizures started in the first days of life and were difficult to control. At age 3 years he experienced multiple seizure types. He had severe developmental delay with no major milestones reached at 3.5 years and showed limited interaction with the environment. Physical examination showed a microcephalic boy with brachyplagiocephaly. He has clouded cornea due to an inability to close his eyes early in life. His facial profile is flat, with arched eyebrows, narrow palpebral fissures, a small mouth, peg shaped teeth, transverse palmar creases. He has radio-ulnar synostosis, cutaneous syndactyly of the 4^{th} and 5^{th} finger, a broad, possibly duplicated hallux on the left and sandal gap on the right. He has truncal hypotonia with spastic tetraplegia. He passed away at age 7 years.

Solid SUBH in peritrigonal optic pathway

LR07-197 is the first child of healthy, non-consanguineous parents of Turkish descent. On prenatal ultrasound oligohydramnios, and IUGR with small head size were noted. She was born at 39 weeks by uncomplicated vaginal delivery. Birth weight was 2930 grams and OFC 31.3 cm. Postnatally, edema of the hands, feet and eyelids were noted. Turner syndrome was excluded by chromosome studies. Increased muscle tone and feeding difficulties occurred in infancy. Around 9 months she was diagnosed with global developmental delay and spastic quadriparesis. She presented with recurrent apnoeic episodes at age 3 years, and EEG showed left occipital epileptiforme

discharges. Seizures responded well to AED. She has mild dysmorphic features with asymmetry of the face and strabismus. Lymphedema of both legs and the right arm persisted causing recurrent skin infections (erysipelas). At age 13 she was diagnosed with scoliosis. Her height and OFC are at -3 SD.

Complex bilateral SUBH

Ribbon-like subcortical heterotopia

LR13-260 was born at 33 3/7 GW by caesarean section performed because of progressive hydrocephalus on ultrasound examinations. A VP-drain was placed after birth. At age 6 years he has profound ID and is wheelchair bound. He has a responsive smile and can roll over. He frequently aspirates on liquids and is unable to eat solid foods. He has short stature (-4 SD) and is macrocephalic (+3.3 SD). He has severe cerebral visual impairment with absence of visual tracking. EEG age 7, when taking keppra and valproic acid, showed severe epileptic encephalopathy and continuous multifocal epileptic discharges and frequent electrodecremental events with accompanied by tonic seizures.

Brain-in-brain

LP99-240 was born at 35 weeks by cesarean section. A VP shunt was placed after birth. Seizures started after birth. An encephalocele was repaired and VP-shunt placed at 5 months. He was diagnosed with craniofacial disproportion and underwent cranial vault expansion and cranioplasty at 11 months. At 4 years he has "focal events" of horizontal eye nystagmus and unresponsiveness lasting ten to fifteen seconds, up to 100 a day. These events were not associated with abnormal EEG activity. He is on phenobarbital, Carbatrol, and Topamax. He is learning sign language and able to sign 4 words. He has spastic quadriparesis and is wheelchair bound. He is fed by a G-tube. He wears a back brace for scoliosis. He is extremely hypotonic and needs necks support, he is able to lift his arms and legs. He is smiling, alert and attentive. He has bilateral esotropia and slow pupil reactions. He is allergic to latex and multiple fruits.

LR00-237: Within a few weeks after birth, seizures started (rhythmic eye twitching, arching of head and back, jerking of arms, lasting 45sec to 3 min) over 30 a day. Examination at 4 weeks showed a microcephalic infant (weight 2.73 kg, OFC 28 cm, ICD 2.0 cm, OCD 5 cm) with a low sloping forehead, high nasal bridge, upslanted palpebral fissures and 4x4x3.5 cm cephalocele at the posterior midline. No other facial anomalies (pictures in db). She had no interaction with the environment and moderate hypotonia. At 4 years she takes lamictal, keppra. She has mild scoliosis. She his hypotonic and has pseudobulbar palsy. Telomere FISH normal. At age 5, seizures frequency had increased to dozens a day, especially at night (under lamictal and keppra). She is allergic to

phenobarbital and penicillin. Weight 20.9 kg, height 96.5 cm, OFC 40.5 cm. She has clonus throughout and fisted hands.

LR13-202: A prenatal ultrasound showed enlarged ventricles and he was diagnosed with hydrocephalus after birth and VP-shunt was placed. He started having seizures in the first weeks, tonic with bending of the arms and drawing the hands in front of the chest, lasting 1-2 minutes. These seizures stopped at 8 months. Around 3 years, shortly after a shunt revision, he started having partial seizures, mostly involving the left arm, but sometimes spreading to a generalized seizures, and also had absence seizures. At age 11, he still has these and they have been difficult to control. He is hypotonic with spastic quadriplegia, has difficulty keeping his head up and is mostly wheelchair bound, although he can stand and take several steps with support. He is a generally happy boy who vocalizes and interacts with his environment. He hears well. His eye movements are limited in both vertical and horizontal gaze, and he has decreased peripheral vision. He has no abnormalities of the retina or optic nerve (according to parents). He has a turricephalic head shape with a soft mass on the top of his skull, covered by an epidermal nevus and a dark lock of hair. He had left-sided temporal alopecia, unclear whether this was congenital or have an extrinsic cause (e.g. caused by a skin infection and/or rubbing of the head). He has small hands, brachydactyly of the toes with a cutaneous 2-3 syndactyly.

Complex chaotic SUBH

LR11-273: Pregnancy history was significant for herpes simplex and valacyclovir exposure. He was born at 39 GW, Apgar scores 8/9, BW 3035 grams (p40-p50). He was referred for multiple congenital anomalies and respiratory distress after birth, including a left pelvic kidney and bilateral hand anomalies consisting on the left of a hypoplastic thumb and 2nd and 5th finger, and on the right an absent thumb, and radioulnar synostosis with short radius. He had a stridor due to laryngomalacia. He was later noted to have a single central incisor, and submucosal cleft palate. At 8 months he has a mild global developmental delay, mild limb hypertonia and is able to sit without support and roll over. His weight is p30, height p20 and OFC 43.5 cm (-1 SD). At 14 months he was babbling and able to say mama.
no increased chromosomal breaks after mitomycin C or DEB treatment in blood cells. Sequencing and MLPA of SHH, SIX3, TGIF, and ZIC2 normal. SNP array showed 420kb deletion of 16q23.1 (bp75,823,175-76,243,191 HGB 36, containing the ADAMST18 gene). Parental studies were pending.

REFERENCES

1. Barkovich AJ, Guerrini R, Kuzniecky RI, Jackson GD, Dobyns WB. A developmental and genetic classification for malformations of cortical development: update 2012. Brain. 2012 May;135(Pt 5):1348-69.
2. Hunter A. Brain. In: Stevenson RE, Hall JG, Goodman R, editors. Human malformations and related anomalies: Oxford University Press; 1993. p. 1-52.
3. Jacobs MP, Fischbach GD, Davis MR, Dichter MA, Dingledine R, Lowenstein DH, *et al.* Future directions for epilepsy research. Neurology. 2001 Nov 13;57(9):1536-42.
4. Kuzniecky R, Murro A, King D, Morawetz R, Smith J, Powers R, *et al.* Magnetic resonance imaging in childhood intractable partial epilepsies: pathologic correlations. Neurology. 1993 Apr;43(4):681-7.
5. Mischel PS, Nguyen LP, Vinters HV. Cerebral cortical dysplasia associated with pediatric epilepsy. Review of neuropathologic features and proposal for a grading system. J Neuropathol Exp Neurol. 1995 Mar;54(2):137-53.
6. Harvey AS, Cross JH, Shinnar S, Mathern GW. Defining the spectrum of international practice in pediatric epilepsy surgery patients. Epilepsia. 2008 Jan;49(1):146-55.
7. Barkovich AJ, Kuzniecky RI, Jackson GD, Guerrini R, Dobyns WB. Classification system for malformations of cortical development: update 2001. Neurology. 2001 Dec 26;57(12):2168-78.
8. Barkovich AJ, Kuzniecky RI, Jackson GD, Guerrini R, Dobyns WB. A developmental and genetic classification for malformations of cortical development. Neurology. 2005 Dec 27;65(12):1873-87.
9. Barkovich AJ, Kuzniecky RI, Dobyns WB, Jackson GD, Becker LE, Evrard P. A classification scheme for malformations of cortical development. Neuropediatrics. 1996 Apr;27(2):59-63.
10. Battaglia G, Arcelli P, Granata T, Selvaggio M, Andermann F, Dubeau F, *et al.* Neuronal migration disorders and epilepsy: a morphological analysis of three surgically treated patients. Epilepsy Res. 1996 Dec;26(1):49-58.
11. Kuzniecky R, Gilliam F, Faught E. Discordant occurrence of cerebral unilateral heterotopia and epilepsy in monozygotic twins. Epilepsia. 1995 Nov;36(11):1155-7.
12. Novegno F, Battaglia D, Chieffo D, Frassanito P, Leoni C, Tamburrini G, *et al.* Giant subcortical heterotopia involving the temporo-parieto-occipital region: a challenging cause of drug-resistant epilepsy. Epilepsy Res. 2009 Nov;87(1):88-94.
13. Poduri A, Golja A, Riviello JJ, Jr., Bourgeois BF, Duffy FH, Takeoka M. A distinct asymmetrical pattern of cortical malformation: large unilateral malformation of cortical development with contralateral periventricular nodular heterotopia in three pediatric cases. Epilepsia. 2005 Aug;46(8):1317-21.
14. Preul MC, Leblanc R, Cendes F, Dubeau F, Reutens D, Spreafico R, *et al.* Function and organization in dysgenic cortex. Case report. J Neurosurg. 1997 Jul;87(1):113-21.
15. Raghavendra S, Krishnamoorthy T, Ashalatha R, Nayak SD, Radhakrishnan K. Hemimegalencephalic appearance of normal hemisphere in unilateral heterotopia and absent corpus callosum. Epilepsy Behav. 2006 Sep;9(2):363-6.
16. Barkovich AJ. Morphologic characteristics of subcortical heterotopia: MR imaging study. AJNR Am J Neuroradiol. 2000 Feb;21(2):290-5.
17. Barkovich AJ. Subcortical heterotopia: a distinct clinicoradiologic entity. AJNR Am J Neuroradiol. 1996 Aug;17(7):1315-22.

18. Barkovich AJ, Kjos BO. Gray matter heterotopias: MR characteristics and correlation with developmental and neurologic manifestations. Radiology. 1992 Feb;182(2):493-9.
19. Friede RL. Dysplasias of Cerebral Cortex. Developmental Neuropathology: Springer-Verlag; 1989.
20. Hansen DV, Lui JH, Parker PR, Kriegstein AR. Neurogenic radial glia in the outer subventricular zone of human neocortex. Nature. 2010 Mar 25;464(7288):554-61.
21. Pollen AA, Nowakowski TJ, Chen J, Retallack H, Sandoval-Espinosa C, Nicholas CR, *et al.* Molecular identity of human outer radial glia during cortical development. Cell. 2015 Sep 24;163(1):55-67.
22. Packard AM, Miller VS, Delgado MR. Schizencephaly: correlations of clinical and radiologic features. Neurology. 1997 May;48(5):1427-34.
23. Barkovich AJR, C. Pediatric Neuroimaging, fifth edition2011.
24. Guerrini R, Dubeau F, Dulac O, Barkovich AJ, Kuzniecky R, Fett C, *et al.* Bilateral parasagittal parietooccipital polymicrogyria and epilepsy. Ann Neurol. 1997 Jan;41(1):65-73.
25. Leventer RJ, Jansen A, Pilz DT, Stoodley N, Marini C, Dubeau F, *et al.* Clinical and imaging heterogeneity of polymicrogyria: a study of 328 patients. Brain. 2010 May;133(Pt 5):1415-27.
26. Curry CJ, Lammer EJ, Nelson V, Shaw GM. Schizencephaly: heterogeneous etiologies in a population of 4 million California births. Am J Med Genet A. 2005 Aug 30;137(2):181-9.
27. Barkovich AJ, Simon EM, Walsh CA. Callosal agenesis with cyst: a better understanding and new classification. Neurology. 2001 Jan 23;56(2):220-7.
28. Baas AF, Gabbett M, Rimac M, Kansikas M, Raphael M, Nievelstein RA, *et al.* Agenesis of the corpus callosum and gray matter heterotopia in three patients with constitutional mismatch repair deficiency syndrome. Eur J Hum Genet. 2013 Jan;21(1):55-61.
29. Breuss M, Heng JI, Poirier K, Tian G, Jaglin XH, Qu Z, *et al.* Mutations in the beta-tubulin gene TUBB5 cause microcephaly with structural brain abnormalities. Cell Rep. 2012 Dec 27;2(6):1554-62.
30. Mishra-Gorur K, Caglayan AO, Schaffer AE, Chabu C, Henegariu O, Vonhoff F, *et al.* Mutations in KATNB1 cause complex cerebral malformations by disrupting asymmetrically dividing neural progenitors. Neuron. 2014 Dec 17;84(6):1226-39.
31. Garfinkle WB. Aventriculy: a new entity? AJNR Am J Neuroradiol. 1996 Oct;17(9):1649-50.
32. Ishak GE, Dempsey JC, Shaw DW, Tully H, Adam MP, Sanchez-Lara PA, *et al.* Rhombencephalosynapsis: a hindbrain malformation associated with incomplete separation of midbrain and forebrain, hydrocephalus and a broad spectrum of severity. Brain. 2012 May;135(Pt 5):1370-86.
33. Kumar S, Jaiswal AK, Rastogi M. Aventriculi associated with holoprosencephaly. J Clin Neurosci. 2006 Apr;13(3):378-80.
34. Sener RN. Schizencephaly and congenital cytomegalovirus infection. J Neuroradiol. 1998 Jul;25(2):151-2.
35. Shaw CM, Alvord EC, Jr. Global cerebral dysplasia due to dysplasia and hyperplasia of periventricular germinal cells. J Child Neurol. 1996 Jul;11(4):313-20.
36. Widjaja E, Massimi L, Blaser S, Di Rocco C, Raybaud C. Midline "brain in brain": an unusual variant of holoprosencephaly with anterior prosomeric cortical dysplasia. Childs Nerv Syst. 2007 Apr;23(4):437-42.
37. Granata T, Farina L, Faiella A, Cardini R, D'Incerti L, Boncinelli E, *et al.* Familial schizencephaly associated with EMX2 mutation. Neurology. 1997 May;48(5):1403-6.

38. Kielar M, Tuy FP, Bizzotto S, Lebrand C, de Juan Romero C, Poirier K, *et al.* Mutations in Eml1 lead to ectopic progenitors and neuronal heterotopia in mouse and human. Nat Neurosci. 2014 Jul;17(7):923-33.
39. Doherty D, Chudley AE, Coghlan G, Ishak GE, Innes AM, Lemire EG, *et al.* GPSM2 mutations cause the brain malformations and hearing loss in Chudley-McCullough syndrome. Am J Hum Genet. 2012 Jun 8;90(6):1088-93.
40. Kau T, Veraguth D, Schiegl H, Scheer I, Boltshauser E. Chudley-McCullough syndrome: case report and review of the neuroimaging spectrum. Neuropediatrics. 2012 Feb;43(1):44-7.
41. Bisschoff IJ, Zeschnigk C, Horn D, Wellek B, Riess A, Wessels M, *et al.* Novel mutations including deletions of the entire OFD1 gene in 30 families with type 1 orofaciodigital syndrome: a study of the extensive clinical variability. Hum Mutat. 2013 Jan;34(1):237-47.
42. Eccles D, Bunyan D, Barker S, Castle B. BRCA1 mutation and neuronal migration defect: implications for chemoprevention. J Med Genet. 2005 Jul;42(7):e42.
43. Dubeau F, Tampieri D, Lee N, Andermann E, Carpenter S, Leblanc R, *et al.* Periventricular and subcortical nodular heterotopia. A study of 33 patients. Brain. 1995 Oct;118 (Pt 5):1273-87.
44. Happle R. Mosaicism in human skin. Understanding the patterns and mechanisms. Arch Dermatol. 1993 Nov;129(11):1460-70.
45. Jamuar SS, Lam AT, Kircher M, D'Gama AM, Wang J, Barry BJ, *et al.* Somatic mutations in cerebral cortical malformations. N Engl J Med. 2014 Aug 21;371(8):733-43.
46. Lee JH, Huynh M, Silhavy JL, Kim S, Dixon-Salazar T, Heiberg A, *et al.* De novo somatic mutations in components of the PI3K-AKT3-mTOR pathway cause hemimegalencephaly. Nat Genet. 2012 Jun 24.
47. Riviere JB, Mirzaa GM, O'Roak BJ, Beddaoui M, Alcantara D, Conway RL, *et al.* De novo germline and postzygotic mutations in AKT3, PIK3R2 and PIK3CA cause a spectrum of related megalencephaly syndromes. Nat Genet. 2012 Aug;44(8):934-40.
48. Eccles DM, Barker S, Pilz DT, Kennedy C. Neuronal migration defect in a BRCA1 gene carrier: possible focal nullisomy? J Med Genet. 2003 Mar;40(3):e24.
49. Del Giudice E, Macca M, Imperati F, D'Amico A, Parent P, Pasquier L, *et al.* CNS involvement in OFD1 syndrome: a clinical, molecular, and neuroimaging study. Orphanet J Rare Dis. 2014;9:74.
50. Rosser T. Aicardi syndrome. Arch Neurol. 2003 Oct;60(10):1471-3.
51. Alcantara D, O'Driscoll M. Congenital microcephaly. Am J Med Genet C Semin Med Genet. 2014 Jun;166C(2):124-39.
52. Mutch CA, Poduri A, Sahin M, Barry B, Walsh CA, Barkovich AJ. Disorders of Microtubule Function in Neurons: Imaging Correlates. AJNR Am J Neuroradiol. 2015 Nov 12.
53. Tang CJ, Fu RH, Wu KS, Hsu WB, Tang TK. CPAP is a cell-cycle regulated protein that controls centriole length. Nat Cell Biol. 2009 Jul;11(7):825-31.
54. Williams SE, Beronja S, Pasolli HA, Fuchs E. Asymmetric cell divisions promote Notch-dependent epidermal differentiation. Nature. 2011 Feb 17;470(7334):353-8.

Chapter 2.2

Recognisable cerebellar dysplasia associated with mutations in multiple tubulin genes

Renske Oegema[*], Thomas D. Cushion[*], Ian G. Phelps, Seo-Kyung Chung, Jennifer C. Dempsey, Sarah Collins, Jonathan G.L. Mullins, Tracy Dudding, Harinder Gill, Andrew J. Green, William B. Dobyns, Gisele E. Ishak, Mark I. Rees[^], Dan Doherty[^]

*,[^] These authors contributed equally to the manuscript

Human Molecular Genetics 2015
Sep 15;24(18):5313-25

ABSTRACT

Mutations in alpha- and beta-tubulins are increasingly recognised as a major cause of malformations of cortical development (MCD), typically lissencephaly, pachygyria and polymicrogyria; however, sequencing tubulin genes in large cohorts of MCD patients has detected tubulin mutations in only 1-13%. We identified patients with a highly-characteristic cerebellar dysplasia but without the lissencephaly, pachygyria and polymicrogyria typically associated with tubulin mutations. Remarkably, in 7 of 9 patients (78%), targeted sequencing revealed mutations in three different tubulin genes (*TUBA1A*, *TUBB2B*, *TUBB3*), occurring *de novo* or inherited from a mosaic parent. Careful re-review of the cortical phenotype on brain imaging revealed only an irregular pattern of gyri and sulci, for which we propose the term tubulinopathy-related dysgyria. Basal ganglia (100%) and brainstem dysplasia (80%) were common features. Based on *in silico* structural predictions, the mutations affect amino acids in diverse regions of the alpha/beta-tubulin heterodimer, including the nucleotide binding pocket. Cell-based assays of tubulin dynamics reveal various effects of the mutations on incorporation into microtubules: TUBB3 p.Glu288Lys and p.Pro357Leu do not incorporate into microtubules at all, while TUBB2B p.Gly13Ala shows reduced incorporation, and TUBA1A p.Arg214His incorporates fully, but at a slower rate than wild-type. The broad range of effects on microtubule incorporation is at odds with the highly stereotypical clinical phenotype, supporting differential roles for the three tubulin genes involved. Identifying this highly characteristic phenotype is important due to the low recurrence risk compared to the other (recessive) cerebellar dysplasias and the apparent lack of non-neurological medical issues.

INTRODUCTION

Since the first discovery in 2007 of *TUBA1A* (OMIM *602529) as a novel gene for lissencephaly, genes encoding alpha- and beta-tubulins, the main components of microtubule polymers, are now being recognised for their major involvement in malformations of cortical development (MCD) [1,2] and these disorders are now collectively termed tubulinopathies. Mutations in *TUBA1A* are predominantly associated with a variable spectrum of lissencephaly, pachygyria, and polymicrogyria-like cortical malformations, with or without microcephaly and abnormalities of other brain structures (in particular the basal ganglia and corpus callosum).[1,3-11] *TUBB2B* (OMIM *612850) mutations frequently cause polymicrogyria-like abnormalities, as well as lissencephaly, cortical dysplasia, schizencephaly, and microcephaly to a lesser extent.[12-17] Two major subgroups of *TUBB3* (OMIM *602661) mutations have been previously described: those associated with mildly abnormal gyral pattern (microgyria, gyral disorganization), and those with congenital fibrosis of the extraocular muscles type 3 (CFEOM3) with neurological symptoms.[2,18,19] Mutations in *TUBB* (OMIM *191130, previously referred to as *TUBB5*) have been associated with microcephaly with structural brain abnormalities, *TUBB4A* (OMIM *602662) variants with hypomyelination [20,21] and, most recently, mutations in *TUBB2A* (OMIM *615101) have been identified in individuals with simplified gyral patterning or unaffected cerebral cortex but with infantile seizures.[22] In addition to alpha- and beta-tubulins, mutations in a gamma-tubulin gene, *TUBG1* (OMIM *191135), have also been associated with pachygyria [10], further highlighting the importance of tubulin and microtubule function during brain development.

Clinically, individuals with tubulin mutations display a range of outcomes, from severe intellectual disability and intractable seizures to learning difficulties and absence of epilepsy. [12,16,18] Screening tubulin genes in large cohorts of MCD patients has yielded a mutation detection rate of only 1-13.3%.[6,8,9,12,13] Selection of MCD patients for sequencing of these genes is difficult because of the variable clinical and imaging features.

It is clear, however, that overall brain development is affected in these patients and, besides predominant cortical malformations, the basal ganglia, corpus callosum, brain stem, and cerebellum are frequently affected. The cerebellum and vermis are often described as hypoplastic or dysplastic, without further specification of the abnormality. [6,19] The range of overlapping phenotypes stemming from tubulin gene variation has been examined extensively; however, all studies published to date have ascertained patients based exclusively on the presence of MCD.

In this study, we present ten patients ascertained due to their characteristic cerebellar dysplasia combined with basal ganglia dysplasia and frequently brainstem asymmetry. Although lissencephaly, pachygyria and polymicrogyria-like malformations were absent, this combination of imaging features prompted us to sequence tubulin genes.

Strikingly, this yielded a high mutation detection rate; as seven out of nine patients carry tubulin mutations (78%, six of eight families).

MATERIALS AND METHODS

Patient selection

From the large cohort of patients with hindbrain imaging abnormalities referred to the University of Washington Hindbrain Research Program, we identified patients with a distinct combination of brainstem asymmetry, superior cerebellar dysplasia and basal ganglia dysplasia and without a diagnosis of MCD (e.g. pachygyria, polymicrogyria). Clinical information was collected through chart review and structured interviews with the parents. All MRIs were systematically reviewed for abnormalities of the cortex, basal ganglia, white matter, ventricles, corpus callosum, hippocampus, brainstem, cerebellum, cerebellar vermis, and cranial nerves (by RO, GI, DD). When possible, DNA was collected from blood and/or saliva. Patients were enrolled through a human subjects research protocol approved at the University of Washington. Informed consent was provided by the patients, their parents or their legal guardians.

Genetic studies

TUBA1A (RefSeq Accession: NC_000012.12), *TUBB3* (NC_000016.10), *TUBB2B* (NC_000006.12), and *TUBA8* (NC_000022.11) were sequenced using molecular inversion probe (MIP) capture and sequencing on a MiSeq as previously described [23]. The MIPs targeted all coding exons and 10bp of exon-flanking intronic sequence. In patients without mutations, we performed Sanger sequencing of *TUBB2A* (NC_000006.12) and *TUBB4A* (NC_000019.10). All variants were confirmed by Sanger sequencing (primer sequences available on request) and checked against four online polymorphism databases: 1,000 genomes (www.1000genomes.org), the Exome Variant Server (http://evs.gs.washington.edu/EVS/), dbSNP (http://www.ncbi.nlm.nih.gov/snp) and ExAC (http://exac.broadinstitute.org).

Bioinformatics Analysis of Tubulin Gene Variants

Combined Annotation–Dependent Depletion 1.0 (CADD; http://cadd.gs.washington.edu) bioinformatics software was used to analyse predicted deleterious effects of identified mutations on protein function. [24] In addition, well-phenotyped *TUBA1A*, *TUBB2B* and *TUBB3* variants included in a study by Bahi-Buisson *et al*. were also analysed to enable comparison between mutations associated with unaffected/simplified gyration and with other, more severe, cortical abnormalities: microlissencephaly, lissencephaly, central pachygyria, central and general polymicrogyria-like cortical malformations.[12]

Homology Modelling

In silico structural predictions of wild-type and variant TUBA1A, TUBB2B and TUBB3 proteins were generated via a previously described homology modelling pipeline. [25] The best homologies for these models were based on 99%, 100% and 94% identities of alpha- and beta-tubulin templates (PDB: 4I4T).[26] Microtubule lattice architecture was based on a previously published template (PDB: 2XRP).[27]

Cell Culture

Human Embryonic Kidney (HEK293) cell culturing, seeding and transfection were performed as previously described.[22]

Expression Construct Generation

In vitro functional analysis of *TUBA1A* and *TUBB2B* variants was performed using expression constructs derived from a C-terminally FLAG-tagged *TUBA1A* (pRK5TUBA1A-CFLAG) clone as previously published. [6] pRK5TUBA1A-FLAG was subsequently modified to reflect wild-type *TUBB2B* (pRK5TUBB2B-CFLAG) by directional cloning. Tubulin gene variants were introduced into wild-type *TUBA1A* and *TUBB2B*, as well as a C-terminally DDK-tagged human *TUBB3* expression construct (OriGene Technologies; pCMV6 entry), using QuickChange site-directed mutagenesis (Stratagene, UK). Entire wild-type and variant transgene coding regions were sequence validated following maxiprep yields (QIAgen). The TUBA1A p.Ile219Val variant was only identified in the final stages of this study and *in vitro* analysis was therefore not available. We included this patient due to the position of the affected amino acid, its *de novo* inheritance, and the similarity of the resulting phenotype with that of others in the cohort.

Immunocytochemistry

HEK293 cells were fixed in -20°C methanol for three minutes and cell membranes subsequently permeablised with Phosphate-Buffered Saline (PBS; Sigma) plus 0.5% Triton X-100 (Sigma) to facilitate immunocytochemical staining of intracellular epitopes. Cells expressing *TUBA1A* and *TUBB2B* constructs were stained using primary antibodies specific to FLAG (Sigma, Cat. F1804; 1:500 dilution), alpha-tubulin (Sigma Cat. T6199; 1:500 dilution) and fluorescently-conjugated secondary antibodies raised against rabbit and mouse (Life Technologies, Cat. A-11011 & A-11001). *TUBB3*-expressing cells were sequentially stained for transgenic and endogenous tubulin protein as previously outlined.[22] Immunostained cells were mounted onto glass slides using ProLong Gold Antifade Reagent (Life Technologies) and images acquired using confocal microscopy (Zeiss LSM 710 & Zen Software).

Microtubule Polymerisation Assay

HEK293 cells expressing wild-type and variant tubulin gene constructs were incubated at 4°C to induce depolymerisation of the microtubule polymer network. After 30 minutes, HEK293s were returned to 37°C. At specified times following their return to optimal temperature, cells were removed, methanol fixed and immunostained to observe the rate of microtubule re-polymerisation in the presence of each tubulin construct.

RESULTS

From the large cohort of patients with hindbrain imaging abnormalities referred to the University of Washington Hindbrain Research Program, we identified ten patients, including two siblings, with a distinct combination of brainstem asymmetry, superior cerebellar dysplasia and basal ganglia dysplasia and without a diagnosis of MCD (e.g. pachygyria, polymicrogyria).

Clinical features

All individuals displayed delayed psychomotor development, with a broad range of severity (Table 1). Motor development was usually more affected than speech. Four patients had documented seizures. Four were reported to have significant behavioural problems, ADHD and aggression being most common. OFC was available for nine individuals, five of whom had microcephaly (>2 standard deviations below the mean) and two of whom had macrocephaly (>2 standard deviations above the mean). Of note, abnormal eye movements were recorded in seven individuals, including oculomotor apraxia (OMA) in four. Strabismus was present in five. Polyneuropathy and/or congenital fibrosis of the extraocular muscles (CFEOM) were not reported in any of the patients. No patients had dysmorphic features, non-central nervous system malformations or hearing loss.

Brain imaging

Brain MRI studies were performed between eight months and eight years of age for all ten individuals (Table 2).

Cerebellum and cerebellar vermis

All patients have a distinct dysplasia of the superior cerebellum, especially the vermis (with "diagonal" folia; folia crossing the midline at an oblique angle), best visible at the midline on axial and coronal views (explained in Supplementary Fig.1, see also Fig. 1 & Supplementary Fig.2, 2nd column). The vermis is hypoplastic in all but three individuals (7/10), with the anterior vermis more severely affected. The cerebellar hemispheres are either normal size or mildly hypoplastic with mild asymmetry.

Table 1. Summary of clinical data

Patient Gender	Mutation	Motor development	Cognition and speech	Seizures	OFC	Behaviour	Eye movements
UW168-3 F	*TUBA1A* c.645G>A (p.R214H)	4yr 3m sitting, not crawling	few single words at 4y 3m	"startle sz" and "absence sz"	<-2.5 SD	NA	roving eye movements
UW167-3 F	*TUBA1A* c.655A>G (p.I219V)	10y walks w/ assistance, ataxia	no speech	IS, recurrence of sz 4y	0 SD	NA	wandering gaze, nystagmoid movements; greatly improved (11y)
UW169-3 F	*TUBB2B* c.38G>C (p.G13A)	NA	NA	no (11y)	-4 SD	Asperger's, ADHD, temper tantrums	strabismus
UW169-4 F	*TUBB2B* c.38G>C (p.G13A)	NA	NA	no (5y)	-4 SD	ADHD symptoms, temper tantrums	strabismus
UW164-3 M	*TUBB3* c.1070C>T (p.P357L)	sitting 14m, walking 28m, no pincer grasp 5y	first word 14m IQ "low end of normal",dysarthric 5y	partial complex	+3 SD	ADHD-like	OMA, strabismus
UW165-3 F	*TUBB3* c.1070C>T (p.P357L)	hypotonia, sitting 10m, walking 26m	first words 18m, normal speech 2y6m	no	0 SD	normal	OMA, abnormal saccades
UW170-3 M	*TUBB3* c.862G>A (p.E288K)	hypotonia, sitting if placed in position at 13m	no words 14m	no	-2 SD	NA	mild OMA, strabismus
UW161-3 F	not tested	sitting 12m, walking 34m	NA	no (9y)	+2 SD	temper tantrums	OMA
UW166-3 F	no	28m: drools, rolls front to back	no words 28m	sz partially responsive to AED (28 m)	- 3.2 SD	normal	abnormal saccades disconjugate gaze
UW146-3 M	no	sitting 10 m, walking 26 m	10 words and 10 signs 2y2m	no	+0.5 SD	temper tantrums (2y)	nystagmus, bilateral ptosis, strabismus

ADHD= attention deficit disorder, OMA= oculomotor apraxia, IS= infantile spasms, y= year(s), m= month(s), NA= not assessed, SD= standard deviation, sz= seizures.

Table 2. Summary of MR imaging

Patient	Age MRI	Vermis	Pons	Medulla	Cortex	Corpus callosum	Enlarged LV	Basal ganglia DYS	Thalami	Hippocampus	CN V HYPO	Other
UW168-3	4y3m	HYPO	ASYM	N	diffuse irregular gyration and sulcation	partial ACC	+	Y	globular	N	++	deficient falx, bilat coloboma
UW167-3	2y1m	HYPO	ASYM	DYSP	diffuse (L>R) irregular gyration and sulcation	partial ACC	++	Y	globular	N	+++	decreased WM
UW169-3	8y7m	N	N	N	irregular gyration and sulcation, multiple shallow sulci	N	+	Y	globular	bilaterally malrotated, left >> right	N	cavum septum pellucidum
UW169-4	2y2m	N	N	N	diffuse irregular gyration and sulcation	N	+	Y	globular	left malrotated, right normal	+	cavum septum pellucidum
UW164-3	6y5m	N	ASYM	DYSP	diffuse irregular gyration and sulcation, multiple shallow sulci	mildly shortened	N	Y	globular	incompletely folded	N	
UW165-3	2y6m	HYPO	ASYM	DYSP	diffuse irregular gyration and sulcation	mildly shortened	+	Y	globular	N	+	deficient falx, prominent perivascular spaces, slightly decreased WM
UW170-3	9m	HYPO	ASYM	N	irregular gyral pattern	thin, hypopl splenium	++	Y	globular	N	++	low resolution MRI
UW161-3	8m	HYPO	ASYM	DYSP	asymmetric gyral pattern, multiple shallow sulci	thin	+	Y	globular	NA (lack of coronal images)	+	
UW166-3	1y3m	HYPO	ASYM	DYSP	irregular gyral pattern	ACC	+++	Y	globular	incompletely folded (HYD)	++	progressive WM loss, communicating HYD
UW146-3	2y2m	HYPO	ASYM	N	diffuse irregular gyration and sulcation	thin , hypoplastic rostrum	++	Y	globular	N	++	decreased WM

+= mild, ++=moderate, +++= severe, ACC=agenesis of the corpus callosum, ASYM= asymmetric, bilat= bilateral, CN= cranial nerve, DYS= dysplasia, HYD= hydrocephalus, HYPO= hypoplasia, LV= lateral ventricles, m= months, N= normal, WM=white matter, y= years.

Brainstem

In eight of 10 individuals, the pons is asymmetrically hypoplastic with a midline ventral indentation and asymmetrical inferior and middle cerebellar peduncles. Additional diffusion tension imaging (DTI) studies of individual UW165-3 showed asymmetry of the corticospinal tracts at the level of the pons (Supplementary Fig. 3). In five of ten, the medulla has a globular contour, with indistinct demarcation between the pyramids and the olivary nuclei.

Basal ganglia, thalami, and corpus callosum

The basal ganglia are asymmetrically dysplastic with bulbous appearance in all individuals, with diffuse, branched, or absent anterior limb of the internal capsule (Fig. 1 & Supplementary Fig. 2, 3rd column). The lateral ventricles have an irregular contour and abnormal rounding of the frontal horns (10/10), likely related to the basal ganglia dysplasia. The thalami are globular-shaped in all. The corpus callosum is variably affected, ranging from almost complete agenesis to normal (Fig. 1 & Supplementary Fig. 2, 4th column).

Cortex

As cortical malformations are considered a key feature in the tubulinopathies, but not reported in our cohort, we carefully re-reviewed the cortex in all individuals. Lissencephaly, pachygyria, and polymicrogyria were not observed; however, patchy and asymmetric abnormalities in gyral size and orientation, and varying sulcal depth are present in all individuals (for example see Supplementary Fig. 1). A pattern involving a cluster of multiple shallow sulci was frequently observed, especially in the frontal lobes. This pattern differs from polymicrogyria (normal cortical thickness, no microgyri, no blurring of the grey-white matter boundaries) and from simplified gyral pattern, where the gyri are too few in number (Barkovich and Raybaud, 2011).

Variants in *TUBA1A*, *TUBB2B*, and *TUBB3*

DNA was available for nine of ten patients, and we identified mutations in seven (78%). In six individuals these were novel, unreported variants: *TUBB2B* c.38G>C (p.Gly13Ala) in two siblings; *TUBB3* c.1070C>T (p.Pro357Leu) in two unrelated patients; *TUBB3* c.862G>A (p.Glu288Lys) and *TUBA1A* c.655A>G (p.Ile219Val) in sporadic patients. In addition, we identified in one patient the previously published missense change *TUBA1A* c.641G>A (p.Arg214His).[12] All variants are *de novo*, except *TUBB2B* p.Gly13Ala, which was inherited by two affected sisters from their mosaic, apparently asymptomatic father (Supplementary Fig. 4). Variants were determined to be absent from 1,000 genomes, the Exome Variant Server, dbSNP142 and ExAC databases. We did not identify mutations in *TUBA8, TUBB2A* or *TUBB4A*.

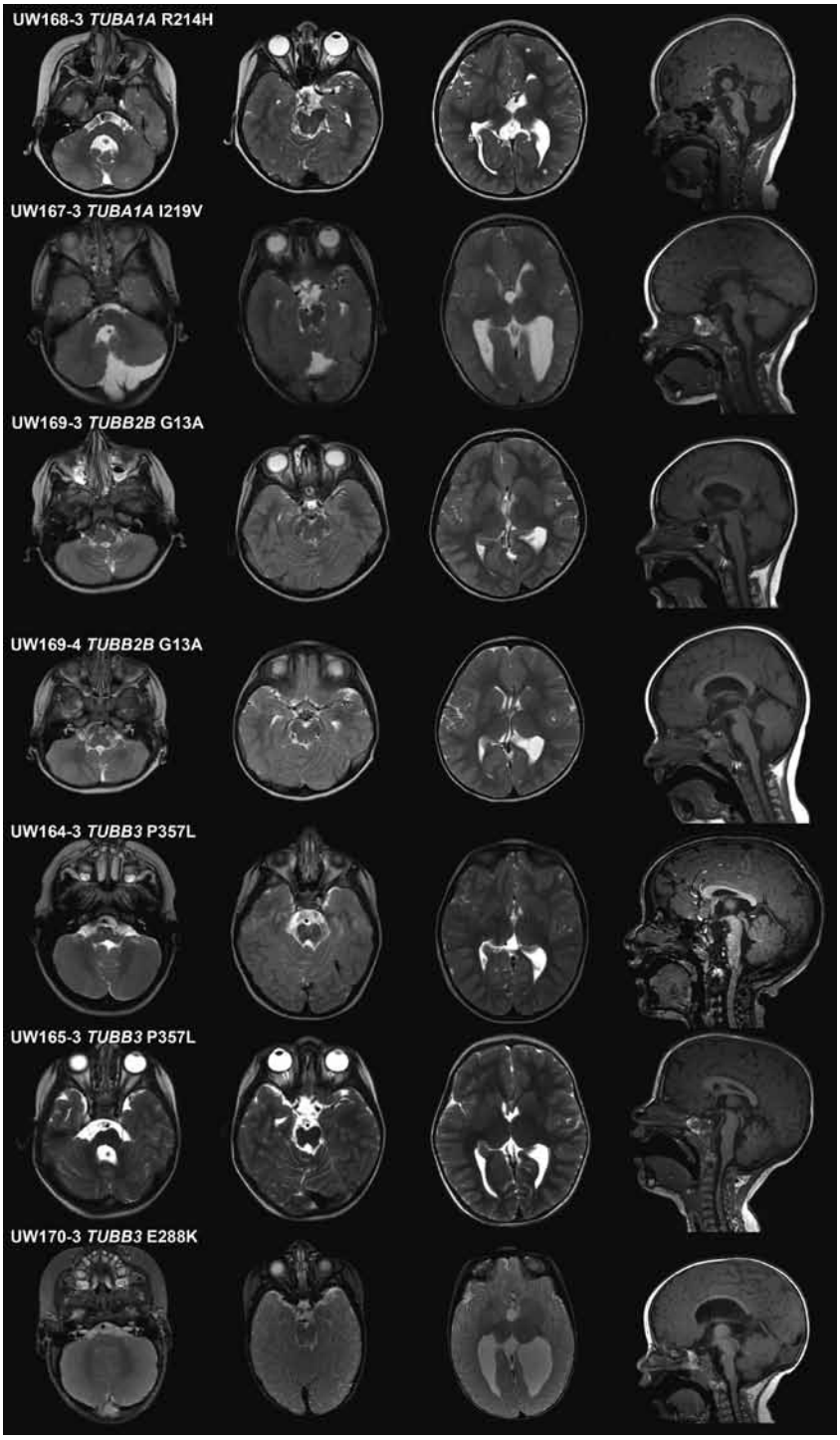

Figure 1. Brain imaging of mutation-positive patients.

CADD scores were generated for each mutation and previously published disease-associated tubulin gene variants (Supplementary Table 1).[12] The *TUBA1A* mutations associated with the mild phenotype (p.Arg214His, p.Ile219Val and p.Val353Ile), have a lower average CADD score than the *TUBA1A* mutations associated with microlissencephaly, consistent with the difference in severity of the phenotypes (Student's T-test, p=0.04). In contrast, CADD scores for *TUBB2B* and *TUBB3* variants did not differ significantly across phenotypic groups, although the sample sizes are small.

Homology Modelling

Altered amino acids are located in a variety of positions throughout the alpha/beta-tubulin heterodimer (Fig. 2A & Fig. 2B; Table 3), with each substitution affecting highly conserved residues (Supplementary Fig. 5). None of the substitutions are predicted to affect interactions with microtubule-associated proteins (MAPs) that predominantly associate with the external face of microtubule polymers.

TUBA1A: p.Arg214His affects an arginine that is conserved in most human alpha-tubulin isoforms. Positioned on alpha-helix 6 of the alpha-tubulin subunit, Arg214 is on the surface of the protein, within the inter-protofilament interface between an adjacent alpha-tubulin subunit when incorporated within a microtubule polymer. It is also in relative proximity to (but not predicted to associate with) helix 10 of the beta-tubulin within the same heterodimer. p.Ile219Val affects an isoleucine conserved throughout alpha-tubulins. Five amino acids from Arg214, this residue is located within a short loop between two alpha-helices at the interface with an adjacent alpha-subunit of a neighbouring microtubule protofilament. The branched isoleucine side chain does not extend into this interface, but is instead orientated towards the centre of the protein. Ile219 is predicted to form a hydrogen bond with Cys213, however this is preserved when substituted with a valine.

TUBB2B: p.Gly13Ala affects a glycine located on the first alpha-helix, within the core of the beta-tubulin subunit. Hyper conserved through alpha- and beta-tubulins, this residue is positioned within a tight groove between the alpha-helix and the preceding

Figure 1 (opposite page). Brain imaging of mutation-positive patients.
Representative images from brain MRI, each row represents one patient. First – third column axial T2 images, fourth column sagittal midline T1 images. First column, level of the cerebellum and brainstem; brainstem asymmetry (except UW169-3, UW169-4) and enlarged 4th ventricle (black asterisks), normal sized cerebellum (except UW167-3). Second column, level of superior cerebellum showing distinct "diagonal" dysplasia of the foliar pattern. Third column, level of basal ganglia; dysplastic and amorphous basal ganglia in all, also note the irregularities in sulcal depth (dysgyria); representative examples in UW168-3 of shallow sulci (marked by white asterisks) and deep sulci (#). Fourth column; thinning of brainstem in all, hypoplastic vermis (except UW169-3, UW169-4, and UW164-3), abnormal corpus callosum (CC) in three (partial agenesis in UW168-3 and UW167-3, thin CC in UW170-3). See Table 2 for details of imaging by individual.

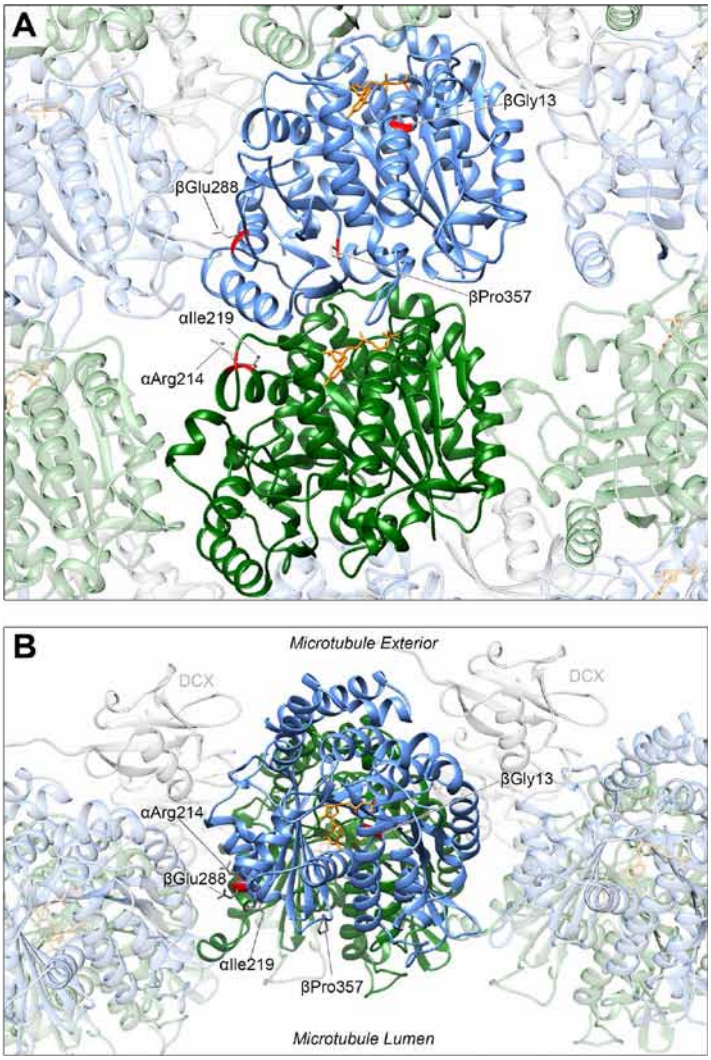

Figure 2. Tubulin variants affect amino acids located in varying regions of the heterodimer. Affected TUBA1A residues (Arg214 & Ile219) are highlighted on an alpha-tubulin protein subunit (green) and TUBB2B Gly13 and TUBB3 Glu288 & Pro357 on a beta-tubulin subunit (blue) as part of a heterodimer incorporated into a microtubule polymer lattice depicted from (A) within the microtubule polymer and (B) from above. TUBA1A Arg214 & Ile219 and TUBB3 Glu288 & Pro357 residues are located at the surface of the heterodimer, whilst TUBB2B Gly13 is buried within the beta-tubulin subunit. αArg214 is positioned towards, but not predicted to directly interact with, both the longitudinal intradimer (between residues of the same heterodimer) and lateral inter-protofilament (adjacent subunits) interfaces. βGlu288 is also positioned at an interface between an adjacent protofilament subunit but with no direct interaction predicted. When incorporated into a polymer, the βPro357 residue faces into the microtubule lumen. It is not predicted to have lateral or longitudinal contact with neighbouring subunits. Due to their location, none of the affected residues are predicted to affect interaction with microtubule-associated proteins that predominantly associate with the exterior surface of the polymer lattice, as demonstrated by DCX in the model (grey).

beta-strand, facilitated by glycine's lack of side chain (Supplementary Fig. 6). As a result of the substitution, the side chain of the resulting alanine is predicted to protrude into the groove. The surrounding residues at the end of the first beta-strand and beginning of the helix are involved in direct interaction with a guanosine nucleotide (GTP/GDP) bound at the Exchangeable (E)-site of the beta-tubulin [28]. Consequently, further subtle changes are predicted in the orientation of additional side chains involved with nucleotide binding, especially Gln11 & Cys12.

TUBB3: p.Glu288Lys is located within the 9th alpha-helix of the beta-tubulin subunit. When incorporated within a microtubule polymer, the acidic glutamate side chain is orientated laterally towards a beta-tubulin subunit of an adjacent protofilament. This residue is conserved through both alpha- and beta-tubulins, and substitution with a basic lysine residue is predicted to disrupt two putative hydrogen bonds between Glu288 and Thr285 within the same subunit (Supplementary Fig. 7). TUBB3, p.Pro357Leu affects one of two neighbouring prolines in a loop between beta-strands 9 and 10 of the beta-tubulin subunit. When incorporated within polymer lattice, Pro357 faces into the microtubule lumen (Fig. 2B). This residue is not predicted to interact with longitudinal or laterally adjacent tubulin subunits.

Table 3. Summary of homology modelling and functional analysis

Gene	Variant	In silico	Conservation	In vitro consequences
TUBA1A	p.Arg214His (c.641G>A)	Alpha-helix 6. Within intradimer and interprotofilament interfaces	αArg214 conserved in most alpha-tubulin isoforms	Incorporates into microtubules but at a reduced rate following cold-induced depolymerisation
	p.Ile219Val (c.655A>G)	Loop between alpha-helices 6 & 7.	αIle219 conserved throughout alpha-tubulin isoforms	Not determined
TUBB2B	p.Gly13Ala (c.38G>C)	Alpha-helix 1. Within beta-tubulin core. 3 predicted H-bonds between β-subunit and GDP disrupted.	βGly13 hyper conserved in both beta- and alpha-tubulin isoforms	Reduced Incorporation into microtubules
TUBB3	p.Glu288Lys (c.862G>A)	Alpha-helix 9. Within interprotofilament interface. Loss of 2 H-bonds with Thr285 (intrasubunit) predicted.	βGlu288 conserved in beta- and most alpha-tubulin isoforms	Does not incorporate into microtubules
	p.Pro357Leu (c.1070C>T)	Loop between beta-strands 9 & 10. Facing microtubule lumen.	βPro357 hyper conserved in both beta- and alpha-tubulin isoforms	Does not incorporate into microtubules

Effect of tubulin gene variants on microtubule incorporation and polymerisation in vitro

To investigate the *in vitro* functional consequences of tubulin gene variants identified, wild-type and variant *TUBA1A*, *TUBB2B* and *TUBB3* constructs were transiently-expressed in HEK293 cells and immunocytochemically stained with antibodies specific to endogenous and transgenic tubulin. Mutations had variable effects on co-assembly with endogenous alpha- or beta-tubulin subunits and incorporation into microtubule polymers (Fig. 3 & Table 3).

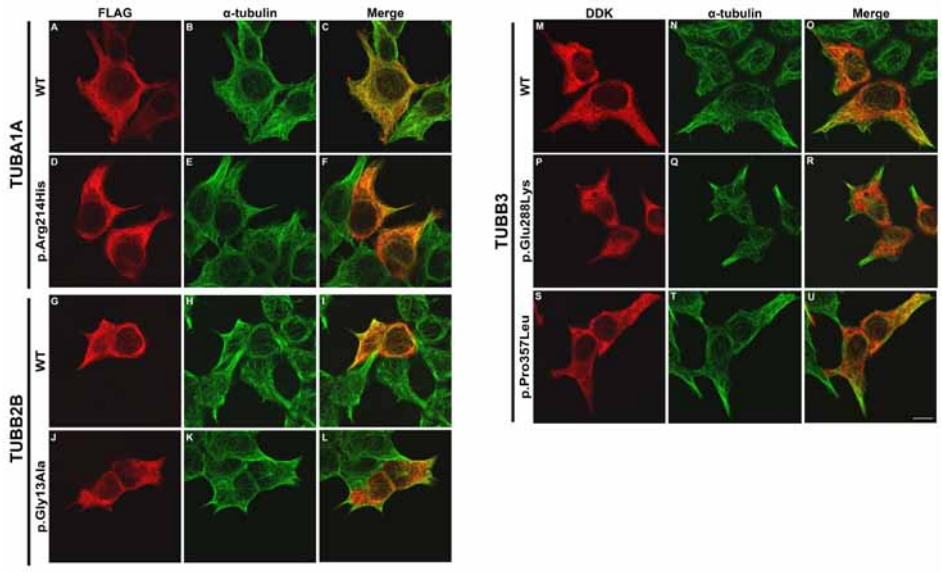

Figure 3. Tubulin gene variants demonstrate varying levels of microtubule incorporation *in vitro*. Wild-type and variant FLAG-tagged *TUBA1A* (A-F), *TUBB2B* (G-L) and DDK-tagged *TUBB3* (M-U) expression constructs were transfected into HEK293 cells to observe incorporation into microtubule polymers during interphase. Cells were fixed for immunocytochemical examination 24h post-transfection, and stained using anti-FLAG (A, D, G, J) or anti-DDK (M, D, G) antibodies to detect the transgenic tubulin, and anti-α-tubulin (B, E, H, K, N, Q, T) to detect the endogenous microtubule network. TUBA1A p.Arg214His successfully incorporates into microtubule polymers, as evident by the presence of fibre-like arrangement in the anti-FLAG channel (D). In comparison to wild-type TUBB2B, p.Gly13Ala also demonstrates integration into microtubules but at a reduced level (J-L); polymer fibres are notably less well-defined in the anti-FLAG channel in comparison to endogenous alpha-tubulin and an increased proportion of the visible p.Gly13Ala beta-tubulin remains unpolymerised in the cell cytoplasm. This is supported by predominantly green polymers observed in the merged cell image (L). Neither TUBB3 p.Glu288Lys nor p.Pro357Leu demonstrate any evidence of microtubule incorporation *in vitro* as indicated by diffuse cytoplasmic staining instead of defined microtubules (M-U). Whereas wild-type TUBB3 can be seen to co-assemble with endogenous alpha-tubulin into microtubule polymers, both variants remain unpolymerised throughout the cell cytoplasm. Images were acquired blind to construct type and are representative of >95% of cells observed. Bar=10μm.

TUBA1A p.Arg214His demonstrates a diminished rate of microtubule reintegration following cold-induced depolymerisation in comparison to wild-type protein (Fig. 4). Despite its ability to polymerise, this suggests that the arginine to histidine substitution subtly perturbs the rate that affected heterodimers integrate into growing microtubules. TUBB2B p.Gly13Ala demonstrates a notable reduction in microtubule incorporation *in vitro*, with very faint polymers visible and the majority of variant beta-tubulin remaining unpolymerised throughout the cell cytoplasm. Neither of the TUBB3 variants demonstrate any signs of microtubule incorporation, as transgenic protein remains diffuse throughout the cell with no polymer arrangement observed.

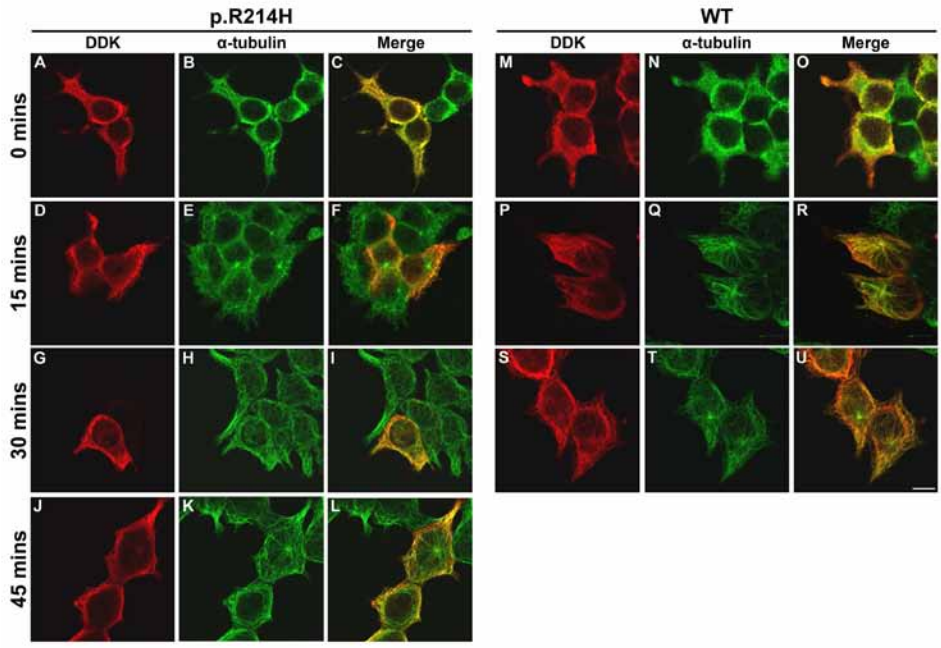

Figure 4. TUBA1A p.Arg214His demonstrates slowed microtubule reincorporation following cold-induced depolymerisation.

To examine the effect of the p.Arg214His amino acid substitution on microtubule dynamics *in vitro*, HEK293 cells expressing wild-type and variant TUBA1A were incubated at 4°C to induce microtubule polymer depolymerisation. After 30 minutes, coverslips were returned to 37°C to promote microtubule re-polymerisation. To observe the rate of microtubule growth in the presence of each construct, cells were removed after 0 (A-C, M-O), 15 (D-F, P-R), 30 (G-I, S-U) and 45 (J-L) minutes of polymer rescue and methanol fixed prior to immunocytochemical staining. Wild-type TUBA1A (M-U) demonstrates reincorporation at a similar rate to endogenous tubulin. After 15 and 30 minutes at 37°C (D-I), microtubule repolymerisation in TUBA1A p.Arg214His-expressing cells can be observed in the endogenous alpha-tubulin channel (E, H), whilst transgenic protein remains unpolymerised with no visible microtubules (D, G). TUBA1A p.Arg214His incorporation is evident after 45 minutes at 37°C (J), however the proportion of variant tubulin appears to be at a markedly lower level than that of endogenous alpha-tubulin (L). Images were acquired blind to construct type and are representative of >95% of cells observed. Bar=10μm.

DISCUSSION

This study describes a highly recognisable pattern of cerebellar dysplasia, brainstem asymmetry and basal ganglia dysplasia without major cortical malformation in 10 patients with developmental delays and eye movement abnormalities. In the majority of tested patients (78%) we identified mutations in *TUBA1A*, *TUBB2B* or *TUBB3* that were either *de novo* or inherited from a mosaic parent. Four out of five mutations identified are novel. Our data add a distinct and recognizable phenotype to the tubulinopathy spectrum, with relatively mild cortical involvement.[12] Although the cohort presented is small, the mutation detection rate suggests that the described pattern of brain abnormalities is highly predictive for tubulin mutations. This detection rate is much higher than any previously published in patients with cortical malformations, ranging from 1-13.3%. [6,8,9,12,13] We expect this number to be higher in selected cohorts of patients with cortical malformations combined with other abnormalities, (e.g. of basal ganglia, corpus callosum) and indeed a detection rate of 30% has been found for the combination of lissencephaly with cerebellar hypoplasia.[6]

Clinical implications

The Baraitser-Winter Neurogenetics Database (www.lmdatabases.com, v 1.0.32) includes 336 conditions encompassing cerebellar vermis hypoplasia or aplasia, making it challenging to identify specific genetic causes in patients with cerebellar malformations. A more detailed understanding of the imaging abnormalities associated with each genetic condition is essential for accurately diagnosing these patients. For example, identifying the characteristic cerebellar dysplasia of the tubulinopathies distinguishes them from other disorders with cerebellar dysplasia that are often autosomal recessive and associated with other medical issues such as hearing loss (Chudley-McCullough syndrome), retinal dystrophy (Poretti-Boltshauser syndrome), muscular dystrophy (dystroglycanopathies), as well as progressive retinal, kidney and liver disease (Joubert syndrome).

While previous studies have not focused on cerebellar abnormalities in tubulinopathies, cerebellar dysplasia has been mentioned in multiple patients (all with cortical malformations), confirming its association with tubulin gene mutations.[11,12,15,16,19] In another study, up to 30% of patients with lissencephaly with cerebellar hypoplasia had mutations in *TUBA1A*, as opposed to only 1% in the classic lissencephaly cohort.[6] It would be interesting to investigate whether cerebellar dysplasia (without hypoplasia) is also a useful diagnostic marker for tubulin mutations in patients with lissencephaly.

While OMA is commonly present in patients with cerebellar abnormalities, OMA has rarely been associated with tubulinopathies, so it is surprising that the majority of our patients presented with gross motor delays and OMA or other impairments of eye movement. In contrast, OMA has only been described in two patients with the distinct

tubulinopathy H-ABC (hypomyelination with atrophy of the basal ganglia and cerebellum) due to *TUBB4A* mutations, and never in patients with *TUBA1A*, *TUBB2B* or *TUBB3* mutations.[21] This may be due to under ascertainment of eye movement abnormalities in patients with severe disability.

Subtle cortical dysgenesis: dysgyria

No findings of lissencephaly, pachygyria, cobblestone cortex, or polymicrogyria (abnormal cortical thickness, irregular cortical surface and grey-white boundary and/or microgyri) were present in the individuals recruited for this study.[29] However we observed abnormal sulci, the majority being shallow, with less frequent areas of sulci extending too deeply into the white matter, the latter predominantly in the perisylvian areas. We therefore consider the terms simplified gyral pattern, polymicrogyria, and polymicrogyria-like cortical dysplasia to be potentially confusing. This is also supported by foetal pathology studies showing atypical features in polymicrogyria-like cortical dysplasia, suggesting a different pathophysiological mechanism from classic polymicrogyria.[11,13] We propose using the term tubulinopathy-associated *dysgyria* for the subtle abnormalities of gyral shape without imaging evidence of lissencephaly, pachygyria, cobblestone cortex, polymicrogyria, or other cortical abnormalities.

Recurrence risk

We identified two affected siblings with a *TUBB2B* mutation, inherited from an asymptomatic father who was found to be mosaic for this mutation. Familial recurrence has previously been described in two sisters with polymicrogyria and a *TUBA1A* mutation with mosaicism in the maternal line.[5] These findings emphasise the importance of careful analysis of the parental sequencing results for evidence of mosaicism and adequate counselling about possible recurrence, as germline mosaicism in a parent can never be fully excluded.

Genotype-phenotype correlations

The same tubulin mutations are frequently observed in unrelated individuals sharing similar brain malformations, e.g. TUBA1A p.Arg264Cys in individuals with characteristic central pachygyria. [3,9,12] Substitutions affecting identical residues but resulting in different amino acids have also produced comparable phenotypes (e.g. TUBA1A p.Arg402Cys and p.Arg402His.[6,12] Consistent with this, in our cohort of patients with strikingly similar MRI findings, we identified one (TUBB3 p.Pro357Leu) mutation in two unrelated patients and a second mutation (TUBB2B p.Gly13Ala) in two siblings. Contrary to this trend, the TUBA1A p.Arg214His variant found in UW168-3 was previously identified in a foetus with a more severe phenotype. [11,12] Other phenotypic dissimilarities have also been described, e.g. *TUBA1A* p.Arg390Cys associated with

both tubulinopathy-associated dysgyria [6] and asymmetrical perisylvian polymicrogyria [10]. While these instances are relatively uncommon, they limit the utility of genotype-phenotype correlations in clinical practice.

The large number of *TUBA1A* mutations that have been identified to date (49 at present), the majority of which are associated with severe brain malformations, makes it possible to evaluate whether *in silico* predictions such as CADD scores correlate with severity of the brain malformation. In fact, the *TUBA1A* variants associated with subtle cortical abnormalities have lower CADD scores than those associated with microlissencephaly, so it may someday be possible to use *in silico* predictions to improve prognostic information for patients and families.

Functional effects of mutations

Our data indicate that mutations in three different tubulin genes lead to a very consistent clinical phenotype, implicating a shared biological mechanism. Surprisingly, the mutations also affect diverse regions of the alpha/beta-tubulin heterodimer, resulting in potential effects on microtubule dynamics, polymer incorporation or guanine nucleotide binding. TUBA1A p.Arg214His was associated with the mildest functional deficit in our *in vitro* pipeline, incorporating into microtubule polymers at comparable levels to wild-type but at a reduced rate. This mild deficit is consistent with the predicted subtle structural effects of TUBA1A p.Arg214His on the alpha-tubulin subunit. Despite residing at the inter-protofilament interface, closer *in silico* inspection suggests neither TUBA1A p.Arg214His nor p.Ile219Val directly affects protein-protein interactions. Interestingly, both variants are in close proximity to a p.Asp218Tyr substitution, previously identified in an individual with lissencephaly.[6] This demonstrates how little one can predict of the resulting phenotype based purely on the affected region of tubulin proteins, as substitutions affecting adjacent residues can result in notably different brain abnormalities.

Structural predictions indicate that TUBB2B p.Gly13Ala affects conserved residues that are part of the nucleotide binding site. GTP hydrolysis at the beta-tubulin subunit is responsible for both polymer incorporation and dynamics.[30] This is consistent with the reduced microtubule incorporation observed *in vitro* and relatively high CADD score, but would be the first association of a mutation potentially affecting guanine nucleotide binding with a mild cerebrocortical phenotype.[12]

As with the *TUBA1A* variants, TUBB3 p.Glu288Lys and p.Pro357Leu substitutions are not predicted to affect specific intra- or intersubunit interactions; however, this observation may be irrelevant, since neither mutant protein incorporates into microtubules *in vitro*. We therefore hypothesise that the p.Glu288Lys and p.Pro357Leu substitutions prevent correct protein processing through one of several possible mechanisms including protein folding, alpha/beta-tubulin heterodimerisation, or subsequent integration into

growing microtubule polymers. This may additionally support the observation by Bahi-Buisson *et al*. that impaired tubulin folding is generally associated with milder cortical phenotypes [12], whilst also emphasising the necessity to support *in silico* predictive modelling with *in vitro* cellular analysis.

Based on our *in vitro* assays, TUBA1A p.Arg214His has the least effect on tubulin polymerization, while TUBB2B p.Gly13Ala has an intermediate effect, and the TUBB3 variants abolish polymerization entirely. The fact that all these mutations lead to the same brain phenotype could be due to a number of different factors, including: 1) a differential requirement for the tubulin proteins during brain development, with TUBA1A being more critical than the beta-tubulins. This may be due to functional redundancy between the different beta-tubulins which are expressed in overlapping patterns during brain development [31]; 2) similar functional effects for all of the mutations. Complete lack of mutant TUBB3 polymerization might result in a similar functional consequence as reduced polymerization of mutant TUBA1A, possibly due to negative effects of mutant TUBA1A incorporated into microtubules; 3) genetic or environmental modifiers contributing to tubulin function and the resulting brain phenotype.

CONCLUSION

In summary, we have identified a highly characteristic combination of cerebellar, brainstem, basal ganglia abnormalities with subtle cortical involvement associated with mutations in three different tubulin genes *TUBA1A*, *TUBB2B* or *TUBB3*. Although tubulin mutations have been commonly associated with severe cortical malformations, this work emphasizes that the cortical involvement can be subtle in patients with more obvious brainstem and basal ganglia involvement. We confirm that a pipeline of *in silico* and *in vitro* work is necessary to add contextual evidence in tubulinopathies and future work will focus on the biochemical and cellular mechanisms by which tubulin mutations disrupt the development of the cortex, basal ganglia, cerebellum and brainstem.

Supplementary Material is available at Human Molecular Genetics online.

ACKNOWLEDGEMENTS

We express our deep appreciation to the patients and families that participated in this work. We also thank Jim Barkovich (University of California, San Francisco, U.S.A.) for helpful discussions of the MRI findings, the cortical abnormalities in particular.

Funding: To M.I.R. lab: National Institute of Social Care and Health Research (NISCHR to M.I.R.), Epilepsy Research UK (ERUK to SK.C. and M.I.R.), and the Waterloo Foundation

(to M.I.R.). To R.O.: EMBO short term fellowship and the Simonsfonds from the Dutch Human Genetics Society (NVHG). To D.D.: University of Washington Pediatrics Department funds and private donations from families of children with brain malformations. The work was also supported by the University of Washington Intellectual and Developmental Disabilities Research Center Genetics Core (National Institutes of Health U54HD083091).

REFERENCES

1. Keays DA, Tian G, Poirier K, Huang GJ, Siebold C, Cleak J, *et al.* Mutations in alpha-tubulin cause abnormal neuronal migration in mice and lissencephaly in humans. Cell. 2007 Jan 12;128(1):45-57.
2. Tischfield MA, Cederquist GY, Gupta ML, Jr., Engle EC. Phenotypic spectrum of the tubulin-related disorders and functional implications of disease-causing mutations. Curr Opin Genet Dev. 2011 Jun;21(3):286-94.
3. Bahi-Buisson N, Poirier K, Boddaert N, Saillour Y, Castelnau L, Philip N, *et al.* Refinement of cortical dysgeneses spectrum associated with TUBA1A mutations. J Med Genet. 2008 Oct;45(10):647-53.
4. Fallet-Bianco C, Loeuillet L, Poirier K, Loget P, Chapon F, Pasquier L, *et al.* Neuropathological phenotype of a distinct form of lissencephaly associated with mutations in TUBA1A. Brain. 2008 Sep;131(Pt 9):2304-20.
5. Jansen AC, Oostra A, Desprechins B, De Vlaeminck Y, Verhelst H, Regal L, *et al.* TUBA1A mutations: from isolated lissencephaly to familial polymicrogyria. Neurology. 2011 Mar 15;76(11):988-92.
6. Kumar RA, Pilz DT, Babatz TD, Cushion TD, Harvey K, Topf M, *et al.* TUBA1A mutations cause wide spectrum lissencephaly (smooth brain) and suggest that multiple neuronal migration pathways converge on alpha tubulins. Hum Mol Genet. 2010 Jul 15;19(14):2817-27.
7. Lecourtois M, Poirier K, Friocourt G, Jaglin X, Goldenberg A, Saugier-Veber P, *et al.* Human lissencephaly with cerebellar hypoplasia due to mutations in TUBA1A: expansion of the foetal neuropathological phenotype. Acta Neuropathol. 2010 Jun;119(6):779-89.
8. Morris-Rosendahl DJ, Najm J, Lachmeijer AM, Sztriha L, Martins M, Kuechler A, *et al.* Refining the phenotype of alpha-1a Tubulin (TUBA1A) mutation in patients with classical lissencephaly. Clin Genet. 2008 Nov;74(5):425-33.
9. Poirier K, Keays DA, Francis F, Saillour Y, Bahi N, Manouvrier S, *et al.* Large spectrum of lissencephaly and pachygyria phenotypes resulting from de novo missense mutations in tubulin alpha 1A (TUBA1A). Hum Mutat. 2007 Nov;28(11):1055-64.
10. Poirier K, Saillour Y, Fourniol F, Francis F, Souville I, Valence S, *et al.* Expanding the spectrum of TUBA1A-related cortical dysgenesis to Polymicrogyria. Eur J Hum Genet. 2013 Apr;21(4):381-5.
11. Fallet-Bianco C, Laquerriere A, Poirier K, Razavi F, Guimiot F, Dias P, *et al.* Mutations in tubulin genes are frequent causes of various foetal malformations of cortical development including microlissencephaly. Acta Neuropathol Commun. 2014;2:69.
12. Bahi-Buisson N, Poirier K, Fourniol F, Saillour Y, Valence S, Lebrun N, *et al.* The wide spectrum of tubulinopathies: what are the key features for the diagnosis? Brain. 2014 Jun;137(Pt 6):1676-700.
13. Cushion TD, Dobyns WB, Mullins JG, Stoodley N, Chung SK, Fry AE, *et al.* Overlapping cortical malformations and mutations in TUBB2B and TUBA1A. Brain. 2013 Feb;136(Pt 2):536-48.
14. Guerrini R, Mei D, Cordelli DM, Pucatti D, Franzoni E, Parrini E. Symmetric polymicrogyria and pachygyria associated with TUBB2B gene mutations. Eur J Hum Genet. 2012 Sep;20(9):995-8.
15. Jaglin XH, Poirier K, Saillour Y, Buhler E, Tian G, Bahi-Buisson N, *et al.* Mutations in the beta-tubulin gene TUBB2B result in asymmetrical polymicrogyria. Nat Genet. 2009 Jun;41(6):746-52.
16. Romaniello R, Arrigoni F, Bassi MT, Borgatti R. Mutations in alpha- and beta-tubulin encoding genes: Implications in brain malformations. Brain Dev. 2015 Mar;37(3):273-80.

17. Romaniello R, Tonelli A, Arrigoni F, Baschirotto C, Triulzi F, Bresolin N*, et al.* A novel mutation in the beta-tubulin gene TUBB2B associated with complex malformation of cortical development and deficits in axonal guidance. Dev Med Child Neurol. 2012 Aug;54(8):765-9.
18. Chew S, Balasubramanian R, Chan WM, Kang PB, Andrews C, Webb BD*, et al.* A novel syndrome caused by the E410K amino acid substitution in the neuronal beta-tubulin isotype 3. Brain. 2013 Feb;136(Pt 2):522-35.
19. Poirier K, Saillour Y, Bahi-Buisson N, Jaglin XH, Fallet-Bianco C, Nabbout R*, et al.* Mutations in the neuronal ss-tubulin subunit TUBB3 result in malformation of cortical development and neuronal migration defects. Hum Mol Genet. 2010 Nov 15;19(22):4462-73.
20. Breuss M, Heng JI, Poirier K, Tian G, Jaglin XH, Qu Z*, et al.* Mutations in the beta-tubulin gene TUBB5 cause microcephaly with structural brain abnormalities. Cell Rep. 2012 Dec 27;2(6):1554-62.
21. Simons C, Wolf NI, McNeil N, Caldovic L, Devaney JM, Takanohashi A*, et al.* A de novo mutation in the beta-tubulin gene TUBB4A results in the leukoencephalopathy hypomyelination with atrophy of the basal ganglia and cerebellum. Am J Hum Genet. 2013 May 2;92(5):767-73.
22. Cushion TD, Paciorkowski AR, Pilz DT, Mullins JG, Seltzer LE, Marion RW*, et al.* De novo mutations in the beta-tubulin gene TUBB2A cause simplified gyral patterning and infantile-onset epilepsy. Am J Hum Genet. 2014 Apr 3;94(4):634-41.
23. O'Roak BJ, Vives L, Fu W, Egertson JD, Stanaway IB, Phelps IG*, et al.* Multiplex targeted sequencing identifies recurrently mutated genes in autism spectrum disorders. Science. 2012 Dec 21;338(6114):1619-22.
24. Kircher M, Witten DM, Jain P, O'Roak BJ, Cooper GM, Shendure J. A general framework for estimating the relative pathogenicity of human genetic variants. Nat Genet. 2014 Mar;46(3):310-5.
25. Mullins JG. Structural modelling pipelines in next generation sequencing projects. Adv Protein Chem Struct Biol. 2012;89:117-67.
26. Prota AE, Bargsten K, Zurwerra D, Field JJ, Diaz JF, Altmann KH*, et al.* Molecular mechanism of action of microtubule-stabilizing anticancer agents. Science. 2013 Feb 1;339(6119):587-90.
27. Fourniol FJ, Sindelar CV, Amigues B, Clare DK, Thomas G, Perderiset M*, et al.* Template-free 13-protofilament microtubule-MAP assembly visualized at 8 A resolution. J Cell Biol. 2010 Nov 1;191(3):463-70.
28. Lowe J, Li H, Downing KH, Nogales E. Refined structure of alpha beta-tubulin at 3.5 A resolution. J Mol Biol. 2001 Nov 9;313(5):1045-57.
29. Barkovich AJ, Raybaud C. Pediatric Neuroimaging. Fifth edition ed. Philadelphia: Lipponcott Williams & Wilkins; 2011.
30. Desai A, Mitchison TJ. Microtubule polymerization dynamics. Annu Rev Cell Dev Biol. 1997;13:83-117.
31. Tischfield MA, Baris HN, Wu C, Rudolph G, Van Maldergem L, He W*, et al.* Human TUBB3 mutations perturb microtubule dynamics, kinesin interactions, and axon guidance. Cell. 2010 Jan 8;140(1):74-87

Chapter 3

Expanding phenotypes

Chapter 3.1

KBG syndrome associated with periventricular nodular heterotopia

Renske Oegema, Rachel Schot, Marie-Claire Y. de Wit, Maarten H. Lequin, Rianne Oostenbrink, Irenaeus F.M. de Coo, Grazia M.S. Mancini

Clinical Dysmorphology 2010;19(3):164-5

INTRODUCTION

KBG syndrome, also known as dento-maxillo-facial syndrome (OMIM 148050), is a rare but well described syndrome of unknown etiology.
Its main features consist of developmental delay, facial dysmorphism, large upper central incisors (macrodontia) and skeletal anomalies. Seizures can also occur. Dominant inheritance with variable expression has been described (Brancati *et al*, 2006).[1]
Periventricular nodular heterotopia (PNH) is a malformation of cortical development characterized by clusters of neurons situated around the cerebral ventricles due to failure of migration to the cortex during development. The causes are heterogeneous including chromosomal, monogenic and exogenous (Andrade, 2009).[2] PNH is associated with epilepsy and developmental delay, but may also remain asymptomatic.
We report on a patient with KGB syndrome and PNH, this combination is to our knowledge not previously reported.

CLINICAL SUMMARY

The propositus, a girl, was born at term after a pregnancy complicated by pre-eclampsia. An emergency caesarian section was performed because of fetal distress. Birth weight was 1895 grams (<p3). She acquired independent walking at age 18 months and spoke her first words at age 12 months. From the age of 3 years, developmental delay was noted by her parents. At the age of 10 years, her TIQ was 69. Her height curve since 12 months of age follows -2 SD, the weight curve between -1 and 0 SD, and head circumference between -2 and -2.5 SD.
On examination at age 10 years she showed brachycephaly, an oval shaped face, a high forehead, lateral sparsity of the eyebrows, a broad nasal tip with hypoplastic flaring nares and a long columnella, macrodontia of the upper central incisors (Fig.1A), a normal palate, and retrognathia. No anomalies of the extremities were noted. Neurological exam revealed no abnormalities besides mild developmental delay.
She is the only child of non-consanguineous Dutch parents. Anamnestically, they have had several miscarriages. The patient's mother has large upper central incisors. She is healthy besides hypertension and has a normal intelligence.

IMAGING

Skeletal maturation was one year delayed on hand X-ray made at age of 10 years. Spinal X-ray revealed failed closure of the arch of the fifth lumbar vertebra and a decreased lumbar lordosis. Skeletal X-rays of the skull, pelvic bones, and chest showed no abnormalities. Macrodontia of central upper incisors is obvious on panoramic radiograph (Fig. 1B).

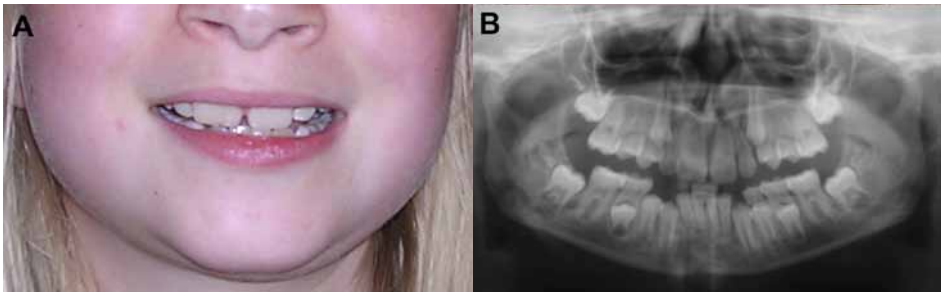

Figure. 1. Note macrodontia of upper incisors; (A) the propositus at age 10 years. Also note broad nasal tip and hypoplastic nares; (B) panoramic radiograph at age 10 years.

On brain MRI performed at age of 11 years periventricular nodular heterotopia at the left lateral ventricle was found. Cortical gyration, central and peripheral CSF spaces were normal (Fig. 2).

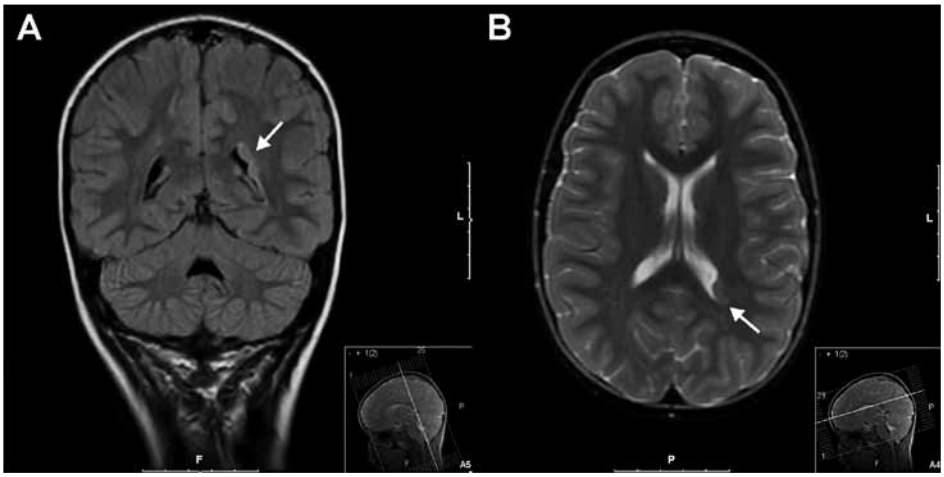

Figure 2. Brain MRI showing unilateral periventricular nodular heterotopia (arrows); (A) coronal FLAIR image and (B) transversal T2-weighted image.

INVESTIGATIONS

Audiogram and tympanometry had normal results. A standard EEG showed a normal background pattern and no epileptic discharges. Cytogenetic analysis in lymphocytes revealed a normal female karyotype (46, XX). Copy number change analysis with Affymetrix Nsp1 250K SNP array did not reveal any submicroscopic chromosomal abnormalities. Metabolic screen in plasma and urine and *Filamin A* sequence analysis were normal.

DISCUSSION

In the propositus, cognitive impairment, dental anomalies, short stature, and skeletal findings suggested the diagnosis of KGB syndrome. We did not detect submicroscopic chromosomal abnormalities as a cause of KBG. In previously published reports, brain anomalies in KBG syndrome were sporadically reported and included hypoplastic cerebellar vermis, enlarged cisterna magna, Chiari malformation type I, meningomyelocele, white matter abnormalities, and microcephaly (Brancati *et al*, 2006, Skjei *et al*, 2007, Kumar *et al*, 2009).[1,3,4] No defect of cortical development has previously been reported in KBG syndrome. PNH may remain asymptomatic but forms a risk factor for epilepsy. The finding of PNH in our propositus indicates that seizures in patients with KBG syndrome may be caused by anomalies of neuronal migration. We suggest that the risk of seizures should be mentioned to families, and that brain MRI should be included in the work-up of KBG patients if there are any abnormal neurological signs or symptoms.

ACKNOWLEDGEMENTS

Authors would like to thank the propositus and her family.

REFERENCES

1. Brancati F, Sarkozy A, Dallapiccola B (2006). KBG syndrome. Orphanet J Rare Dis, 1:50
2. Andrade D (2009). Genetic basis in epilepsies caused by malformations of cortical development and in those with structurally normal brain. Hum Genet, 126(1):173-93
3. Skjei KL, Martin MM, Slavotinek AM (2007). KBG syndrome: report of twins, neurological characteristics, and delineation of diagnostic criteria. Am J Med Gen Part A, 143A:292-300.
4. Kumar H, Prabhu N, Cameron A (2009). KBG syndrome : review of the literature and findings of 5 affected patients. Oral Surg Oral Med Oral Pathol Oral Radiol Endod, 108:e72-e79

Chapter 3.2

Distinctive phenotypic abnormalities associated with submicroscopic 21q22 deletion including *DYRK1A*

Renske Oegema*, Annelies de Klein*, Annemieke J. Verkerk, Rachel Schot, Belinda Dumee, Hannie Douben, Bert Eussen, Lorette Dubbel, Pino J. Poddighe, Ingrid van der Laar, William B. Dobyns, Peter J. van der Spek, Maarten H. Lequin, Irenaeus F.M. de Coo, Marie-Claire Y. de Wit, Marja W. Wessels, Grazia M.S. Mancini

* These authors contributed equally to the manuscript

Molecular Syndromology 2010;1:113–120

ABSTRACT

Partial monosomy 21 has been reported, but the phenotypes described are variable with location and size of the deletion. We present two patients with a partially overlapping microdeletion of 21q22 and a striking phenotypic resemblance.
They both presented with severe psychomotor delay, behavioral problems, no speech, microcephaly, feeding problems with frequent regurgitation, idiopathic thrombocytopenia, obesity, deep set eyes, down turned corners of the mouth, dysplastic ears, and small chin. Brain MRI showed cerebral atrophy mostly evident in frontal and temporal lobes, widened ventricles and thin corpus callosum in both cases, and in one patient evidence of a migration disorder. The first patient also presented with epilepsy and a VSD. The second patient had a unilateral Peters anomaly. Microarray analysis showed a partially overlapping microdeletion spanning about 2.5 Mb in the 21q22.1-q22.2 region including the *DYRK1A* gene and excluding *RUNX1*. These patients present with a recognizable phenotype specific for this 21q22.1-q22.2 locus. We searched literature for patients with overlapping deletions including the *DYRK1A* gene, in order to define other genes responsible for this presentation.

INTRODUCTION

Chromosome 21 has been the subject of extensive studies. Trisomy 21 causing Down syndrome [DS, OMIM #190685] is one of the few trisomy syndromes compatible with life and is common with an incidence of about 1 in 800 live births. However, (partial) monosomy 21 is much rarer and few patients have been reported in literature.[1-22] The region of the monosomy and the phenotype of reported cases are variable. The 21q22 region seems associated with the most severe phenotype exhibiting mental retardation and microcephaly.[23] Disruption of *DYRK1A* (*Drosophila "minibrain"* homologue gene, OMIM *600855) in this region has been associated with microcephaly, mental retardation and dysmorphisms in two patients [24]. Studying similar patients potentially reveals valuable information regarding the function of the chromosome 21 genes.
We present two unrelated individuals with a partial monosomy 21 with strikingly similar facial features giving them a 'moody' appearance, similar brain imaging and a partially overlapping 21q22 microdeletion. This overlapping 2.5 Mb region contains amongst others the *DYRK1A* gene and covers the DS critical region [OMIM #190685]. Combining our data with previously published reports by others, we delineate a recognizable phenotype of chromosome 21q22.1-q22.2 microdeletions including the *DYRK1A* gene.

CLINICAL REPORTS

Patient 1 was referred to our department at 18 months of age. Clinical data are summarized in Table 1. He was born after an uneventful pregnancy at 38 weeks of gestation as the 10th child to non-consanguineous healthy Dutch parents. His birth weight was 2140 grams (-2 SD) and head circumference 31 cm (-2.8 SD). The neonatal period was complicated by cardiac decompensation due to a persistent ductus arteriosus and a perimembranous ventricular septum defect (VSD). The duct closed spontaneously at cardiologic follow-up, the VSD was managed conservatively.
Clinical genetic examination at age 18 months showed micro- and brachycephaly, square forehead, deep-set eyes with long eyelashes, small nose, large pupils, thin lips with down-turned corners of the mouth, micrognathia, large, low-set ears, and weight and head circumference at -4 SD (Fig. 1).
His developmental milestones were delayed. Severe feeding problems and gastro-esophageal reflux necessitated gastric tube feeding and Nissen fundoplication. He suffered from recurrent upper respiratory tract infections and had severe constipation. He developed epilepsy with tonic-clonic seizures requiring antiepileptic drug (AED) therapy.
At follow-up at age 7 years he was severely mentally retarded and exhibited no speech. He had a flat forehead, broad eyebrows extending onto the eyelids, deep-set eyes with

Table 1. Summary of patients described in literature with an 21q22 (micro)deletion including *DYRK1A*

	Patient 1 (this paper)	**Patient 2 (this paper)**	**Bartsch**	**Fujta et al**	**Matsu-moto et al**	**Shinawi et al Patient 3**	**Theodoropoulos et al**	**Yao et al Case 2**	**Yao et al Case 3**
Chromosomal aberration	del(21) (q22.13q22.2) (mosaic)	del(21) (q22.12q22.2)	der(21) t(18;21) (q23;q22.1)	Del(21) (q22.12q22.2)	del(21) (q22.1)	del(21) (q22.1) (mosaic)	del(21) (q22)	del(21) (q22.1)	del(21) (q22.1q22.3) (mosaic)
Deletion size	4.1 Mb	4.2 Mb	> 10.4 Mb <12.1 Mb	3.97 Mb		19.8 Mb		12.87 Mb	12.6 Mb
Sex	M	F	F	M	M	F	F	F	F
MR / DD	Y	Y	Y	Y	Y	Y		Y	Y
IUGR	Y	Y	Y	Y	Y	Y		Y	Y
Height (SD)	<-3 SD	<2.5 SD	-2.5 SD	-3 SD	-1.4 SD				
Obesity	Y	Y	N	N	N				
OFC at birth	<-2.5 SD	<-2.5 SD	-3 SD	-3.2 SD	-1.5 SD		p25		
OFC	-4 SD	-2 SD	-2.3 SD	<p3	-2.5 SD	<p3		Micro-cephaly	Microcephaly
Facial dysmorphism									
Full eyebrows	Y	Y		Y					
Long eyelashes	Y	Y							
Deep-set eyes	Y	Y	Y			Y			
Peri-orbital fullness	Y	Y	Y	Y		Y			
Epicanthal folds	N	Y	N	Y		Y		Y	Y
Hypertelorism				Y		Y			
Deep nasal bridge	Y	Y	Broad			Y	N	Broad	N
Prominent nose					Y				
Anteverted nares	Y	Y	Y						

Table 1. Summary of patients described in literature with an 21q22 (micro)deletion including *DYRK1A* (continued)

	Patient 1 (this paper)	Patient 2 (this paper)	Bartsch	Fujta et al	Matsu-moto et al	Shinawi et al Patient 3	Theodoropoulos et al	Yao et al Case 2	Yao et al Case 3
Featureless/prominent philtrum	Y	Y	Y	N					
Down-turned corners mouth	Y	Y	Y	Y					
Teeth	Decay	Decay, abnormal	Small, widely spaced	Peg-shaped, prominent incisors					
Retro/micrognathia	Y	Y	Y	Y	Y		Y	Y	Y
Low-set/dysplastic ears	Y, large	Y, earpit	Y	Y, earpit	Y	Small ears	Y, cup-shaped, tag	N	Y
Neurology									
Epilepsy/seizures	Y	Y	Y	N		Y		Y	Y
Speech	N	N	N	N		Y			
Brain imaging (MRI if not stated otherwise)	EV, decreased WM, underdeveloped frontal lobes, hypopl. CC	EV, decreased WM, underdeveloped frontal lobes, thin optic chiasm and CC		CTscan: normal		Normal	Ultrasound: germinal matrix bleed, EV, thin CC	CD, CC and WM hypolasia,	CT-scan: hydrocephalus ex vacuo, CD, hypoplasia WM and CC, hypoplasia cerebellum
Other features									
Thrombocytopenia	Y	N		N		Y			
Heart	VSD, Persistent DAB	Persistent DAB	Murmur	N		Murmur	Coarctation aorta, hypoplastic left heart, thick valves, PFO	Unknown defect	Unknown defect

Table 1. Summary of patients described in literature with an 21q22 (micro)deletion including *DYRK1A* (continued)

	Patient 1 (this paper)	**Patient 2 (this paper)**	**Bartsch**	**Fujta et al**	**Matsu-moto et al**	**Shinawi et al Patient 3**	**Theodoropoulos et al**	**Yao et al Case 2**	**Yao et al Case 3**
Extremities	Small hands and feet	Triggerfinger, single palmar crease	Short hands and legs, small flat feet	Thick toenails			Camptodactyly, overlapping fingers		
Miscellaneous	Cryptorchism	Peters anomaly, inverted nipples	Abnormal cervical vertebrae	Hypospadias, corneal cloud-ing, bifid uvula	Short neck	Strabismus, inverted nipples, thin/sparse hair	Microphthalmia, cloudy cornea, short neck, anterior anus, kidney dysplasia, skeletal abnormali-ties	Webbed neck	Webbed neck

Unknown features are left blank. Y= yes, N= no, NA= not applicable, SD= standard deviation, DAB= ductus arteriosus Botalli, CC= corpus callosum, CD= cortical dys-plasia, CT-scan = computed tomopgraphy scan, EV= enlarged ventricles, ITP= idiopathic thrombocytopenia, IUGR= intra-uterine growth retardation, MR/DD= mental retardation/ developmental delay, PFO= patent foramen ovale, PVL= periventricular leukomalacia, VSD= ventricular septum defect, WM= white matter.

long eyelashes, large pupils, wide nasal ridge, large, low-set ears, full cheeks, dental caries, micrognathia, small hands and feet, a sandal gap between 1st and 2nd toes, joint hyperlaxity, pectus excavatum, truncal obesity, and cryptorchism (Fig. 1). His height was 110 cm (-3 SD), weight 20 kg (+1 SD), and head circumference 45.5 cm (-4 SD). Abdominal ultrasound and skeletal X-rays revealed no abnormalities. A post-operative (tonsillectomy) hemorrhage prompted studies of bleeding diathesis, this revealed low platelet counts ranging from 82 – 149 x 10^9 /L (normal range: 199- 369 x10^9/L).
Brain MRI performed at 1 year of age (Fig. 3A, B) showed small frontal lobes, enlarged lateral and third ventricles with high signal of periventricular white matter on T2 weighted images, a thin corpus callosum and brain stem, and delayed myelination.
At two years of age, brain MRI showed similar features, although myelination had progressed.
He died at age 11 of a bronchopneumonia complicated by pulmonary hemorrhage.

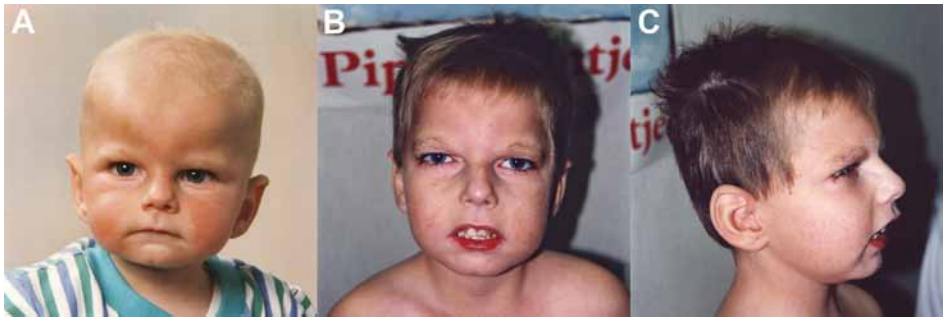

Figure 1. Facial features of patient 1.
(A) Age unknown. Note the full upper eyelids and cheeks, anteverted nares, down-turned corners of the mouth and large ears. (B and C) Age 7 years. Note thick eyebrows, full upper eye lids and cheeks, slightly anteverted nares, down-turned corners of the mouth, dental decay and large, low-set ears.

Patient 2 was referred to our department of Clinical Genetics at the age of 8 months because of progressive microcephaly and dysmorphic features. She was born after an uneventful pregnancy at 42 weeks of gestation as the first child of non-consanguineous healthy Chinese parents. Her birth weight was 2765 grams (-2 SD), length 46 cm (-3 SD) and head circumference 31 cm (-3.5 SD). She had a systolic murmur due to a persistent ductus arteriosus. It has closed spontaneously on follow-up. In infancy she suffered from episodic attacks of blue discoloration of the extremities. She has had two seizures suspect of epilepsy and one EEG showed dubious epileptic activity, requiring AED therapy.
On clinical examination dysmorphic features included square forehead with nevus flammeus, low-set and thick eyebrows, long eyelashes, peri-orbital fullness with deep set eyes, wide nasal ridge, anteverted nares, down-turned corners of the mouth, small

chin, round ears with broad helices and a left-sided ear pit, inverted nipples, a closed sacral dimple, a congenital nevus on the back, a single palmar crease on the left hand, a contracture of the left thumb, deep set nails of the toes, and bilateral short proximally implanted first toes (Fig. 2)

Figure 2. Facial features of patient 2.
(A) Age 8 months. Note the full upper eye lids and cheeks, anteverted nares and down-turned corners of the mouth. (B and C) Age 7 years. Note thick eyebrows, Peters anomaly of the right eye, full upper eye lids and cheeks, anteverted nares and down-turned corners of the mouth, malformed ears and moody expression. (D) Severe dental decay and malshaped teeth.

Her developmental milestones were delayed. She started walking independently at age 2. She suffered from feeding problems which required gastric tube feeding in infancy. During follow-up up to 7 years of age she exhibited severe mental retardation with absent speech, no eye contact, hyperactive behavior and poor interaction with people. Teeth grinding was noted and diffuse dental decay was striking. At that age, her height was 110 cm (-3 SD), weight 25 kg (2.5 SD), and head circumference 48 cm (-2 SD). She has severe constipation.

Ophthalmic examination revealed bilateral hypermetropia, amblyopia of the right eye, and a unilateral corneal opacity area consistent with a Peters anomaly. Her platelet counts were below normal range on two separate occasions, 104 and 137x 10^9/L (normal range: 199- 369 x10^9/L). Craniosynostosis was excluded with a skull X-ray. Congenital CMV-infection was excluded by PCR of neonatal screening blood spot. No skeletal abnormalities were detected.

Brain MRI performed at age 5 months and repeated MRI at age 15 months (Fig. 3C,D) showed cerebral atrophy with deep sulci, mostly evident in frontal and temporal lobes, underdeveloped frontal gyri, a thin corpus callosum with loss of periventricular white matter and widened lateral and third ventricles both at frontal and occipito-temporal areas, a thin brain stem, and no evidence for active demyelination.

Recent brain MRI at age 8 years showed evidence for a periventricular nodular heterotopia located in the frontal horn of the right lateral ventricle. The inferior part of the right frontal cortex is abnormal and suspect for polymicrogryia (Fig. 3E,F).

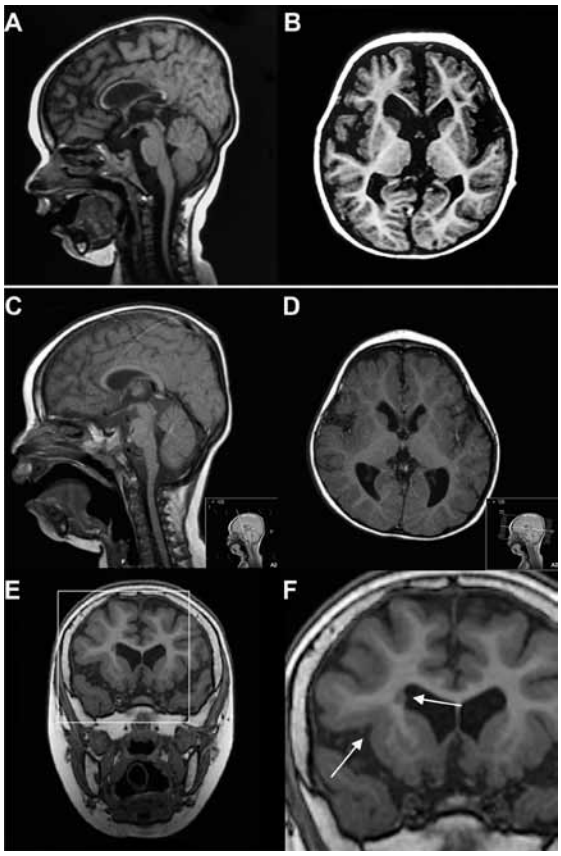

Figure 3. Brain T1 weighted MRI images. (A,B,C, and D) Note cerebral atrophy/underdevelopment of frontal and temporal lobes, widened ventricles including the third ventricle, thin corpus callosum and brain stem. (A) Patient 1, mid sagittal section (B) Patient 1, transversal section (C) Patient 2, midsagittal section (D) Patient 2, transversal section. E,F patient 2, note periventricular nodular heterotopia and area suspect of polymicrogyria in left frontal lobe (E) Coronal section (F) Magnification of E, upper arrow points to heterotopia, lower arrow points to area suspect of polymicrogyria.

CYTOGENETIC AND MICROARRAY RESULTS

Routine cytogenetic analysis of patients 1 and 2 revealed a normal karyotype. DNA of the patients was hybridized to Affymetrix 250K SNP arrays according to the Affymetrix standard protocol for the GeneChip Mapping 250K NspI arrays. Copy number analysis using the Copy Number Analyzer for GeneChip (CNAG) v3.0 [25] indicated in patient 1 a 4.1 Mb deletion (arr 21q22.13q22.2(37053718-41102161 [hg18]x1, see Fig. 4). In patient 2, a 4.2 Mb deletion (arr 21q22.12q22.2(35337577-39585051 [hg18])x1) was observed, (Fig. 4). In both cases parental DNA analysis by quantitative PCR showed a *de novo* origin of the deletion. The deletions were confirmed by fluorescent in situ hybridization (FISH) with chromosome 21 BAC clones (RP11-166F15 absent, RP1-63H24 present). Analysis of the B allele ratio of the Affymetrix array in Nexus Copy Number software (Biodiscovery) revealed the possibility that in patient 1 the deletion was present in mosaic form in leukocyte DNA. Additional FISH analysis confirmed the mosaic in cultured lymphocytes where 50% of the nuclei showed the presence of two normal copies of chromosome 21. In order to define the deletion breakpoint in patient 2 more precisely, qPCR experiments were performed on patient DNA (primer sequences

available on request). This resulted in refinement of the borders, defining the deletion from basepair 35346296 to 39576472 (NCBI built 36.3), and, using extra- and intragenic probes *RUNX1* was excluded from the proximal end of the deletion.
The deletion areas of the two patients partially overlap from base pair 37053718 to 39585051 spanning 2.5 Mb on chromosome 21q22.13q22.2 , encompassing 27 genes (15 protein coding genes, 3 non-protein coding gene, 4 pseudogenes and 5 hypothetical genes) according to the NCBI and Ensembl database annotations build 36.3 (Table 2). The *DYRK1A* gene, previously associated with neurodevelopmental anomalies and microcephaly [24], is included in the shared deletion area.

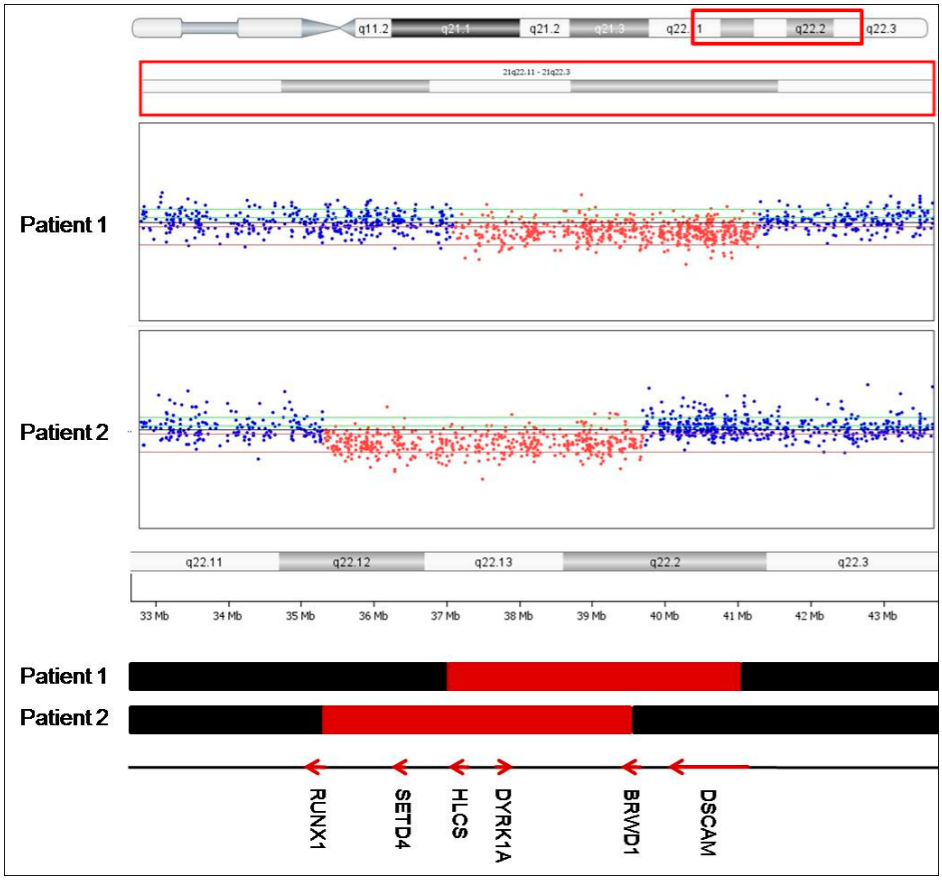

Figure 4. Array results.
Under the schematic representation of chromosome 21 the actual results in the 21q22.11-q22.3 region of the two 250K SNP arrays are shown. In the bottom panel the overlapping segments and several genes in the area are depicted.

Table 2. Known genes in overlapping deletion area

Gene symbol	Name	OMIM
HLCS	Holocarboxylase synthethase	609018
DSCR6	Down syndrome critical region gene 6	609892
PIGP	Phosphatidylinositol glycan anchor biosynthesis, class P	605938
TTC3	Tetratricopeptide repeat domain 3	602259
DSCR9	Down syndrome critical region gene 9	-
DSCR3	Down syndrome critical region gene 3	605298
DYRK1A	Dual-specificity tyrosine- (Y)- phosphorylation regulated kinase 1A	600855
KCNJ6	Potassium channel, inwardly rectifying, subfamily J, member 6	600877
DSCR4	Down syndrome critical region gene 4	604829
DSCR8	Down syndrome critical region gene 8	-
DSCR10	Down syndrome critical region gene 10	-
KCNJ15	Potassium channel, inwardly rectifying, subfamily J, member 15	602106
ERG	V-ets erythroblastosis virus E26 onco gene homolog	165080
C21orf24	Chromosome 21 open reading frame 24	611723
ETS2	V-ets erythroblastosis virus E26 onco gene homolog 2	164740
AP001042.1	FLJ45139 protein	-
PSMG1	Proteasome assembly chaperone 1 (DSCR2)	605296
BRWD1	Bromodomain and WD repeat domain 1	-

REVIEW OF 21Q22 DELETIONS INCLUDING *DYRK1A*

Several features have been repeatedly described in partial monosomy 21 including intrauterine and postnatal growth retardation, down-slanting palpebral fissures, low-set ears, arthrogryposis-like signs, hypertonia, heart defect, and mental retardation [19]. In order to delineate a more specific phenotype relating to 21q22 deletions we searched Pubmed, Decipher and Ensembl databases for patients with these deletions. Most of the patients reported in literature have microscopic deletions with poorly defined breakpoints. We review only those where we can deduce overlap with the 21q22.13q22.2 critical region of our patients and where the phenotypic description is sufficient for comparison. These are summarized in Table 1. The findings are fairly consistent regarding intra-uterine growth retardation (IUGR), microcephaly, mental retardation, seizures, corpus callosum abnormalities and facial features (deep-set eyes, micrognathia, and dysplastic ears).

Of note, also one patient described by Shinawi et al. [26] and one by Yao et al. [20] show the deletion in mosaic form.

DISCUSSION

The two patients presented in this paper show a distinctive phenotype that to our knowledge has not previously been recognized in patients with 21q22 deletions. They

exhibit severe mental retardation with absence of speech, microcephaly, short stature, and distinct cerebral abnormalities. Their facial features with square forehead, full eyebrows and eyelids, deep-set eyes, broad nasal ridge, and down-turned corners of the mouth are strikingly alike and give them a "moody" appearance. Brain MRI findings are quite similar in the patients, showing underdevelopment of frontal lobes with evidence of a migration disorder in patient 2, deep frontotemporal sulci, large lateral and third ventricles, loss of periventricular white matter, callosal dysgenesis and thin brain stem. The low resolution MRI of patient 1 did not allow recognition of minor cortical malformations.

Because of their resembling features, it is likely that genes in their common deleted area are causative of their phenotype. *DYRK1A* [OMIM 600855] maps to chromosome 21q22.13 and is included in the deleted area of both patients. With its location within the Down syndrome critical region, *DYRK1A* has been suggested to play a crucial role in brain alterations both in trisomy and monosomy 21 patients.[27] Møller et al [24] reported two patients with a translocation truncating the *DYRK1A* gene. Both patients exhibited prenatal onset microcephaly, intrauterine growth retardation, feeding problems, developmental delay and seizures. In the first patient retardation was mild, and he had large, low-set ears, long philtrum, and micrognathia. On brain MRI hypogenesis of the corpus callosum was described without other abnormalities. The second patient had severe mental retardation, absent speech, large ears, flat philtrum and a ventricular septum defect. Brain MRI showed enlarged ventricles. The *DYRK1A* gene is the human homolog of the Drosophila *minibrain* gene.[28] It is highly conserved in mammals. In mice, *Dyrk1a* haploinsuffiency leads to a reduced body size with a disproportionate brain reduction, and developmental delay.[29] In particular, underdevelopment of the ventral mid- and hindbrain structures was present in *Dyrk1A*$^{+/-}$ mice. The MRI findings of our patients with large third ventricle, thin corpus callosum and brain stem might relate to the *DYRK1A* haploinsufficiency.

Besides *DYRK1A*, there are 14 protein coding and 3 non-protein coding genes annotated in the common deleted area, each of which might contribute to the phenotype. Six of these are Down-syndrome critical region (DSCR) genes of unknown function. Among the genes with known function, *TTC3*, *KCNJ6* and *BRDW1* are also interesting candidates.

The *TTC3* (tetratricopeptide repeat domain 3) gene is involved in neuronal cell differentiation and particularly in regulation of neurite extension [30], suggesting that absence of *TTC3* could be related to in cognitive problems and brain underdevelopment. The tetratricopeptide domain is also present in kinesins responsible for organization of axonal microtubules and cytoskeleton dynamics and in *KIAA1279*, the gene mutated in Goldberg-Sphrintzen syndrome.[31]

KCNJ6 [OMIM 600877], also known as *GIRK2*, is expressed in the brain and the pancreatic β-cell. Homozygous *GIRK2* missense mutation in *weaver* mice causes severe

cerebellar ataxia and altered behavioral pattern.[32,33] Heterozygous *weaver* mice have a decreased number of surviving granule cells and suffer sporadically from tonic-clonic seizures.[32] Also, homozygous *weaver* mice have decreased levels of circulating IGF-I and responded to GH-treatment.[34] The postnatal growth retardation in our patients might be partially explained by a deficient GH/IGF-I axis, as seen in mutant *weaver* mice.
Mutations in the *RUNX1* gene [OMIM 151385] cause familial platelet disorder with propensity to acute myeloid leukemia [FPD/AML; OMIM 601399]. Shinawi et al [26] reviewed platelet pool storage disease caused by *RUNX1* haploinsufficiency and described multiple problems of microdeletions at 21q22 ascribed to *RUNX1* and *DYRK1A*. Surprisingly, both our patients were diagnosed with low platelet counts, although *RUNX1* is not deleted. Possibly, regulatory elements of *RUNX1* are affected by the deletion or other genes in the critical area are involved in platelet disorders. In mice, regulatory elements have been identified distant (300 kb) from *Runx1*.[35]
Periventricular nodular heterotopia (PNH) are a new finding in 21q22 deletion. PNH is considered a malformation of cortical development. Of note, other cortical malformations, that is polymicrogyria [20,21] and lissencephaly [22], have been associated with 21q deletions. Yao et al [20] propose that an 8.4 Mb region on 21q22.11-q22.3 is associated with cortical dysplasia. However, the large size of this area and lack of break point details make comparison of these patients with ours incomplete.
Our findings suggest that a minimum 2.5 Mb microdeletion at chromosome 21q22.13q22.2 including *DYRK1A* and excluding *RUNX1* is responsible for a characteristic syndrome with recognizable facial features, severe developmental delay, brain abnormalities, IUGR, and eye and platelet abnormalities. Our observation reduces the chromosomal area to which these abnormalities have been previously ascribed, and should encourage high resolution array analysis in patients with a similar phenotype. It could be worthwhile searching for mutations in *DYRK1A* in patients with a similar phenotype in whom microdeletions have been excluded.

ACKNOWLEDGEMENTS

We would like to thank the patients and their families for their cooperation to this manuscript and Ruud Koppenol for kindly providing the figures.

ONLINE RESOURCES

NCBI: http://www.ncbi.nlm.nih.gov/
Decipher: https://decipher.sanger.ac.uk/application/
ECARUCA: http://agserver01.azn.nl:8080/ecaruca/ecaruca.js

REFERENCES

1. Bartsch O, Hinkel GK, Petersen MB, Konig U, Bugge M, Mikkelsen M, Avramopoulos D, Morris M, Antonarakis SE. A large family with subtelomeric translocation t(18;21)(q23;q22.1) and molecular breakpoint in the Down syndrome critical region. Hum Genet. 1997 Oct;100(5-6):669-75.
2. Dobyns WB, Mirzaa G, Christian SL, Petras K, Roseberry J, Clark GD, Curry CJ, McDonald-McGinn D, Medne L, Zackai E, Parsons J, Zand DJ, Hisama FM, Walsh CA, Leventer RJ, Martin CL, Gajecka M, Shaffer LG. Consistent chromosome abnormalities identify novel polymicrogyria loci in 1p36.3, 2p16.1-p23.1, 4q21.21-q22.1, 6q26-q27, and 21q2. Am J Med Genet A. 2008 Jul 1;146A(13):1637-54.
3. Ehling D, Kennerknecht I, Junge A, Prager B, Exeler R, Behre B, Horst J, Schmitt-John T, Bartsch O, Wirth J. Mild phenotype in two unrelated patients with a partial deletion of 21q22.2-q22.3 defined by FISH and molecular studies. Am J Med Genet A. 2004 Dec 15;131(3):265-72.
4. Fryns JP, D'Hondt F, Goddeeris P, van den Berghe H. Full monosomy 21: a clinically recognizable syndrome? Hum Genet. 1977 Jun 30;37(2):155-9.
5. Fujita H, Torii C, Kosaki R, Yamaguchi S, Kudoh J, Hayashi K, Takahashi T, Kosaki K. Microdeletion of the Down syndrome critical region at 21q22. Am J Med Genet A. 2010 Apr;152A(4):950-3.
6. Huret JL, Leonard C, Chery M, Philippe C, Schafei-Benaissa E, Lefaure G, Labrune B, Gilgenkrantz S. Monosomy 21q: two cases of del(21q) and review of the literature. Clin Genet. 1995 Sep;48(3):140-7.
7. Joosten AM, De Vos S, Van Opstal D, Brandenburg H, Gaillard JL, Vermeij-Keers C. Full monosomy 21, prenatally diagnosed by fluorescent in situ hybridization. Prenat Diagn. 1997 Mar;17(3):271-5.
8. Korenberg JR, Kalousek DK, Anneren G, Pulst SM, Hall JG, Epstein CJ, Cox DR. Deletion of chromosome 21 and normal intelligence: molecular definition of the lesion. Hum Genet. 1991 Jun;87(2):112-8.
9. Krasikov N, Takaesu N, Hassold T, Knops JF, Finley WH, Scarbrough P. Molecular and cytogenetic investigation of complex tissue-specific duplication and loss of chromosome 21 in a child with a monosomy 21 phenotype. Am J Med Genet. 1992 Jun 1;43(3):554-60.
10. Lindstrand A, Malmgren H, Sahlen S, Schoumans J, Nordgren A, Ergander U, Holm E, Anderlid BM, Blennow E. Detailed molecular and clinical characterization of three patients with 21q deletions. Clin Genet. 2010 Feb;77(2):145-54.
11. Lyle R, Bena F, Gagos S, Gehrig C, Lopez G, Schinzel A, Lespinasse J, Bottani A, Dahoun S, Taine L, Doco-Fenzy M, Cornillet-Lefebvre P, Pelet A, Lyonnet S, Toutain A, Colleaux L, Horst J, Kennerknecht I, Wakamatsu N, Descartes M, Franklin JC, Florentin-Arar L, Kitsiou S, Ait Yahya-Graison E, Costantine M, Sinet PM, Delabar JM, Antonarakis SE. Genotype-phenotype correlations in Down syndrome identified by array CGH in 30 cases of partial trisomy and partial monosomy chromosome 21. Eur J Hum Genet. 2009 Apr;17(4):454-66.
12. Matsui I, Yamamoto Y, Kuroki Y. [Down's syndrome and its countertype (21q-)]. Nihon Rinsho. 1978 May;Suppl:1452-3.
13. Matsumoto N, Ohashi H, Tsukahara M, Kim KC, Soeda E, Niikawa N. Possible narrowed assignment of the loci of monosomy 21-associated microcephaly and intrauterine growth retardation to a 1.2-Mb segment at 21q22.2. Am J Hum Genet. 1997 Apr;60(4):997-9.

14. Mori MA, Lapunzina P, Delicado A, Nunez G, Rodriguez JI, de Torres ML, Herrero F, Valverde E, Lopez-Pajares I. A prenatally diagnosed patient with full monosomy 21: ultrasound, cytogenetic, clinical, molecular, and necropsy findings. Am J Med Genet A. 2004 May 15;127A(1):69-73.
15. Pellissier MC, Philip N, Voelckel-Baeteman MA, Mattei MG, Mattei JF. Monosomy 21: a new case confirmed by in situ hybridization. Hum Genet. 1987 Jan;75(1):95-6.
16. Theodoropoulos DS, Cowan JM, Elias ER, Cole C. Physical findings in 21q22 deletion suggest critical region for 21q- phenotype in q22. Am J Med Genet. 1995 Nov 6;59(2):161-3.
17. Tuschl K, Fritz B, Herle M, Fonatsch C, Bodamer OA. Trisomy 1q42.3-qter and monosomy 21q22.3-qter associated with ear anomaly, facial dysmorphology, psychomotor retardation, and epilepsy: delineation of a new syndrome. Am J Med Genet A. 2007 Sep 1;143A(17):2065-9.
18. Holbek S, Friedrich U, Brostrom K, Petersen GB. Monosomy for the centromeric and juxtacentromeric region of chromosome 21. Humangenetik. 1974;24(3):191-5.
19. Chettouh Z, Croquette MF, Delobel B, Gilgenkrants S, Leonard C, Maunoury C, Prieur M, Rethore MO, Sinet PM, Chery M, et al. Molecular mapping of 21 features associated with partial monosomy 21: involvement of the APP-SOD1 region. Am J Hum Genet. 1995 Jul;57(1):62-71.
20. Yao G, Chen XN, Flores-Sarnat L, Barlow GM, Palka G, Moeschler JB, McGillivray B, Morse RP, Korenberg JR. Deletion of chromosome 21 disturbs human brain morphogenesis. Genet Med. 2006 Jan;8(1):1-7.
21. Beri-Dexheimer M, Latger-Cannard V, Philippe C, Bonnet C, Chambon P, Roth V, Gregoire MJ, Bordigoni P, Lecompte T, Leheup B, Jonveaux P. Clinical phenotype of germline RUNX1 haploinsufficiency: from point mutations to large genomic deletions. Eur J Hum Genet. 2008 Aug;16(8):1014-8.
22. Miller AC, Rashid RM, Muraskas JK. A novel presentation of a rare chromosome 21q22.2 deletion. Clin Dysmorphol. 2009 Jan;18(1):57-8.
23. Yamamoto Y, Ogasawara N, Gotoh A, Komiya H, Nakai H, Kuroki Y. A case of 21q—syndrome with normal SOD-1 activity. Hum Genet. 1979 May 10;48(3):321-7.
24. Moller RS, Kubart S, Hoeltzenbein M, Heye B, Vogel I, Hansen CP, Menzel C, Ullmann R, Tommerup N, Ropers HH, Tumer Z, Kalscheuer VM. Truncation of the Down syndrome candidate gene DYRK1A in two unrelated patients with microcephaly. Am J Hum Genet. 2008 May;82(5):1165-70.
25. Nannya Y, Sanada M, Nakazaki K, Hosoya N, Wang L, Hangaishi A, Kurokawa M, Chiba S, Bailey DK, Kennedy GC, Ogawa S. A robust algorithm for copy number detection using high-density oligonucleotide single nucleotide polymorphism genotyping arrays. Cancer Res. 2005 Jul 15;65(14):6071-9.
26. Shinawi M, Erez A, Shardy DL, Lee B, Naeem R, Weissenberger G, Chinault AC, Cheung SW, Plon SE. Syndromic thrombocytopenia and predisposition to acute myelogenous leukemia caused by constitutional microdeletions on chromosome 21q. Blood. 2008 Aug 15;112(4):1042-7.
27. Song WJ, Sternberg LR, Kasten-Sportes C, Keuren ML, Chung SH, Slack AC, Miller DE, Glover TW, Chiang PW, Lou L, Kurnit DM. Isolation of human and murine homologues of the Drosophila minibrain gene: human homologue maps to 21q22.2 in the Down syndrome "critical region". Genomics. 1996 Dec 15;38(3):331-9.
28. Tejedor F, Zhu XR, Kaltenbach E, Ackermann A, Baumann A, Canal I, Heisenberg M, Fischbach KF, Pongs O. minibrain: a new protein kinase family involved in postembryonic neurogenesis in Drosophila. Neuron. 1995 Feb;14(2):287-301.

29. Fotaki V, Dierssen M, Alcantara S, Martinez S, Marti E, Casas C, Visa J, Soriano E, Estivill X, Arbones ML. Dyrk1A haploinsufficiency affects viability and causes developmental delay and abnormal brain morphology in mice. Mol Cell Biol. 2002 Sep;22(18):6636-47.
30. Berto G, Camera P, Fusco C, Imarisio S, Ambrogio C, Chiarle R, Silengo L, Di Cunto F. The Down syndrome critical region protein TTC3 inhibits neuronal differentiation via RhoA and Citron kinase. J Cell Sci. 2007 Jun 1;120(Pt 11):1859-67.
31. Brooks AS, Bertoli-Avella AM, Burzynski GM, Breedveld GJ, Osinga J, Boven LG, Hurst JA, Mancini GM, Lequin MH, de Coo RF, Matera I, de Graaff E, Meijers C, Willems PJ, Tibboel D, Oostra BA, Hofstra RM. Homozygous nonsense mutations in KIAA1279 are associated with malformations of the central and enteric nervous systems. Am J Hum Genet. 2005 Jul;77(1):120-6.
32. Patil N, Cox DR, Bhat D, Faham M, Myers RM, Peterson AS. A potassium channel mutation in weaver mice implicates membrane excitability in granule cell differentiation. Nat Genet. 1995 Oct;11(2):126-9.
33. Pravetoni M, Wickman K. Behavioral characterization of mice lacking GIRK/Kir3 channel subunits. Genes Brain Behav. 2008 Jul;7(5):523-31.
34. Yao W, Bethin K, Yang X, Zhong J, Lee WH. Role of the GH/IGF-I axis in the growth retardation of weaver mice. Endocrine. 2007 Oct;32(2):227-34.
35. Soler E, Andrieu-Soler C, de Boer E, Bryne JC, Thongjuea S, Stadhouders R, Palstra RJ, Stevens M, Kockx C, van Ijcken W, Hou J, Steinhoff C, Rijkers E, Lenhard B, Grosveld F. The genome-wide dynamics of the binding of Ldb1 complexes during erythroid differentiation. Genes Dev. 2010 Feb 1;24(3):277-89.

Chapter 3.3

Asymmetric polymicrogyria and periventricular nodular heterotopia due to mutation in *ARX*

Renske Oegema, Anneke Maat-Kievit, Maarten H. Lequin, Rachel Schot, Veerle M.H. Nanninga- van den Neste, Marianne E. Doornbos, Marie C.Y. de Wit, Dicky Halley, Grazia M.S. Mancini

American Journal Medical Genetics part A. 2012 Jun;158A(6):1472-6

ABSTRACT

Mutations in the *ARX* gene, at Xp22.3, cause a broad spectrum of disorders, including infantile spasms, X-linked lissencephaly with abnormal genitalia (XLAG), callosal agenesis and isolated intellectual disability. Genotype/phenotype studies suggested that polyalanine tracts expansion is associated with non-malformative phenotypes, while missense and nonsense mutations cause cerebral malformations, however, patients with structural normal brain and missense mutations have been reported. We report on a male patient born with cleft lip and palate who presented with infantile spasms and hemiplegia. MRI showed agenesis of corpus callosum (ACC), an interhemispheric cyst, periventricular nodular heterotopia (PVNH), and extensive left frontal polymicrogyria (PMG). Sequencing of the *ARX* gene in the patient identified a six basepair insertion (c.335ins6, exon 2). The insertion leads to a two-residue expansion of the first polyalanine tract and was described previously in a family with non-syndromic X-linked mental retardation. To our knowledge, *ARX* mutation causing PMG and PVNH is unique, but the spasms and ACC are common in *ARX* mutations. Clinicians should be aware of the broad clinical range of *ARX* mutations, and further studies are necessary to investigate the association with PMG and PVNH and to identify possible modifying factors.

INTRODUCTION

The *ARX* gene (Aristaless-related homeobox, X-linked, OMIM *300382) encodes a homeodomain transcription factor. These factors play crucial roles in cerebral development and patterning.[1] The broad range of disorders associated with mutations in the *ARX* gene, at Xp22.3, includes X-linked infantile spasms, X-linked lissencephaly with abnormal genitalia (XLAG), agenesis of corpus callosum with abnormal genitalia, and isolated X-linked non-syndromic intellectual disability (NSID).[2] The most severe forms are hydranencephalic patients [3], but little is known of the mechanisms leading to the different presentations.

Genotype/phenotype studies suggest that polyalanine tract expansions cause non-malformative phenotypes, while loss-of-function mutations and missense mutations located in the homeodomain and near the aristaless domain cause brain malformations.[2,3] However, intra- and interfamilial and genetic heterogeneity is observed [2,4] and several missense mutations have been shown to cause a seizure phenotype without gross structural brain malformations.[5-7]

We report a boy with infantile spasms, polymicrogyria (PMG) and periventricular nodular heterotopia (PVNH), further expanding the spectrum of the *ARX*-related disorders and emphasizing the phenotypic variability of these mutations.

CLINICAL REPORT

The parents of our patient are healthy, non-consanguineous and of Dutch descent. The mother had a spontaneous abortion prior to this pregnancy. Prenatal ultrasound during this pregnancy showed a cleft lip, otherwise the pregnancy was uneventful. The patient was born after 41 weeks and 5 days of gestation, his birth weight was 3190 g (25th percentile), and length 51 cm (25th percentile), OFC at birth was not noted. Delivery was uncomplicated and Apgar scores were 9 and 10, after 1 and 5 minutes, respectively. Right cleft lip and palate were confirmed. Cardiac findings were normal. At age 2 months he developed infantile spasms with the EEG showing unilateral left hypsarrhythmia. He had a severe developmental delay, axial hypotonia, right spastic hemiplegia, and he was unable to sit or stand independently at age 18 months. No dystonic movements were noted at this age.

At age 3.5 months he was a boy with an OFC of 39.5 cm (-1.5 SD), brachycephaly, large anterior fontanel, hypertelorism, unilateral cleft lip and palate extending into the right nostril, "square-shaped" ears, loose nuchal skin, inverted nipples, normal male genitalia, and slight cutis marmorata. He had bilateral ptosis and upgaze paresis (Fig. 1). Ophthalmological examination showed a pigmented ring around the optic nerve, the significance of which is unclear. Brain MRI performed at age 3 months showed several abnormalities: agenesis of corpus callosum, interhemispheric cyst, dilatation of the

anterior left ventricle with periventricular nodular heterotopia (PVNH), and extensive left frontal polymicrogyria (PMG). MRI at age 2 years showed similar abnormalities (Fig. 2) and additionally demonstrated PMG in the right frontal lobe, although less extensive than the left.

His seizures responded inadequately to anti-epileptic therapy (including vigabatrin, ACTH, valproate, levetiracetam, clobazam, and a ketogenic diet). He experienced continued tonic spasms, up to 8 times per day. At age 26 months a functional hemispherectomy was performed, resulting in a dramatic decrease of seizure frequency and improvement of alertness and psychomotor development. No tissue was taken for pathology studies.

Metabolic analysis (plasma amino acids, cholesterol synthesis, acylcarnitine pattern and sialotransferrines; urine amino- and organic acids, sialic acid, imidazoles, guanidinoacetic acid, creatine, and sulfite) gave normal results.

Figure 1. Frontal view of the patient showing lateral downslant of eyebrows, bilateral ptosis, divergent strabismus, hypertelorism, low nasal bridge, and status after repair of right cleft lip.

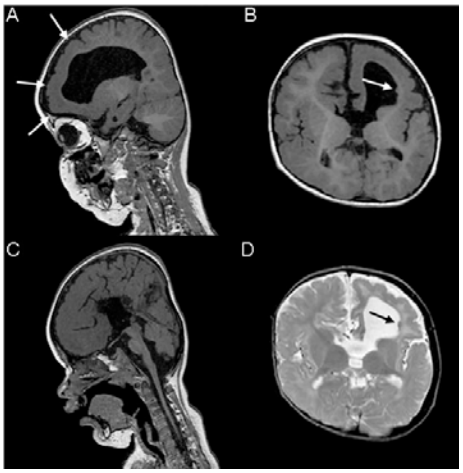

Figure 2. Brain MR imaging of the patient at age 2 years.
(A) sagittal T1-weighted gradient echo image shows extensive left frontal PMG (arrows) and dilated lateral ventricle, (B) transverse T1-weighted gradient echo image shows heterotopia on ventricular wall (arrow), left frontal PMG, and PMG in the right medial anterior part of frontal lobe, (C) sagittal T1-weighted gradient echo image shows absence of corpus callosum. (D) transverse T2-weighted image showing PMG and heterotopia (arrow).

MOLECULAR STUDIES

Routine cytogenetic analysis showed a normal male karyotype (46,XY), and subsequent genomic analysis by Affymetrix 6.0 K SNP array showed no pathogenic copy number variants. Sequencing of the *FLNA* gene was normal. With sequencing of the *ARX* gene, a 6- basepair insertion (335ins6, exon 2) was identified, which is expected to lead to a two alanine residue elongation of the first polyalanine tract. The boy's mother, who is clinically unaffected, was found to be a heterozygous carrier of this insertion.

DISCUSSION

The combination of callosal agenesis and infantile spasms prompted *ARX* analysis in our patient, and a pathogenic mutation was identified. Interestingly, this boy also has PMG and PVNH, not been reported previously in *ARX*. This combination of findings may be coincidental in this boy, but could also be a manifestation of the *ARX* mutation.
The *ARX* gene encodes for 4 polyalanine tracts. Around 60% of known mutations in *ARX* are GCG repeat-encoded polyalanine tract expansions, and in 17 of 97 reported cases the first polyalanine tract is expanded, as in our patient.[2] The 335ins6 mutation (under different nomenclature; c304ins$(GCG)_2$), causes nonsyndromic X-linked mental retardation[1], however, no data on brain imaging of these patients were presented. Another mutation of the first polyalanine tract, the c.304ins$(GCG)_7$ mutation, has been reported in several phenotypes including NSID, Partington syndrome and X-linked infantile spasms.[2,8] The role of the polyalanine tracts in the *ARX* protein is not well understood. Some authors have reported aggregation of the protein in the cytoplasm or nucleus in polyalanine expansion mutations.[2,9] It has been suggested that the severity of the clinical phenotype may reflect increasing length of the expansion [10-12], however, others have reported great intra- and interfamilial variability.[4,13,14]
PMG and PVNH are considered *m*alformations of *c*ortical *d*evelopment (MCD) [15] which are caused by failure of neurons to correctly migrate from the subventricular zone and to organize during fetal development. Evident asymmetric PMG was described in 22q11 microdeletion syndrome and *TUBB2B* mutations but the cause of PMG is heterogenous, genetic and non-genetic.[16,17] Lissencephaly, another form of MCD, is, in combination with ambiguous genitalia (XLAG), a well-recognized disorder due to *ARX* mutations. The role of ARX in neuronal migration has been studied; and in the brain of an *ARX* patient, clusters of immature neurons were found in the white matter [18]; these authors hypothesized that ARX is necessary for the correct tangential migration of preplate GABAergic interneurons derived from the lateral ganglionic eminences. Silencing of *ARX* expression in neural progenitors causes failure of cells to migrate to the cortical plate.[19] *Arx* mutant mice show reduced neuronal migration out of the subventricular zone *in utero*, leading to ectopic periventricular accumulation of neurons [20], which

mimics the human PVNH phenotype. Both PMG and PVNH are not an indication for *ARX* screening and there are no studies systematically screening MCD (except lissencephaly) patients for *ARX* mutations. It would be of interest to perform analysis of the *ARX* gene in more patients with MCD to determine the significance of our finding. Over 1,000 targets of *Arx* have been identified [21], and recently, an 8 alanine expansion of the first polyalanine tract of *Arx* was shown to prevent repression of a subset of *Arx* targets.[22] We hypothesize that genetic variations of *ARX* targets can contribute to the variable phenotype of *ARX* mutations and possibly for the unique aspects of our patient, already suggested for other genes involved in cortical development.[23]
Cleft lip and palate is an uncommon finding in *ARX* patients, but was reported once.[24] This patient also presented with hypertelorism, mental retardation, agenesis of corpus callosum, transsphenoidal encephalocele, and partial anterior hypopituitarism. This phenotype overlaps partly with that of our patient and also shows resemblance to frontonasal dysgenesis. A group of *aristaless-like* homeobox genes (ALX) genes is known to cause "frontonasal dysplasia". Mutations in *ALX3* cause frontorhiny [25] and isolated clefting [26]. Mutations in *ALX4* cause "frontonasal dysplasia" associated with alopecia and genital abnormalities.[27] Recently, *ALX1* mutations were found in patients with a severe form of autosomal recessive "frontonasal dysplasia", with microphthalmia and facial clefting.[28] Post-mortem brain studies of two affected fetuses showed corpus callosum agenesis, cerebellar hypoplasia and neuronal heterotopia of the pons in one.
In conclusion, we report a unique presentation of an *ARX* mutation associated with infantile spasms, PMG, PVNH, and cleft lip/palate. Screening of the *ARX* gene in a cohort of MCD patients with this combination would clarify the significance of our finding. The broad phenotype and inter/intra familial variability observed in *ARX* mutations suggests that other contributing factors, either genetic or environmental, are involved in determination of the phenotype. Identifying the genetic factors among these, e.g. by exome sequencing, in the future will be important for adequate counselling of families with potentially high recurrence risk, for adequate therapy, and for further understanding of brain development.

ACKNOWLEDGEMENTS

The authors are grateful to the family for their collaboration in the preparation of the manuscript. They would like to thank Ruud Koppenol for help with the illustrations.

REFERENCES

1. Bienvenu T, Poirier K, Friocourt G, Bahi N, Beaumont D, Fauchereau F, Ben Jeema L, Zemni R, Vinet MC, Francis F, Couvert P, Gomot M, Moraine C, van Bokhoven H, Kalscheuer V, Frints S, Gecz J, Ohzaki K, Chaabouni H, Fryns JP, Desportes V, Beldjord C, Chelly J. ARX, a novel Prd-class-homeobox gene highly expressed in the telencephalon, is mutated in X-linked mental retardation. Hum Mol Genet. 2002 Apr 15;11(8):981-91.
2. Shoubridge C, Fullston T, Gecz J. ARX spectrum disorders: making inroads into the molecular pathology. Hum Mutat. 2010 Aug;31(8):889-900.
3. Kato M, Das S, Petras K, Kitamura K, Morohashi K, Abuelo DN, Barr M, Bonneau D, Brady AF, Carpenter NJ, Cipero KL, Frisone F, Fukuda T, Guerrini R, Iida E, Itoh M, Lewanda AF, Nanba Y, Oka A, Proud VK, Saugier-Veber P, Schelley SL, Selicorni A, Shaner R, Silengo M, Stewart F, Sugiyama N, Toyama J, Toutain A, Vargas AL, Yanazawa M, Zackai EH, Dobyns WB. Mutations of ARX are associated with striking pleiotropy and consistent genotype-phenotype correlation. Hum Mutat. 2004 Feb;23(2):147-59.
4. Turner G, Partington M, Kerr B, Mangelsdorf M, Gecz J. Variable expression of mental retardation, autism, seizures, and dystonic hand movements in two families with an identical ARX gene mutation. Am J Med Genet. 2002 Nov 1;112(4):405-11.
5. Giordano L, Sartori S, Russo S, Accorsi P, Galli J, Tiberti A, Bettella E, Marchi M, Vignoli A, Darra F, Murgia A, Bernardina BD. Familial Ohtahara syndrome due to a novel ARX gene mutation. Am J Med Genet A. 2010 Dec;152A(12):3133-7.
6. Marsh E, Fulp C, Gomez E, Nasrallah I, Minarcik J, Sudi J, Christian SL, Mancini G, Labosky P, Dobyns W, Brooks-Kayal A, Golden JA. Targeted loss of Arx results in a developmental epilepsy mouse model and recapitulates the human phenotype in heterozygous females. Brain. 2009 Jun;132(Pt 6):1563-76.
7. Scheffer IE, Wallace RH, Phillips FL, Hewson P, Reardon K, Parasivam G, Stromme P, Berkovic SF, Gecz J, Mulley JC. X-linked myoclonic epilepsy with spasticity and intellectual disability: mutation in the homeobox gene ARX. Neurology. 2002 Aug 13;59(3):348-56.
8. Cossee M, Faivre L, Philippe C, Hichri H, de Saint-Martin A, Laugel V, Bahi-Buisson N, Lemaitre JF, Leheup B, Delobel B, Demeer B, Poirier K, Biancalana V, Pinoit JM, Julia S, Chelly J, Devys D, Mandel JL. ARX polyalanine expansions are highly implicated in familial cases of mental retardation with infantile epilepsy and/or hand dystonia. Am J Med Genet A. 2011 Jan;155A(1):98-105.
9. Nasrallah IM, Minarcik JC, Golden JA. A polyalanine tract expansion in Arx forms intranuclear inclusions and results in increased cell death. J Cell Biol. 2004 Nov 8;167(3):411-6.
10. Albrecht A, Mundlos S. The other trinucleotide repeat: polyalanine expansion disorders. Curr Opin Genet Dev. 2005 Jun;15(3):285-93.
11. Kato M, Das S, Petras K, Sawaishi Y, Dobyns WB. Polyalanine expansion of ARX associated with cryptogenic West syndrome. Neurology. 2003 Jul 22;61(2):267-76.
12. Kato M, Saitoh S, Kamei A, Shiraishi H, Ueda Y, Akasaka M, Tohyama J, Akasaka N, Hayasaka K. A longer polyalanine expansion mutation in the ARX gene causes early infantile epileptic encephalopathy with suppression-burst pattern (Ohtahara syndrome). Am J Hum Genet. 2007 Aug;81(2):361-6.
13. Laperuta C, Spizzichino L, D'Adamo P, Monfregola J, Maiorino A, D'Eustacchio A, Ventruto V, Neri G, D'Urso M, Chiurazzi P, Ursini MV, Miano MG. MRX87 family with Aristaless X dup24bp mutation and implication for polyAlanine expansions. BMC Med Genet. 2007;8:25.

14. Partington MW, Turner G, Boyle J, Gecz J. Three new families with X-linked mental retardation caused by the 428-451dup(24bp) mutation in ARX. Clin Genet. 2004 Jul;66(1):39-45.
15. Barkovich AJ, Kuzniecky RI, Jackson GD, Guerrini R, Dobyns WB. A developmental and genetic classification for malformations of cortical development. Neurology. 2005 Dec 27;65(12):1873-87.
16. Jaglin XH, Poirier K, Saillour Y, Buhler E, Tian G, Bahi-Buisson N, Fallet-Bianco C, Phan-Dinh-Tuy F, Kong XP, Bomont P, Castelnau-Ptakhine L, Odent S, Loget P, Kossorotoff M, Snoeck I, Plessis G, Parent P, Beldjord C, Cardoso C, Represa A, Flint J, Keays DA, Cowan NJ, Chelly J. Mutations in the beta-tubulin gene TUBB2B result in asymmetrical polymicrogyria. Nat Genet. 2009 Jun;41(6):746-52.
17. Robin NH, Taylor CJ, McDonald-McGinn DM, Zackai EH, Bingham P, Collins KJ, Earl D, Gill D, Granata T, Guerrini R, Katz N, Kimonis V, Lin JP, Lynch DR, Mohammed SN, Massey RF, McDonald M, Rogers RC, Splitt M, Stevens CA, Tischkowitz MD, Stoodley N, Leventer RJ, Pilz DT, Dobyns WB. Polymicrogyria and deletion 22q11.2 syndrome: window to the etiology of a common cortical malformation. Am J Med Genet A. 2006 Nov 15;140(22):2416-25.
18. Marcorelles P, Laquerriere A, Adde-Michel C, Marret S, Saugier-Veber P, Beldjord C, Friocourt G. Evidence for tangential migration disturbances in human lissencephaly resulting from a defect in LIS1, DCX and ARX genes. Acta Neuropathol. 2010 Oct;120(4):503-15.
19. Friocourt G, Kanatani S, Tabata H, Yozu M, Takahashi T, Antypa M, Raguenes O, Chelly J, Ferec C, Nakajima K, Parnavelas JG. Cell-autonomous roles of ARX in cell proliferation and neuronal migration during corticogenesis. J Neurosci. 2008 May 28;28(22):5794-805.
20. Colombo E, Collombat P, Colasante G, Bianchi M, Long J, Mansouri A, Rubenstein JL, Broccoli V. Inactivation of Arx, the murine ortholog of the X-linked lissencephaly with ambiguous genitalia gene, leads to severe disorganization of the ventral telencephalon with impaired neuronal migration and differentiation. J Neurosci. 2007 Apr 25;27(17):4786-98.
21. Quille ML, Carat S, Quemener-Redon S, Hirchaud E, Baron D, Benech C, Guihot J, Placet M, Mignen O, Ferec C, Houlgatte R, Friocourt G. High-throughput analysis of promoter occupancy reveals new targets for arx, a gene mutated in mental retardation and interneuronopathies. PLoS One. 2011;6(9):e25181.
22. Nasrallah MP, Cho G, Putt ME, Kitamura K, Golden JA. Differential effects of a polyalanine tract expansion in Arx on neural development and gene expression. Hum Mol Genet. 2011 Dec 2.
23. Manzini MC, Walsh CA. What disorders of cortical development tell us about the cortex: one plus one does not always make two. Curr Opin Genet Dev. 2011 Jun;21(3):333-9.
24. Van Esch H, Poirier K, de Zegher F, Holvoet M, Bienvenu T, Chelly J, Devriendt K, Fryns JP. ARX mutation in a boy with transsphenoidal encephalocele and hypopituitarism. Clin Genet. 2004 Jun;65(6):503-5.
25. Twigg SR, Versnel SL, Nurnberg G, Lees MM, Bhat M, Hammond P, Hennekam RC, Hoogeboom AJ, Hurst JA, Johnson D, Robinson AA, Scambler PJ, Gerrelli D, Nurnberg P, Mathijssen IM, Wilkie AO. Frontorhiny, a distinctive presentation of frontonasal dysplasia caused by recessive mutations in the ALX3 homeobox gene. Am J Hum Genet. 2009 May;84(5):698-705.
26. Jugessur A, Shi M, Gjessing HK, Lie RT, Wilcox AJ, Weinberg CR, Christensen K, Boyles AL, Daack-Hirsch S, Trung TN, Bille C, Lidral AC, Murray JC. Genetic determinants of facial clefting: analysis of 357 candidate genes using two national cleft studies from Scandinavia. PLoS One. 2009;4(4):e5385.

27. Kayserili H, Uz E, Niessen C, Vargel I, Alanay Y, Tuncbilek G, Yigit G, Uyguner O, Candan S, Okur H, Kaygin S, Balci S, Mavili E, Alikasifoglu M, Haase I, Wollnik B, Akarsu NA. ALX4 dysfunction disrupts craniofacial and epidermal development. Hum Mol Genet. 2009 Nov 15;18(22):4357-66.
28. Uz E, Alanay Y, Aktas D, Vargel I, Gucer S, Tuncbilek G, von Eggeling F, Yilmaz E, Deren O, Posorski N, Ozdag H, Liehr T, Balci S, Alikasifoglu M, Wollnik B, Akarsu NA. Disruption of ALX1 causes extreme microphthalmia and severe facial clefting: expanding the spectrum of autosomal-recessive ALX-related frontonasal dysplasia. Am J Hum Genet. 2010 May 14;86(5):789-96.

Chapter 3.4

Novel no-stop *FLNA* mutation causes multi-organ involvement in males

Renske Oegema, Jessie M. Hulst, Sabine D.M. Theuns-Valks, Leontine M.A. van Unen, Rachel Schot, Grazia M.S. Mancini, Marguerite E.I. Schipper, Marie C.Y. de Wit, Barbara J. Sibbles, Irenaeus F.M. de Coo, Veerle Nanninga, Robert M.W. Hofstra, Dicky J.J. Halley, Alice S. Brooks

American Journal Medical Genetics part A. 2013 Sep;161A(9):2376-84.

ABSTRACT

Mutations in *FLNA* (Filamin A, OMIM 300017) cause X-linked periventricular nodular heterotopia (XL-PNH). XL-PNH-associated mutations are considered lethal in hemizygous males. However, a few males with unusual mutations (including distal truncating and hypomorphic missense mutations), and somatic mosaicism have been reported to survive past infancy. Two brothers had an atypical presentation with failure to thrive and distinct facial appearance including hypertelorism. Evaluations of these brothers and their affected cousin showed systemic involvement including severe intestinal malfunction, malrotation, congenital short bowel, PNH, pyloric stenosis, wandering spleen, patent ductus arteriosus, atrial septal defect, inguinal hernia, and vesicoureteral reflux. The unanticipated finding of PNH led to *FLNA* testing and subsequent identification of a novel no-stop *FLNA* mutation (c.7941_7942delCT, p.(*2648Serext*100)). Western blotting and qRT-PCR of patients' fibroblasts showed diminished levels of protein and mRNA. This *FLNA* mutation, the most distal reported so far, causes in females classical XL-PNH, but in males an unusual, multi-organ phenotype, providing a unique insight into the *FLNA*-associated phenotypes.

INTRODUCTION

Mutations in *FLNA* (Filamin A, OMIM 300017, Xq28) cause several allelic X-linked disorders, including periventricular nodular heterotopia (XL-PNH), skeletal syndromes (e.g. Melnick-Needles syndrome), cardiac valvular dystrophy, chronic idiopathic intestinal pseudo-obstruction, FG syndrome, and terminal osseous dysplasia.[1-3] Filamin A is widely expressed during development and has an important function in actin cytoskeletal organisation and cell signalling.[4] In a study of PNH patients, *FLNA* mutations were found in 83% of familial and 19% of sporadic cases.[5] Genotype-phenotype correlations exists, and most of PNH patients are females with protein-truncating mutations, which are lethal in males. Rare cases of surviving males have been reported, and they usually presented with seizures and/or PNH [5-10] or (isolated) gastro-intestinal symptoms.[11, 12] In contrast to the disruptive mutations in females, males were mosaic for the mutation or had missense, splice site, or distal truncating mutations.[3, 5, 8, 13] These observations in males point to the obligatory presence of filamin A during human embryonic development.[1]

Here, we present a family where in 3 males and 4 females a novel no-stop *FLNA* mutation (c.7941_7942delCT, p.(*2648Serext*100)) was identified. The family was originally referred because of failure to thrive and facial appearance in the affected males. Their extensive medical history, with unusual multi-systemic presentation, provides a unique insight into the *FLNA*-associated phenotypes.

CLINICAL REPORTS

A pedigree of the family is provided in Figure 1. Informed consent for participation in this study was obtained from all patients, according to the local IRB requirements.

The male propositus (III-1)was born at term as the first child of non-consanguineous Dutch parents. His birth weight was 3200 g (-1 SD). Neonatally, he underwent surgery for pyloric stenosis. Thereafter unexplained feeding difficulties required gastric tube feeding till age 7 months. Evaluation at 2 months, showed a malnourished, normocephalic (0 SD) and hyperteloric (ICD +2 SD) boy who had orbital fullness, a low nasal bridge, broad nasal base, broad mouth, micrognathia, left ear pit, narrow chest, V-shaped sacral dimple, crowded toes (Fig. 2A), an inguinal hernia and a persistent ductus arteriosus (PDA). Appearance became more normal with age (Fig. 2D). He had always had a tendency toward constipation, but from age 4 years, he developed progressive abdominal pain and flatulence. Celiac disease was excluded by duodenal biopsies. At age 6, he was diagnosed with intestinal malrotation and a short small bowel, estimated to be 1/3 of normal length. On a medium chain triglycerides (MCT) diet episodes of abdominal pain and flatulence decreased. Brain MRI at 4 years showed bilateral PNH, partial agenesis of the corpus callosum and a retrocerebellar cyst. A

24-hour EEG registered epileptic activity in the frontal lobes during sleep, although he never had overt seizures. His development is normal.

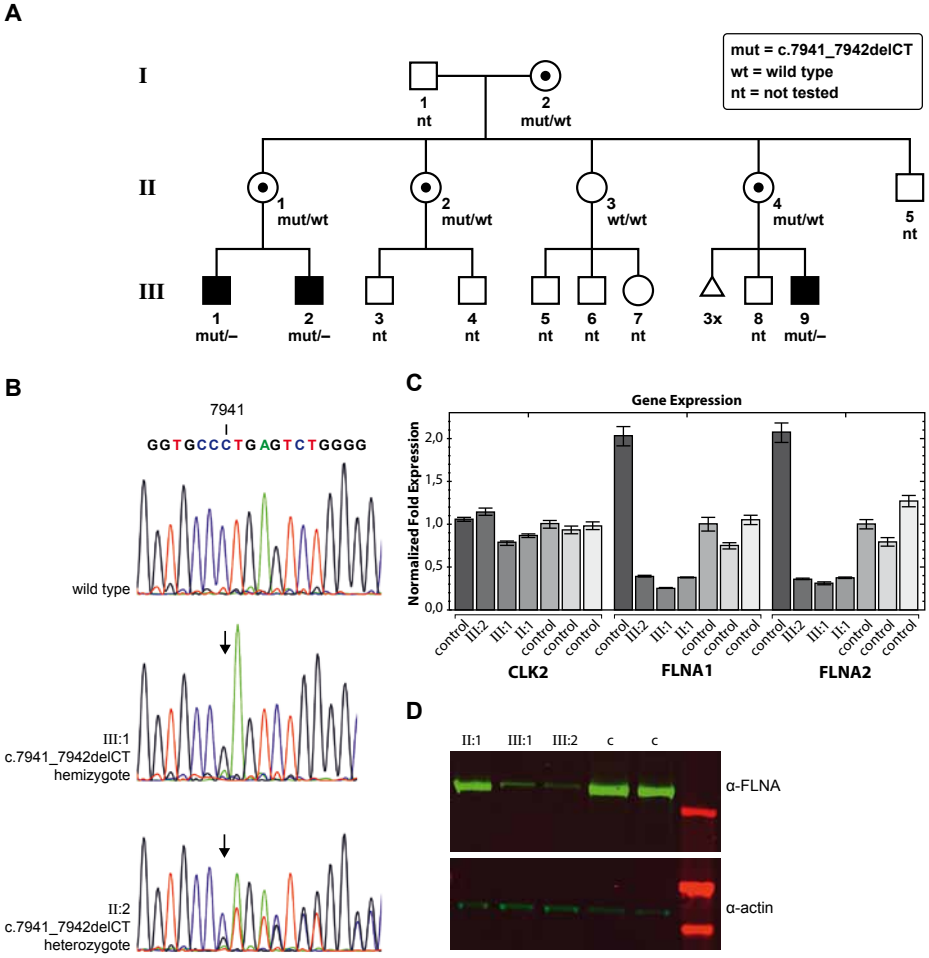

Figure 1.

(A) Pedigree. Black boxes represent affected males, dotted circles represent heterozygous females. (B) Sanger sequencing results showing wild type sequence, hemizygous male (patient III-1) and heterozygous female (patient II-2). Arrow points to first position of the CT deletion (c.7941). (C) Result of qRT-PCR showing *FLNA* expression (normalized to *COPS5* expression) in fibroblast cell lines from patients III-2 (2) , III-1 (3), and II-1 (4); and from four healthy control individuals (1=male, 5=male, 6=female, 7= female). Primers were designed against exon 2-3 (FLNA1) and exon 42-43 (FLNA2).Expression of *FLNA* is significantly lowered in the patients versus controls. *CLK2* expression (housekeeping gene) is normal in all cell lines. (D) Western blot analysis in fibroblasts using FLNA monoclonal antibodies (Abnova, clone 4E10-1B2, diluted 1:1000) showing lowered FLNA expression in male patients (III:1 and III:2) compared to their mother (II-1) and two controls.

His younger brother (III-2) was born at term with a weight 3715 g (0 SD). Neonatally he was diagnosed with vesicoureteral reflux (VUR), a mildly dysplastic mitral valve, and a PDA. He suffered from recurrent upper respiratory tract infections and severe constipation. Hirschsprung disease was excluded by suction rectal biopsy. At age 6 months he presented with colitis due to severe cow's milk protein intolerance, symptoms improved with a diet. Physical examination showed a prominent forehead, hypertelorism (ICD >2SD), orbital fullness, a short nose with anteverted nares, low-set ears, large mouth (rectangular-shaped when crying), crowded toes, deep plantar creases (Fig. 2G-H), longitudinal sacral dimple, and mild pectus excavatum. Hypotonia, drooling, and a mildly delayed motor development were noted. Appearance became more normal with age (Fig. 2B, E). Brain MRI at age 21 months demonstrated bilateral PNH and a retrocerebellar cyst (Fig. 2J, K). He never had seizures and attends regular education. At age 4 he presented acutely with vomiting and upper abdominal pain, peristaltic sounds were indicative of ileus, imaging (contrast radiographs and MRI) showed signs of gastro- intestinal obstruction. On laparotomy, the terminal ileum was distended over a distance of 10 cm, without functional obstruction. Two months later he experienced a similar episode which responded well to conservative therapy. An upper gastrointestinal contrast study showed a short small bowel, estimated 1/3 of normal. He also responded well to a MCT diet. He presented again with acute abdominal pain at age 4.5 years and abdominal ultrasound and CT imaging showed an enlarged and dislocated ("wandering") spleen and multiple accessory spleens (Fig. 2I). Splenopexy was performed successfully.

Their mother (II-1) is healthy. Results of cardiac evaluation (ECG and cardiac ultrasound) were normal.

The proband's cousin (III-9) was born at 38 weeks, weighing 2865 g (-1 SD). During pregnancy his mother (II-4) was on carbamazepine therapy. Feeding difficulties were present from birth and at day 7 he was admitted because of bilious vomiting, diarrhea, and weight loss, requiring tube feeding. Examination (Fig. 2C) showed a malnourished infant with a mildly turricephalic head shape, prominent forehead creases, arched eyebrows, hypertelorism, almond-shaped eyes, a low nasal bridge, anteversion of the nares, broad mouth (rectangular-shaped when crying), abnormal palmar creases, sacral dimple, and a left inguinal hernia. A diagnosis of congenital short bowel and malrotation was made. Shortly thereafter, he deteriorated with progressive vomiting. At laparotomy a malrotated, distended but vital intestine was seen, most likely due to a resolved volvulus. He underwent a Ladd's procedure but feeding problems persisted thereafter with frequent vomiting. At 10 weeks a jejunostomy and gastrostomy were placed and currently at age 5 months he is only partly tolerating enteric feeding and needs additional parenteral nutrition. Jejunal full thickness biopsies showed absence of FLNA immunostaining, without evident structural abnormalities (revised by R. Kapur,

Seattle Children's Hospital). He experienced 2 urinary tract infections. Brain MRI at 2 weeks of age showed PNH, hypoplastic cerebellum and vermis. He was diagnosed with an atrial septal defect (ASD) II. He has frequent episodes of tachypnea with oxygen need, lung CT imaging at age 5 weeks suggested presence of bronchomalacia.
His mother (II-4) has had three miscarriages. Her chromosomes and those of her husband were normal. She presented with seizures during her fourth pregnancy and subsequently PNH was identified on brain MRI. She has hypertelorism, and prolaps of the mitral valve with mild insufficiency.
The proband's maternal aunt (II-2) suffers from mild constipation and uses a SSRI for depression and anxiety. She suffers from joint pains due to "loose ligaments". As a child she had splint therapy because of congenital hip dysplasia. At age 30, she underwent repair of an umbilical hernia. She has downslanting palpebral fissures and small, low-set ears. She complains of palpitations, however results of cardiac examination were normal. A common trunk of the truncus brachiocephalica and the left carotid artery was noted. Brain MRI showed PNH and retrocerebellar cyst (Fig. 2L).
The maternal grandmother (I:2) has an uterus bicornus and has suffered from depressive episodes. Cardiac status was normal. She has mild hypertelorism.

LABORATORY INVESTIGATIONS

Patients III-1 and III-2 both have a normal male karyotype (46,XY). In III-2 results of a telomeric screen, (MLPA MRC Holland, SALSA P036C and P070), FISH analysis of the 22q11 region and routine metabolic investigations were normal. Sanger sequencing of *FLNA* (reference sequence NM_01110556.1) showed a novel two base-pair deletion in exon 48; c.7941_7942delCT, p.(*2648Serext*100)), affecting the stop codon. This no-stop variant is predicted to elongate the coding RNA and create a novel stop codon in the polyadenylation signal of the 3´UTR. Subsequent targeted testing led to identification of this variant in their mother, grandmother, two maternal aunts and their clinically affected cousin (Fig. 1A, B). Skin fibroblast cell lines were obtained from patients III-1 and III-2 and their mother, II-1. Western blot using FLNA monoclonal antibodies (Abnova, clone 4E10-1B2, diluted 1:1000) showed diminished protein levels in fibroblast homogenates from the brothers, compared to their mother's and two independent control cell lines (confirmed in triplicate) (Fig. 1D). QRT-PCR primers were designed against exon 2-3 (Ensembl FLNA_002, forward CATCAAACTGGTGTCCATCGA, reverse GGAGATGGAGTAGTGCAGGATCA) and exon 42-43 (forward TCTTTTGAG-GACCGCAAGGA, reverse CCTCGTTGAACTTGACTGAGACTTC). Expression of mRNA was downregulated in both patients and their mother compared to three unrelated controls, normalized to *COPS5* expression (Fig. 1C).

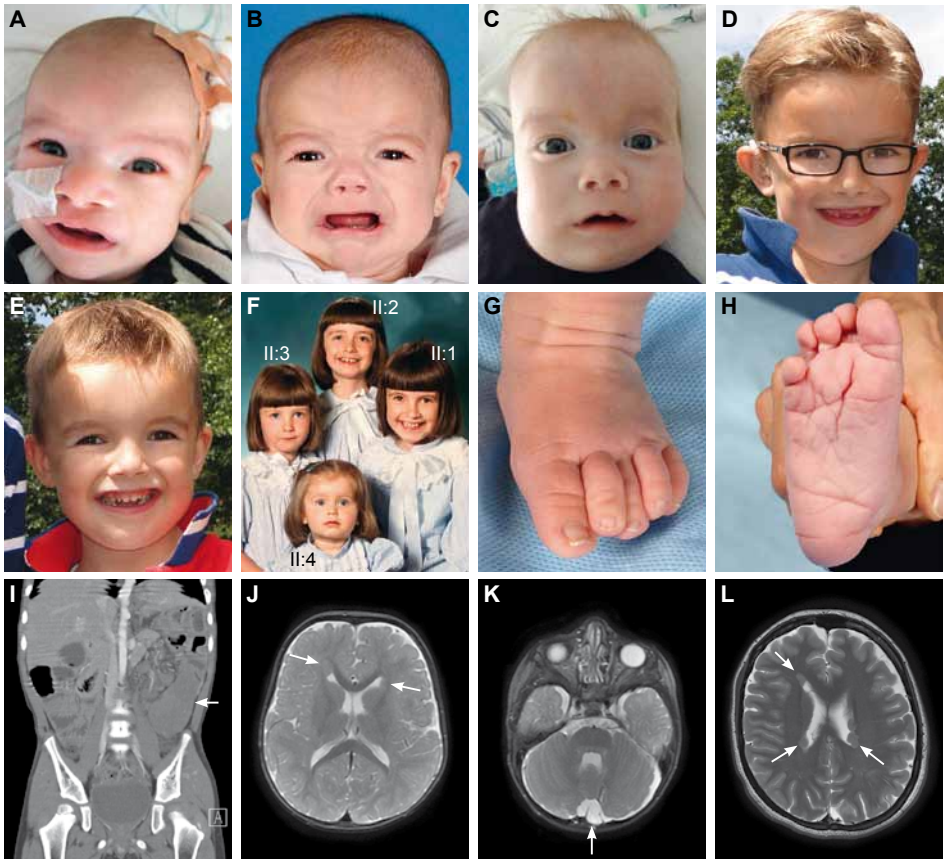

Figure 2.
(A-F) facial appearance of patients. (A) patient III-1, age 2 months with hypertelorism, orbital fullness, broad nasal base, and broad mouth (B) patient III-2, age 3.5 months, showing hypertelorism, orbital fullness, anteverted nares, rectangular-shaped mouth. (C) patient III-9, age 4 months, with hypertelorism, almond-shaped eyes, infra-orbital creases, low nasal bridge, and anteverted nares. (D) patient III-1, age 7. E: patient III-2, age 4. (F) sisters in childhood, only individual II:3 does not carry the mutation. (G, H) foot of patient III-2 with crowded toes and deep plantar creases. (I) Abdominal CT-scan image of patient III-2, arrow points to dislocated spleen. (J-L) brain MRI, T2-weighted images. (J) patient III-2 transverse view, note PNH along frontal horns of lateral ventricles. (K) patient III-2 transversal view shows retrocerebellar cyst. (L) patient II-2, showing PNH along the walls of the lateral ventricles.

DISCUSSION

We describe three boys with a novel *FLNA* variant who have an unusual non-lethal phenotype and atypical presentation with failure to thrive and minor facial anomalies. On examination they had extensive and variable multi-organ involvement including congenital short bowel with malrotation, "wandering spleen", PNH, PDA, and urinary tract abnormalities. Only one of the affected females had presented with seizures and PNH, the others were ascertained through affected relatives. The unanticipated finding

Table 1. Summary of males with *FLNA* mutations surviving past infancy

Reference	Molecular	Neurological	Gastro-intestinal	Cardiovascular	Facial	Miscellaneous
This report (patient 1)	c.7941_7942delCT (no-stop)	PNH, ACC, retrocerebellar cyst	Constipation, bowel malrotation, short small bowel, pyloric stenosis	PDA	Full upper eyelids, hypertelorism, broad mouth, low-set ears, earpit	Irregular toe implant, sacral dimple
This report (patient 2)	c.7941_7942delCT (no-stop)	PNH, retrocerebellar cyst, delayed motor development, hypotonia	Constipation, intestinal pseudoobstruction, short small bowel, milk protein intolerance	PDA, dysplastic mitral valve	Full upper eyelids, hypertelorism, anteverted nares, broad mouth	VUR, irregular toe implant, sacral dimple, URTI
This report (patient 4)	c.7941_7942delCT (no-stop)	hypotonia, PNH, retrocerebellar cyst	Malrotation, short small bowel, intestinal pseudoobstruction.	ASD	Forehead creases, hypertelorism, anteverted nares, broad mouth	Respiratory problems eci, inguinal hernia, sacral dimple
Fitzpatrick et al. 1997 Clayton-Smith et al. 2009 (family 8)	intragenic duplication (exon 4, 11 included)	-	Intestinal pseudoobstruction, malrotation	PDA, ASD	Smooth philtrum, large jaw, low set ears, downslant, hyper-telorism	Thrombocytopenia, cryptorchidism, hydrone-phrosis
Clayton-Smith et al. 2009 (family 9)	intragenic duplication (exon 4, 11 included)	-	Bowel malrotation, intestinal pseudoobstruction	PDA, PFO	No dysmorphic features	SUA, thrombocytopenia
Sheen et al. 2001 (M1)	c.6915C>G (distal nonsense)	PNH, enlarged cisterna magna, seizures	-	-	-	-
Sheen et al. 2001 (M2)	c.1966C>T (missense)	PNH (few), seizures	-	-	-	-
Guerrini et al. 2004	c.304A>G (missense)	PNH, PDA, mega cisterna magna, cerebellar hypoplasia,	-	-	-	cryptorchidism
Guerrini et al. 2004 (family 2)	c.446C>T (missense)	PNH (single nodule)	-	Aortic valve insufficiency	-	-

Table 1. Summary of males with *FLNA* mutations surviving past infancy (continued)

Reference	Molecular	Neurological	Gastro-intestinal	Cardiovascular	Facial	Miscellaneous
Guerrini et al. 2004 (family 3)	c.1692-2A>G (mosaic splice site> skipping of exon 12)	PNH, cerebellar hypoplasia, seizures, IQ 72	-	Aortic aneurysm	-	Bifid epiglottis, pes cavus
Hehr et al. 2006	c.1923C>T (splice site> 2 transcripts)	PNH, retrocerebellar cyst	Poor feeding, severe constipation, malrotation	Septal defect, pulmonary valve prolapse, dysplastic tricuspid valve	Hypertelorism, downslant, low-set posterior rotated ears	Inguinal hernia, clubfoot
Gerard-Blanluet et al. 2006	c.7922C>T (missense)	PNH, polymicrogyria, enlarged ventricles, microcephaly, thin corpus callosum, seizures, IQ 50	-	PDA	Enlarged anterior fontanel	Premature birth
Gargiolo et al. 2007	c.65-66delAC (frameshift affecting long transcript)	Abnormal signal white matter, seizures, spastic diplegia	Intestinal pseudoobstruction, malrotation, short small bowel, pyloric hypertrophy, ileal volvulus, parenteral nutrition	-	-	-
Unger et al. 2007	c.3872C>T (missense)	-	Severe constipation	-	Prominent forehead, frontal upsweep, small mouth, simple ears	-
Kapur 2010 Patient 1	duplication first 28 exons	Partial ACC, PNH, moyamoya disease	Intestinal pseudoobstruction, short small bowel, parenteral nutrition, malrotation, cholelithiasis	PDA, VSD		Cryptorchidism, distended bladder, bifid uvula, anemia, thrombocytopenia with giant platelets
Kapur 2010 Patient 5	c.7021C>T (nonsense)	PNH, posterior fossa arachnoid cyst	Intestinal pseudoobstruction, short small bowel, malrotation	-	Coarse facial features, square face, flat philtrum, wide metopic suture, anchored frenulum, high-arched palate	Diafragmatic hernia, spina bifida occulta, natal tooth, proximally placed thumbs, died at 6 weeks of age

Table 1. Summary of males with *FLNA* mutations surviving past infancy (continued)

Reference	Molecular	Neurological	Gastro-intestinal	Cardiovascular	Facial	Miscellaneous
Parrini et al. 2011 Patient III:2	c.7865_7870del (in-frame deletion)	PNH, CC hypoplasia, mega cisterna magna, hypoplastic cerebellar vermis	-	-	Epicanthic folds, downslanting palpebral fissures, depressed nasal root, anteverted nares, low and rotated ears, flat face	Skeletal abnormalities
Parrini et al. 2011 Patient III:3	c.7865_7870del (in-frame deletion)	PNH, CC hypoplasia, mega cisterna magna	Gut malrotation	-	Epicanthic folds, depressed nasal root, anteverted nares, low and rotated ears, flat face	Hypospadias, cryptorchidism, skeletal abnormalities
Masurel-Paulet et al. 2011	c.994delG (mosaic nonsense)	PN, cerebellar hypoplasia, mega cisterna magna, mild developmental delay, hypotonia	Inability to feed orally	PDA, aortic root dilatation	-	pulmonary emphysema, tracheobronchomalacia, bifid urinary system, supraumbilical hernia, macrothrombocytes
Fergelot 2012 (patient 1)	c.356T>A (mosaic missense)	PNH, mega cisterna magna	-	Aortic regurgitation and root dilatation	-	Died during surgery of bleeding complications
Fergelot 2012 (patient 2)	c.116C>A (missense)	Neonatal convulsions, hemiplegia and seizures after head trauma, asymmetric PNH, mega cisterna magna	-	Prolapse mitral valve, mild aortic regurgitation	Epicanthic folds, telecanthus, anteverted nares, anteverted helices	-
Reinstein 2012 (M1)	c.853C>T (missense)	Seizures, PNH		Prolapse mitral valve	Non-dysmorphic	Thin, doughy skin, joint hypermobility, supraumbilical hernia
Reinstein 2012 (M2)	c.5498_5504delCACCCACinsAC (indel)	PNH, hypoplasia CC, syringomelia	Intestinal malrotation	Dilated aorta, dysplastic valves, tortuous vessels	Non-dysmorphic	Joint laxity, elastic skin
Reinstein 2012 (M3)	c.381G>C (missense)	PNH	-	Thick mitral valve w/ prolapse, dilated aorta	-	Joint hypermobility, pectus carinatum, scoliosis, pneumothrorax, eventration diaphragm

Table 1. Summary of males with *FLNA* mutations surviving past infancy (continued)

Reference	Molecular	Neurological	Gastro-intestinal	Cardiovascular	Facial	Miscellaneous
Reinstein 2012 (M4)	c.387C>G (missense)	PNH	-	Dysplastic valves	-	Cutis laxa
Van der Werf 2012 (family 1)	c.16-17delCT (frameshift affecting long transcript)	No clinical signs	Short small bowel	-	-	-
Van der Werf 2012 (Family 2)	c.16-17delCT (frameshift affecting long transcript)	No clinical signs	Short small bowel	-	-	Synovial lipomatosis

The otopalatodigital syndromes which have a recognizable presentation and isolated cardiovascular disease were not included in the table.
Abrreviations used: ACC= agenesis of corpus callosum, ASD= atrial septum defect, IQ= intelligence quotient, PDA= patent ductus arteriosus, PFO= patent foramen ovale, PNH= periventricular nodular heterotopia, SUA=single umbilical artery, URTI= upper respiratory tract infections, - = not mentioned.

of PNH in the two brothers led to identification of the c.7941_7942delCT no-stop variant. Although variable congenital malformations are associated with *FLNA* mutations, PNH seems to be the most constant finding and therefore provides a valuable clue to diagnosis in these patients. PNH has occurred in females with classic XL-PNH, with MNS-like facial appearance [14, personal observation] and with an Ehlers-Danlos-like joint hypermobility syndrome [15, 16], and in rare surviving males (summarized in Table 1).
Brain MRI is not routinely performed in neurologically normal patients presenting with congenital abnormalities, therefore the frequency of *FLNA* mutations might be underestimated. Table 1, summarizing the phenotypes of surviving males, presents additional symptoms which might lead to consideration of *FLNA* testing in males. Feeding problems, severe constipation and/or intestinal pseudoobstruction are frequent and 5 other patients have been diagnosed with congenital short bowel.[11, 12, 17] The latter is a rare anomaly, and only one other gene for congenital short bowel syndrome, *CLMP*, is known to date.[18] *FLNA* is a second gene to consider in the differential diagnosis, especially in males presenting with additional findings outside the gastrointestinal tract**.** Cardiovascular anomalies are also common, and a number of males have been described with familial isolated polyvalvular cardiac disease.[19, 20] Seldomly, the face is described, but this proved to be of diagnostic value in this family.
Although the *FLNA* mutations in surviving males are non-recurrent, all are relatively mild (e.g. non-truncating or mosaic). The frameshift induced by the c.7941_7942delCT deletion disrupts the original stopcodon, and creates a novel stopcodon 100 amino acids downstream in the 3´UTR polyadenylation signal. This might lead to increased mRNA degradation due to lack of a protective polyA tail, which is supported by the lowered expression we observed in the patients with qRT-PCR experiments. As these males present with a non-lethal phenotype, and Western blot shows residual protein levels, we hypothesize that a small amount of RNA escapes degradation and leads to low levels of functional protein.
Originally, gastro-intestinal features in *FLNA* patients were considered due to impaired gastrointestinal motility because of inadequate migration of neurons to the bowel during embryonic development [11]. However, recently the neurogenic hypothesis was doubted and in five male patients with *FLNA*-related X-linked pseudo-obstruction abnormal layering of the muscularis propria was shown, without abnormalities of the enteric nervous system.[12] Smooth muscle dysfunction might be an explanation for the frequently observed PDA in *FLNA* patients and the pyloric stenosis in patient III-2, yet jejunal biopsies from patient III-9 did not show evident smooth muscle abnormalities. Filamin A has a wide range of functions, and this family shows that its presence is essential for proper development of the gastro-intestinal, cardiovascular, genito-urinary and central nervous system. Clinicians should be aware of the differential diagnosis of acute abdomen in *FLNA* patients, which can include intestinal pseudoobstruction,

malrotation, volvulus, and wandering spleen, whilst chronic abdominal complaints and failure to thrive can be due to a short bowel. The findings in this family together with a few prior reports emphasize the high frequency of gastrointestinal symptoms in these patients, and as this family shows, one diagnosis does not exclude the other. Due to its variable presentation, the prevalence of *FLNA* mutations might very well be underestimated. Testing should be considered in patients presenting with a wide range of symptoms, and this report adds wandering spleen to its presentation. A proper diagnosis makes adequate monitoring of all involved organs possible and informs families of recurrence risks. We suggest a thorough work up of the different organ systems in each (male) patient, including diagnostic workup and careful monitoring of gastrointestinal complaints, a renal ultrasound, and a cardiac examination.

ACKNOWLEDGEMENTS

The authors are grateful for the kind collaboration of the family in this study and to Dr. Raj Kapur, Seattle Children's Hospital, WA, USA for pathology studies. They would like to thank Tom de Vries-Lentsch for assistance with the figures.

ONLINE RESOURCES

Ensembl –www.ensembl.org
OMIM –www.omim.org

REFERENCES

1. Robertson SP. Filamin A: phenotypic diversity. Curr Opin Genet Dev. 2005;15(3):301-7.
2. Sun Y, Almomani R, Aten E, Celli J, van der Heijden J, Venselaar H, et al. Terminal osseous dysplasia is caused by a single recurrent mutation in the FLNA gene. Am J Hum Genet. 2010;87(1):146-53.
3. Unger S, Mainberger A, Spitz C, Bahr A, Zeschnigk C, Zabel B, et al. Filamin A mutation is one cause of FG syndrome. Am J Med Genet A. 2007;143A(16):1876-9.
4. Feng Y, Walsh CA. The many faces of filamin: a versatile molecular scaffold for cell motility and signalling. Nat Cell Biol. 2004;6(11):1034-8.
5. Sheen VL, Dixon PH, Fox JW, Hong SE, Kinton L, Sisodiya SM, et al. Mutations in the X-linked filamin 1 gene cause periventricular nodular heterotopia in males as well as in females. Hum Mol Genet. 2001;10(17):1775-83.
6. Fergelot P, Coupry I, Rooryck C, Deforges J, Maurat E, Sole G, et al. Atypical male and female presentations of FLNA-related periventricular nodular heterotopia. Eur J Med Genet. 2012;55(5):313-8.
7. Gerard-Blanluet M, Sheen V, Machinis K, Neal J, Apse K, Danan C, et al. Bilateral periventricular heterotopias in an X-linked dominant transmission in a family with two affected males. Am J Med Genet A. 2006;140(10):1041-6.
8. Guerrini R, Mei D, Sisodiya S, Sicca F, Harding B, Takahashi Y, et al. Germline and mosaic mutations of FLN1 in men with periventricular heterotopia. Neurology. 2004;63(1):51-6.
9. Parrini E, Ramazzotti A, Dobyns WB, Mei D, Moro F, Veggiotti P, et al. Periventricular heterotopia: phenotypic heterogeneity and correlation with Filamin A mutations. Brain. 2006;129(Pt 7):1892-906.
10. Parrini E, Rivas IL, Toral JF, Pucatti D, Giglio S, Mei D, et al. In-frame deletion in FLNA causing familial periventricular heterotopia with skeletal dysplasia in males. Am J Med Genet A. 2011;155A(5):1140-6.
11. Gargiulo A, Auricchio R, Barone MV, Cotugno G, Reardon W, Milla PJ, et al. Filamin A is mutated in X-linked chronic idiopathic intestinal pseudo-obstruction with central nervous system involvement. Am J Hum Genet. 2007;80(4):751-8.
12. Kapur RP, Robertson SP, Hannibal MC, Finn LS, Morgan T, van Kogelenberg M, et al. Diffuse abnormal layering of small intestinal smooth muscle is present in patients with FLNA mutations and x-linked intestinal pseudo-obstruction. Am J Surg Pathol. 2010;34(10):1528-43.
13. Kasper BS, Kurzbuch K, Chang BS, Pauli E, Hamer HM, Winkler J, et al. Paternal inheritance of classic X-linked bilateral periventricular nodular heterotopia. Am J Med Genet A. 2013;161(6):1323-8.
14. Zenker M, Rauch A, Winterpacht A, Tagariello A, Kraus C, Rupprecht T, et al. A dual phenotype of periventricular nodular heterotopia and frontometaphyseal dysplasia in one patient caused by a single FLNA mutation leading to two functionally different aberrant transcripts. Am J Hum Genet. 2004;74(4):731-7.
15. Reinstein E, Frentz S, Morgan T, Garcia-Minaur S, Leventer RJ, McGillivray G, et al. Vascular and connective tissue anomalies associated with X-linked periventricular heterotopia due to mutations in Filamin A. Eur J Hum Genet. 2012.
16. Sheen VL, Jansen A, Chen MH, Parrini E, Morgan T, Ravenscroft R, et al. Filamin A mutations cause periventricular heterotopia with Ehlers-Danlos syndrome. Neurology. 2005;64(2):254-62.

17. van der Werf CS, Sribudiani Y, Verheij JB, Carroll M, O'Loughlin E, Chen CH, et al. Congenital short bowel syndrome as the presenting symptom in male patients with FLNA mutations. Genet Med. 2013;15(4):310-3.
18. Van Der Werf CS, Wabbersen TD, Hsiao NH, Paredes J, Etchevers HC, Kroisel PM, et al. CLMP is required for intestinal development, and loss-of-function mutations cause congenital short-bowel syndrome. Gastroenterology. 2012;142(3):453-62 e3.
19. Bernstein JA, Bernstein D, Hehr U, Hudgins L. Familial cardiac valvulopathy due to filamin A mutation. Am J Med Genet A. 2011;155A(9):2236-41.
20. Kyndt F, Gueffet JP, Probst V, Jaafar P, Legendre A, Le Bouffant F, et al. Mutations in the gene encoding filamin A as a cause for familial cardiac valvular dystrophy. Circulation. 2007;115(1):40-9.
21. Clayton-Smith J, Walters S, Hobson E, Burkitt-Wright E, Smith R, Toutain A, Amiel J, Lyonnet S, Mansour S, Fitzpatrick D, Ciccone R, Ricca I, Zuffardi O, Donnai D. 2009. Xq28 duplication presenting with intestinal and bladder dysfunction and a distinctive facial appearance. Eur J Hum Genet;17(4):434-43

Chapter 3.5

Progressive cerebellar atrophy and polyneuropathy: expanding the spectrum of *PNKP* mutations

Cathryn Poulton*, Renske Oegema*, Daphne Heijsman, Jeannette Hoogeboom, Rachel Schot, Hans Stroink, Michèl A. Willemsen, Frans W. Verheijen, Peter van de Spek, Andreas Kremer, Grazia M.S. Mancini
*these authors contributed equally to the manuscript

Neurogenetics 2013 Feb;14(1):43-5

ABSTRACT

We present a neurodegenerative disorder starting in early childhood of two brothers consisting of severe progressive polyneuropathy, severe progressive cerebellar atrophy, microcephaly, mild epilepsy and intellectual disability. The cause of this rare syndrome was found to be a homozygous mutation (c.1250_1266dup, resulting in a frameshift p.Thr424GlyfsX48) in *PNKP,* identified by applying homozygosity mapping and whole genome sequencing. Mutations in *PNKP* have previously been associated with a syndrome of primary microcephaly and seizures (MCSZ syndrome, MIM 613402), but not with a neurodegenerative disorder. PNKP is a dual function enzyme with a key role in different pathways of DNA damage repair. DNA repair disorders can result in accelerated cell death, leading to underdevelopment and neurodegeneration. In skin fibroblasts from both affected individuals we show increased susceptibility to apoptosis under stress conditions and reduced *PNKP* expression. PNKP is known to interact with DNA repair proteins involved in the onset of polyneuropathy and cerebellar degeneration, therefore our findings explain this novel phenotype.

INTRODUCTION

From the first identification of the basis of mendelian disorders using whole exome sequencing (WES) [1] and whole genome sequencing (WGS) [2, 3] these techniques have rapidly emerged as effective methods in finding disease-causing mutations. In consanguineous pedigrees this can be combined with homozygosity mapping for rapid candidate gene filtering.[4] Two siblings from a Dutch isolated population presented to our clinic with a rare combination of features starting in early childhood consisting of ataxia caused by progressive cerebellar atrophy, progressive debilitating polyneuropathy, microcephaly, severe intellectual disability (ID) and mild epilepsy. No ocular signs or involvement of other organs were present. No known disorder was compatible with this phenotype (including known DNA repair disorders and hereditary neuropathies), extensive metabolic work-up was normal. The MRI patterns were not typical for known cerebellar ataxia with polyneuropathy syndromes, such as infantile neuroaxonal dystrophy or neuroacanthocytosis.

Despite multiple expert opinions and laboratory studies we were unable to establish a definitive clinical diagnosis. We therefore pursued a genotype-first approach and chose a combination of homozygosity mapping and whole genome sequencing approach in order to minimize the chance of missing known and putative pathogenic mutation(s) in both coding regions and splice sites.[5] The same strategy has been successfully used to screen all known and identify new hereditary motor and sensory neuropathy (HMSN) genes.[2] To our surprise we identified a homozygous mutation in *PNKP* (MIM 605610) in both affected siblings by WGS and confirmed the disease locus with homozygosity mapping. Mutations in *PNKP* (polynucleotide kinase 3`-phosphatase) have been described in an autosomal recessive disorder characterized by microcephaly, seizures and developmental delay (MCSZ, one of the early infantile epileptic encephalopathies, EIEE10, MIM 613402).[6] The MCSZ patients are phenotypically very different to the patients described, who did not show any clinical progression, or any neurodegenerative symptoms. Additional studies in patient cells indicate a role of increased apoptosis in the pathogenesis of this novel degenerative phenotype.

CLINICAL REPORTS

The parents of our patients are healthy and originate from an isolated community in the southwest of the Netherlands. Genealogical studies of the family pedigree showed a loop of consanguinity (Fig. 1A).

Patient 1 was born at term with microcephaly (occipito-frontal circumference, OFC -3.25 SD), and weight and length at -1 SD. He had developmental delay, at 15 months he was able to take a few supported steps, and say 'daddy' and 'mama'. At this age his OFC was -5.7 SD. At 23 months he walked independently, with a broad based ataxic

gait. He had brisk tendon reflexes. He presented with a series of febrile seizures at 2.5 years, and experienced occasional seizures, mostly febrile, thereafter. His global development was compatible with 17 months at age 4.5 years (Bayley scale of development). The boy was hyperactive and always had an extreme happy behaviour. The diagnosis Angelman syndrome was considered, but DNA testing was negative. At age 9 he was a restless boy with severe progressive microcephaly (-6 SD), short stature (-4 SD), ataxic gait, speaking 5 to 10 words. A brain MRI at age 16 showed severe cerebellar atrophy (Fig. 2, A-C), while a CT made at the age of 10 months showed no atrophy of the cerebellum at all.

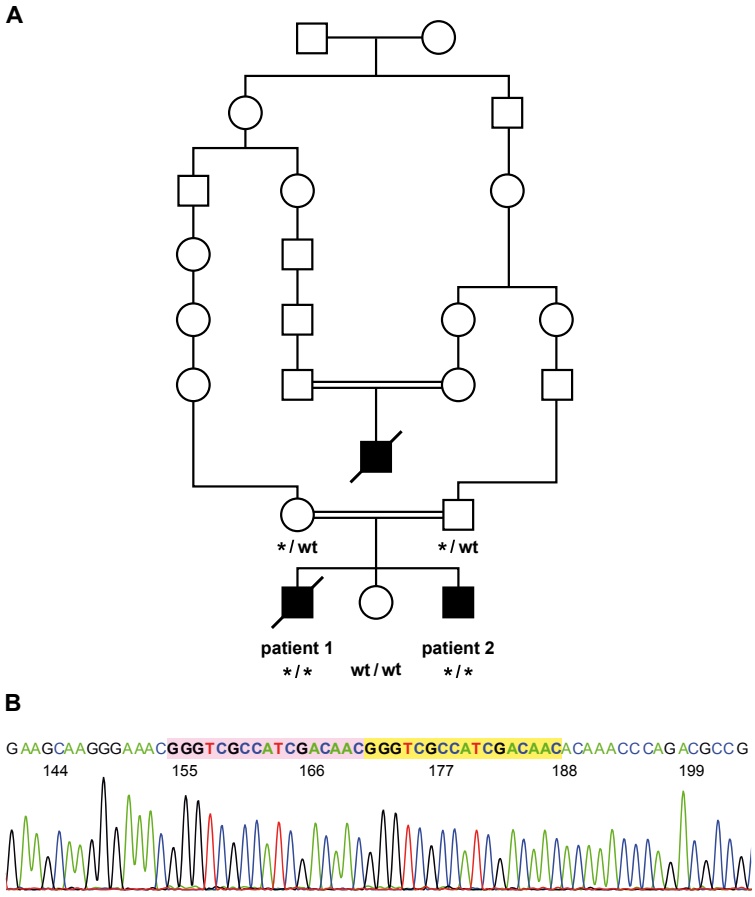

Figure 1.
(A) Pedigree of the family showing common ancestor couple and the link to a possibly third affected family member. *PNKP* genotype is shown below individuals: *= 1250_1266 dup, wt= "wild type" *PNKP* sequence, black boxes represent affected persons. (B) Sanger sequencing results of *PNKP* in patient 2, the sequence present *in duplo* is shaded in pink and yellow.

A slow deterioration of motor skills became evident, and he became wheelchair bound at age thirteen (see supplemental video). Motor function further deteriorated over the next few years, mostly as the consequence of progressive signs of the peripheral neuropathy, i.e. paresis of arms and legs accompanied by hypotonia, muscular atrophy, loss of the initially brisk tendon reflexes, and the development of contractures. A progressive severe motor and sensory demyelinating polyneuropathy with axonal degeneration was shown on EMG at age 11 and 16 (Tables 1 and 2). In contrast to the motor deterioration, cognitive functions and speech performance remained stable, while the epilepsy improved. He retained a happy demeanour, but had temper tantrums in adolescence. He died of pneumonia at 25 years.

Patient 2, the younger brother of patient 1, was born at term with birth weight at +0.5 SD, length at -0.25 SD, and OFC at -1.5 SD. At 3 months microcephaly (-3.5 SD) and developmental delay were noted. His first seizure occurred at 12 months. He walked independently at 18 months and showed also hyperactive and happy behaviour. At five years he developed strabismus and papilloedema consistent with raised intracranial pressure and a ventriculo-peritoneal shunt was placed. He slowly lost his ability to walk, and started using a wheel chair from age 7 (supplemental video). At age 14 his OFC was -4.75 SD, and he was a hyperactive boy who could speak about 10 words. EMG at age 10 and 16 showed demyelinating polyneuropathy (Tables 1 and 2). Brain MRI at age 15 months showed enlarged lateral ventricles and thin corpus callosum (Fig. 2, D-F), and at age 9 and 18 years, after placement of the VP drain, showed a severe progressive cerebellar atrophy, and mild cerebral atrophy (Fig. 2, G-L). Seizures occurred 3-4 times a year while on carbamazepine therapy, but later on the frequency decreased. No eye problems, skin rash or susceptibility to infection were ever observed in the brothers.

A second-degree cousin of the father (Fig. 1A) had a similarly affected son who died around 30 years of age of a progressive neurological disease. No medical records are available. He had a small head, seizures and had lost the ability to walk.

Metabolic investigations including lactate, vitamin A and E, very long chain fatty acids, sialotransferrin isoforms, erythrocyte and leukocyte morphology, lysosomal enzymes, urine organic acids, mucopolysaccharides and amino acids, and CSF neurotransmitters were normal in both brothers. Transcription-coupled nucleotide excision repair after UV treatment (diagnostic test for Cockayne syndrome) and inhibition of DNA synthesis after X-ray irradiation (diagnostic test for ataxia-telangiectasia) were normal in patient fibroblasts (see below).

A video of patient 1 and 2 at different ages showing ataxia and progressive deterioration is included in the supplemental data (with consent of the family).

Table 1. Nerve conduction studies

	Nerve	Muscle	DML (ms)	NCV (m/s)	SNAP (uV)	CMAP: distal stimulation (mV)	CMAP: proximal stimulation (mV)
Patient 1							
(11 years)	Motor:						
	R ant tib	EDB	10.4	72		0.4	0.6
	R median	APB	3.5	41		5.0	4.5
Patient 1							
(16 years)	R ant tib	EDB				0	
	R post tib	AH				0	
	L post tib	AH				0	
	R median	APB	5.3	34		4.5	2.1
	Sensory:						
	L sural				0		
	R median (digit 3)				0		
Patient 2							
(11 years)	Motor:						
	R ant tib	EDB				0	0
	R post tib	AH	6.5	34		2.8	1.5
	L post tib	AH	4.9	37		2.7	2.4
	Sensory:						
	L sural nerve				0		
Patient 2							
(16 years)	Motor:						
	R ulnar nerve	ADM	4.4	31		0.7	0.8
	R post tib	Soleus					0
	L post tib	AH				0	
	Sensory:						
	R sural nerve				0		
	R median (digit 3)				0		

Nerve conduction velocity (NCV) and distal motor latency (DML) values for patients 1 and 2 show slowing and loss of conduction in motor and sensory nerves, and conduction block consistent with a severe mixed demyelinating/axonal sensorimotor polyneuropathy. Normal values: NCV > 50 m/s in the arms, > 40 m/s in the legs; compound motor action potential (CMAP) extensor digitorum brevis (EDB) > 5 mV, CMAP muscles hand > 10 mV. *ADM* abductor digiti minimi, *AH* abductor hallucis, *ant tib* anterior tibial nerve, *APB* abductor pollicis brevis, *L* left side, *post tib* posterior tibial nerve, *R* right side (R), *SNAP* sensory nerve action potential.

Table 2. Needle EMG results

	Muscle	FP	PSW	Maximal pattern	Polyphasic MUAP
Patient 1					
(16 years)	L TA	+	+	0	
	L Q	+	-	mixed	+
Patient 2					
(11 years)	L TA	-	-	mixed	-
Patient 2					
(16 years)	R TA	++	-	0	
	R FR	++	+++	0	
	R BB	-	-	mixed	+

Needle EMG in both patients shows fibrillations (FP), positive sharp waves (PSW), and polyphasic motor unit action potentials (MUAP) consistent with denervation.
BB biceps brachii, *FR* femoris rectus, *L* left side, *Q* quadriceps, *R* right side, *TA* tibialis anterior.

MATERIALS AND METHODS

Patient material and informed consent

All the family members and legal patient guardians provided written informed consent for participation in the study, which is embedded in a broader study of the cause of brain malformation at the Erasmus MC.

SNP arrays

500 ng of total genomic DNA extracted from peripheral leucocytes of the two affected brothers and their unaffected sister was hybridized to Genome-Wide Human SNP Array 6.0 according to the manufacturer's protocol (Affymetrix, Santa Clara, CA). Affymetrix Genotyping Console (GTC4.1.0) was used for genotyping and both GTC4.1.0 and CNAG v3.3.0.1 Beta were used for regions of homozygosity (ROH) analysis as well as copy number analysis.[7]

Whole genome sequencing

DNA from the mother and two affected sons was extracted from peripheral leucocytes (mother) and fibroblast cell lines (sons) and sent to Complete Genomics (Mountain View, US), for whole genome sequencing.[8] This technique was preferred above exome sequencing in order to minimize the chance of missing the mutations by exon capturing techniques.[9]

Reads were mapped to the National Center for Biotechnology Information (NCBI) reference genome, build 36. Analysis of the whole genome sequencing data was done using CGA tools version 1.3.0 and TIBCO Spotfire version 3.3.1. The initial analysis was restricted to nonsynonymous variants, variants disrupting the acceptor or donor splice

site or small insertions or deletions (up to approximately 50 bp) in the homozygous area that were fully called and were not present in dbSNP129, or in data from the 1000 genome database and Exome variant sever (Washington university), or in 100 control samples from our in-house database (HuVariome). Additionally, variants should follow the expected autosomal homozygous recessive inheritance pattern. When this analysis did not lead to a result, the stringency of the filtering was lowered by allowing no-calls or half-calls at potential variant positions, as long as one of the family members showed a variant on at least one allele. As a compound heterozygous recessive or X-linked inheritance could not be excluded by the pedigree of this family, we also performed analyses for these inheritance models.

Sanger sequencing

Verification of the mutation was performed by Sanger sequencing of exon 14 of the *PNKP* gene (RefSeq NG_027717) on DNA isolated from peripheral leucocytes. PCR amplification reactions were performed and products were purified with ExoSAP-IT (USB). Direct sequencing of both strands was performed using Big Dye Terminator chemistry ver. 3.1 (Applied Biosystems). DNA fragment analysis was performed using capillary electrophoresis on an ABI 3130 Genetic Analyzer (Applied Biosystems) and the software package Seqscape (Applied Biosystems, version 2.1). Primer sequences are available upon request.

DNA repair and apoptosis studies

In cultured skin fibroblasts from patient 1 and 2, transcription-coupled nucleotide excision repair after UV treatment was used as diagnostic test for Xeroderma pigmentosum and Cockayne syndrome as described and resistance to inhibition of DNA synthesis after X-ray irradiation (cell cycle arrest) was used as a diagnostic test for mutations in the ATM pathway (ataxia-telangiectasia and Nijmegen breakage syndrome).[10-12]
Using cultured skin fibroblasts from both patients bearing the homozygous *PNKP* mutation, and 5 healthy control cells lines, we tested for susceptibility to apoptosis. In order to detect apoptosis the cells were stained with the FlicaTM (Fluorescent-Labeled Inhibitor of Caspases) apoptosis multi-caspase detection kit (Immunochemistry Technologies, LLC), which makes use of an inhibitor sequence of active caspases and was performed according to the manufacturer instructions. Fluorescent cells were scored (as a percentage of apoptotic fibroblasts) before and after stress induction by 24 hours serum deprivation and then a further 24 hours exposure to 5 mM dithiothreitol (DTT) by two blinded investigators. Necrosis versus apoptosis was tested by vital staining exclusion with propidium iodide. The experiment was repeated three times and each time performed in triplicate.

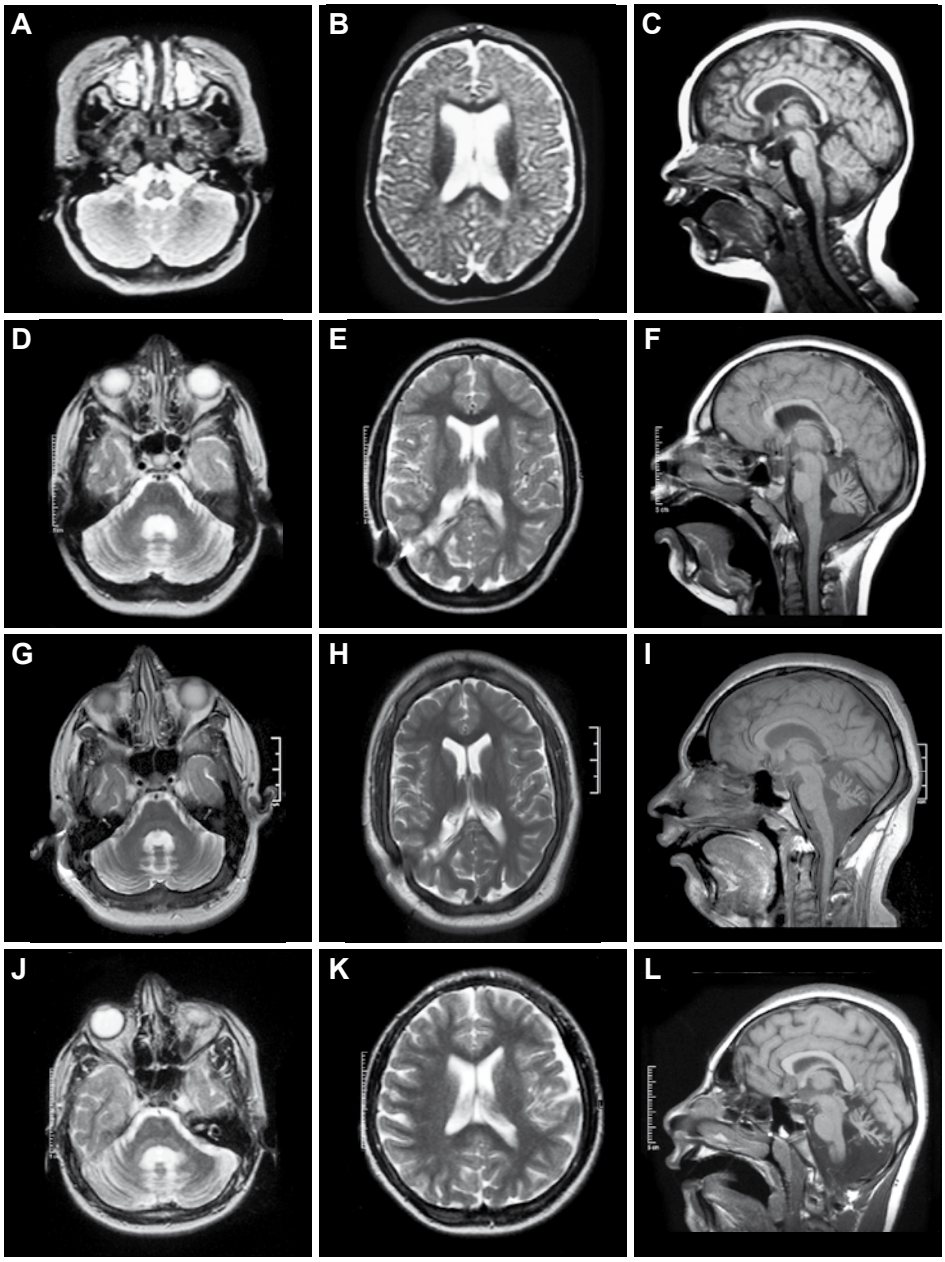

Figure 2.
MRI imaging of patient 1 (A-C) and patient 2 (D-L). First two columns show transversal T2-weighted images, the third column shows sagittal T1-weighted images. (A-C) patient 1 age 16 years, microcephaly, generalized atrophy, enlarged ventricles, and severe cerebellar atrophy. (D-F) patient 2 age 15 months, mild generalized atrophy, enlarged lateral ventricles and thin corpus callosum. (G-I) age 9 years, and (J-L) age 18 years, show decrease of lateral ventricle sizes after placement of VP-drain, severe and progressive cerebellar atrophy.

Quantitative PCR

Analysis of gene expression by qRT-PCR was carried out using a KAPA SYBRH FAST qPCR Kit (Kapa Biosystems) in the CFX96 Real-Time system (BioRad). Thermal cycling conditions were as follows: denaturing step (95˚C for 3 minutes), followed by 35 cycles of denaturing (95˚C for 5"), annealing and extension (60˚C for 30"). Fluorescence detection and data analysis were performed by BioRad CFX Manager 2.0. Experiments were performed in triplicate using as the reference *GAPDH* (MIM 138400) and *ACTB* (MIM 102630) for gene expression normalization.[13] Primers are listed in supplemental Table S3.

RESULTS

SNP arrays and WGS

ROH analysis of the two affected brothers and an unaffected sister was performed in CNAG 3.3.0.1 Beta. Two regions of overlapping ROH were found in the two affected brothers and not in the unaffected sister on chromosome 11q23 (bp 117,449,498-118,276,116, build 37) and chromosome 19q13 (bp 34,230,986-51,258,314, build 37). Considering the consanguinity loop and the size of the area (17 Mb), the region on chromosome 19q13 can be confidently considered identical by descent rather than identical by state and would putatively contain the genetic mutation (Fig. S1). The mapped whole genome sequence of the three samples (mother and two sons) varied between 183 and 192 Gb, resulting in a good average coverage between 66x and 68x per genome (Table S1). Confident diploid calls could be made for approximately 97% of the reference genome in all cases. On average, 3.75 million genetic variants were identified per sample, including single nucleotide variants and short insertions, deletions and substitutions up to ~50 bp.

Filtering for a homozygote recessive mutation present in both affected individuals was applied and after allowing no calls, variations in only 3 genes in the homozygous regions were found: *ZNF285A*, *FCGRT* and *PNKP* (Fig. S2). We excluded FCGRT as this encodes a protein only expressed in placental tissue and responsible for transferring IgG from mother to fetus therefore is not relevant to the phenotype. *ZNF285A* is 100% identical to human gene *ZNF806* and *ZNF678*, it has no mouse ortholog which throws doubt onto the physiological mechanism, and is in a cluster of more then 25 similar ZNF genes on chromosome 19. Which makes it unlikely that this is the causative gene for this phenotype.

The *PNKP* variant was confirmed by Sanger sequencing, which showed an insertion of 17 bp corresponding to a duplication in exon 14 of PNKP (c.1250_1266dup) resulting in a frameshift (p.Thr424GlyfsX48, PNKP-201 Ensembl database). This insertion is within the largest candidate ROH (Fig. S1 and Table S1). The *PNKP* gene was recently described in literature to be related to microcephaly, seizures and developmental delay (MCSZ)

syndrome and one of the mutations was the same variant that we identified in our family [6]. Although heterozygous for the duplication, the mother was homozygous for the haplotype previously described. This confirms the association of the duplication with this haplotype in different ethnic backgrounds, and suggests this haplotype might predispose to the occurrence of the duplication, instead of being a founder effect. Analysis of WGS data for compound heterozygous and X-linked inheritance did not lead to any additional causative variants being found. We also specifically looked into genes known to be involved in neuropathy (Table S4) and found sufficient coverage and sequencing depth to confidently exclude a causative mutation.

qRT-PCR

In order to confirm the 17 bp duplication in exon 14 and to study its effect on *PNKP* expression we studied transcripts by qRT-PCR. Using primers against *PNKP* and designed over exon 3 and 4 and exon 15 and 16 we showed that the expression of PNKP was consistently decreased, however there was still expression of mRNA for PNKP in the homozygous state (Fig. S3). These results support the effect of the mutation as a loss of PNKP function.

Apoptosis studies

One of the effects of DNA damage is that, due to overall cell stress, cells have an increased susceptibility to undergo apoptosis. It has also been hypothesized that abnormal apoptosis is the pathogenic mechanism leading to microcephaly in MCSZ [6]. Cultured skin fibroblasts from both patients had indeed a significantly increased tendency to undergo apoptosis (Student's unpaired *t*-test $p<0.0001$) when under stress conditions in comparison to 5 control cell lines (Fig. 3).

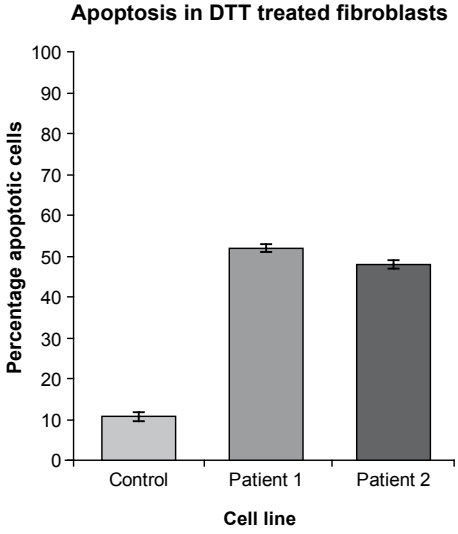

Figure 3. Patient 1 and patient 2 fibroblasts have an increased tendency to undergo apoptosis when treated with 5mM DTT in comparison to 5 control cell lines, each experiment involved testing 5 control cell lines and 2 patient cell lines on 3 separate occasions. ($p<0.001$, unpaired *t*-test, SPSS v17.0). Rates are shown as a mean of 3 experiments (+/- SEM).

DISCUSSION

We successfully applied WGS to identify the disease causing *PNKP* mutations in two brothers with a novel phenotype consisting of progressive cerebellar atrophy, severe polyneuropathy, microcephaly, and severe ID. There were occasional seizures, but no history of early infantile epileptic encephalopathy.

The same 17 bp duplication in exon 14 (c.1250_1266dup, resulting in a frame shift Thr424GlyfsX48) in *PNKP* in homozygous and compound heterozygous state has been identified in patients with a different syndrome (MCSZ/EIEE10, microcephaly, intractable seizures and developmental delay syndrome).[6] The published three patients who were homozygous for this mutation within an identical haplotype were not described as having progressive neurodegeneration. However, our patients clearly showed progressive disease in childhood, with loss of motor milestones (supplemental video), development of severe neuropathy and cerebellar atrophy. The MCSZ syndrome was not considered in our patients because of these symptoms. The extensive diagnostic investigations, the combined autozygosity mapping and WGS approach makes very unlikely that in this family we missed another genetic mutation accounting for the disorder.

PNKP is a dual function protein that has a polynucleotide 3'phosphatase and a polynucleotide 5` hydroxylkinase domain and has an important role in repair of both single strand breaks (SSB) and double-strand breaks (DSB).[14, 15] Fibroblast cell lines from our PNKP patients showed an increased tendency to go into apoptosis, supporting a role of apoptosis in the pathogenesis. Our observations suggest that stress placed on the cell by the DNA repair defect causes insufficient proliferation and cell death. Increased apoptosis was shown in mouse neuronal precursors and differentiated neurons with reduced *Pnkp* levels.[6]

We looked at PNKP's interacting partners using STRING analysis, which combines information from different sources to identify known and putative protein interactions (Fig. 4). This shows interaction with known neurodegenerative disease-associated proteins (Fig. 4). Mutations in *TDP1* cause autosomal recessive spinocerebellar ataxia with axonal neuropathy (SCAN1, MIM 607250) [16], and this has led to the previous suggestion that *PNKP* could be a gene for SCAN [17]. *APTX* mutations cause ataxia-oculomotor apraxia type 1 (AOA1, MIM 606350). *PNKP*, *TDP1*, and *APTX* defects all lead to abnormal SSB repair, which provides experimental evidence for a common mechanism of neurodegeneration.[18]

Severe microcephaly is observed in the autosomal recessive primary microcephaly syndromes (MCPH). One of the genes involved in this disorder, MCPH1, links the MCPH genes to DNA repair by activating ATM and ATR (respectively associated with ataxia-telangiectasia and Seckel syndrome) [14, 19], which in turn phosphorylate and activate PNKP.

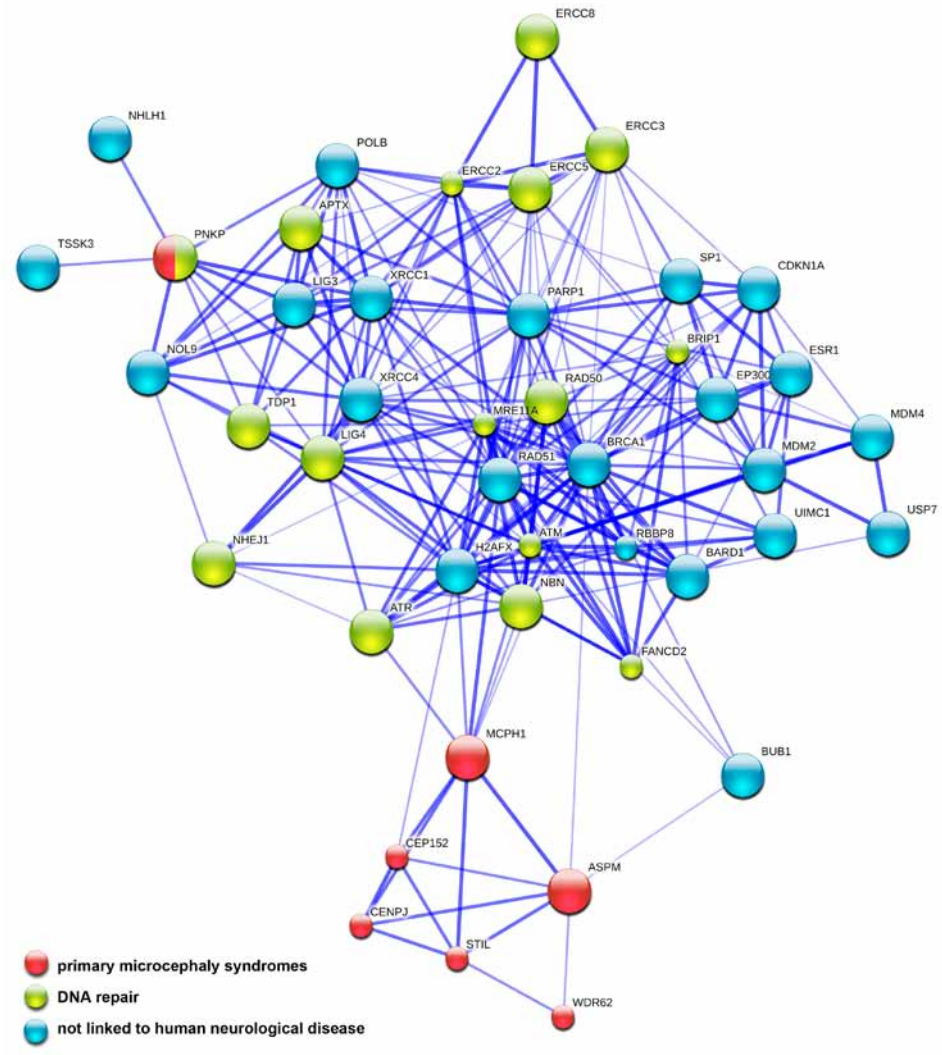

Figure 4. STRING analysis showing PNKP interactions between known proteins which are encoded by genes associated with primary microcephaly syndromes (red filled circles), DNA repair disorders (green filled circles), proteins not yet associated with human neurological disease (candidate genes, blue filled circles). The blue line between the proteins indicate known interactions and the thickness of the line is representative of the confidence of evidence (the thicker the line, the more evidence to support the interaction).

In the DSB repair, which is particularly important in dividing cells during development, PNKP directly interacts with the scaffold XRCC4 and activates LIG4. *LIG4* mutations cause immunodeficiency with microcephaly (MIM 606593).[19, 20] *DNA ligase 4 -/-* mice show increased apoptosis throughout the nervous system and die in the embryonic period. *Lig4* conditional KO mice (*Lig4 Nes-Cre*) have a pronounced microcephaly and show increased apoptosis from E13.5, peaking at E15.[21] This apoptosis is apparently mediated by the intact pro-apoptotic function of ATM in *Lig4* mutants.[22] Microcephaly due to increased apoptosis of neuroprogenitors during embryonic development has been shown by our group in a syndrome with congenital microcephaly and diabetes.[23] Therefore, the function and interactions of PNKP supports a role in the neurodegenerative phenotype as well as microcephaly, possibly by increased apoptosis.
In conclusion, we have described a neurodegenerative phenotype not previously described with *PNKP* mutations and used a combined approach of autozygosity mapping and whole genome sequencing as a valuable tool for diagnosis.

Supplementary information is available online at the Neurogenetics website.

ACKNOWLEDGEMENTS

We thank Dr N.G. Jaspers at the department of Genetics, Erasmus Medical Center for critically reading the manuscript. We acknowledge the collaboration of the members of the patients' family. We thank J. Meulstee for help with interpretation of EMG data. We also thank Tom de Vries Lentsch for the figures and Petra Veraart for the genealogical study.

ONLINE RESOURCES

Online Mendelian Inheritance in Man (OMIM):www.ncbi.nlm.nih.gov/omim.
cga tools: www.completegenomics.com/sequence-data/cgatools/
TIBCO Spotfire: http://spotfire.tibco.com/
STRING 9.0: http://string-db.org.
Ensembl: www.ensembl.org

REFERENCES

1. Hoischen A, van Bon BW, Gilissen C, Arts P, van Lier B, Steehouwer M, et al. De novo mutations of SETBP1 cause Schinzel-Giedion syndrome. Nat Genet. 2010;42(6):483-5. Epub 2010/05/04.
2. Lupski JR, Reid JG, Gonzaga-Jauregui C, Rio Deiros D, Chen DC, Nazareth L, et al. Whole-genome sequencing in a patient with Charcot-Marie-Tooth neuropathy. N Engl J Med. 2010;362(13):1181-91. Epub 2010/03/12.
3. Roach JC, Glusman G, Smit AF, Huff CD, Hubley R, Shannon PT, et al. Analysis of genetic inheritance in a family quartet by whole-genome sequencing. Science. 2010;328(5978):636-9. Epub 2010/03/12.
4. Pippucci T, Benelli M, Magi A, Martelli PL, Magini P, Torricelli F, et al. EX-HOM (EXome HOMozygosity): a proof of principle. Hum Hered. 2011;72(1):45-53. Epub 2011/08/19.
5. Dixon-Salazar TJ, Silhavy JL, Udpa N, Schroth J, Bielas S, Schaffer AE, et al. Exome sequencing can improve diagnosis and alter patient management. Sci Transl Med. 2012;4(138):138ra78. Epub 2012/06/16.
6. Shen J, Gilmore EC, Marshall CA, Haddadin M, Reynolds JJ, Eyaid W, et al. Mutations in PNKP cause microcephaly, seizures and defects in DNA repair. Nat Genet. 2010;42(3):245-9. Epub 2010/02/02.
7. Nannya Y, Sanada M, Nakazaki K, Hosoya N, Wang L, Hangaishi A, et al. A robust algorithm for copy number detection using high-density oligonucleotide single nucleotide polymorphism genotyping arrays. Cancer Res. 2005;65(14):6071-9. Epub 2005/07/19.
8. Drmanac R, Sparks AB, Callow MJ, Halpern AL, Burns NL, Kermani BG, et al. Human genome sequencing using unchained base reads on self-assembling DNA nanoarrays. Science. 2010;327(5961):78-81. Epub 2009/11/07.
9. Lam HY, Clark MJ, Chen R, Natsoulis G, O'Huallachain M, Dewey FE, et al. Performance comparison of whole-genome sequencing platforms. Nat Biotechnol. 2012;30(6):562. Epub 2012/06/09.
10. Kleijer WJ, van der Kraan M, Los FJ, Jaspers NG. Prenatal diagnosis of ataxia-telangiectasia and Nijmegen Breakage syndrome by the assay of radioresistant DNA synthesis. Int J Radiat Biol. 1994;66(6 Suppl):S167-74. Epub 1994/12/01.
11. Mallery DL, Tanganelli B, Colella S, Steingrimsdottir H, van Gool AJ, Troelstra C, et al. Molecular analysis of mutations in the CSB (ERCC6) gene in patients with Cockayne syndrome. Am J Hum Genet. 1998;62(1):77-85. Epub 1998/03/07.
12. Zafeiriou DI, Thorel F, Andreou A, Kleijer WJ, Raams A, Garritsen VH, et al. Xeroderma pigmentosum group G with severe neurological involvement and features of Cockayne syndrome in infancy. Pediatr Res. 2001;49(3):407-12. Epub 2001/03/03.
13. Bustin SA, Benes V, Garson JA, Hellemans J, Huggett J, Kubista M, et al. The MIQE guidelines: minimum information for publication of quantitative real-time PCR experiments. Clin Chem. 2009;55(4):611-22. Epub 2009/02/28.
14. Caldecott KW. Single-strand break repair and genetic disease. Nat Rev Genet. 2008;9(8):619-31. Epub 2008/07/16.
15. Weinfeld M, Mani RS, Abdou I, Aceytuno RD, Glover JN. Tidying up loose ends: the role of polynucleotide kinase/phosphatase in DNA strand break repair. Trends Biochem Sci. 2011;36(5):262-71. Epub 2011/03/01.
16. Sano Y, Date H, Igarashi S, Onodera O, Oyake M, Takahashi T, et al. Aprataxin, the causative protein for EAOH is a nuclear protein with a potential role as a DNA repair protein. Ann Neurol. 2004;55(2):241-9. Epub 2004/02/03.

17. Plo I, Liao ZY, Barcelo JM, Kohlhagen G, Caldecott KW, Weinfeld M, et al. Association of XRCC1 and tyrosyl DNA phosphodiesterase (Tdp1) for the repair of topoisomerase I-mediated DNA lesions. DNA Repair (Amst). 2003;2(10):1087-100. Epub 2003/09/19.
18. Reynolds JJ, Walker AK, Gilmore EC, Walsh CA, Caldecott KW. Impact of PNKP mutations associated with microcephaly, seizures and developmental delay on enzyme activity and DNA strand break repair. Nucleic Acids Res. 2012. Epub 2012/04/18.
19. McKinnon PJ. DNA repair deficiency and neurological disease. Nat Rev Neurosci. 2009;10(2):100-12. Epub 2009/01/16.
20. Mani RS, Yu Y, Fang S, Lu M, Fanta M, Zolner AE, et al. Dual modes of interaction between XRCC4 and polynucleotide kinase/phosphatase: implications for nonhomologous end joining. J Biol Chem. 2010;285(48):37619-29. Epub 2010/09/21.
21. Gatz SA, Ju L, Gruber R, Hoffmann E, Carr AM, Wang ZQ, et al. Requirement for DNA ligase IV during embryonic neuronal development. J Neurosci. 2011;31(27):10088-100. Epub 2011/07/08.
22. Shull ER, Lee Y, Nakane H, Stracker TH, Zhao J, Russell HR, et al. Differential DNA damage signaling accounts for distinct neural apoptotic responses in ATLD and NBS. Genes Dev. 2009;23(2):171-80. Epub 2009/01/28.
23. Poulton CJ, Schot R, Kia SK, Jones M, Verheijen FW, Venselaar H, et al. Microcephaly with simplified gyration, epilepsy, and infantile diabetes linked to inappropriate apoptosis of neural progenitors. Am J Hum Genet. 2011;89(2):265-76. Epub 2011/08/13.

Chapter 3.6

A single strand that links multiple neuropathologies in human disease

Renske Oegema*, Cathryn J Poulton*, and Grazia M.S. Mancini
*these authors contributed equally to the manuscript

Brain 2014 Apr;137(Pt 4):e266

Sir,

We read with great interest the review by Reynolds and Stewart in the January issue reviewing three neurological disorders associated with defective single strand break repair: ataxia oculomotor apraxia 1 (AOA1), spinocerebellar ataxia with axonal neuropathy 1 (SCAN1) and microcephaly, early-onset, intractable seizures and developmental delay (MCSZ) syndrome.[1] The authors discuss in detail the clinical features and underlying pathologic mechanisms. We noted that they focus on the differences in clinical presentation between AOA1, SCAN1 and MCSZ syndrome; the first two having progressive cerebellar ataxia as a major symptom, and the latter retaining normal brain structures and lacking sign of neurodegeneration or ataxia. They hypothesize that the hypomorphic nature of the mutation with preservation of DNA 3' phosphatase activity of PNKP leads to this attenuated phenotype.

Indeed, the individuals described in the first report of MCSZ syndrome lack cerebellar symptoms.[2] However our group recently published clinical details of two brothers with *PNKP* mutation who, besides the congenital microcephaly, presented in early childhood with a neurodegenerative disorder consisting of progressive cerebellar ataxia and severe polyneuropathy leading to loss of motor milestones, wheel chair dependence, and in one, premature death at age 25 years.[3] Intensive investigations including repeated brain imaging and EMGs showed progressive cerebellar atrophy and severe mixed demyelinating/axonal sensorimotor polyneuropathy (Fig. 1). In addition they had mild epilepsy, not meeting criteria for early infantile epileptic encephalopathy, and moderate/severe intellectual disability). Through homozygosity mapping and whole genome sequencing a homozygous mutation (c.1250_1266dup resulting in a frameshift p.Thr424GlyfsX48) in *PNKP* was identified. This is exactly the same homozygous duplication already described in the 3 patients with MCSZ syndrome who did not show any evidence of neurodegeneration.[2] In light of the knowledge about the PNKP function we can fully explain the phenotype of our patients and agree with the prediction that this protein plays a major role in development of the CNS and in maintenance of normal functions of both CNS and PNS throughout life.

PNKP is a dual function enzyme which functions in both single strand and double strand break repair. PNKP directly interacts with TDP1, associated with SCAN1, and this has led to the previous suggestion that *PNKP* could be a candidate gene for spinocerebellar ataxia with neuropathy.[4] PNKP is involved in single strand break (SSB) DNA repair by binding to a scaffold provided by XRCC1 and processing the repaired strands for the DNA ligase LIG3.[5] Interestingly, *XRCC1* knock-out mice show loss of cerebellar purkinje cells, ataxia and seizures.[6]

PNKP is also involved in double strand base repair and directly interacts with XRCC4 to activate LIG4. Conditional knock-out mice (*Lig4 Nes-Cres*) show microcephaly and have increased apoptosis in the brain at E23.5-E15.[7]

There is therefore sufficient knowledge to support and to expect the presentation of microcephaly, cerebellar ataxia and polyneuropathy, which we observed in case of *PNKP* mutation.

We showed in patient-derived fibroblasts harbouring the *PNKP* duplication an increased tendency to undergo apoptosis, thus supporting the theory that their microcephaly is caused by an increased apoptosis in neuronal precursors with unrepaired DNA breaks. We hypothesize that PNKP's dual function in single and double strand break explains the combination of cerebellar atrophy and microcephaly.

It is not clear at the moment why the neurodegenerative symptoms were not present in the early description of the same *PNKP* mutation, but this is very interesting to address in future studies, particularly whether additional genetic, epigenetic or environmental factors contribute to this variability, as some of these could be modifiable and amenable to intervention.

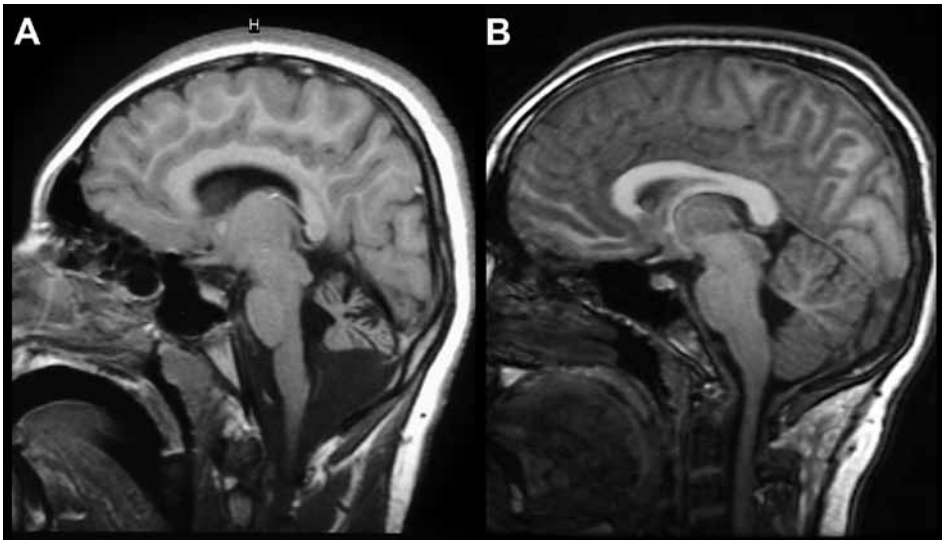

Figure 1. Brain sagittal T1 magnetic resonance imaging of one of the brothers (A), age 16, showing microcephaly and profound cerebellar atrophy compared to age-matched control (B).

REFERENCES

1. Reynolds JJ, Stewart GS. A single strand that links multiple neuropathologies in human disease. Brain : a journal of neurology. 2013;136(Pt 1):14-27. Epub 2013/02/01.
2. Shen J, Gilmore EC, Marshall CA, Haddadin M, Reynolds JJ, Eyaid W, et al. Mutations in PNKP cause microcephaly, seizures and defects in DNA repair. Nat Genet. 2010;42(3):245-9. Epub 2010/02/02.
3. Poulton C, Oegema R, Heijsman D, Hoogeboom J, Schot R, Stroink H, et al. Progressive cerebellar atrophy and polyneuropathy: expanding the spectrum of PNKP mutations. Neurogenetics. 2013;14(1):43-51. Epub 2012/12/12.
4. Plo I, Liao ZY, Barcelo JM, Kohlhagen G, Caldecott KW, Weinfeld M, et al. Association of XRCC1 and tyrosyl DNA phosphodiesterase (Tdp1) for the repair of topoisomerase I-mediated DNA lesions. DNA Repair (Amst). 2003;2(10):1087-100. Epub 2003/09/19.
5. Caldecott KW. Single-strand break repair and genetic disease. Nat Rev Genet. 2008;9(8):619-31. Epub 2008/07/16.
6. Lee Y, Katyal S, Li Y, El-Khamisy SF, Russell HR, Caldecott KW, et al. The genesis of cerebellar interneurons and the prevention of neural DNA damage require XRCC1. Nat Neurosci. 2009;12(8):973-80. Epub 2009/07/28.
7. Gatz SA, Ju L, Gruber R, Hoffmann E, Carr AM, Wang ZQ, et al. Requirement for DNA ligase IV during embryonic neuronal development. J Neurosci. 2011;31(27):10088-100. Epub 2011/07/08.

Chapter 4

New gene and mechanism

Chapter 4.1

Human *INTS8* mutations link brain development and transcriptome integrity to the Integrator complex

Renske Oegema[*], David Baillat[*], Daphne Heijsman, Rachel Schot, Sima Kheradmand Kia, A. Jeannette M. Hoogeboom , Zheng Xia, Wei Li, Matteo Cesaroni, Maarten H. Lequin[7], Cathryn J. Poulton, William B. Dobyns, Irenaeus F.M. de Coo, Frans W.Verheijen, Andreas Kremer, Peter J. van der Spek, Rob Willemsen, Adriana I. Iglesias, Leontine van Unen, Eric J. Wagner[^], Maarten Fornerod[^], Grazia M.S. Mancini

[*,^] these authors contributed equally to the manuscript

Manuscript submitted

ABSTRACT

Integrator (INT) is an RNA polymerase II (RNAPII)-associated complex that was recently identified to have a broad role in both RNA processing and transcription regulation. Despite the size of INT (>14 subunits), no germline mutations causing human disease in any subunit have been reported. Here, we show that *Integrator Complex Subunit 8* gene (*INTS8)* mutation causes a rare human neurodevelopmental syndrome. Patient cells display significant disruptions in gene expression and RNA processing, while depletion of INTS8 in zebrafish embryos lead to prominent underdevelopment of the head. Therefore, our results point to an evolutionary conserved requirement of INT in brain development.

INTRODUCTION

The Integrator complex (INT) associates with the C-terminal domain of the largest subunit of the RNA polymerase II (RNAPII). It was first discovered to mediate the co-transcriptional 3'-end processing of the U-rich small nuclear RNAs (UsnRNAs), the RNA components of the spliceosome.[1, 2] Recently, the scope of INT function has broadened through the discoveries of a general role in RNAPII promoter proximal pause-release and in the processing of enhancer RNAs.[3-7] INT consists of at least 14 subunits and is phylogenetically conserved among metazoans.[1, 8] To the exception of INT subunits INTS9 and INTS11, that are paralogues of the cleavage and polyadenylation specificity factor (CPSF) subunits CPSF100 and CPSF73 respectively, and which form the endonuclease factor responsible for cleavage of pre-mRNA [9, 10], the other INT subunits bear no homology to any RNA processing machinery or transcriptional regulators that would allow a predictable function within the complex.[11] Although animal studies suggest an evolutionary conserved requirement of INT subunits for normal embryonic development [12-17], human INT germline mutations have not been linked to any disease. Mutations in U snRNA have been previously linked to splicing alterations leading to brain disorders. For example, mutations in the mouse *Rnu2-8*, coding for U2 snRNA, results in cerebellar degeneration [18] and *U4atac* mutations in humans result in extreme microcephaly.[19] Besides its role in UsnRNA 3'-end processing, recent studies identified INT as a regulator of gene expression through RNAPII-dependent transcriptional initiation, pause-release and elongation.[3, 5, 6] Promoter-proximal pausing affects up to 40% of the genes and is particularly important during development.[20, 21] Paused RNAPII is preferentially encountered at developmentally-regulated genes where it can orchestrate the synchronous gene activation necessary for pattern formation.[22-25] This process is particularly important during neuronal development, synapse plasticity and maturation.[26-28] Given the established function for INT in UsnRNA biogenesis and RNAPII pause-release it would be predicted that reduced INT activity could disrupt normal human neurodevelopment. Here, we demonstrate for the first time that mutation in the *Integrator Complex Subunit 8* gene (*INTS8*) causes a rare neurodevelopmental syndrome through loss of INT integrity and function leading to broad transcriptome alterations.

RESULTS AND DISCUSSION

Three siblings presented with a distinct and recognizable neurodevelopmental syndrome. In summary, they had severe intellectual disability, spastic tetraplegia, epilepsy, microcephaly, and cerebral blindness (Fig. 1A and see clinical reports in supplement). Brain imaging showed periventricular nodular heterotopia (PNH) and cerebellar hypoplasia (Fig. 1B, S1). Whole genome sequencing (WGS) using DNA from

six family members identified bi-allelic mutations in the *Integrator Complex subunit 8* gene (*INTS8*) in the affected siblings (Table S1). The first mutation is a nine-base-pair deletion leading to the deletion of three amino acids (c.2917_2925del, p.Glu972_Leu-974del; simplified as INTS8ΔEVL), while the second mutation is a predicted missense mutation (c.893A>G, p.Asp298Gly). The mutations and their segregation in the family were confirmed by Sanger sequencing (Fig. 1C, 1D). INTS8 is a 995-amino-acid protein,

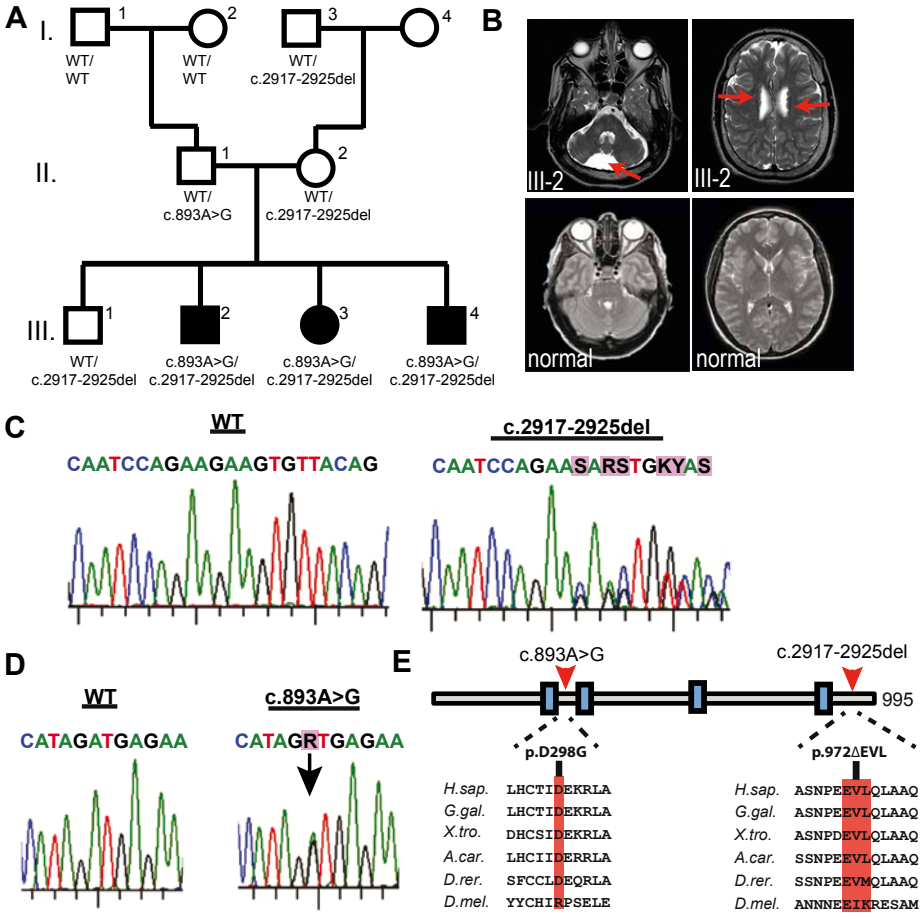

Figure 1. Biallelic *INTS8* mutations in a family with a severe neurodevelopmental syndrome. (A) Pedigree of the extended family; filled symbols represent affected individuals. Below each individual the *INTS8* alleles (WT= wild type) are shown. (B, upper panel) magnetic resonance imaging (MRI) of affected individual III-2 showing cerebellar hypoplasia (left, arrow) and periventricular nodular heterotopia (right, arrows). (B, lower panel) normal MRI from unaffected individual for comparison. (C,D) Electropherograms from Sanger sequencing of *INTS8* wild type and mutant alleles. (E) Graphical depiction of INTS8 including the four tetratricopeptide (TPR) motifs (blue blocks), the patient mutations and in the lower panel the conservation of the affected amino acids residues.

containing four predicted tetratricopeptide (TPR) motifs, which are versatile protein-protein interaction domains. Both mutations reside in conserved regions of the protein and INTS8ΔEVL is located at the C-terminus of the TPR4 domain in a predicted alpha helix (Fig. 1E). In spite of sequencing *INTS8* in 25 PNH patients and 266 other patients with brain malformations, we did not observe additional bi-allelic *INTS8* mutations, which suggests that this is a gene with a very low mutational rate. This is supported by the high combined annotation dependent depletion (CADD) score of the mutations (Table S2).[29]

To study whether and how these mutations affect *INTS8* expression we obtained primary fibroblasts from the three affected siblings and their unaffected brother, who is heterozygous only for the INTS8ΔEVL mutations. qRT-PCR indicates that *INTS8* expression is reduced in patient cells (~50% reduction) suggesting that one of the INTS8 genes is not expressed (Fig. 2A). To confirm this, we designed an amplicon incapable of amplifying the INTS8ΔEVL allele and found that the expression of the INTS8 c.893A>G allele is almost undetectable in patients (Fig. 2A).

Close analysis of known INTS8 transcripts in the NCBI RefSeq database indicates that the INTS8 c.893A>G mutation is located at position +1 of an exon (exon 8) of an annotated alternative 3¢ splice site used by isoform NR_073445.1 (variant 3, Fig. 2B). This variant is predicted to generate a premature stop codon within exon 8 and to be subjected to rapid degradation through nonsense mediated decay (NMD). To test the impact of c.893A>G on exon 8 splicing, we designed an INTS8-GFP minigene-reporter construct (Fig. 2C). Wild-type-*INTS8* minigenes transfected into HeLa or HEK293T cells generated two distinct exon inclusion products (Fig. 2D), confirmed by Sanger sequencing to be variants 1 and 3 (not shown). Strikingly, introduction of the single base c.893A>G mutation into the *INTS8* reporter was sufficient to completely change the splicing of exon 8 such that the distal 3¢ splice site used in the *INTS8* variant 3 was now exclusively utilized (Fig. 2D). Cloning and sequencing of this single spliced product confirmed the predicted exon junction (Fig. S3A). Both endogenous isoforms can be detected in HeLa cells but variant 3 constitutes only 6% of total cellular *INTS8* mRNA (Fig. S3B and S3C). Treatment in HeLa or HEK293T cells with puromycin or cycloheximide increased variant 3 RNA levels to 43% and 34%, respectively (Fig. S3C), supporting the model that variant 3 is subject to NMD.[30] In patient cells, baseline levels of *INTS8* variant 3 also increased after mRNA stabilization (Fig. S3D). Collectively, these results show that the c.893A>G mutation dramatically alters the splicing of *INTS8* exon 8, producing a premature stop codon and an unstable transcript.

As the c.893A>G allele produces an unstable mRNA, we deduced that the mutant INTS8ΔEVL is the preponderant protein expressed as suggested by the levels of mRNA expression in patient cells (Fig 2A, middle panel). Further, we could detect comparable levels and nuclear localization of INTS8ΔEVL protein in patient cells suggesting that

removal of these three amino acids does not overtly impact protein folding and accumulation (Fig S4, S5 and S6). Therefore, we investigated whether the INTS8ΔEVL protein could impact INTS8 interaction with the other subunits in the complex. To that end, we established HEK293T cells stably expressing wild-type (WT) or mutant (ΔEVL) INTS8 bearing an N-terminal 3XFLAG tag and purified the associated INT using anti-FLAG affinity resin. While WT and mutant INTS8-associated peptides showed a very similar pattern by SDS-PAGE (Fig. S7). Probing for the presence of specific INT subunits revealed differential association with the two proteins. The ΔEVL-FLAG-INTS8 eluates contained nearly undetectable amounts of INTS1,-12 and RPB1, reduced levels of associated INTS4,-9,-11, but similar levels of endogenous INTS5 and INTS3, compared to WT-FLAG-INTS8 (Fig. 2E). Thus, the ΔEVL mutation appears to impact the ability of INTS8 to associate with other members of the INT complex. In patient cells we found reduced levels of INTS4, INTS9, and INTS11 and normal levels of INTS3 (Fig. 2F) suggesting that the reduced association of INTS8 with other members of INT leads to an overall loss in INT integrity and stability of some of its subunits. Consistent with this observation, we measured slight but significantly elevated amounts of misprocessed snRNA in patient cells (Fig. 2G), although total snRNA levels did not significantly differ between patient and control cells (Fig. S8). Taken together, these results indicate that in patient cells, there is both a reduction in integrity and function of INT.

To investigate the extent of INTS8 dysfunction on transcription and splicing, we conducted both exon array analysis and RNA-seq on patient cells relative to controls. Differential gene expression (DGE) data from exon arrays performed on fibroblasts showed a large number of significantly dysregulated genes in the patients' vs. control cells (n=682; $p<0.02$, Table S3). To confirm results attained by exon array and to further explore a genome-wide effect on splicing we subjected poly(A) mRNA fractions from patient III-2 and III-4 and 2 controls to high depth RNAseq analysis (~65-fold average coverage, Table S4). We found an even larger number of genes (N=3,002; $p< 0.02$) that were significantly up- or downregulated in patient cells vs. control cells (Table S5). We validated 17 of these potential target genes by qRT-PCR (Fig. 3A,3B, S9). Comparison of DGE data between exon arrays (3x3 design) and RNAseq (2x2 design) showed a correlation coefficient of 0.66 between the two data sets (Fig. 3C) and, interestingly, that a majority of the genes that are significantly dysregulated in both datasets (N=82) are expressed in the CNS (Table S6).

In addition to transcriptional deregulation, we also detected significant splicing changes in 215 genes ($p<0.01$, 292 total events, Table S7) and confirmed the *INTS8* alternative splicing induced by the c. 893A>G mutation in patient cells. The vast majority of affected splicing events are skipped exons (65%) and mutually exclusive exons (19%, Fig. 3D). We selected five alternatively spliced genes and confirmed the corresponding splicing changes (Fig. 3E, 3F, S10). In mammals, it is estimated that 90%

of protein-coding genes are subject to alternative splicing (AS) and that the brain in particular relies heavily on AS to regulate neuronal development.[31-33] Among the AS genes, the *SPTAN1* gene is particularly interesting because in patient cells, exon 37 of

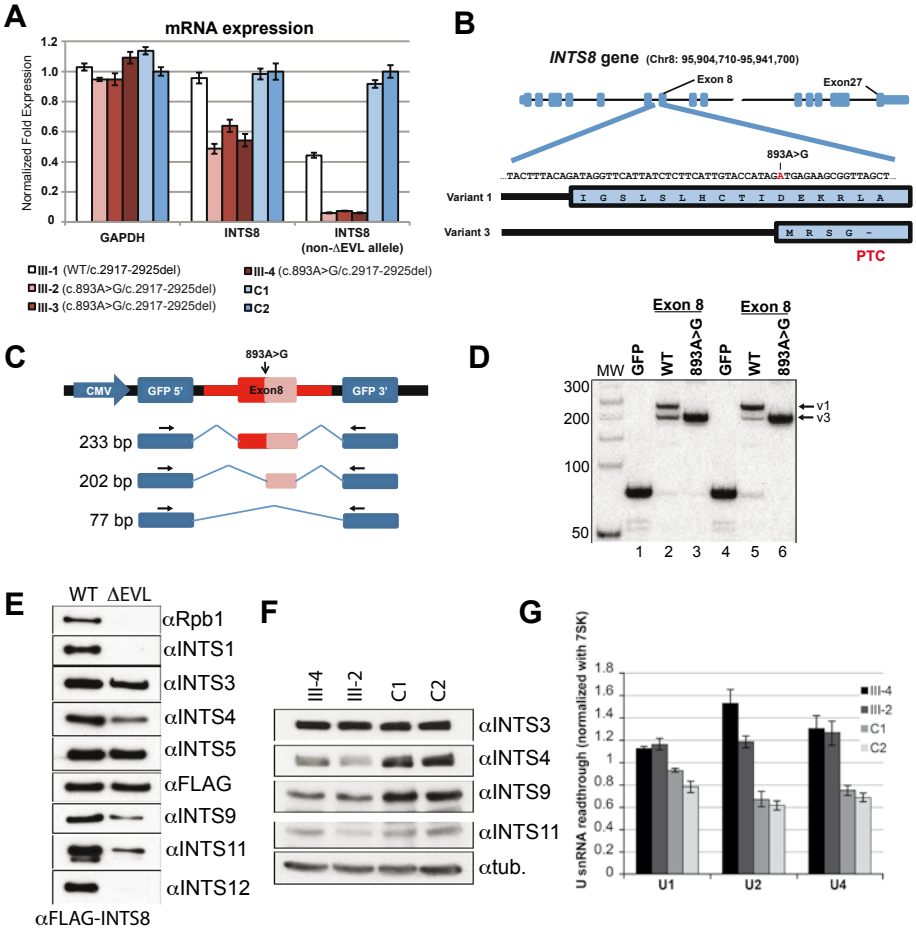

Figure 2. Effect of the *INTS8* mutations.
(A) qRT-PCR on fibroblast-derived RNA of the patients (III-2, III-3, III-4), their unaffected sibling (III-1), and two control cell lines (C1, C2), normalized for *GAPDH* expression. Expression of the c.893A>G allele vs. wild type was measured using a primer designed at the c.2917-2925del (INTS8 non-ΔEVL allele). (B) Schematic overview of INTS8 genomic and protein sequence. The c.893A>G mutation is present at the start of the exon8 of transcript variant 3 that contains a premature stop codon. (C) Schematic of the GFP-minigene reporter construct used to evaluate the effect of the c.893A>G mutation on *INTS8* exon 8 splicing pattern. (D) RT-PCR analysis of RNA isolated from HeLa (lanes 1-3) or HEK293T cells (lanes 4-6) transfected with the GFP-minigene constructs. The empty reporter (GFP) is used as a control. (E) Western blot analysis of flag-affinity eluates from HEK293T stable lines expressing 3xFlag-tagged INTS8 wild type (WT) or INTS8ΔEVL. (F) Western blots on total cell extracts from patient and control primary fibroblasts. (G) qRT-PCR showing normalized expression of misprocessed U1, U2 and U4 snRNAs in total RNA extracted from patient III-2 and III-4 fibroblasts compared to two controls.

the gene is exclusively skipped. *SPTAN1*-deficient patients share many features with the *INTS8* patients as they present with severe intellectual disability, no visual tracking, epilepsy and spastic tetraplegia and brain imaging shows cerebellar hypoplasia, acquired microcephaly and hypomyelination.[34] Interestingly, the skipped exon (exon 37) is normally specific to brain and muscle tissues and codes for a predicted protein-protein interaction motif suggesting a potential loss of function in *INTS8* patients.[35-37] Altogether, these results indicate that INT-deficient patient cells contain global transcriptome perturbations manifesting as both altered splicing patterns and gene

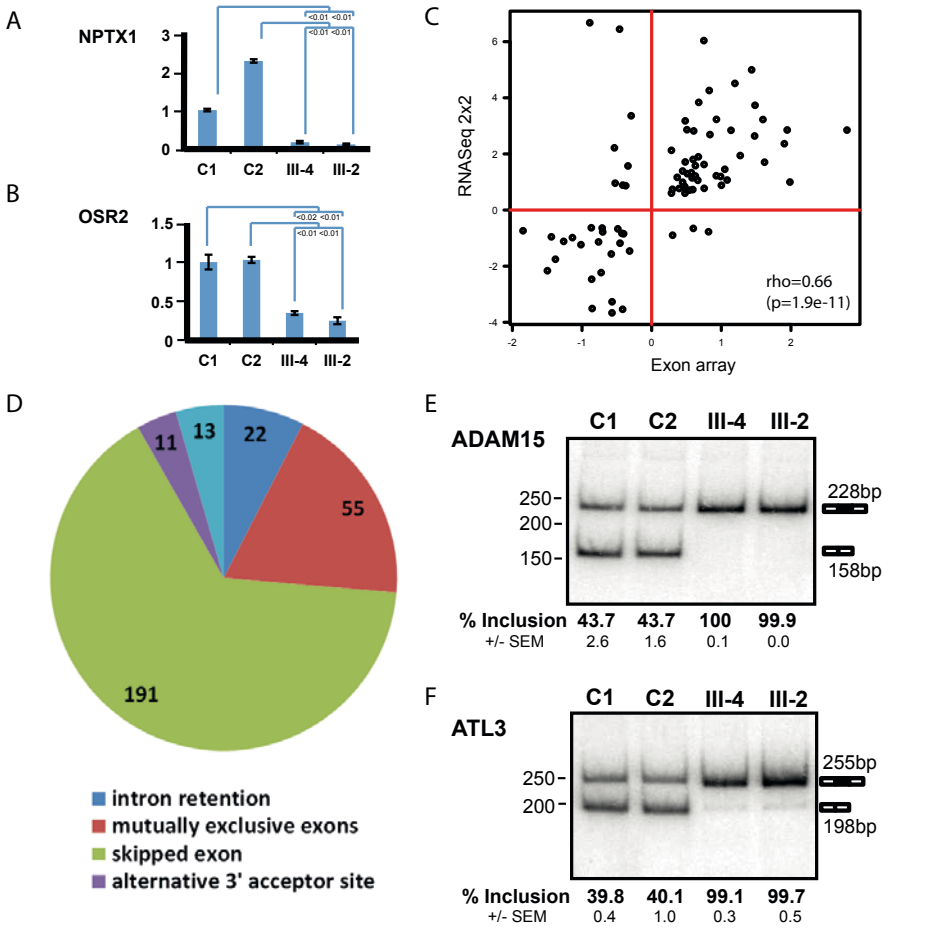

Figure 3. Dysregulated transcriptome in patient cells.
(A, B) qRT-PCR validation of gene expression variation in patient cells for *NPTX1* and *OSR2* mRNAs. (C) Correlation analysis of DGE data from exon arrays (X axis) and RNAseq (Y axis). (D) Pie chart representing the different types of AS detected in patient cells vs control in RNA-seq data (n=215, p<0.01, 292 total events). (E, F) Experimental verification by RT-PCR of the splicing changes associated with INTS8 mutations for *ADAM15* (E) and *ATL3* (F) mRNAs.

expression, which are supported by INT's emerging role in both UsnRNA processing and transcription regulation.

In view of the severe developmental brain defects observed in the patients, and the peak of *INTS8* expression in the human and mouse fetal brain (Fig. S11, S12), we studied the effect of INTS8 depletion in zebrafish embryos using a morpholino antisense oligonucleotide (MO) approach directed against the zebrafish homolog of human *INTS8* (NP_001018592.2, Text S1). We designed two splice-blocking MO against *ints8*, MO1 and MO2, and both were able to down-regulate *ints8* mRNAs levels by more than 90% (Fig. S13, S14). The MO1 morphants showed severe developmental defects detectable as early as one day post fertilization (dpf) and readily visible at 2 dpf. Notably, *ints8* morphants presented central nervous system defects characterized by a smaller and structurally abnormal brain compared to wild type (Fig. 4A-F). In addition, they had near-absent pigmentation, underdevelopment of the eye, swelling of the yolk sac, and pericardial edema. Not only were the effects visible at relatively low MO doses, but we also observed a dose-dependent response from 2 to 8 ng (Fig. 4B-D). Morphants developed microcephaly as their head size was significantly smaller in 4 ng and 8 ng morphants compared to uninjected embryos (Fig. 4G). More importantly, we found that the head size/body length ratio was also significantly smaller in the morphants (Fig. 4H). This suggests that there is a specific effect of *ints8* depletion on head development independent from an overall developmental growth defect. To rule out the possibility that the observed developmental defects were caused by off-target p53-mediated apoptosis [38], we co-injected MO1 with p53-MO. The phenotype of these morphants did not differ from that observed in the MO1 morphants (Fig. S15). Injections with MO2 replicated the MO1 phenotype, as these morphants also had significantly smaller heads and smaller head size/ length ratio (Fig. S16). Altogether these results indicate that *ints8* expression is required in the developing zebrafish brain and that its depletion causes microcephaly, as we also observed in patients.

Our study provides the first evidence for an evolutionary conserved requirement of INTS8 and crucial role of INT during human brain development. INTS8 is essential for the structural and functional integrity of INT, and mutated INTS8 causes increased U snRNA misprocessing, increased AS events and altered gene expression, confirming a central INT role in transcriptional regulation.

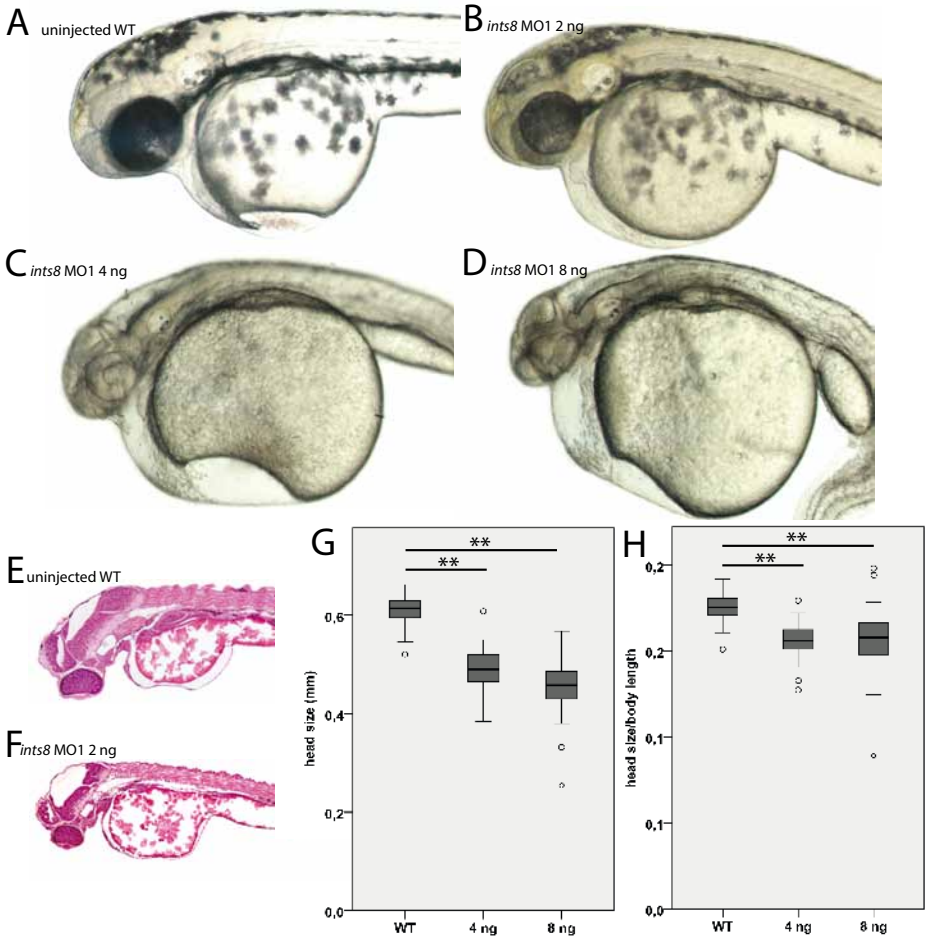

Figure 4. Underdevelopment of the head in ints8 zebrafish morphants.
(A-D) Close view of zebrafish embryos at 2 dpf treated with increasing *ints8* MO1 doses (WT= uninjected). (E, F) Representative pictures of histology sections of uninjected WT and embryos injected with 2ng MO1 at 2 dpf. (G) Comparison of head size at 3 dpf between WT and embryos treated with 4 and 8 ng of *ints8* MO1 (n=40, ** p=<0.001, Kruskal-Wallis). (H) Comparison of head size/body length ratio at 3 dpf between WT and embryos treated with 4 and 8 ng of *ints8* MO1 (n=40, ** p=<0.001, Kruskal-Wallis).

MATERIALS AND METHODS

Subject recruitment

All study participants or their legal caretakers gave written informed consent to participate in this study, and for publication of images, according to Erasmus MC institutional review board requirements (protocol METC-2011253, METC-2012387).

Whole genome and Sanger sequencing

Whole-genome sequencing (WGS) using DNA from the four siblings and their parents was performed using the Complete Genomics platform (Mountain View, US), details are provided in File S1. Data are deposited internally at the Erasmus MC to acknowledge the privacy of the family.

qRT-PCR of endogenous INTS8

Quantitative (q)RT-PCR of RNA extracted from cultured fibroblasts of the affected siblings, their unaffected brother, and two control cell lines was carried out using a KAPA SYBR FAST qPCR Kit (Kapa Biosystems) in the CFX96 Real-Time system (BioRad), details are provided in Supplemental Methods.

qRT-PCR of misprocessed UsnRNA and Integrator target gene expression in primary fibroblasts

qRT-PCR was performed using RNA from cultured fibroblasts on a Stratagene Mx3000P real-time PCR system (Agilent) using the KAPA SYBR FAST qPCR Kit (Kapa Biosystems) according to manufacturer's instructions, details are provided in Supplemental Methods.

Splicing assays

Exon 8 and flanking intronic sequences of human *INTS8* gene were amplified from HEK293T genomic DNA by PCR (primers in Supplemental Methods). The amplicon was cloned into the pGint vector [39] using BamHI and SalI restriction sites. The A893G mutation was introduced by site directed mutagenesis (primers in Supplemental Methods). The resulting constructs were transfected in HEK293T and HeLa cells using Lipofectamine2000 (Thermo Fisher). After 48h, total RNA was extracted, purified and used to generate cDNA. PCR amplification of the corresponding splicing product was performed. For detection and quantification, oligonucleotides were 5' radiolabeled using 32P-γATP and T4 Polynucleotide Kinase (Thermo Fisher) and added in a 1/10 ratio with unlabeled oligonucleotides. The corresponding PCR reactions were resolved onto a 6% non-denaturing acrylamide gel, fixed and dried. The gels were scanned using a storage phosphor screen and a Storm scanner (GE Healthcare) and quantified using ImageQuant software (GE Healthcare).

INTS8 stable cell lines and Flag-affinity purification

The human *INTS8* cDNA was amplified by PCR from HeLa cell cDNA and the corresponding PCR product was cloned into a modified pCDNA6 plasmid containing an N-terminal 3XFlag tag using EcoRI and XhoI restriction sites. The EVL deletion was introduced by site directed mutagenesis. HEK293T cells were transfected with either

construct. Flag-affinity purification was performed as in [1] using nuclear extracts from approximately 10^9 cells. Integrator subunits in the eluate were detected by Western blot using the following antibodies: anti-FLAG M2 (Sigma), INTS1 (Bethyl, A300-361A), INTS3 (Bethyl, A302-050A), INTS4 (Bethyl, A301-296A), INTS5 (Abcam, ab74405), INTS9 (Bethyl, A300-422A), INTS11 (Bethyl, A301-274A) and INTS12 (Proteintech, 16455-1-AP). Oligonucleotide sequences are listed in File S1.

Western blot of Integrator complex components

Cultured fibroblasts were used for western blots of INT components. Approximately 75 µg of the clarified whole cell extract were separated on an 8% acrylamide SDS-PAGE gel. After transfer to a PVDF membrane, the presence of the different INT subunits was assessed by Western blot using the antibodies listed above.

Exon arrays

Six Affymetrix GeneChip Human Exon 1.0 arrays of RNA extracted from cultured fibroblasts of all three affected siblings and three age and sex-matched controls were rma normalized on transcript level using the R package (http://www.r-project.org). Top down- and upregulated genes with p values <0.02 were analyzed for enriched gene ontology terms (goterms_BP_all) using DAVID (medium stringency) to identify clusters with significant enrichment (enriched score ≥ 1.3). CEL file microarray data are available under GEO accession number GSE48849 (http://www.ncbi.nlm.nih.gov/geo/).

RNA-Seq analysis

Poly(A) mRNA fractions isolated from cultured fibroblasts from patient III-2, III-4, and two controls were subjected to RNA-Seq analysis. In order to detect even slight changes in splicing, we utilized high depth RNA sequencing (RNA-Seq, ~1.5 x 10^7 reads). The resulting data was analysed using a recently developed pipeline specifically designed to monitor splicing efficiency.[40] In addition, we analysed patient and control RNA-Seq data for differences in gene expression at steady state levels using EdgeR. Data are deposited in Gene Expression Omnibus (GSE76878).

Zebrafish *ints8* morpholino design and microinjections

All zebrafish procedures and conditions were in accordance with the Dutch animal welfare legislation, details are provided in supp. Two Morpholino antisense oligo-nucleotides (MO1 and MO2) predicting abnormal splicing were obtained from Gene Tools (Philomath, OR, USA). MO1 was designed against zebrafish ints8 targeting the intron 2 exon 3 donor site. The second morpholino (MO2) targets the exon 6 intron 7 boundary. Indicated amounts of MOs solutions were injected into the yolk of one to two cells stage zebrafish embryos (Danio rerio,Tupfel long fin strain) using a pneumatic

picopump (World Precision Instruments, Berlin, Germany). In addition, a previously described MO against p53 was used to detect possible off-target effects due to activation of p53 expression.[38] For measurements, pictures were taken with a Leica M165 MC stereo microscope and Leica Application Suite v4.4.0 software. Measurements were made using the Fiji software (ImageJ 1.50a, http://imagej.nih.gov/ij). For body length, total distance from head to tail was measured. For head size, we measured the distance from head till the posterior part of the otic vesicle. The head size/body length ratio was calculated for each larva using Excel software. The Kruskal-Wallis test for non-parametric statistical testing of independent samples was performed using IBM SPSS software (v21).

Supplementary information is available online at http://cluster15.erasmusmc.nl/oegema. Username oegema, password renske.

ACKNOWLEDGEMENTS

We thank the family, object of this study, for the trust and collaboration throughout the years.
Also we would like to thank Dr. Annemieke J. Verkerk for support during the early stages of the project.

Funding

Work in the Wagner laboratory is funded from the Welch Foundation (H-1889). Work in the Mancini laboratory was supported by the Erasmus MC grant (Mrace nr. 104673 to GMSM). Work in the Erasmus MC Bioinformatics department was supported by CTMM and Lygature grants.

REFERENCES

1. Baillat D, Hakimi MA, Naar AM, Shilatifard A, Cooch N, Shiekhattar R. Integrator, a multiprotein mediator of small nuclear RNA processing, associates with the C-terminal repeat of RNA polymerase II. Cell. 2005;123(2):265-76. Epub 2005/10/22.
2. Peart N, Sataluri A, Baillat D, Wagner EJ. Non-mRNA 3′ end formation: how the other half lives. Wiley Interdiscip Rev RNA. 2013;4(5):491-506. Epub 2013/06/12.
3. Gardini A, Baillat D, Cesaroni M, Hu D, Marinis JM, Wagner EJ, et al. Integrator regulates transcriptional initiation and pause release following activation. Mol Cell. 2014;56(1):128-39. Epub 2014/09/10.
4. Latos PA, Goncalves A, Oxley D, Mohammed H, Turro E, Hemberger M. Fgf and Esrrb integrate epigenetic and transcriptional networks that regulate self-renewal of trophoblast stem cells. Nat Commun. 2015;6:7776. Epub 2015/07/25.
5. Skaar JR, Ferris AL, Wu X, Saraf A, Khanna KK, Florens L, et al. The Integrator complex controls the termination of transcription at diverse classes of gene targets. Cell Res. 2015;25(3):288-305. Epub 2015/02/14.
6. Stadelmayer B, Micas G, Gamot A, Martin P, Malirat N, Koval S, et al. Integrator complex regulates NELF-mediated RNA polymerase II pause/release and processivity at coding genes. Nat Commun. 2014;5:5531. Epub 2014/11/21.
7. Lai F, Gardini A, Zhang A, Shiekhattar R. Integrator mediates the biogenesis of enhancer RNAs. Nature. 2015;525(7569):399-403. Epub 2015/08/27.
8. Chen J, Ezzeddine N, Waltenspiel B, Albrecht TR, Warren WD, Marzluff WF, et al. An RNAi screen identifies additional members of the Drosophila Integrator complex and a requirement for cyclin C/Cdk8 in snRNA 3′-end formation. RNA. 2012;18(12):2148-56. Epub 2012/10/26.
9. Mandel CR, Kaneko S, Zhang H, Gebauer D, Vethantham V, Manley JL, et al. Polyadenylation factor CPSF-73 is the pre-mRNA 3′-end-processing endonuclease. Nature. 2006;444(7121):953-6. Epub 2006/11/28.
10. Albrecht TR, Wagner EJ. snRNA 3′ end formation requires heterodimeric association of integrator subunits. Mol Cell Biol. 2012;32(6):1112-23. Epub 2012/01/19.
11. Baillat D, Wagner EJ. Integrator: surprisingly diverse functions in gene expression. Trends Biochem Sci. 2015;40(5):257-64. Epub 2015/04/18.
12. Ezzeddine N, Chen J, Waltenspiel B, Burch B, Albrecht T, Zhuo M, et al. A subset of Drosophila integrator proteins is essential for efficient U7 snRNA and spliceosomal snRNA 3′-end formation. Mol Cell Biol. 2011;31(2):328-41. Epub 2010/11/17.
13. Han SM, Lee TH, Mun JY, Kim MJ, Kritikou EA, Lee SJ, et al. Deleted in cancer 1 (DICE1) is an essential protein controlling the topology of the inner mitochondrial membrane in C. elegans. Development. 2006;133(18):3597-606. Epub 2006/08/18.
14. Hata T, Nakayama M. Targeted disruption of the murine large nuclear KIAA1440/Ints1 protein causes growth arrest in early blastocyst stage embryos and eventual apoptotic cell death. Biochim Biophys Acta. 2007;1773(7):1039-51. Epub 2007/06/05.
15. Rutkowski RJ, Warren WD. Phenotypic analysis of deflated/Ints7 function in Drosophila development. Dev Dyn. 2009;238(5):1131-9. Epub 2009/03/28.
16. Tao S, Cai Y, Sampath K. The Integrator subunits function in hematopoiesis by modulating Smad/BMP signaling. Development. 2009;136(16):2757-65. Epub 2009/07/17.

17. Kapp LD, Abrams EW, Marlow FL, Mullins MC. The integrator complex subunit 6 (Ints6) confines the dorsal organizer in vertebrate embryogenesis. PLoS Genet. 2013;9(10):e1003822. Epub 2013/11/10.
18. Jia Y, Mu JC, Ackerman SL. Mutation of a U2 snRNA gene causes global disruption of alternative splicing and neurodegeneration. Cell. 2012;148(1-2):296-308. Epub 2012/01/24.
19. Edery P, Marcaillou C, Sahbatou M, Labalme A, Chastang J, Touraine R, et al. Association of TALS developmental disorder with defect in minor splicing component U4atac snRNA. Science. 2011;332(6026):240-3. Epub 2011/04/09.
20. Muse GW, Gilchrist DA, Nechaev S, Shah R, Parker JS, Grissom SF, et al. RNA polymerase is poised for activation across the genome. Nat Genet. 2007;39(12):1507-11. Epub 2007/11/13.
21. Guenther MG, Levine SS, Boyer LA, Jaenisch R, Young RA. A chromatin landmark and transcription initiation at most promoters in human cells. Cell. 2007;130(1):77-88. Epub 2007/07/17.
22. Zeitlinger J, Stark A, Kellis M, Hong JW, Nechaev S, Adelman K, et al. RNA polymerase stalling at developmental control genes in the Drosophila melanogaster embryo. Nat Genet. 2007;39(12):1512-6. Epub 2007/11/13.
23. Lagha M, Bothma JP, Esposito E, Ng S, Stefanik L, Tsui C, et al. Paused Pol II coordinates tissue morphogenesis in the Drosophila embryo. Cell. 2013;153(5):976-87. Epub 2013/05/28.
24. Gaertner B, Zeitlinger J. RNA polymerase II pausing during development. Development. 2014;141(6):1179-83. Epub 2014/03/07.
25. Williams LH, Fromm G, Gokey NG, Henriques T, Muse GW, Burkholder A, et al. Pausing of RNA polymerase II regulates mammalian developmental potential through control of signaling networks. Mol Cell. 2015;58(2):311-22. Epub 2015/03/17.
26. Saha RN, Dudek SM. Splitting hares and tortoises: a classification of neuronal immediate early gene transcription based on poised RNA polymerase II. Neuroscience. 2013;247:175-81. Epub 2013/05/29.
27. Korb E, Finkbeiner S. Arc in synaptic plasticity: from gene to behavior. Trends Neurosci. 2011;34(11):591-8. Epub 2011/10/04.
28. West AE, Greenberg ME. Neuronal activity-regulated gene transcription in synapse development and cognitive function. Cold Spring Harb Perspect Biol. 2011;3(6). Epub 2011/05/11.
29. Kircher M, Witten DM, Jain P, O'Roak BJ, Cooper GM, Shendure J. A general framework for estimating the relative pathogenicity of human genetic variants. Nat Genet. 2014;46(3):310-5. Epub 2014/02/04.
30. Noensie EN, Dietz HC. A strategy for disease gene identification through nonsense-mediated mRNA decay inhibition. Nat Biotechnol. 2001;19(5):434-9.
31. Pan Q, Shai O, Lee LJ, Frey BJ, Blencowe BJ. Deep surveying of alternative splicing complexity in the human transcriptome by high-throughput sequencing. Nat Genet. 2008;40(12):1413-5. Epub 2008/11/04.
32. Wang ET, Sandberg R, Luo S, Khrebtukova I, Zhang L, Mayr C, et al. Alternative isoform regulation in human tissue transcriptomes. Nature. 2008;456(7221):470-6. Epub 2008/11/04.
33. Norris AD, Calarco JA. Emerging Roles of Alternative Pre-mRNA Splicing Regulation in Neuronal Development and Function. Front Neurosci. 2012;6:122. Epub 2012/09/01.
34. Tohyama J, Nakashima M, Nabatame S, Gaik-Siew C, Miyata R, Rener-Primec Z, et al. SPTAN1 encephalopathy: distinct phenotypes and genotypes. J Hum Genet. 2015;60(4):167-73. Epub 2015/01/30.
35. Cianci CD, Zhang Z, Pradhan D, Morrow JS. Brain and muscle express a unique alternative transcript of alphaII spectrin. Biochemistry. 1999;38(48):15721-30. Epub 2000/01/08.

36. Heery DM, Kalkhoven E, Hoare S, Parker MG. A signature motif in transcriptional co-activators mediates binding to nuclear receptors. Nature. 1997;387(6634):733-6. Epub 1997/06/12.
37. Savkur RS, Burris TP. The coactivator LXXLL nuclear receptor recognition motif. J Pept Res. 2004;63(3):207-12. Epub 2004/03/31.
38. Robu ME, Larson JD, Nasevicius A, Beiraghi S, Brenner C, Farber SA, et al. p53 activation by knockdown technologies. PLoS Genet. 2007;3(5):e78. Epub 2007/05/29.
39. Bonano VI, Oltean S, Garcia-Blanco MA. A protocol for imaging alternative splicing regulation in vivo using fluorescence reporters in transgenic mice. Nat Protoc. 2007;2(9):2166-81. Epub 2007/09/15.
40. Singh RK, Xia Z, Bland CS, Kalsotra A, Scavuzzo MA, Curk T, et al. Rbfox2-coordinated alternative splicing of Mef2d and Rock2 controls myoblast fusion during myogenesis. Mol Cell. 2014;55(4):592-603. Epub 2014/08/05.

Chapter 5

GENERAL DISCUSSION

GENERAL DISCUSSION

The main purpose of my research was to expand our knowledge regarding malformations of cortical development (MCD). Our studies provide novel data with respect to their presentation, classification and etiology. Although our knowledge on MCD has expanded substantially, we have also learned that MCD are far more diverse on the clinical and genetic level than we had ever anticipated.
This general discussion will highlight my most important findings and place them in the context of the current knowledge on cortical development. It starts with a discussion of the phenotypic heterogeneity and the importance of thorough phenotyping. Next, I will show that this heterogeneity is also present at the genetic level, but at the cellular level many MCD-associated genes can be linked to similar underlying pathways. Regulation of gene expression is presented as a novel mechanism. Finally , the future perspectives and challenges in diagnostics and research will be discussed.

MCD PHENOTYPING

For many rare disorders, knowledge on the full clinical spectrum and/or the molecular background is lacking, therefore the individuals described in this thesis were carefully phenotyped. We showed that this can lead to a clinical diagnosis, targeted identification of the molecular cause, or expansion of the phenotype associated with a known gene. The latter will provide better counseling of the affected families on the prognosis of their disorder and the possibility to anticipate on specific symptoms.

Imaging-based diagnosis

Chapter 2.1 showed that regarding subcortical heterotopia the current MCD classification is not comprehensive and many subtypes exist. Also it showed that an imaging-based diagnosis can be very helpful in predicting the likelihood of a genetic etiology with high recurrence risk or rather a sporadic occurrence.
Chapter 2.2 illustrates the emerging importance of tubulinopathies, e.g. disorders caused by a mutation in a tubulin gene. Likely, any clinician involved in the care of MCD patients will encounter tubulinopathy patients. The first studies screening tubulin genes in large cohorts of MCD patients has yielded a mutation detection rate of 1-10%.[1-4] Although the phenotypic spectrum is extremely broad, including microcephaly, lissencephaly, pachygyria, polymicrogyria and simplified gyral pattern, it has become evident that tubulinopathies share a complex but recognizable brain imaging pattern. Often the corpus callosum is agenetic or hypogenetic, the basal ganglia are dysmorphic with absence of the internal capsule, and the brain stem and cerebellum are hypoplastic and dysplastic (Fig. 1). A recent study has shown that selecting MCD patients for these additional abnormalities substantially increased the mutation

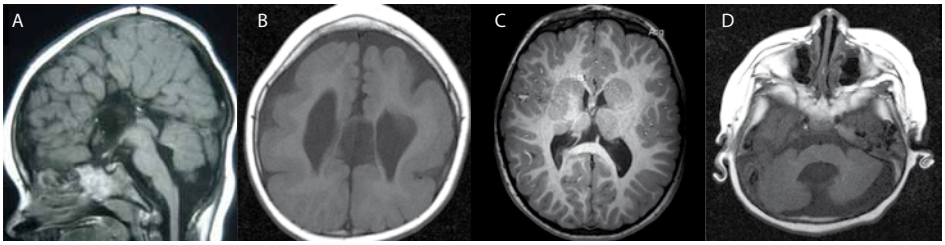

Figure 1. Typical MR imaging abnormalities observed in tubulinopathies
(all T1 weighted). (A) Agenesis of the corpus callosum in patient with *TUBA1A* c.410T>A. (B) Pachygyria with an asymmetric gyral pattern in patient with *TUBA1A* c.1265G>A. (C) Asymmetric dysmorphic basal ganglia and thalami with fusion of the caudate and putamen in patient with *TUBB3* c.1070C>T. Also note the normal cortical thickness , with irregular sulcal depth, especially evident in the frontal lobes (dysgyria). (D) Asymmetric cerebellar hypoplasia (*TUBA1A* c.1265G>A).

detection rate, up to 42% for *TUBA1A*. [5] We show in Chapter 2.2 that a distinct cerebellar dysplasia is highly predictive of finding tubulin mutations, as we found mutations in 7 out of 9 tested patients. None of the scans of these patients were classified as MCD, although re-review showed a clearly abnormal gyral pattern. This pattern, however, did not classify as either polymicrogyria, pachygyria or simplified gyral pattern. Instead, the cortical thickness was near-normal, but the gyri were irregular in size and in depth. As nomenclature was lacking, we proposed the term dysgyria. This term has also been adopted by the Barkovich group.[6] Also, a feature which had been noted by others, but had not received much attention, is the marked asymmetry of the abnormalities.

Phenotypic expansion

An imaging diagnosis and a syndrome diagnosis can be complementary to each other and the clinical geneticist plays an essential role in this by carrying out a thorough dysmorphology exam in every child with MCD. This is illustrated in Chapter 3.1, where we expanded the clinical spectrum of KBG syndrome with PNH. The MCD itself did not offer a clue to the diagnosis in this child, as PNH were, at this time, never described in patients with KBG syndrome. Similarly, in chapter 3.3, we described for the first time, PNH and polymicrogyria in a patient with a known *ARX* mutation. The finding of MCD in this boy eventually led to successful epilepsy surgery. This illustrates how clinical observations remain essential, even in the background of a molecular diagnosis.
The proband from the family described in chapter 3.4 had extensive multi-organ involvement, but not until the finding of PNH this led to the identification of the *FLNA* mutation. We show through our study and extensive literature review that the common assumption that *FLNA* mutations are embryonically lethal in males is untrue. Moreover, these males commonly present with multi-organ involvement and the gastro-intestinal symptoms in particular can be debilitating. The symptoms associated

with FLNA mutations are extremely variable, even within the same family. For example, we observed severe respiratory disease in one affected boy, but not in his two cousins. Similar observations have been made in other families.[7,8] Future studies should aim at identifying possible modifying factors, genetic or environmental, as these might offer clues to therapeutic interventions.

In chapter 3.5 we expanded the phenotype associated with a known mutation in *PNKP* with severe neurodegeneration. Our finding should therefore change the counseling on prognosis and the clinical care for patients with *PNKP* mutations. The finding of neurodegenerative features has been confirmed in a subsequent Portuguese study, where *PNKP* was found to be a major gene associated with autosomal recessive dystonia, ataxia and oculomotor apraxia.[9] As we have observed an increased susceptibility to undergo apoptosis in patient cells , one could hypothesize that the microcephaly and seizures are due to increased apoptosis in the brain. A similar mechanism has been proposed for the microcephaly, epilepsy, and diabetes syndrome.[10] Of note, the Portuguese patients did not have microcephaly nor seizures, and therefore the susceptibility to apoptosis might depend on the genotype, or on an additional event triggering the onset of apoptosis.

In conclusion, mutations in the same gene can cause extreme phenotypic variability, and, vice-versa, MCD are caused by mutations in many different genes.

Future perspectives

Ultra-high field 7T MRI has already proved its superiority in diagnosing polymicrogyria, focal cortical dysplasia type IIb, and subcortical heterotopia in small cohorts.[11-13] This highly detailed imaging with a microscopic resolution enables visualization of small anatomic structures not previously appreciated at lower fields, and therefore more accurate identification of the location and extent of the malformation.[11] Several other technical advances also aid to provide more detailed and accurate imaging, adding valuable information on prognosis and when planning epilepsy surgery.[14,15] These novel techniques need experienced neuroradiologists to interpret and classify the imaging data, acting in close collaboration with neurologists and clinical geneticists. Clinical geneticists in particular are trained in pattern recognition by incorporating all the typical features of a patient, and a dysmorphologist eye on the brain scan could prove essential in this process. Clinical geneticists also serve as a bridge between the laboratory and the clinic.

MOLECULAR MECHANISMS

Subcortical heterotopia

A subset of rare forms of subcortical heterotopia has been shown to be caused by genetic mutations (discussed below). However, it is striking that for the large majority of subcortical heterotopia, especially the deeply infolded and the curvilinear subtypes, the molecular basis is unknown. We hypothesize that those are caused by either *de novo* mutations, possibly mosaic or somatic, vascular disruptive events or by a complex interplay of genetic and environmental factors. Vascular disruptive events have already been associated with the occurrence of schizencephaly and polymicrogyria.[16,17] A complex etiology is also observed in families with cerebrovascular disease (and also rare instances of schizencephaly, polymicrogyria and cortical dysplasia) due to *COL4A1* mutations; the penetrance is low and modifying factors are required for developing disease.[18] Epilepsy is a major, but potentially treatable complication of subcortical heterotopia and recent studies have shown that the underlying etiology of epilepsy can affect therapy outcome.[19] For epilepsies with a possible genetic basis, efforts should be made to identify its cause paving the way for individualized treatment. MCD is a major cause of epilepsy, as several studies have shown that MCD is found in 25% of pediatric partial seizures, 5-15% of adult epilepsy, and 20-40% of therapy-resistant epilepsy.[20-23] A large-scale sequencing effort, preferably in affected brain tissue, is needed to answer questions regarding etiology and to identify potential targets for therapy.

Periventricular nodular heterotopia

Although mutations in *FLNA* are the most frequent cause of PNH, its etiology is far more complex. This is demonstrated by the findings in our study cohort and is also illustrated by Table 1 in Chapter 1, which list many genes and chromosomal aberrations that have been associated with PNH, many only in sporadic reports. *FLNA* encodes an important regulator of the actin cytoskeleton, which is connected to the plasma membrane through integrins, hence to the extra-cellular matrix. The discovery that the majority of X-linked PNH can be explained by mutations in *FLNA* has led to the hypothesis that PNH are the result of an intrinsic defect in migration of the neuronal progenitor cell.[24] This was supported by the earlier finding that melanoma cell lines lacking FLNA show defective motility.[25] However, in the majority of patients, the cortex is normally or near-normally developed. This suggests that neuronal progenitors harbouring pathogenic mutations can successfully complete migration. Moreover, FLNA has a wide range of functions and dozens of interacting partners.[26] More recent studies have emphasized an important role for the radial glial cell in the pathogenesis of PNH.[27] Brain pathology of deceased *FLNA* patients showed a disruption of the ependymal lining and diminished radial glia processes and these findings were

reproduced by *Flna* knockdown in developing rat brain.[28] In addition, disruption of the radial glial scaffold in animal models leads to heterotopia.[29,30]
Other genes that have been definitely related to periventricular heterotopia are involved in subcellular vesicle trafficking (*ARFGEF2*)[31] and the Hippo pathway, disturbance of which led to increased proliferation of early progenitors and a block in their subsequent differentiation (*DCHS1*, *FAT4*).[32] Interestingly, FLNA has also been implicated in vesicle trafficking and it binds to the *ARGEF2* encoded protein BIG2.[33] It has been suggested that impairment of vesicle trafficking leads to loss of cell adhesion molecules and thus loss of ependymal integrity.[33]
In conclusion of the available data, PNH could be due to a subtle disturbance of intricate processes and a complex interplay of the migrating neuron and its supporting matrix. This disturbance could be caused by either one or a combination of defects in the connection to the ependymal lining, the cytoskeleton, the responsiveness to extracellular cues, the cell cycle, the polarity of the migrating progenitor or of the radial glial cell, neuronal adhesion and disassembly and premature differentiation.[27,34-36] Further studies are necessary to elucidate the full profile of this intriguing process. Animal models have provided great insights into neuronal migration, however they cannot always replicate the cortical malformations observed in humans.[37,38] As mice lack a gyrencephalic cortex, other mammals, for example ferrets serve as better models of human brain development.[39,40] Cerebral organoids offer a simplified model of early brain development, enabling the study of gene expression patterns and the effect of gene knockdowns on proliferation, migration, differentiation, and organisation of human neuronal cells.[41,42]

INTS8

A potential novel mechanism is highlighted by our discovery of *INTS8* mutations in a syndromal form of PNH (chapter 4.1). This study represents the first identification of germline mutations in an Integrator Complex component and shows that this complex is required for brain development in both humans and zebrafish. The Integrator complex associates with RNA polymerase II and regulates snRNA processing, and transcriptional regulation of protein-coding genes through at least transcription initiation and RNA polymerase II pause release.[43]
We propose several mechanisms through which *INTS8* mutations lead to this severe brain developmental disorder. Firstly, altered expression of one particular gene could cause the observed phenotype. Several dysregulated genes in patients cells can be related to early brain development by their function and/or expression profile (Appendix). Secondly, we showed that in patient cells many genes are alternatively spliced. This is in line with the role of the Integrator complex in the processing of snRNAs, major components of the spliceosome. Several studies have demonstrated that the

brain relies heavily on alternative splicing during neuronal development.[44-46] This is supported by the finding that mutations in the splicing factor RNA-binding motif *RBM10* cause abnormal mRNA splicing and intellectual disability, microcephaly, PNH, and cerebellar hypoplasia.[47,48] Similarly, mutations in the minor spliceosome U4atac snRNA gene in human results in splicing defects and cause microcephalic osteodysplastic primordial dwarfism.[49,50] Thirdly, the development of the brain, more than that of any other organ, is finely tuned by RNA transcriptional and post-transcriptional processes.[51] It could be that this fine-tuning is disturbed leading to global transcriptome alterations in the developing brain. Studies in patient cells also support a broader disruption of both gene expression levels and alternative splicing. Finally, it has been shown that the Integrator complex is required for ciliogenesis.[52] SiRNA mediated depletion of several Integrator components led to a significantly decreased number of ciliated cells.[52] It is unclear whether the Integrator complex is directly involved in ciliogenesis or that this is an indirect effect of the altered gene expression or RNA splicing. Because ciliogenesis is crucial during brain development (see below) we studied the cilia in patient cells by immunocytochemistry but observed no obvious structural abnormalities (F. Verheijen, unpublished data). This does not, however, exclude a more subtle effect of these or of other, currently unrecognized, *INTS8* mutations on cilia structure or function.[53,54]

The importance of microtubule dynamics in MCD

Tubulinopathies

Many MCD, including heterotopia and microcephaly, the objects of this study, have a link to abnormalities of microtubules. The recent discoveries of mutations in alpha- and beta-tubulin encoding genes in MCD patients have greatly emphasized the importance of microtubule dynamics. Mutations causing MCD have now been identified in *TUBA1A*, *TUBB2A, TUBB2B*, *TUBB3*, and *TUBB*.[55] In addition to the alpha- and beta-tubulins, mutations in many microtubule-associated genes cause MCD (Fig. 2). In Chapter 2.1 we show that mutations in *EML1*, encoding a microtubule-associated protein cause a rare syndrome characterized by ribbon-like subcortical heterotopia and megalencephaly.[56] This is one of the most rare types of SUBH and one of the few of which the genetic cause has been determined.

Microtubules are an important component of the cytoskeleton and in addition facilitate intracellular transport and nuclear movement, an essential process in cell migration. Microtubules are expressed in many cell types throughout the body. However, mutations in the above-mentioned genes primarily affect the nervous system. This is probably explained by the fact that microtubules are heterodimers build of alpha- and a beta-tubulin isotypes in a variable mixture, as each isotype has its specific temporospatial expression pattern.[57,58] Therefore, the composition of microtubules in neuronal cells differs greatly from that in non-neuronal cells.[58]

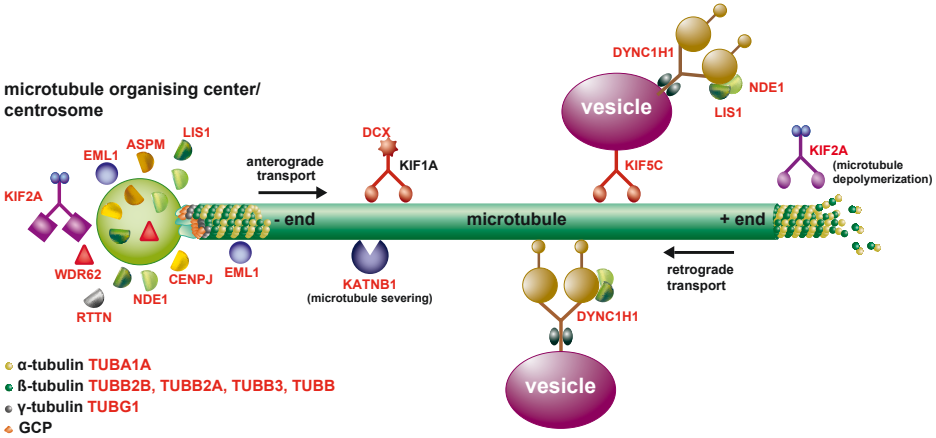

Figure 2. Microtubule with microtubule-associated proteins/genes.
Those associated with MCD are depicted in red. Primary microcephaly genes are not included unless they are associated with structural MCD. [Adapted from Poirier *et al*., 2013, with permission from Nature Publishing group.]

Centrosome

The major microtubule-organizing center is the centrosome (Fig. 2). During cell division, the centrosome duplicates and forms the base of the mitotic spindle which separates the chromosomes. Mutations in many centrosomal components have been shown to cause primary microcephaly.[59] This strengthened the concept that neuronal proliferation is the main process affected in these patients.[60] Although per definition major structural brain abnormalities are absent in individuals with primary microcephaly, very little brain imaging from this group has been published. Our observation of subcortical heterotopia in a girl with primary microcephaly due to *CENPJ* mutations was therefore surprising. However, careful literature study showed that MCD occurs in patients with microcephaly caused by *KATNB1*, *WDR62*, *STIL*, *ASPM*, and *RTTN* mutations suggesting that brain malformations are more frequently observed in patients initially diagnosed as having primary microcephaly.[54,61-64] Hence the original definition of primary microcephaly might become obsolete as there is a broad and continuous spectrum of associated brain abnormalities, similar to the microtubule-associated disorders.

Primary cilium

Microtubules form major building blocks for the primary cilium. This organelle protrudes its axoneme from the cell surface and plays and important role in major cellular signalling pathways, including the Hedgehog and Wnt signaling pathways. The base of the primary cilium is the basal body, a structure derived from the centrioles. The

axoneme consists of a core of microtubule doublets.[65] The significance of cilia function for brain development is evident from the spectrum of neurodevelopmental disorders associated with ciliopathies, e.g. Bardet-Biedl syndrome and Joubert syndrome. A growing number of studies point to an essential role of the primary cilium in mammalian corticogenesis [29,66-69], and we have observed several patients with MCD and defective ciliogenesis ([53] and F. Verheijen and G. Mancini, unpublished data).

Microtubule – actin interactions

Another major cytoskeletal component, the actin network, also plays an important role in cortical development.[70] Filamin A binds to and is an organizer of the actin cytoskeleton.[71] Its importance is also supported by the recent identification of mutations in genes encoding actin components (*ACTB* and *ACTG1*) causing a syndromic form of lissencephaly.[72] Accumulating evidence suggests that there is an important crosstalk between the microtubule and the actin neuronal networks.[73] The microtubule-associated protein doublecortin (DCX, figure 1) can be translocated to F-actin[74], and interestingly, the centrosome can act as an organizer of the actin network.[75] Several actin-related genes had an altered expression in *INTS8* mutant cells, indicating another potential pathway through which the *INTS8* mutations influenced brain development.

DYRK1A and brain development

We described a recognizable syndrome associated with chromosomal microdeletions involving the *DYRK1A* gene (chapter 3.2). Since then, small deletions and point mutations of the *DYRK1A* gene have been identified in patients with similar features.[76-79] This reinforces our assumption that *DYRK1A* haploinsufficiency was the main driver of the phenotype of the patients we described. Importantly, *DYRK1A* has now been recognized as one of the major ID genes, being found in 0.1%-0.5% of patients in large NGS studies.[80,81] Review of (scarce) published imaging data revealed that at least an additional three patients have cortical dysplasia, although this is not mentioned by the authors.[79] *DYRK1A* is a highly conserved gene located in the so-called Down Syndrome critical region (DSCR), a part of chromosome 21 that is responsible for the majority of phenotypic features in Down syndrome (OMIM *600855). It encodes a member of the dual-specificity tyrosine phosphorylation-regulated kinase (DYRK) family and is involved in neuronal proliferation, neuronal differentiation, cell death and synaptic plasticity.[82] In primary hippocampal rat neurons, Dyrk1a overexpression reduced overall axon growth.[83] The precise molecular mechanism through which DYRK1A regulates neuronal development remains to be elucidated, but interestingly it has been found be essential to several pathways related to MCD. For example, Dyrk1a is able to alter DCX expression, to down-regulate hedgehog signalling and to affect F-actin remodelling.[83,84] DYRK1A has also been shown to regulate cell cycle exit and

differentiation of neural precursors.[85] Taken together, the effect of DYRK1A deficiency on brain development is probably multifold, affecting proliferation leading to microcephaly, affecting cytoskeleton dynamics leading to MCD in a subset of patients, and affecting axon outgrowth and synaptic plasticity leading to moderate to severe ID in all patients.

New developments and challenges in molecular diagnostics

The chapters in this thesis not only present characterisation of MCD-associated phenotypes , but also illustrate the rapid evolution in genetic testing over the past few years. Starting with a clinical syndrome description (chapter 3.1), to targeted gene testing (3.3, 3.4) and submicroscopic aberrations (3.2) to finally mutations detected by whole-exome and whole genome sequencing (WES and WGS, 2.1, 3.6, 4.1).
Detection of submicroscopic copy-number variants with SNP-array, targeted next-generation sequencing and whole-exome sequencing have now become the primary diagnostic procedure for this group of patients. In intellectual disability, this has been shown to increase the chance of establishing a genetic diagnosis substantially, and is expected to increase further with the diagnostic implementation of whole-genome sequencing.[86,87] However, we are still far away from a 100% mutation discovery rate for MCD. An NGS approach using a targeted panel by our center and by others gave a detection rate of 6-18%.[88,89] No numbers for WES/ WGS have been published, however in our center we observe many unsolved cases after WES, especially patients with polymicrogyria remain without a molecular diagnosis (G. Mancini, personal observation). Most of the diagnoses involve genes with an autosomal recessive, autosomal dominant *de novo*, or X-linked inheritance patterns. We might have to expand our search to mutations which are more difficult to identify, for example those with an autosomal dominant inheritance pattern with reduced penetrance, mutations in regulatory non-coding regions of the genome, oligogenic inheritance, or mosaic mutations (see next paragraph). Also, non-genetic causes like *in utero* infections and vascular disruptions should be considered.
The discovery of novel variants in known or novel genes in only one or few patients complicates the interpretation regarding pathogenicity. To overcome this problem, a large effort is needed to develop and implement functional studies of unclassified variants in the diagnostic trajectory. Possible assays range from relatively simple (e.g. measuring gene expression), to mutant protein expression, localization and interaction patterns to more complicated and time-consuming animal studies. In addition, data sharing amongst laboratories facilitates the recognition of genotype-phenotype correlations regarding rare diseases. However, it does raise other difficulties regarding privacy protection of the patients, data ownership, and authorship of scientific publications.

Mosaicism

An important theme is the relative high prevalence of mosaic mutations which complicates molecular testing. Several groups have now published this occurrence in a range of MCD including *LIS1*- and *DCX*-related subcortical band heterotopia [90,91], X-linked PNH [92], the PI3K-AKT pathway-related megalencephaly/overgrowth syndromes [93], *PIK3R2*-related bilateral perisylvian polymicrogyria [94], and *TUBB2B*-related pachygyria/polymicrogyria.[88]

Mosaic mutations have also been detected in apparently unaffected parents of children with germline mutations and full-blown phenotypes (chapter 2.2).[95-97] These findings impose a high recurrence risk on families compared to true *de novo* germline mutations in the offspring. More importantly, sibling recurrences without identification of the mutation in either parent have been reported.[97,98] For counselling of recurrence risks and prenatal diagnostics, careful investigation of parental samples is warranted. An accurate estimation of the recurrence risk will remain difficult and the possibility of targeted prenatal testing should be considered in the counselling of families with apparent *de novo* inheritance. Even with increased awareness, detection of mosaic variants remains extremely difficult with levels as low as a few percent of NGS reads.[94] Analysing whole-exome data with such a low threshold for detection would be an immense, if not impossible task for the diagnostic laboratory. Therefore the clinical geneticist should make an effort in predicting the possibility of mosaicism during the process of clinical phenotyping and to select the genes to be analysed in more detail. Detection of somatic mutations present only in affected brain tissue is even more difficult and will only be possible in a small group of patients undergoing epilepsy surgery.[99-101] The potential diagnostic pitfalls and challenges need to be thoroughly explained when counselling families of potential mosaic MCD patients.

CONCLUDING REMARKS

Over the past 20 years, with the emergence of high resolution brain imaging and next-generation sequencing in clinical diagnostics, our knowledge on MCD has expanded exponentially. Nevertheless, this has also taught us that MCD are far more heterogeneous on the clinical and genetic level than anyone had ever anticipated. Many challenges lay ahead, and research is hampered by lack of recognition, lack of funding, and small study cohorts. Rapid and inexpensive functional tests should be developed to test the pathogenicity of novel genomic variants. The patient benefits from knowledge of the optimal treatment, prognosis, developmental outcome, and risks of developing complications. Clinicians should therefore encourage their patients to reach out to each other and form international forums, as to efficiently collect and exchange this information and prioritize research themes. This approach has already

been applied successfully for other rare disorders.[102-104] In addition, scientists and molecular geneticists should unite and share their data, feel encouraged to form international consortia and publish their findings in open-access journals. Altogether, the impact of these measures could become greater than that of the technological advances we have witnessed over the past decades.

REFERENCES

1. Morris-Rosendahl DJ, Najm J, Lachmeijer AM, Sztriha L, Martins M, Kuechler A, et al. Refining the phenotype of alpha-1a Tubulin (TUBA1A) mutation in patients with classical lissencephaly. Clin Genet. 2008 Nov;74(5):425-33.
2. Cushion TD, Dobyns WB, Mullins JG, Stoodley N, Chung SK, Fry AE, et al. Overlapping cortical malformations and mutations in TUBB2B and TUBA1A. Brain. 2013 Feb;136(Pt 2):536-48.
3. Kumar RA, Pilz DT, Babatz TD, Cushion TD, Harvey K, Topf M, et al. TUBA1A mutations cause wide spectrum lissencephaly (smooth brain) and suggest that multiple neuronal migration pathways converge on alpha tubulins. Hum Mol Genet. 2010 Jul 15;19(14):2817-27.
4. Poirier K, Keays DA, Francis F, Saillour Y, Bahi N, Manouvrier S, et al. Large spectrum of lissencephaly and pachygyria phenotypes resulting from de novo missense mutations in tubulin alpha 1A (TUBA1A). Hum Mutat. 2007 Nov;28(11):1055-64.
5. Bahi-Buisson N, Poirier K, Fourniol F, Saillour Y, Valence S, Lebrun N, et al. The wide spectrum of tubulinopathies: what are the key features for the diagnosis? Brain. 2014 Jun;137(Pt 6):1676-700.
6. Mutch CA, Poduri A, Sahin M, Barry B, Walsh CA, Barkovich AJ. Disorders of Microtubule Function in Neurons: Imaging Correlates. AJNR Am J Neuroradiol. 2015 Nov 12.
7. Clapham KR, Yu TW, Ganesh VS, Barry B, Chan Y, Mei D, et al. FLNA genomic rearrangements cause periventricular nodular heterotopia. Neurology. 2012 Jan 24;78(4):269-78.
8. de Wit MC, Tiddens HA, de Coo IF, Mancini GM. Lung disease in FLNA mutation: confirmatory report. Eur J Med Genet. 2011 May-Jun;54(3):299-300.
9. Bras J, Alonso I, Barbot C, Costa MM, Darwent L, Orme T, et al. Mutations in PNKP cause recessive ataxia with oculomotor apraxia type 4. Am J Hum Genet. 2015 Mar 5;96(3):474-9.
10. Poulton CJ, Schot R, Kia SK, Jones M, Verheijen FW, Venselaar H, et al. Microcephaly with simplified gyration, epilepsy, and infantile diabetes linked to inappropriate apoptosis of neural progenitors. Am J Hum Genet. 2011 Aug 12;89(2):265-76.
11. De Ciantis A, Barkovich AJ, Cosottini M, Barba C, Montanaro D, Costagli M, et al. Ultra-high-field MR imaging in polymicrogyria and epilepsy. AJNR Am J Neuroradiol. 2015 Feb;36(2):309-16.
12. Guerrini R, Dobyns WB. Malformations of cortical development: clinical features and genetic causes. Lancet Neurol. 2014 Jul;13(7):710-26.
13. Guerrini R, Duchowny M, Jayakar P, Krsek P, Kahane P, Tassi L, et al. Diagnostic methods and treatment options for focal cortical dysplasia. Epilepsia. 2015 Nov;56(11):1669-86.
14. Pascher B, Kroll J, Mothersill I, Kramer G, Huppertz HJ. Automated morphometric magnetic resonance imaging analysis for the detection of periventricular nodular heterotopia. Epilepsia. 2013 Feb;54(2):305-13.
15. Zhang H, Schneider T, Wheeler-Kingshott CA, Alexander DC. NODDI: practical in vivo neurite orientation dispersion and density imaging of the human brain. Neuroimage. 2012 Jul 16;61(4):1000-16.
16. Curry CJ, Lammer EJ, Nelson V, Shaw GM. Schizencephaly: heterogeneous etiologies in a population of 4 million California births. Am J Med Genet A. 2005 Aug 30;137(2):181-9.
17. Stutterd CA, Leventer RJ. Polymicrogyria: a common and heterogeneous malformation of cortical development. Am J Med Genet C Semin Med Genet. 2014 Jun;166C(2):227-39.
18. Meuwissen ME, Halley DJ, Smit LS, Lequin MH, Cobben JM, de Coo R, et al. The expanding phenotype of COL4A1 and COL4A2 mutations: clinical data on 13 newly identified families and a review of the literature. Genet Med. 2015 Nov;17(11):843-53.

19. Dhindsa RS, Goldstein DB. Genetic Discoveries Drive Molecular Analyses and Targeted Therapeutic Options in the Epilepsies. Curr Neurol Neurosci Rep. 2015 Oct;15(10):70.
20. Jacobs MP, Fischbach GD, Davis MR, Dichter MA, Dingledine R, Lowenstein DH, et al. Future directions for epilepsy research. Neurology. 2001 Nov 13;57(9):1536-42.
21. Kuzniecky R, Murro A, King D, Morawetz R, Smith J, Powers R, et al. Magnetic resonance imaging in childhood intractable partial epilepsies: pathologic correlations. Neurology. 1993 Apr;43(4):681-7.
22. Mischel PS, Nguyen LP, Vinters HV. Cerebral cortical dysplasia associated with pediatric epilepsy. Review of neuropathologic features and proposal for a grading system. J Neuropathol Exp Neurol. 1995 Mar;54(2):137-53.
23. Papayannis CE, Consalvo D, Kauffman MA, Seifer G, Oddo S, D'Alessio L, et al. Malformations of cortical development and epilepsy in adult patients. Seizure. 2012 Jun;21(5):377-84.
24. Sheen VL, Dixon PH, Fox JW, Hong SE, Kinton L, Sisodiya SM, et al. Mutations in the X-linked filamin 1 gene cause periventricular nodular heterotopia in males as well as in females. Hum Mol Genet. 2001 Aug 15;10(17):1775-83.
25. Cunningham CC, Gorlin JB, Kwiatkowski DJ, Hartwig JH, Janmey PA, Byers HR, et al. Actin-binding protein requirement for cortical stability and efficient locomotion. Science. 1992 Jan 17;255(5042):325-7.
26. Nakamura F, Stossel TP, Hartwig JH. The filamins: organizers of cell structure and function. Cell Adh Migr. 2011 Mar-Apr;5(2):160-9.
27. Bizzotto S, Francis F. Morphological and functional aspects of progenitors perturbed in cortical malformations. Front Cell Neurosci. 2015;9:30.
28. Carabalona A, Beguin S, Pallesi-Pocachard E, Buhler E, Pellegrino C, Arnaud K, et al. A glial origin for periventricular nodular heterotopia caused by impaired expression of Filamin-A. Hum Mol Genet. 2012 Mar 1;21(5):1004-17.
29. Higginbotham H, Guo J, Yokota Y, Umberger NL, Su CY, Li J, et al. Arl13b-regulated cilia activities are essential for polarized radial glial scaffold formation. Nat Neurosci. 2013 Aug;16(8):1000-7.
30. Schmid MT, Weinandy F, Wilsch-Brauninger M, Huttner WB, Cappello S, Gotz M. The role of alpha-E-catenin in cerebral cortex development: radial glia specific effect on neuronal migration. Front Cell Neurosci. 2014;8:215.
31. Sheen VL, Ganesh VS, Topcu M, Sebire G, Bodell A, Hill RS, et al. Mutations in ARFGEF2 implicate vesicle trafficking in neural progenitor proliferation and migration in the human cerebral cortex. Nat Genet. 2004 Jan;36(1):69-76.
32. Cappello S, Gray MJ, Badouel C, Lange S, Einsiedler M, Srour M, et al. Mutations in genes encoding the cadherin receptor-ligand pair DCHS1 and FAT4 disrupt cerebral cortical development. Nat Genet. 2013 Nov;45(11):1300-8.
33. Zhang J, Neal J, Lian G, Hu J, Lu J, Sheen V. Filamin A regulates neuronal migration through brefeldin A-inhibited guanine exchange factor 2-dependent Arf1 activation. J Neurosci. 2013 Oct 2;33(40):15735-46.
34. Solecki DJ. Sticky situations: recent advances in control of cell adhesion during neuronal migration. Curr Opin Neurobiol. 2012 Oct;22(5):791-8.
35. Munji RN, Choe Y, Li G, Siegenthaler JA, Pleasure SJ. Wnt signaling regulates neuronal differentiation of cortical intermediate progenitors. J Neurosci. 2011 Feb 2;31(5):1676-87.
36. Tang BL. Rab, Arf and Arl-Regulated Membrane Traffic in Cortical Neuron Migration. J Cell Physiol. 2015 Nov 20.

37. Cahana A, Escamez T, Nowakowski RS, Hayes NL, Giacobini M, von Holst A, et al. Targeted mutagenesis of Lis1 disrupts cortical development and LIS1 homodimerization. Proc Natl Acad Sci U S A. 2001 May 22;98(11):6429-34.
38. Feng Y, Chen MH, Moskowitz IP, Mendonza AM, Vidali L, Nakamura F, et al. Filamin A (FLNA) is required for cell-cell contact in vascular development and cardiac morphogenesis. Proc Natl Acad Sci U S A. 2006 Dec 26;103(52):19836-41.
39. de Juan Romero C, Bruder C, Tomasello U, Sanz-Anquela JM, Borrell V. Discrete domains of gene expression in germinal layers distinguish the development of gyrencephaly. EMBO J. 2015 Jul 14;34(14):1859-74.
40. Masuda K, Toda T, Shinmyo Y, Ebisu H, Hoshiba Y, Wakimoto M, et al. Pathophysiological analyses of cortical malformation using gyrencephalic mammals. Sci Rep. 2015;5:15370.
41. Lancaster MA, Knoblich JA. Generation of cerebral organoids from human pluripotent stem cells. Nat Protoc. 2014 Oct;9(10):2329-40.
42. Camp JG, Badsha F, Florio M, Kanton S, Gerber T, Wilsch-Brauninger M, et al. Human cerebral organoids recapitulate gene expression programs of fetal neocortex development. Proc Natl Acad Sci U S A. 2015 Dec 22;112(51):15672-7.
43. Baillat D, Wagner EJ. Integrator: surprisingly diverse functions in gene expression. Trends Biochem Sci. 2015 May;40(5):257-64.
44. Grabowski P. Alternative splicing takes shape during neuronal development. Curr Opin Genet Dev. 2011 Aug;21(4):388-94.
45. Yeo G, Holste D, Kreiman G, Burge CB. Variation in alternative splicing across human tissues. Genome Biol. 2004;5(10):R74.
46. Norris AD, Calarco JA. Emerging Roles of Alternative Pre-mRNA Splicing Regulation in Neuronal Development and Function. Front Neurosci. 2012;6:122.
47. Gripp KW, Hopkins E, Johnston JJ, Krause C, Dobyns WB, Biesecker LG. Long-term survival in TARP syndrome and confirmation of RBM10 as the disease-causing gene. Am J Med Genet A. 2011 Oct;155A(10):2516-20.
48. Johnston JJ, Sapp JC, Curry C, Horton M, Leon E, Cusmano-Ozog K, et al. Expansion of the TARP syndrome phenotype associated with de novo mutations and mosaicism. Am J Med Genet A. 2014 Jan;164A(1):120-8.
49. Edery P, Marcaillou C, Sahbatou M, Labalme A, Chastang J, Touraine R, et al. Association of TALS developmental disorder with defect in minor splicing component U4atac snRNA. Science. 2011 Apr 8;332(6026):240-3.
50. He H, Liyanarachchi S, Akagi K, Nagy R, Li J, Dietrich RC, et al. Mutations in U4atac snRNA, a component of the minor spliceosome, in the developmental disorder MOPD I. Science. 2011 Apr 8;332(6026):238-40.
51. Tebbenkamp AT, Willsey AJ, State MW, Sestan N. The developmental transcriptome of the human brain: implications for neurodevelopmental disorders. Curr Opin Neurol. 2014 Apr;27(2):149-56.
52. Jodoin JN, Shboul M, Albrecht TR, Lee E, Wagner EJ, Reversade B, et al. The snRNA-processing complex, Integrator, is required for ciliogenesis and dynein recruitment to the nuclear envelope via distinct mechanisms. Biol Open. 2013;2(12):1390-6.
53. Kheradmand Kia S, Verbeek E, Engelen E, Schot R, Poot RA, de Coo IF, et al. RTTN mutations link primary cilia function to organization of the human cerebral cortex. Am J Hum Genet. 2012 Sep 7;91(3):533-40.

54. Shamseldin H, Alazami AM, Manning M, Hashem A, Caluseiu O, Tabarki B, et al. RTTN Mutations Cause Primary Microcephaly and Primordial Dwarfism in Humans. Am J Hum Genet. 2015 Dec 3;97(6):862-8.
55. Romaniello R, Arrigoni F, Bassi MT, Borgatti R. Mutations in alpha- and beta-tubulin encoding genes: implications in brain malformations. Brain Dev. 2015 Mar;37(3):273-80.
56. Kielar M, Tuy FP, Bizzotto S, Lebrand C, de Juan Romero C, Poirier K, et al. Mutations in Eml1 lead to ectopic progenitors and neuronal heterotopia in mouse and human. Nat Neurosci. 2014 Jul;17(7):923-33.
57. Tischfield MA, Engle EC. Distinct alpha- and beta-tubulin isotypes are required for the positioning, differentiation and survival of neurons: new support for the 'multi-tubulin' hypothesis. Biosci Rep. 2010 Oct;30(5):319-30.
58. Guo J, Qiang M, Luduena RF. The distribution of beta-tubulin isotypes in cultured neurons from embryonic, newborn, and adult mouse brains. Brain Res. 2011 Oct 28;1420:8-18.
59. Alcantara D, O'Driscoll M. Congenital microcephaly. Am J Med Genet C Semin Med Genet. 2014 Jun;166C(2):124-39.
60. Barkovich AJ, Kuzniecky RI, Jackson GD, Guerrini R, Dobyns WB. A developmental and genetic classification for malformations of cortical development. Neurology. [Review]. 2005 Dec 27;65(12):1873-87.
61. Passemard S, Titomanlio L, Elmaleh M, Afenjar A, Alessandri JL, Andria G, et al. Expanding the clinical and neuroradiologic phenotype of primary microcephaly due to ASPM mutations. Neurology. 2009 Sep 22;73(12):962-9.
62. Kakar N, Ahmad J, Morris-Rosendahl DJ, Altmuller J, Friedrich K, Barbi G, et al. STIL mutation causes autosomal recessive microcephalic lobar holoprosencephaly. Hum Genet. 2015 Jan;134(1):45-51.
63. Mishra-Gorur K, Caglayan AO, Schaffer AE, Chabu C, Henegariu O, Vonhoff F, et al. Mutations in KATNB1 cause complex cerebral malformations by disrupting asymmetrically dividing neural progenitors. Neuron. 2014 Dec 17;84(6):1226-39.
64. Yu TW, Mochida GH, Tischfield DJ, Sgaier SK, Flores-Sarnat L, Sergi CM, et al. Mutations in WDR62, encoding a centrosome-associated protein, cause microcephaly with simplified gyri and abnormal cortical architecture. Nat Genet. 2010 Nov;42(11):1015-20.
65. Jana SC, Marteil G, Bettencourt-Dias M. Mapping molecules to structure: unveiling secrets of centriole and cilia assembly with near-atomic resolution. Curr Opin Cell Biol. 2014 Feb;26:96-106.
66. Dixon-Salazar T, Silhavy JL, Marsh SE, Louie CM, Scott LC, Gururaj A, et al. Mutations in the AHI1 gene, encoding jouberin, cause Joubert syndrome with cortical polymicrogyria. Am J Hum Genet. 2004 Dec;75(6):979-87.
67. Higginbotham H, Eom TY, Mariani LE, Bachleda A, Hirt J, Gukassyan V, et al. Arl13b in primary cilia regulates the migration and placement of interneurons in the developing cerebral cortex. Dev Cell. 2012 Nov 13;23(5):925-38.
68. Field M, Scheffer IE, Gill D, Wilson M, Christie L, Shaw M, et al. Expanding the molecular basis and phenotypic spectrum of X-linked Joubert syndrome associated with OFD1 mutations. Eur J Hum Genet. 2012 Jul;20(7):806-9.
69. Guemez-Gamboa A, Coufal NG, Gleeson JG. Primary cilia in the developing and mature brain. Neuron. 2014 May 7;82(3):511-21.
70. Moon HM, Wynshaw-Boris A. Cytoskeleton in action: lissencephaly, a neuronal migration disorder. Wiley Interdiscip Rev Dev Biol. 2013 Mar-Apr;2(2):229-45.

71. Sheen VL. Filamin A and Big2: a shared endocytic pathway. Bioarchitecture. 2014 Mar-Apr;4(2):53-7.
72. Riviere JB, van Bon BW, Hoischen A, Kholmanskikh SS, O'Roak BJ, Gilissen C, et al. De novo mutations in the actin genes ACTB and ACTG1 cause Baraitser-Winter syndrome. Nat Genet. 2012 Apr;44(4):440-4, S1-2.
73. Coles CH, Bradke F. Coordinating neuronal actin-microtubule dynamics. Curr Biol. 2015 Aug 3;25(15):R677-91.
74. Tsukada M, Prokscha A, Ungewickell E, Eichele G. Doublecortin association with actin filaments is regulated by neurabin II. J Biol Chem. 2005 Mar 25;280(12):11361-8.
75. Farina F, Gaillard J, Guerin C, Coute Y, Sillibourne J, Blanchoin L, et al. The centrosome is an actin-organizing centre. Nat Cell Biol. 2016 Jan;18(1):65-75.
76. Courcet JB, Faivre L, Malzac P, Masurel-Paulet A, Lopez E, Callier P, et al. The DYRK1A gene is a cause of syndromic intellectual disability with severe microcephaly and epilepsy. J Med Genet. 2012 Dec;49(12):731-6.
77. van Bon BW, Hoischen A, Hehir-Kwa J, de Brouwer AP, Ruivenkamp C, Gijsbers AC, et al. Intragenic deletion in DYRK1A leads to mental retardation and primary microcephaly. Clin Genet. 2011 Mar;79(3):296-9.
78. Ruaud L, Mignot C, Guet A, Ohl C, Nava C, Heron D, et al. DYRK1A mutations in two unrelated patients. Eur J Med Genet. 2015 Mar;58(3):168-74.
79. Ji J, Lee H, Argiropoulos B, Dorrani N, Mann J, Martinez-Agosto JA, et al. DYRK1A haploinsufficiency causes a new recognizable syndrome with microcephaly, intellectual disability, speech impairment, and distinct facies. Eur J Hum Genet. 2015 Oct;23(11):1473-81.
80. Redin C, Gerard B, Lauer J, Herenger Y, Muller J, Quartier A, et al. Efficient strategy for the molecular diagnosis of intellectual disability using targeted high-throughput sequencing. J Med Genet. 2014 Nov;51(11):724-36.
81. van Bon BWM, Coe BP, de Vries BBA, Eichler EE. DYRK1A-Related Intellectual Disability Syndrome. 2015.
82. Tejedor FJ, Hammerle B. MNB/DYRK1A as a multiple regulator of neuronal development. FEBS J. 2011 Jan;278(2):223-35.
83. Slepak TI, Salay LD, Lemmon VP, Bixby JL. Dyrk kinases regulate phosphorylation of doublecortin, cytoskeletal organization, and neuronal morphology. Cytoskeleton (Hoboken). 2012 Jul;69(7):514-27.
84. Schneider P, Bayo-Fina JM, Singh R, Kumar Dhanyamraju P, Holz P, Baier A, et al. Identification of a novel actin-dependent signal transducing module allows for the targeted degradation of GLI1. Nat Commun. 2015;6:8023.
85. Soppa U, Schumacher J, Florencio Ortiz V, Pasqualon T, Tejedor FJ, Becker W. The Down syndrome-related protein kinase DYRK1A phosphorylates p27(Kip1) and Cyclin D1 and induces cell cycle exit and neuronal differentiation. Cell Cycle. 2014;13(13):2084-100.
86. Gilissen C, Hehir-Kwa JY, Thung DT, van de Vorst M, van Bon BW, Willemsen MH, et al. Genome sequencing identifies major causes of severe intellectual disability. Nature. 2014 Jul 17;511(7509):344-7.
87. Taylor JC, Martin HC, Lise S, Broxholme J, Cazier JB, Rimmer A, et al. Factors influencing success of clinical genome sequencing across a broad spectrum of disorders. Nat Genet. 2015 Jul;47(7):717-26.
88. Jamuar SS, Lam AT, Kircher M, D'Gama AM, Wang J, Barry BJ, et al. Somatic mutations in cerebral cortical malformations. N Engl J Med. 2014 Aug 21;371(8):733-43.

89. Mancini G. Diagnostic yield of targeted next generation sequencing panel for cortical malformations ESHG; Glasgow2015.
90. Gleeson JG, Minnerath S, Kuzniecky RI, Dobyns WB, Young ID, Ross ME, et al. Somatic and germline mosaic mutations in the doublecortin gene are associated with variable phenotypes. Am J Hum Genet. 2000 Sep;67(3):574-81.
91. Sicca F, Kelemen A, Genton P, Das S, Mei D, Moro F, et al. Mosaic mutations of the LIS1 gene cause subcortical band heterotopia. Neurology. 2003 Oct 28;61(8):1042-6.
92. Guerrini R, Mei D, Sisodiya S, Sicca F, Harding B, Takahashi Y, et al. Germline and mosaic mutations of FLN1 in men with periventricular heterotopia. Neurology. 2004 Jul 13;63(1):51-6.
93. Riviere JB, Mirzaa GM, O'Roak BJ, Beddaoui M, Alcantara D, Conway RL, et al. De novo germline and postzygotic mutations in AKT3, PIK3R2 and PIK3CA cause a spectrum of related megalencephaly syndromes. Nat Genet. 2012 Aug;44(8):934-40.
94. Mirzaa GM, Conti V, Timms AE, Smyser CD, Ahmed S, Carter M, et al. Characterisation of mutations of the phosphoinositide-3-kinase regulatory subunit, PIK3R2, in perisylvian polymicrogyria: a next-generation sequencing study. Lancet Neurol. 2015 Oct 28.
95. Jansen AC, Oostra A, Desprechins B, De Vlaeminck Y, Verhelst H, Regal L, et al. TUBA1A mutations: from isolated lissencephaly to familial polymicrogyria. Neurology. 2011 Mar 15;76(11):988-92.
96. Oegema R, Cushion TD, Phelps IG, Chung SK, Dempsey JC, Collins S, et al. Recognizable cerebellar dysplasia associated with mutations in multiple tubulin genes. Hum Mol Genet. 2015 Sep 15;24(18):5313-25.
97. Zillhardt JL, Poirier K, Broix L, Lebrun N, Elmorjani A, Martinovic J, et al. Mosaic parental germline mutations causing recurrent forms of malformations of cortical development. Eur J Hum Genet. 2015 Sep 23.
98. Mroske C, Rasmussen K, Shinde DN, Huether R, Powis Z, Lu HM, et al. Germline activating MTOR mutation arising through gonadal mosaicism in two brothers with megalencephaly and neurodevelopmental abnormalities. BMC Med Genet. 2015;16:102.
99. D'Gama AM, Geng Y, Couto JA, Martin B, Boyle EA, LaCoursiere CM, et al. Mammalian target of rapamycin pathway mutations cause hemimegalencephaly and focal cortical dysplasia. Ann Neurol. 2015 Apr;77(4):720-5.
100. Lee JH, Huynh M, Silhavy JL, Kim S, Dixon-Salazar T, Heiberg A, et al. De novo somatic mutations in components of the PI3K-AKT3-mTOR pathway cause hemimegalencephaly. Nat Genet. 2012 Jun 24.
101. Leventer RJ, Scerri T, Marsh AP, Pope K, Gillies G, Maixner W, et al. Hemispheric cortical dysplasia secondary to a mosaic somatic mutation in MTOR. Neurology. 2015 May 19;84(20):2029-32.
102. Shaw AC, van Balkom ID, Bauer M, Cole TR, Delrue MA, Van Haeringen A, et al. Phenotype and natural history in Marshall-Smith syndrome. Am J Med Genet A. 2010 Nov;152A(11):2714-26.
103. Baas M, Huisman S, van Heukelingen J, Koekkoek G, Laan HW, Hennekam RC. Building treasures for rare disorders. Eur J Med Genet. 2015 Jan;58(1):11-3.
104. Unique. [cited 2015]; Available from: www.rarechromo.org.

Chapter 6

Appendix

SUMMARY

In **Chapter 1**, the general introduction, our current knowledge on cortical development and malformations of cortical development (MCD) is summarized, with a focus on heterotopia and microcephaly. Also, an outline of the thesis is provided.
Chapter 2 presents imaging characteristics of subcortical heterotopia (**2.1**) and a cerebellar dysplasia associated with tubulinopathies (**2.2**).
Searching four MCD databases worldwide, we were able to collect imaging data of 107 patients with subcortical heterotopia, which is the largest study of this malformation to date **(2.1).** The majority (83%) of patients were scanned during childhood and 79% had abnormal cognitive and/or motor development. Seizures were reported in 69% with age of onset significantly skewed towards early childhood. We proposed a new imaging classification for subcortical heterotopia, with four main groups. We showed that several rare bilateral forms can have a genetic etiology but that for the curvilinear and deeply infolded subcortical heterotopia a prenatal vascular disruptive etiology should be considered. However, *de novo* germline or mosaic mutations cannot be excluded at this point.
In **chapter 2.2**, we present ten patients with a highly characteristic cerebellar dysplasia. Remarkably, in seven of nine patients (78%), targeted sequencing revealed mutations in three different tubulin genes (*TUBA1A*, *TUBB2B* and *TUBB3*), occurring *de novo* or inherited from a mosaic parent. In cellular studies, all the studied mutations lead to impaired microtubule incorporation. As mutations in tubulin genes are known to cause MCD, we carefully re-reviewed the cortex on brain imaging and this revealed only an irregular pattern of gyri and sulci, for which we propose the term tubulinopathy-related dysgyria.
In **Chapter 3** the phenotype of several disorders is expanded.
In **chapter 3.1** we describe for the first time the presence of periventricular nodular heterotopia with KBG syndrome.
In **chapter 3.2**, two patients are described with an overlapping 21q22 microdeletion. We propose that they represent a new syndrome caused by haploinsufficiency of the *DYRK1A* gene. This syndrome is characterized by intellectual disability, absent speech, and distinct facial features.
Chapter 3.3 describes the occurrence of periventricular nodular heterotopia and polymicrogyria in a patient with an *ARX* two-residue expansion of the first polyalanine tract. The same mutation had been previously reported in a family with non-syndromic XLID. Furthermore, the only MCD that had previously been related to *ARX* was an occipital-predominant lissencephaly, being caused by truncating mutations or missense mutations in the region encoding the homeodomain.

For the research described in **chapter 3.4**, we had the unique opportunity to study a family of which seven members were shown to harbor a novel no-stop *FLNA* mutation. Five individuals underwent brain imaging and all had periventricular nodular heterotopia. In addition, the three affected males survived into childhood but with multi-organ involvement which included severe gastro-intestinal symptoms.

In **chapters 3.5 and 3.6** we show that a homozygous frameshift mutation in *PNKP* causes a neurodegenerative disorder starting in early childhood and consisting of severe progressive polyneuropathy and cerebellar atrophy, microcephaly, mild epilepsy, and intellectual disability. Mutations in *PNKP* had previously been associated with a syndrome of microcephaly, seizures and developmental delay, but without neurodegeneration. We showed that patient cells have an increased tendency to undergo apoptosis under stress conditions which is in line with the function of PNKP in DNA damage repair.

In **chapter 4.1** we report that mutations in the *Integrator complex subunit 8* gene (*INTS8)* cause a rare neurodevelopmental syndrome. The affected patients, three siblings, had profound intellectual disability, seizures and microcephaly. Brain imaging showed periventricular nodular heterotopia and cerebellar hypoplasia. Knockdown of *ints8* in zebrafish embryos led to abnormal brain development. This study therefore unveils an essential and evolutionary conserved role of the Integrator complex in brain development.

Chapter 5, the general discussion, highlights the main findings of this thesis and places these in the context of the current knowledge on cortical development.

SAMENVATTING

In **hoofdstuk 1**, de algemene inleiding, is de huidige kennis betreffende de ontwikkeling van de hersenschors en aanlegstoornissen van de hersenschors (MCD) samengevat. Er wordt gefocust op twee aandoeningen, heterotopieën en microcefalie. Ook wordt in dit hoofdstuk de opbouw van het proefschrift gepresenteerd.
Hoofstuk 2.1 beschrijft een studie van 107 patiënten met subcorticale heterotopieën. Dit vormt de tot nu toe grootste studie naar deze hersenafwijking. De meerderheid van de patiënten (83%) had op de kinderleeftijd een hersenscan ondergaan. Een afwijkende cognitieve en/of motorische ontwikkeling werd gerapporteerd in 79% van de patiënten en epilepsie in 69%. De leeftijd van de eerste epileptische aanval vond significant vaker plaats op de jonge kinderleeftijd. We stellen een nieuw classificatiesysteem voor bestaande uit vier hoofdgroepen. Een aantal zeldzame, bilaterale afwijkingen hebben een genetische oorzaak. De oorzaak van *curvilinear* en *deeply infolded* subcorticale heterotopieën zou goed een vasculaire disruptie tijdens de zwangerschap kunnen zijn. In deze groepen kunnen echter *de novo* kiembaan en somatische mutaties niet worden uitgesloten.
Tien patiënten met een duidelijk herkenbare cerebellaire dysplasie worden beschreven in **hoofdstuk 2.2**. In 7 van de 9 (78%) vonden we mutaties in een tubuline-gen (*TUBA1A*, *TUBB2B* en *TUBB3)*, nieuw ontstaan of geërfd van een ouder met een mutatie in mozaïek vorm. Gebruik makend van een celsysteem laten we zien dat het gemuteerde eiwit niet normaal in microtubuli wordt geïncorporeerd. Omdat mutaties in deze genen zijn geassocieerd met MCD hebben we de MRI's van alle patiënten opnieuw goed bekeken. We vonden een afwijkend patroon van gyri en sulci, en we stellen voor hier de term dysgyrie voor te gebruiken.
Onze observaties beschreven in **hoofdstuk 3** verbreden het klinische spectrum van verschillende aandoeningen. In **hoofdstuk 3.1** beschrijven we voor het eerst een patiënt met KBG syndroom en periventriculaire nodulaire heterotopieën.
In **hoofdstuk 3.2** beschrijven we twee patiënten met een overlappende 21q22 microdeletie. Zij hebben een syndroom dat wordt gekenmerkt door een verstandelijke beperking, afwezige spraak en bijzondere uiterlijke kenmerken en wat wordt veroorzaakt door haplo-insufficiëntie van het *DYRK1A* gen.
Hoofdstuk 3.3 beschrijft een patiënt met periventriculaire nodulaire heterotopieën en polymicrogyrie die een mutatie in het *ARX* gen bleek te hebben. Dezelfde mutatie was eerder beschreven in een familie met niet-syndromale X-gebonden verstandelijke beperking. Deze vormen van MCD waren nooit eerder geassocieerd met *ARX* mutaties.
Voor **hoofdstuk 3.4** beschreven wij een unieke familie waarin 7 individuen een nieuwe *no-stop* mutatie in het *FLNA* gen hadden. Bij alle vijf familieleden die een hersenscan ondergingen werden periventriculaire nodulaire heterotopieën aangetoond. Hiernaast

hadden drie jongens in deze familie aandoeningen van verschillende organen waaronder ernstige gastro-intestinale symptomen.

Hoofdstukken 3.5 en 3.6 laten zien dat een homozygote frameshift mutatie in het *PNKP* gen in twee broers een ernstige neurodegeneratieve aandoening veroorzaakte. Deze broers presenteerden zich op de vroege kinderleeftijd met progressieve polyneuropathie, cerebellaire atrofie en microcefalie, met daarnaast epilepsie en een verstandelijke beperking. Mutaties in het *PNKP* gen waren eerder beschreven als oorzaak van een syndroom met microcefalie, epilepsie en ontwikkelingsachterstand, maar zonder neurodegeneratieve afwijkingen. We laten zien dat cellen van patiënten onder stressvolle omstandigheden in apoptose gaan, wat past bij de functie van PNKP in de reparatie van DNA schade.

Hoofdstuk 4.1 laat zien dat mutaties in *Integrator complex subunit 8* (*INTS8*) een zeldzaam syndroom veroorzaken dat wordt gekenmerkt door een ernstige verstandelijke beperking, epilepsie en microcefalie. Hersenscans van de patiënten lieten periventriculaire nodulaire heterotopieën en onderontwikkeling van het cerebellum zien. Uitschakeling van *ints8* in zebravis embryo's leidde tot ernstige afwijkingen in de hersenontwikkeling. Nooit eerder werden mutaties in dit complex beschreven en wij laten hiermee zien dat het Integrator complex een essentiële rol heeft in de hersenontwikkeling en dat deze rol evolutionair geconserveerd is.

In **hoofdstuk 5**, de algemene beschouwing, worden de belangrijkste bevindingen van dit proefschrift uitgelicht en in de context geplaatst van onze huidige kennis betreffende de ontwikkeling van de hersenschors.

LEKENSAMENVATTING

Ik heb onderzoek gedaan naar **aangeboren afwijkingen van de hersenen** (*malformations of cortical development*). Deze afwijkingen kun je zien op een hersenscan (MRI). In totaal zijn er nu meer dan 200 verschillende soorten bekend, die allemaal zeldzaam zijn. De meest frequente komen voor bij 1 op de 2500 personen. Desondanks vormen ze een belangrijke oorzaak van epilepsie, ontwikkelingsachterstand, spasticiteit en verstandelijke beperking. De twee aandoeningen waar ik mij in dit promotieonderzoek op heb gericht, zijn hersencellen die op de verkeerde plek in de hersenen zitten (**heterotopieën**) en hersenen die te klein zijn (**microcefalie**). Deze twee aandoeningen kunnen samen voorkomen bij een persoon, maar dat hoeft niet.

Veel hersenafwijkingen zijn nog niet of nauwelijks beschreven in de medische literatuur. Ik beschrijf in detail de klachten van patiënten en de bij hen geconstateerde afwijkingen op de hersenscan. Voor een specifieke afwijking beschrijven we meer dan honderd patiënten, de grootste studie tot nu toe. Ook laten we zien dat deze afwijking niet per sé een erfelijke (genetische) oorzaak heeft, maar bijvoorbeeld ook het gevolg kan zijn van een probleem in de zwangerschap, zoals een verminderde hersendoorbloeding.

Bij sommige patiënten vond ik wel een afwijkende samenstelling van de chromosomen en het DNA wat daarop ligt (het erfelijk materiaal). We hebben een afwijking op chromosoom 21 vastgesteld en veranderingen (mutaties) in verschillende erfelijke eigenschappen (genen) die hersenafwijkingen veroorzaken. Een belangrijke ontdekking is dat mutaties in het *INTS8* gen een hersenaandoening veroorzaken met een ernstige verstandelijke beperking, spasticiteit en epilepsie.

Mijn onderzoek laat zien dat deze aandoeningen een veelheid aan klachten kunnen veroorzaken en dat ook de onderliggende oorzaken erg verschillen, meer dan we ooit hadden gedacht. Ondanks de ontwikkeling van nieuwe technologieën op het gebied van genetisch onderzoek en hersenscans, is bij veel patiënten de oorzaak van hun hersenaandoening nog steeds onbekend. Hiervoor zijn verschillende redenen te bedenken: (1) de technieken zijn nog niet goed genoeg om elke erfelijke variant op te sporen; (2) de afwijkingen van het erfelijk materiaal komen niet voor in elke lichaamscel en worden daarom niet gevonden (mozaïek); (3) door de zeldzaamheid van de aandoeningen zijn er te weinig patiënten om goed onderzoek te kunnen doen; en (4) er zijn gespecialiseerde artsen nodig om de diagnose te stellen.

In de toekomst moeten we daarom nog gerichter op zoek naar erfelijke varianten, en moeten internationale netwerken worden ontwikkeld waar zowel patiënten als artsen en onderzoekers veilig hun data van zeldzame aandoeningen kunnen delen.

CURRICULUM VITAE

Renske Oegema werd op 26 april 1981 geboren te Zaanstad. In 1997/1998 volgde zij een schooljaar in de Verenigde Staten. Zij behaalde in 2000 haar V.W.O. diploma aan 't Zaanlands Lyceum te Zaandam, waar zij slaagde met een gemiddelde 8. Aansluitend begon zij aan haar studie geneeskunde in Amsterdam (AMC-UvA). Tijdens haar wetenschappelijke stage in 2004 onderzocht zij het voorkomen van dengue en leptopspirosis in Honduras. Na haar arts-examen in 2007 was zij een jaar werkzaam als arts-assistent kindergeneeskunde in het Meander Medisch Centrum te Amersfoort. Vervolgens startte zij als arts-assistent klinische genetica in het Erasmus MC, waar zij in 2011 aan haar opleiding tot klinisch geneticus begon onder supervisie van dr. Anneke Kievit. In de tussentijd werkte zij aan haar onderzoek naar aanlegstoornissen van de hersenschors (*malformations of cortical development*) onder leiding van dr. Grazia Mancini en prof. dr. Robert Hofstra. In 2013 heeft ze drie maanden stage gelopen bij prof. Bill Dobyns in Seattle. In 2016 volgde zij de epilepsiestage op de afdeling Genetica van het UMC Utrecht (prof. dr. Nine Knoers). Op 16 mei 2016 zal zij haar opleiding tot klinisch geneticus afronden en gaan werken als neurogeneticus in het UMC Utrecht.
Renske is getrouwd met Edwin Scherbeijn en samen hebben zij een zoon; Casper (2014).

Renske Oegema was born in Zaanstad on April 26th, 1981. In Zaandam she attended primary and secondary schools. In 1997/1998, she spend one year as an high school exchange student in the U.S.A. In 2000, she graduated from high school ('t Zaanlands Lyceum). After graduation, she started medical school at the AMC-UvA in Amsterdam. During her training she spent four months studying the incidence of leptospirosis and dengue in Honduras. After obtaining her medical degree, she worked one a year as a pediatric resident in the Meander Medisch Centrum in Amersfoort. Next, in 2008, she started working at the department of Clinical Genetics at the Erasmus MC. In 2011, she started her clinical genetics training, under supervision of dr. Anneke Kievit. In parallel, under supervision of dr. Grazia Mancini and prof. dr. Robert Hofstra, she studied malformations of cortical development, the work which has resulted in this thesis. In 2013, Renske went to professor Bill Dobyns' lab in Seattle for a three-month training focusing on heterotopia and tubulinopathies; in 2016 she followed at three-month training in epilepsy at the Genetics department of the UMC Utrecht (prof. dr. Nine Knoers). Renske will finish her clinical genetics training on May 16th 2016, after which she will be employed as a neurogeneticist at the UMC Utrecht.
Renske is married to Edwin Scherbeijn, they have a son Casper (born 2014).

PHD PORTFOLIO

Courses	Year	Work load (ECTS)
Fourth European Course in Clinical Dysmorphology, Rome, Italy	2011	0.6
Desiderius Evidence-based medicine, Rotterdam	2011	0.8
MolMed Grasduinen in Genome Browsers	2011	0.3
Course in Medical Genetics, Bologna, Italy	2012	1.4
Rekenen aan Genen, Amsterdam	2013	2.0
Write an article and get it published, Utrecht	2013	0.2
MolMed Microsoft Access – Basic, Rotterdam	2015	0.3
MolMed Microsoft Access – Advanced, Rotterdam	2015	0.3
MolMed Biomedical Research Techniques XIV, Rotterdam	2015	1.5
MolMed Basic Introduction Course on SPSS	2015	1.0
Erasmus MC CPO Course – Patient-oriented research, Rotterdam	2015	0.3
MGC 'Share your biotechnology research with a broad audience', Leiden	2015	0.5
Wetenschappelijke integriteit, Rotterdam	2015	0.3
Browsing genes and genomes with UCSC, Rotterdam	2015	0.6
Biomedical English Writing and Communication (7/10 classes)	2015-2016	3.0
National conferences		
15th Molecular Medicine Day, Rotterdam (poster presentation)	2011	1.0
NVHG najaarssymposium (poster presentation)	2012	1.0
Vereniging Klinische Genetica Nederland – LOG (2x/year)	2010-2014	1.0
International conferences		
Joint UK-Dutch Clinical Genetics Conference, Amsterdam (oral presentation)	2010	1.0
16th Mediterranean Meeting of Child Neurology, Mykonos, Greece (oral presentation)	2010	1.0
European Society of Human Genetics, Amsterdam (poster presentation)	2011	1.0
European Dysmorphology Club, Rome, Italy (oral presentation)	2011	1.0
Joint UK-Dutch Clinical Genetics Conference, Newcastle upon Tyne, UK (oral presentation)	2012	1.0
European Society of Human Genetics, Paris (oral presentation)	2013	1.0
PVNH World Conference, Waltham, USA (oral presentation)	2013	1.0
American Society of Human Genetics, Boston, USA	2013	1.0
Dysmorphology Club, ASHG, Boston (oral presentation)	2013	1.0
Joubert syndrome biennial conference, Boston (poster presentation)	2013	1.0
Dobyns & Millen Lab Research Meeting, Center for Integrative Brain Research, Seattle, USA (oral presentation)	2013	1.0
Joint UK-Dutch Clinical Genetics Conference, Leiden (oral presentation)	2014	1.0
European Society of Human Genetics, Glasgow, UK (poster presentation)	2015	1.0

Teaching		
College genetica voor verpleegkundigen, Sint Franciscus Gasthuis	2013	0.3
College Minor "Klinische Genetica in de Maatschappij" Erasmus MC	2012&2015	0.5
Vaardigheidsonderwijs geneeskunde Erasmus MC	2010-2015	0.5
Other		
Attending Clinical Genetics Work Discussion	2010-2015	1.0
Attending Journal Club (counseling/ research)	2010-2015	1.0
Co-organizer Refereeravond Neurogenetica "Big brains, small brains, genes and mechanisms	2015	0.5
Reviewer for international journals & funding organisation	2012-2015	1.0
Member of VKGN werkgroep Ethiek en Recht	2013-today	1.0
Member Stuurgroep B: METAB, ENZYM, FU	2013-today	1.0
Writing international grant application: COST Action (pending)	2015	1.0

LIST OF PUBLICATIONS

Oegema R, Cushion TD, Phelps IG, Chung SK, Dempsey JC, Collins S, Mullins JG, Dudding T, Gill H, Green AJ, Dobyns WB, Ishak GE, Rees MI, Doherty D. Recognizable cerebellar dysplasia associated with mutations in multiple tubulin genes. Human Molecular Genetics. 2015 Sep 15;24(18):5313-25.

Kalscheuer VM, James VM, Himelright ML, Long P**, Oegema R**, Jensen C, Bienek M, Hu H, Haas SA, Topf M, Hoogeboom AJ, Harvey K, Walikonis R, Harvey RJ. Novel Missense Mutation A789V in *IQSEC2* Underlies X-Linked Intellectual Disability in the MRX78 Family. Frontiers in Molecular Neuroscience. 2015;8:85.

Oegema R, Poulton CJ, Mancini GM. A single strand that links multiple neuropathologies in human disease. Brain. 2014 Apr;137(Pt 4):e266.

Kielar M, Tuy FP, Bizzotto S, Lebrand C, de Juan Romero C, Poirier K, **Oegema R**, Mancini GM, Bahi-Buisson N, Olaso R, Le Moing AG, Boutourlinsky K, Boucher D, Carpentier W, Berquin P, Deleuze JF, Belvindrah R, Borrell V, Welker E, Chelly J, Croquelois A, Francis F. Mutations in *Eml1* lead to ectopic progenitors and neuronal heterotopia in mouse and human. Nature Neuroscience. 2014 Jul;17(7):923-33.

Poulton C, **Oegema R**, Heijsman D, Hoogeboom J, Schot R, Stroink H, Willemsen MA, Verheijen FW, van de Spek P, Kremer A, Mancini GM. Progressive cerebellar atrophy and polyneuropathy: expanding the spectrum of *PNKP* mutations. Neurogenetics. 2013 Feb;14(1):43-51.

Oegema R, Hulst JM, Theuns-Valks SD, van Unen LM, Schot R, Mancini GM, Schipper ME, de Wit MC, Sibbles BJ, de Coo IF, Nanninga V, Hofstra RM, Halley DJ, Brooks AS. Novel no-stop *FLNA* mutation causes multi-organ involvement in males. American Journal of Medical Genetics A. 2013 Sep;161A(9):2376-84.

Verbeek E, Meuwissen ME, Verheijen FW, Govaert PP, Licht DJ, Kuo DS, Poulton CJ, Schot R, Lequin MH, Dudink J, Halley DJ, de Coo RI, den Hollander JC, **Oegema R**, Gould DB, Mancini GM. *COL4A2* mutation associated with familial porencephaly and small-vessel disease. European Journal of Human Genetics. 2012 Aug;20(8):844-51.

van den Bosch BJ, Gerards M, Sluiter W, Stegmann AP, Jongen EL, Hellebrekers DM, **Oegema R**, Lambrichs EH, Prokisch H, Danhauser K, Schoonderwoerd K, de Coo IF,

Smeets HJ. Defective *NDUFA9* as a novel cause of neonatally fatal complex I disease. Journal of Medical Genetics. 2012 Jan;49(1):10-5.

Srebniak MI, Boter M, Oudesluijs GO, Cohen-Overbeek T, Govaerts LC, Diderich KE, **Oegema R**, Knapen MF, van de Laar IM, Joosten M, Van Opstal D, Galjaard RJ. Genomic SNP array as a gold standard for prenatal diagnosis of foetal ultrasound abnormalities. Molelcular Cytogenetics. 2012;5(1):14.

Oegema R, van Zutven LJ, van Hassel DA, Huijbregts GC, Hoogeboom AJ. Unbalanced three-way chromosomal translocation leading to deletion 18q and duplication 20p. European Journal of Medical Genetics. 2012 Apr;55(4):265-8.

Oegema R, Maat-Kievit A, Lequin MH, Schot R, Nanninga-van den Neste VM, Doornbos ME, de Wit MC, Halley DJ, Mancini GM. Asymmetric polymicrogyria and periventricular nodular heterotopia due to mutation in *ARX*. American Journal of Medical Genetics A. 2012 Jun;158A(6):1472-6.

Kheradmand Kia S, Verbeek E, Engelen E, Schot R, Poot RA, de Coo IF, Lequin MH, Poulton CJ, Pourfarzad F, Grosveld FG, Brehm A, de Wit MC, **Oegema R**, Dobyns WB, Verheijen FW, Mancini GM. *RTTN* mutations link primary cilia function to organization of the human cerebral cortex. American Journal of Human Genetics. 2012 Sep 7;91(3):533-40.

Oegema R, Schram P, Nuboer R. Diabetesbehandeling bij kinderen: intensief is niet altijd beter. Nederlands Tijdschrift voor Geneeskunde. 2011;155:A802.
Oegema R, Schot R, de Wit MC, Lequin MH, Oostenbrink R, de Coo IF, Mancini GM. KBG syndrome associated with periventricular nodular heterotopia. Clinical Dysmorphology. 2010 Jul;19(3):164-5.

Oegema R, de Klein A, Verkerk AJ, Schot R, Dumee B, Douben H, Eussen B, Dubbel L, Poddighe PJ, van der Laar I, Dobyns WB, van der Spek PJ, Lequin MH, de Coo IF, de Wit MC, Wessels MW, Mancini GM. Distinctive Phenotypic Abnormalities Associated with Submicroscopic 21q22 Deletion Including *DYRK1A*. Molecular Syndromology. 2010 Sep;1(3):113-20.

DANKWOORD

Mijn dank gaat uit naar de vele patiënten en hun families beschreven in dit proefschrift, die zonder aarzeling hun medische voorgeschiedenis hebben gedeeld voor onderzoek en publicatie. Dankzij hen weten we nu meer over de vele uitingsvormen en oorzaken van corticale malformaties.

Zoveel collega's hebben bijgedragen aan dit proefschrift, ik zal niet iedereen hier kunnen bedanken, maar een aantal van hen wil ik hier zeker noemen.

Beste Grazia, het moge duidelijk zijn dat zonder jou dit proefschrift er niet was geweest. Naast mijn copromotor, was je ook nog mijn inspirator en opleider. Je hebt me laten zien dat binnen de genetica patiëntenzorg en onderzoek onlosmakelijk met elkaar verbonden zijn. Bedankt dat je zoveel van je kennis en tijd met mij hebt gedeeld. Beste Robert, veel dank dat je mijn promotor wilde zijn. Je gaf mij de kans mijn eigen pad uit te stippelen, dank voor je vertrouwen. Ik wil de leden van de kleine commissie prof.dr. Nine Knoers, prof.dr. Anna Jansen en dr. Annelies de Klein bedanken voor de tijd die zij hebben gestoken in het zorgvuldig lezen van mijn proefschrift. Prof.dr. Vincenzo Bonifati and prof.dr. Daniela Pilz, what an honour that you were willing to take place in the committee. Maarten Lequin, bedankt voor het delen van je kennis van de neuroradiologie, ik kijk uit naar onze verdere samenwerking in Utrecht.

Rachel, ik ben blij dat jij straks naast me staat. Je bent bij heel veel artikelen in dit boekje nauw betrokken geweest (en nog een aantal meer) dus het was niet meer dan logisch dat jij mijn paranimf moest zijn. Ik bewonder je om je scherpe blik en gestructureerde denkwijze. Leontine, naast al je eigen experimenten had je altijd tijd om mij te helpen, bedankt voor je enthousiasme. Frans, je hebt bij mij de interesse in de ciliopathieën en de microscopie gewekt, ik heb veel van je geleerd. Cathryn, our collaboration did not last very long but has been very productive. Elly, aan jouw hand zette ik de eerste stapjes in het lab. Maarten Fornerod, jij hebt de *INTS8* paper met jouw analyses naar een hoger plan getild.
Heel veel personen op het lab van de 9e, maar ook op de 20e en 24e hebben de afgelopen jaren mij met hun tijd, hulp en tips vooruit geholpen. Adriana and Herma, without your help with the "visjes" I would have been completely lost. I realize I have asked quite a lot of your time, thank you for that. Simone and Isa, I am grateful to have you around in the last phases of my PhD. You were an invaluable source of tips and tricks.
Professor Bill Dobyns, I am very grateful for our collaboration, it has been an inspiring and stimulating experience which has led to a vital section of this thesis. Thank you for

welcoming me to your lab, sharing the data from your huge database and teaching me your incredible understanding of MCD. Professor Jim Barkovich and Professor Renzo Guerrini thank you for your invaluable input into the heterotopia study, and your willingness to share your data and your extensive knowledge. This has taken the heterotopia project to a significantly higher level, it has been an honour and a privilege working with you. Many aspects of the study were made so much easier by the wonderful assistance of Carissa and Brandi. Dan Doherty and Thomas Cushion, many miles over land and over sea did not stop us from successfully collaborating on the tubulins. Ghayda Mirzaa, my Seattle buddy, so glad we became colleagues and friends. I look forward to future collaborations.

Ik wil graag alle collega's van de klinische genetica in het Erasmus MC bedanken, klinisch genetici, secretariaat, datateam, diagnostiek en research. Jullie hebben mij gevormd tot de klinisch geneticus die ik nu (bijna) ben en hebben mij in Rotterdam een onvergetelijke tijd bezorgd. Fred, bedankt dat je zoveel moeite hebt gedaan een plek voor mij te creëren. Anneke, dank voor het vertrouwen dat je in mij hebt gesteld, en mij al in een vroeg stadium zeker te stellen van een opleidingsplek. Dank ook voor je flexibele opstelling waardoor je voor mij de mogelijkheden schiep om elders stages te lopen en mij verder in de neurogenetica te bekwamen. Alice, bedankt voor al je hulp bij het *FLNA* artikel en voor heel veel meer. Tom de Vries-Lentsch en Ruud Koppenol dank voor jullie tomeloze inzet en geduld bij het maken van al die figuren.
Mijn collega arts-assistenten uit Rotterdam, altijd een gezellig clubje waar ik veel goede herinneringen aan bewaar. In het bijzonder Marije, vanaf dag 1 in Rotterdam was jij mijn neurogenetica buddy, je emigratie is een groot gemis voor mij en voor genetisch Nederland. En Judith, van ANIOS naar AIOS naar promovendus, onze loopbaan verliep parallel. Net zoals onze reizen Den Haag – Rotterdam v.v. Je onderzoek gaat als een speer, je bent slim en gedreven, jij komt er wel. Ik ben heel blij met jou als paranimf. Nog veel succes en plezier met je promotie. Lieve Lieke, jouw optimistische en constructieve blik op de wereld heeft je door heel wat moeilijke momenten gesleept. Heel jammer dat we geen collega's meer zijn, ze hebben veel geluk gehad in Grun. Iris, Laura, Shimriet, Myrthe, Virginie en Serwet, ik wens jullie heel veel succes en plezier in jullie opleiding. Anne en Shimriet, veel succes (en sterkte) bij het afronden van jullie promotie.
René de Coo, onder jouw supervisie op de neurogenetica poli heb ik mijn neurologische blik verder kunnen ontwikkelen.

Ik wil mijn nieuwe collega's van de afdeling Genetica in het UMC Utrecht bedanken voor het hartelijke welkom op de afdeling. Ik kijk uit naar onze samenwerking, en in het bijzonder met mijn neurogenetica collega's Eva, Nienke en Mariëlle.

De afgelopen jaren zijn er ook momenten geweest dat ik niet aan het werk was, en deze momenten heb ik met heel veel dierbare en gezellige mensen kunnen delen. Mijn lieve Amsterdamse vriendinnen, met name Soetinah, Annemarie, Lidewine en Annemiek, jullie zijn er altijd voor mij, en ik kijk uit naar vele gezellige etentjes in het post-baby, -opleiding en -promotietijdperk. Simone, Jana, Yvonne, Sonja; we kennen elkaar al zo lang, het is altijd fijn en vertrouwd om jullie weer te zien. Alle Haagse vrienden en de Veldheertjes, wat heerlijk om zulke betrokken mensen vlak om je heen te hebben. Juist de vrienden die wat verder weg wonen bedank ik voor hun trouwe vriendschap en ik hoop jullie in de nabije toekomst weer wat vaker op te kunnen zoeken.
Wat ben ik blij met zo'n leuke familie. Natuurlijk mijn ouders Bob en Jacobien ben ik dankbaar voor hoe jullie ons al die jaren hebben gesteund en gestimuleerd. Ook Els en Henk spelen een belangrijke rol in ons leven, net als Kyane, Loran, Dorine, Arjen en Bart. Oma Joke en oma Alie, ik ben heel trots af te stammen van deze twee vitale en ietwat eigenwijze dames. Gerard en Emmie, Erwin en Saskia, ik bof met zo'n geïnteresseerde en hartelijke schoonfamilie, en natuurlijk Jesse en Esra, ik hoop op nog vele gezellige logeerpartijtjes.
Tot slot, bedank ik de leukste mannen van de hele wereld. Het is altijd heerlijk thuiskomen bij jullie na een drukke werkdag. Lieve Edwin, je kent me niet anders dan bezig met werk en promotie. Bedankt voor al je geduld en support. Tijdens moeilijke momenten week jij nooit van mijn zijde. Met je brede interesse en enthousiasme voor de mooie dingen geef je het leven meer glans. Lieve Casper, je bent lief, vrolijk en ondeugend, en ik geniet van je gebrabbel en alle grote kleine avonturen die je beleefd. De wereld ligt op je te wachten, en we gaan haar met z'n drieën ontdekken.